The pore size distribution and permeability of cement pastes containing varying proportions of fly ash or blastfurnace slag.

Mansoor, Monther Hadi

THE PORE SIZE DISTRIBUTION AND PERMEABILITY OF CEMENT PASTES CONTAINING VARYING PROPORTIONS OF FLY ASH OR BLASTFURNACE SLAG

by

Monther Hadi Mansoor, B.Sc., M.Sc.

A Thesis for the degree of Ph.D.

submitted to

The University of London

Department of Civil Engineering
University of London
King's College
Strand
London

1983

ABSTRACT

The effects on the pore size distribution and permeability of cement pastes of replacing varying proportions of the cement by Fly ash or ground granulated Blastfurnace slag were studied in this work.

Mercury intrusion porosimetry was used to measure pores in the range 37 - 75,000 Angstrom , and oven drying of saturated samples at 105°C to measure the total porosities of Fly ash or Blastfurnace slag replaced cement pastes, at water/cement ratios of 0.3 and 0.4 at ages 3, 7, 28, 90, 270 and 560 days. Water permeabilities were measured by applying direct hydrostatic pressures to specimens, with a back pressure, and measuring the flows in a specially constructed apparatus at 20°C.

The replaced cement pastes showed useful reductions in water permeability provided high levels of replacement were avoided (less than 40% for Fly ash, or less than 80% for Blastfurnace slag. The parameter defined as the ratio of total intruded pore volume (maximum pressure 2000 kg/cm^2) to total porosity followed the same general trend as water permeability and is a useful parameter in assessing a cement.

The reduction in water permeability of cement pastes with various replacement levels of Fly ash or Blastfurnace slag is not due to a reduction in total porosity, which increases, but is caused by a shift of pore size distribution to finer pores, together with a blocking of capillary pores by increased gel product.

The bleeding rate and capacity were reduced for increasing Fly ash or Blastfurnace slag replacement.

ACKNOWLEDGEMENTS

The author wishes to express his profound gratitude to Dr. S.A. Jefferis who continually provided inspiration, constant help and encouragement during the course of this study, without whom this thesis could not have been completed. My deep appreciation to Dr. J.M. Illston and Dr. H.G. Midgely of Hatfield Polytechnic for the use of the Mercury Porosimetry and Volumeter equipment, Mr. D. Oxley for technical assistance, and the workshop staff at King's College for their assistance.

I should like to thank my family for their unfailing support over a period of many years.

TABLE OF CONTENTS

Page

CHAPTER TWO: THE CHARACTERISTICS OF ORDINARY PORTLAND CEMENT, FLY ASH, AND BLASTFURNACE SLAG AND MATERIALS USED IN THE PRESENT WORK

CHAPTER ONE

INTRODUCTION

CHAPTER ONE

INTRODUCTION

1.1 INTRODUCTION

The durability of cement can be improved by the addition of Fly Ash or Blastfurnace slag which are the relatively cheap waste products of the power and steel industries. Interest in cements containing these materials is sufficiently great that considerable data on properties is already available and various standards exist in many countries governing the quality and permitted proportions of such substances in cement. However, at present, there is an absence of data concerning the effect of replacement of the cement by Fly ash or Blastfurnace slag upon the pore structure or the water permeabilities which develop. Hence in this research the major aim was to investigate how the pore structure and water permeabilities were affected by varying replacement levels of Fly ash or ground granulated Blastfurnace slag.

Much data on the porosity characteristics of hardened cement pastes is confined to the range of 100-1000 Angstrom but it was felt that the research here should not be so confined and data should be collected on porosity characteristics extending each side of this range, in particular over the full range currently possible by mercury intrusion porosimetry 37-75,000 Angstrom. As discussed below pores exist mainly in two forms in hardened cement paste, gel pores and capillary pores, and the methods of determining pore structure and permeability will be given.

Some relationship between water permeability and porosity characteristics of a cement paste is expected, but this relationship for Fly ash or Blastfurnace slag replaced cement pastes is not a simple one, as becomes apparent from the research data presented here, and will be discussed.

It has been necessary to select starting materials carefully so that the conclusions reached in this research typefy the various Fly ashes or Blastfurnace slags used in the cement industry. The considerable experimentation required in obtaining data for just one Fly ash and one Blastfurnace slag composition may, however represent some limitation. To facilitate the scientific interpretation of data obtained it has been necessary to use replacement levels covering a range greater than the levels permitted by various standards.

During the progress of this research, it has been necessary to check properties such as compressive strength to ensure compatibility between samples tested here and those of other researches. Inevitably additional data, such as bleeding characteristics was required to confirm that segregation did not occur in the test mixes.

1.2 PORE STRUCTURE

1.2.1 PORE STRUCTURE OF CEMENT PASTES

In the Powers model (1958, 1960, 1964), at any stage of hydration, the hardened cement paste is considered to be a conglomerate of cement gel, calcium hydroxide, unhydrated cement and capillary pores. The capillary pores are due to the water filled spaces between the cement grains which remain after the cement has set. The hydrated product, gel which will fill most of the capillary pores is regarded as containing gel pores. As hydration proceeds, the amount and distribution of porosity between capillary and gel pores changes considerably. Initially all the pores are capillary pores. As hydration proceeds, the capillary pore volume is reduced because the capillary pores become filled with hydration products, and the gel porosity increases. There is a net reduction in total porosity because hydration increases the solid phase volume in mature and dense pastes and the capillaries become blocked by gel and

segmented so that they are inter-connected solely by gel pores.

At a certain critical water/cement ratio near to 0.38, according to Powers and Neville, fully hydrated cement paste would have no capillary porosity. It would have only gel pores, which would occupy about 28 per cent of the gel volume. At higher water/cement ratios and at complete hydration, there would be about 28 per cent gel pores plus capillary pores due to excess water. Thus in hydrated paste there are two distinct classes of pores and these are represented diagrammatically in Figure 1.1. The gel pores, according to Powers, are orders of magnitude smaller than the capillary pores, though they are greater in size than molecules of water.

Feldman and Sereda (1968) concluded that cement gel has a layered structure, with water separating the layers. This water is called inter-layer hydrate water, or "solid" water chemically bound to the hydrate crystals. They also divided the water in cement paste into three physical categories: (i) water of crystallisation, (ii) free water saturated with calcium hydroxide in the capillary pore spaces in the cement paste and (iii) adsorbed water on the walls. A diagrammatic representation of this is given in Figure 1.2.

Powers and Brownyard (1947) were the first to arbitrarily divide the water in cement paste into evaporable and non-evaporable types. Basically, the non-evaporable water is the water of hydration. The evaporable water is the water that is removed by drying at a temperature of 105^{o}C. The evaporable water is the gel water and capillary water which is held in the gel pores and the capillary pores respectively.

A part of this evaporable water is within the field of force of the solid phase, i.e. it is adsorbed. This water is often regarded as having a high viscosity but being nevertheless sufficiently mobile to take part in the flow (Nyame and Illston, 1981; Neville, 1981).

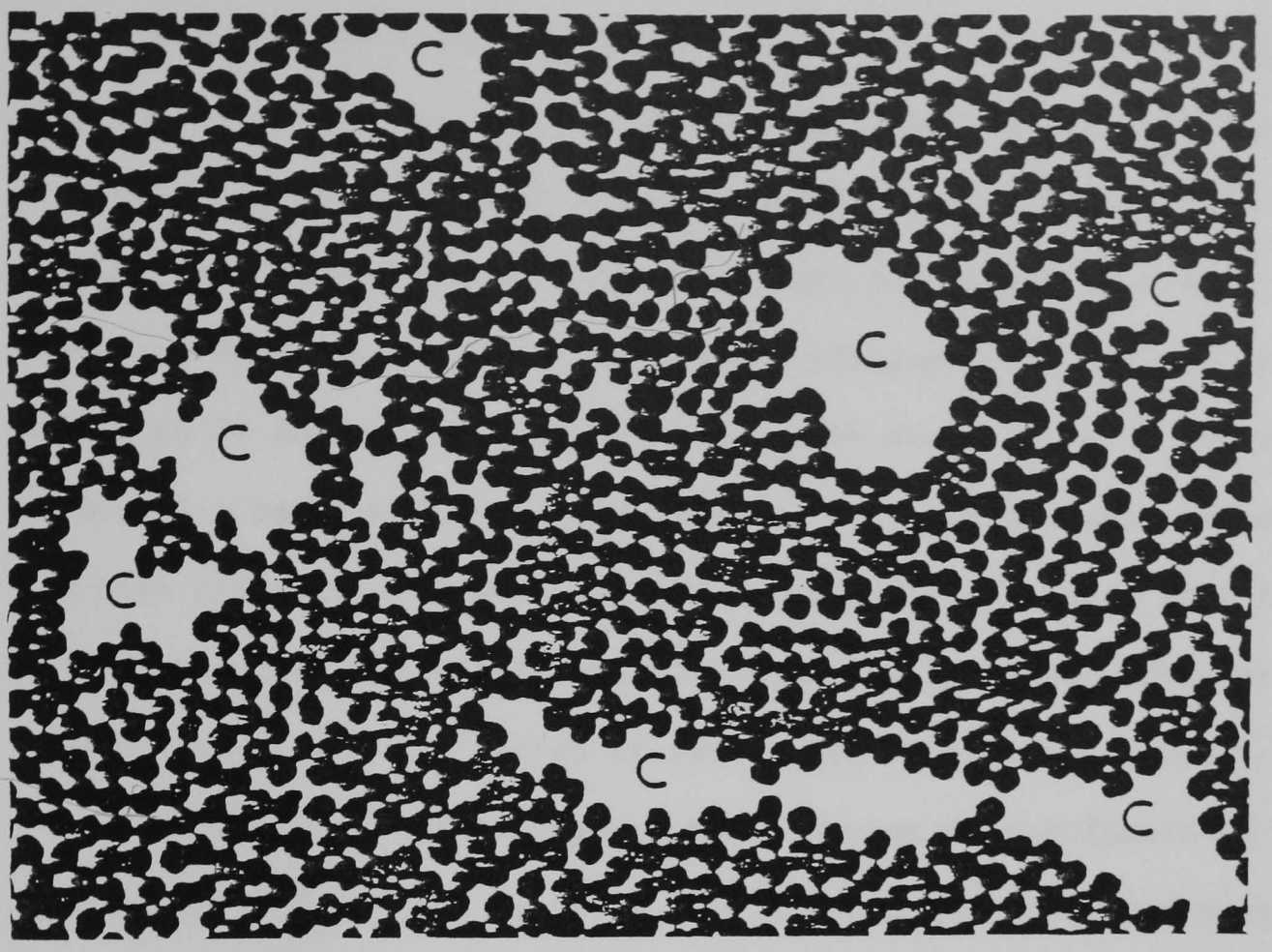

Figure 1.1. Simplified model of paste structure, solid dots represent gel particles; interstitial spaces are gel pores; spaces such as those marked C are capillary pores (the size of gel pores is exaggerated for clarity) (after Neville, 1981).

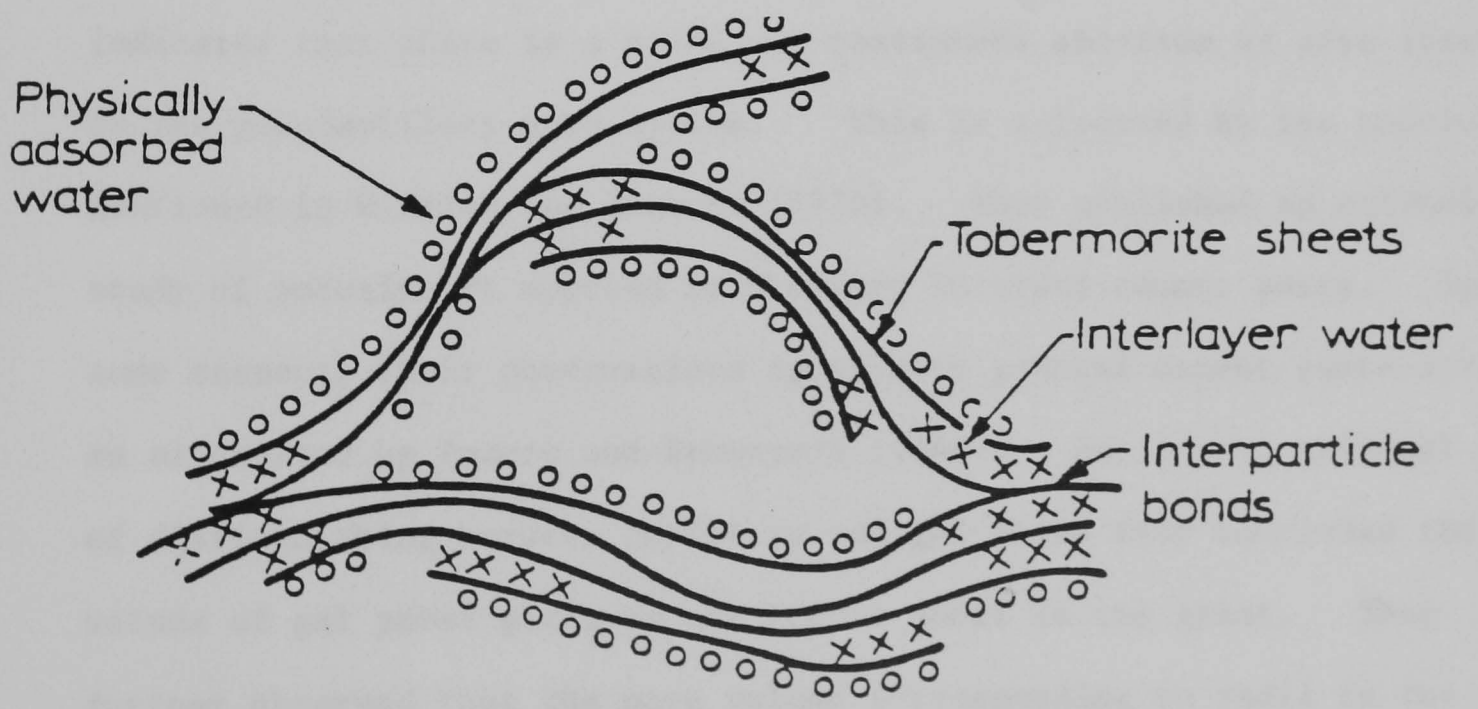

Figure 1.2. Probable structure of hydrated calcium silicates (after Neville, 1981). (Tobermorite refers to hydrated calcium silicates).

The average size of gel pores may be interpreted in terms of a hydraulic radius, defined as the reciprocal of the specific surface area expressed in units of area per unit volume. Estimates of the hydraulic radius as of the order of 7 Angstrom have been cited by Powers (1960, 1964). This value implies an average distance from surface to surface of 15 to 20 Angstrom depending on the pore shape factor. Powers favoured a best estimate of 18 Angstrom for this average surface to surface distance. Powers and Brownyard (1947) suggested that the capillary pores constitute an interconnected continuous network in fresh cement paste, but for pastes of reasonable water/cement ratios it was considered that the capillary pores would become discontinuous as hydration proceeded. When this occurred, any transmission of fluid between capillary pores would involve its passing through gel pores of very much smaller size.

One of the important questions that does not appear to have been completely resolved is whether or not the pore size distribution is continuous over the range from gel to capillary pores. In Verbeck's (1966) discussion of pore size distribution by nitrogen adsorption he indicated that there is a broad and continuous spectrum of pore sizes in the gel-capillary pore system. This is supported by the conclusions mentioned in Winslow and Diamond (1970). They published an extensive study of porosimetry applied to Ordinary Portland cement paste. In some respects their observations agree with general cement paste structure as elucidated by Powers and Brownyard (1948). But in the critical area of distinguishing between capillary and gel pores they concluded that the volume of gel pores given by the Powers model is too great. They further observed that the pore volume corresponding to radii in the range of 100-1000 Angstrom is substantial at all ages, that is the pore volume is generally considered to lie between gel pores and capillary pores. From this evidence Winslow and Diamond suggested that "most of

the volume in cement paste is neither capillary nor gel porosity per se, but consists of spaces left between particulate hydration products, supplemented by pores in spongy hydration products found to be present by scanning electron microscope observation".

Verbeck (1966) arbitrarily divided the pore system into two regions. Gel pores, considered to vary from 10 to 80 Angstrom and the capillary system from 80 Angstrom to 1.3 microns.

Diamond (1971) critically compared sorption and mercury porosimetry methods of pore structure analysis and concluded that mercury intrusion is relatively more efficient in assessing the distribution of the relatively large pore structure characteristic of hardened cement paste.

Auskern and Horn (1973) mentioned that there is not much capillary porosity less than 60 Angstrom in diameter. The maximum capillary porosity is a function of water/cement ratio and maturity. For a mature paste of water/cement ratio equal to 0.55, the maximum pore diameter is about 2000 Angstrom. Also they mentioned that the difference in capillary pore structure between cement pastes of different water/cement ratios lies mainly in the region of large pores; pastes with higher water/cement ratio having a group of large pores not present in lower water/cement ratio pastes.

In the present work high pressure mercury porosimetry measurements were made on cement pastes (prepared at water/cement ratios of 0.3 and 0.4) with varying proportions of the cement replaced by Fly ash or Blastfurnace slag , for reasons discussed later in relation to bleeding.

1.2.2 MEASUREMENT OF PORE STRUCTURE

Determination of total pore volume is a routine measurement in most laboratories dealing with porous materials. The value usually is calculated as the difference of two specific volumes. Thus the internal pore volume is calculated from the difference between the bulk density and particle density (McBain 1932).

A complete description of pore structure requires the measurement of the distributions of pore sizes, volumes, shapes and surfaces over the entire range of the pore size spectrum within the porous solid. Several authors (Diamond and Dolch 1972, Auskern and Horn 1973, Diamond 1973, Sellevold 1974 and Nyame 1980) have successfully measured the distribution of large pores in hardened cement paste, by mercury porosimetry. Sorption methods tend to be more efficient for the smaller pores (Diamond 1971). The helium comparison pycnometer does not give information on pore sizes but it has been usefully applied to study the collapse or re-expansion of interlayer spaces within the calcium silicate hydrates of hydrated cement paste (Feldman 1972).

1.2.2.1 MERCURY POROSIMETRY METHODS

Mercury porosimetry has been reviewed in detail by Rootare 1967, Orr 1970 and Diamond 1971. The method is based on the fact that a liquid, which does not wet a solid, can only enter pores in that solid under an applied pressure.

The amount of work, W required to force the liquid into a pore of

radius r and length L is proportional to the increased surface exposed to the mercury at the pore wall. Assuming cylindrical pores (Ritter and Drake 1945) showed that

$$W = 2\pi r L \gamma \cos \theta \qquad (1.1)$$

where

γ = surface tension of the liquid(mercury), defined as the work required to produce one square centimetre of surface.

θ = contact angle between the liquid and the wall of pore.

For a liquid which does not wet the solid ($\theta > 90^{o}$) a positive pressure is required to force it into the pores, increasing as the radius of the pores decreases. This is consistent with capillary fall as opposed to capillary rise when $\theta < 90^{o}$. See Figure 1.3.

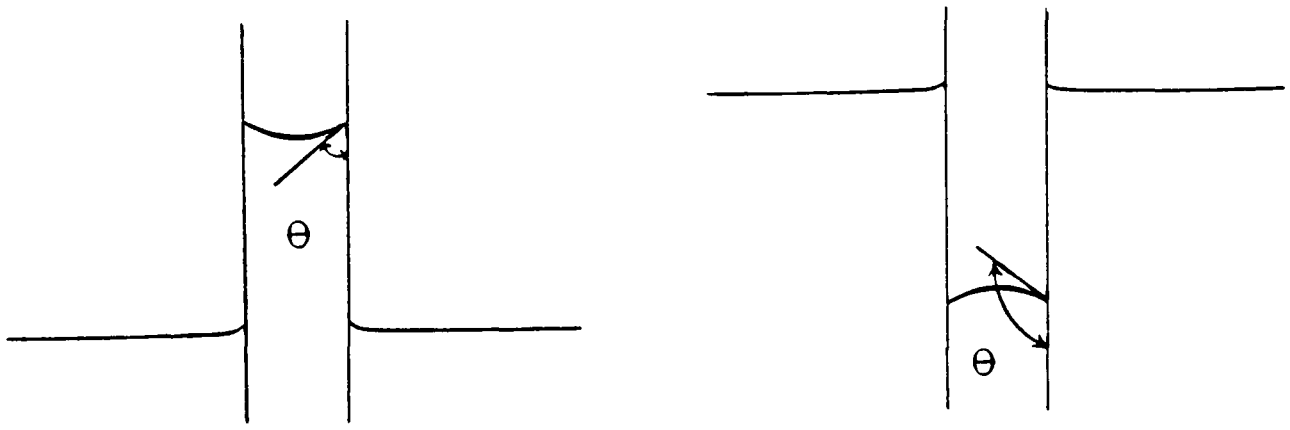

Figure 1.3 Left : Capillary rise : liquid wets the solid; $\theta < 90$

Right : Capillary depression: liquid does not wet solid; $\theta > 90$

Thus work must be done to force mercury into a pore. When a volume of mercury V is forced into a pore under external pressure P the amount of work W is given by:

$$W = P\ V = P\pi r^{2} L \qquad (1.2)$$

At equilibrium, equations 1.1 and 1.2 may be combined to give

$$Pr = -2\gamma \cos\theta \qquad (1.3)$$

Equation 1.3 was developed by Washburn, 1921 and is often referred to as the "Washburn equation."

Ritter and Drake (1945), published experimental data obtained by mercury porosimetry. They used a resistance wire to make contact with mercury in a capillary stem to monitor volume changes. They also developed one of the earliest high pressure porosimeters and measured the contact angle between mercury and variety of materials, which they found to be between 135° and 142°. They selected 140° as a reasonable average.

Winslow and Diamond (1970) determined the contact angle for oven dried specimens of hardened cement pastes and found it to be 117° (and the mercury surface tension to be 484 dyne/cm), though they found that the contact angle tended to vary with drying conditions.

For the present work a commercial Carlo Erba 200 series mercury porosimeter was used. In this the volume of the mercury which penetrates the pores of the sample is measured with a dilatometer and it is recorded automatically as a function of pressure. The general technique for mercury porosimetry is described more fully in Chapter 3.

1.2.2.2 SORPTION METHODS

Total pore volume and pore size distribution may be determined from gas adsorption isotherms, provided that the amount of gas adsorbed on the pore surfaces is small compared with the amount adsorbed at the saturation pressure. With many adsorbents a

hysteresis loop occurs between the adsorption and desorption curves provided a monolayer has been completed. This has been explained as being due to capillary condensation in the pores of the adsorbent. As the pressure is reduced, the adsorbate does not evaporate as readily from the capillaries as it does from a flat surface due to a lowering of the vapour pressure over the concave meniscus formed by the condensed vapour in the pores (Skalny and Odler 1972, Brunauer et al. 1970, Gregg and Sing 1967). The lowering of the vapour pressure for a cylindrical pore of radius r is given by the Kelvin equation, (Gregg and Sing 1967).

$$\ln(P/Po) = \frac{-2\gamma V_L \cos\theta}{RT\ r} \qquad (1.4)$$

where r = pore radius

γ = liquid surface tension

θ = contact angle of liquid and the walls of the pore

Po = saturation vapour pressure of the adsorbate

P/Po = relative gas pressure

V_L = molar volume of adsorbate in liquid form

T = temperature (K)

R = molar gas constant

This equation may be further developed from thermodynamic considerations or by using the method of Young and Laplace (Gregg and Sing 1967). The two forms of the equation that develop are respectively

$$\ln(P/Po) = -\gamma V_L\ S \cos\theta/RTV_v \qquad (1.5)$$

and

$$\ln(P/Po) = -\gamma V_L \cos\theta\ (1/r_1+1/r_2)/RT \qquad (1.6)$$

where S = surface area

V_v = volume of pores

r_1 and r_2 are the radii of curvature of the curved surface of the meniscus in mutually perpendicular planes.

The pore radius given by the Kelvin equation is in fact the radius of that part of the pore which is not covered by the adsorbed molecular layer, therefore a correction to the volume of vapour absorbed needs to be made to allow for the thickness of the adsorbed film to obtain the true pore radius. If allowance is made for the thickness of the adsorbed film t, the relevant radius for the relative pressure, P/Po would be r-t and the volume adsorbed would be made up of two parts, the volume filling capillary pores and the volume which increases the thickness of the adsorbed layer on pores with radii greater than r. In order to determine the pore size distribution, it is therefore necessary to know t. This problem is discussed more fully by Gregg and Sing, 1967.

Oulton (1948) assumed the thickness of the adsorbed layer remains constant over the whole pressure region. Schull (1948) pointed out that this gave too high a value for t in the high pressure region and he determined multilayer thicknesses from experimental data with non-porous solids. However, their distributions do tend to agree with those obtained by mercury-intrusion methods (Jayner et al. 1951), so

the assumptions are perhaps not particularly significant.

Cranston and Inkley (1957) derived a curve of thickness of adsorbed layer, t against relative pressure, P/Po from published isotherms on fifteen non-porous materials by dividing the volume of nitrogen adsorbed by the BET surface area. They stated that their method may be applied either to the adsorption or desorption branch of the isotherm and that the indications were that the adsorption branch should be used, a proposal which is at variance with current practice.

Gregg and Sing 1967, Brunauer et al.1967 and Roberts 1967, agreed that the shape of the t-curve depends on the energy of adsorption, t increasing at the same relative pressure with increasing energy. Mikhail et al. 1972 and Hagymassy et al. 1967 supplied suitable t curves for hardened cement pastes.

1.2.2.3. HELIUM PYCNOMETER

In the helium pycnometer technique one may obtain the "solid volume" of a sample by helium displacement. The solid volume is considered to exclude all pores, but include interlayer spaces which may or may not be occupied by water. Helium can be assumed to flow rapidly into all pores except the interlayer spaces (Feldman 1971).

The technique has been used successfully to study the collapse and re-expansion of interlayer spaces due to penetration and withdrawal of interlayer hydrate water (Feldman and Sereda 1970, 1968). Though, according to Brunauer (1972) and Feldman (1972), the interpretation of

the data is questionable.

Nyame (1980) found that the measurement of total porosity by a simple oven drying procedure was more successful than the helium inflow method.

1.3 BLEEDING

1.3.1 BLEEDING PHENOMENA

The process of bleeding is a familiar one and has been studied extensively by many investigators, particularly Powers, 1939 and Steinour, 1944. Immediately, after the placing of cement paste there is a tendency for the solid particles to settle due to gravitational forces and for water to collect at the surface, this is called bleeding (Powers 1939).

Bleeding may take place gradually by uniform seepage over the whole surface. In addition to general seepage, a number of localized "pipes" or channels from the interior to the surface may sometimes develop. From these the water may flow with sufficient velocity to transport small solid particles and build up miniature craters around the mouth of each of the channels which is called excessive bleeding. The formation of channels and craters is characteristic of rather wet consistency. It shows a need for corrective measures. On the other hand, when bleeding occurs by uniform seepage only, the composition of the mix is probably homogenous within reasonable bounds, and the bleeding itself is not necessarily undesirable. Such bleeding is called normal bleeding.

There are two aspects of bleeding to be considered, the rate at which it occurs, and the total amount.

The rate of bleeding under fully saturated conditions where capillary tension cannot develop can be conveniently divided into two stages: a stage at which bleeding occurs at a constant rate, followed by a period of diminishing rate. The conditions which determine the length of the period of constant rate are various and are considered in more detail later.

The total settlement tends to be proportional to the depth of the freshly placed mass. The amount of settlement divided by the depth of the mass is called the bleeding capacity.

The bleeding capacity can be expressed as the total loss per unit of water originally in the mixture. The nature of the phenomenon is such that the loss of water is not the same from the upper and lower parts of the mass. Under some circumstances, the water content of the upper part may remain unchanged all the loss being from the lower part.

Powers (1939) distinguished three zones in a sufficiently deep semi-infinite sample of paste after settlement:

1. A zone of clear water at the top.

2. A zone of uniform density equal to the original density.

3. A compressed zone in which there is a gradient of density, increasing towards the bottom (see Figure 1.4).

Although free water accumulates at the top, it is immediately above a zone of uniform density equal to the original density implying that there is no apparent segregation in this zone; this water effectively comes from the compression zone lower down. The compression zone begins at the depth where the hydrostatic pressure exceeds the interparticle repulsion. Powers, 1939 noted that "a fourth zone of maximum compression with uniform density, which was thought could exist, did not develop under the compressive forces of the magnitude developed from the weight of the sediment".

The bleeding curve (see Figure 1.4) can be divided into sections: a straight line that indicates a period of constant rate of bleeding, followed by a period of diminishing rate, then a zero rate.

Bleeding characteristics, that is, initial rate of bleeding, and the bleeding capacity as characterized by the shape of the bleeding curve (Figure 1.4) depend mainly on effective specific surface particle interaction and chemical composition (Steinour, 1945). Additionally mixing method and equipment affect these characteristics since they control the initial degree of dispersion (Powers, 1945; Valore et al. 1949; Bruthans 1963) and, therefore rate of hydration and surface

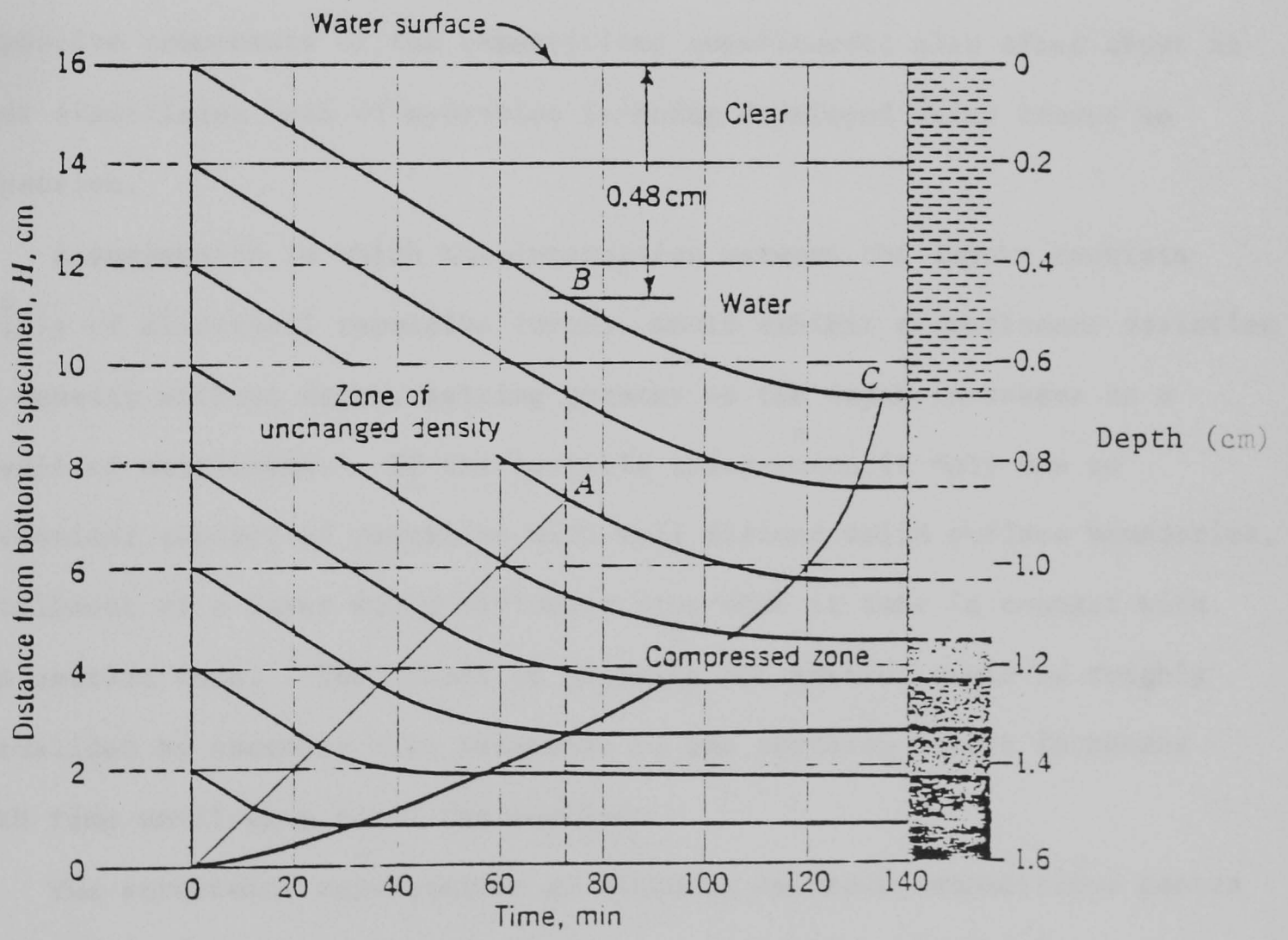

Figure 1.4. Development of sedimentation (compression) zones in a semi-infinite sample. (After Powers, 1939).

adsorption. Powers (1939, 1968) discussed in detail the effect of the dimensions of sample based on development of peripheral and sedimentation zones.

The initial linear part of the bleeding curve suggests the sedimentation of the porous layer of paste is uninfluenced by particle interaction. With time, the compressed zone builds up. The continuous variation of the density in the bottom compression zone decreasing from the base up to the uniform density zone is an indication of the effect of the interparticle electrical repulsion and time-dependent development of mechanical resistance. If the rate of development of mechanical resistance is high, discontinuities may occur in the bleeding curve. A post-bleeding expansion may also be observed (see Figures 1.6 to 1.10 inclusive) due to expansive components of the cementitious constituent; also after about an hour significant heat of hydration is being developed which causes an expansion.

A suspension in which the interaction between the layers consists solely of electrical repulsive forces would exhibit a continuous variation of density without depth, getting greater as the depth increases as a result of settlement. If the particle interaction is only due to mechanical contact of particles with well defined solid surface boundaries, settlement of a layer would virtually stop when it came in contact with the settled zone. The effect of gelation and setting could be roughly visualized by assuming that thickness of the settling layers increases with time until they touch one another.

The structural consequences of bleeding on fresh cementitious pastes can be divided into two broad groups, (i) Those related mainly to rate of bleeding, such as channelling and consolidation, (ii) Differential settlement, when water bleeding from some layers can cause water gains in other layers, a more important factor in the setting of mortars and concretes. Water gain is the dilution of the subsequent layer of

material by the bleeding water that collects on the previous layers (Powers, 1968).

In cases of high rates of bleeding, the flaws (water pockets or channels) within the fresh paste matrix may result in an unsatisfactory performance of the material and may cause failure to seal the voids (Jefferis, 1972). However if the paste settles as a whole by normal bleeding at moderate rate it may consolidate to give practically a flaw-free mass (Powers, 1968).

Hughes and Ash (1969) found that increasing the ratio of surface area of solids to the water in a mix reduces the anistropic effect and therefore the water gain.

Hughes and Ash (1969) found that test cubes gave different compressive strengths when tested in the vertical and horizontal directions; they attributed this anisotropy to the effects of water gain. Their work demonstrated that increasing the ratio of surface area of solids to the water in a mix reduced these undesirable effects and suggested various remedies including adding Fly ash to maintain the workability.

1.3.2 MEASUREMENT OF BLEEDING AND BLEEDING-TIME CURVES

Powers (1939, 1968) and Steinour (1944, 1945) made extensive studies of bleeding in cement pastes and suspensions of fine powders. Valore et al.(1949) developed an apparatus for continuous measurement of bleeding in cement pastes.

Test methods developed for the measurement of bleeding fall into two general categories :

1. Methods based on the measurement of subsidence of the surface, the subsidence can be measured by following the surface with a probe connected to a micrometer or by following the subsidence of a float placed on the surface of the paste with a cathetometer. These two techniques called "probe method" and "float method" respectively and are shown in Figure 1.5.

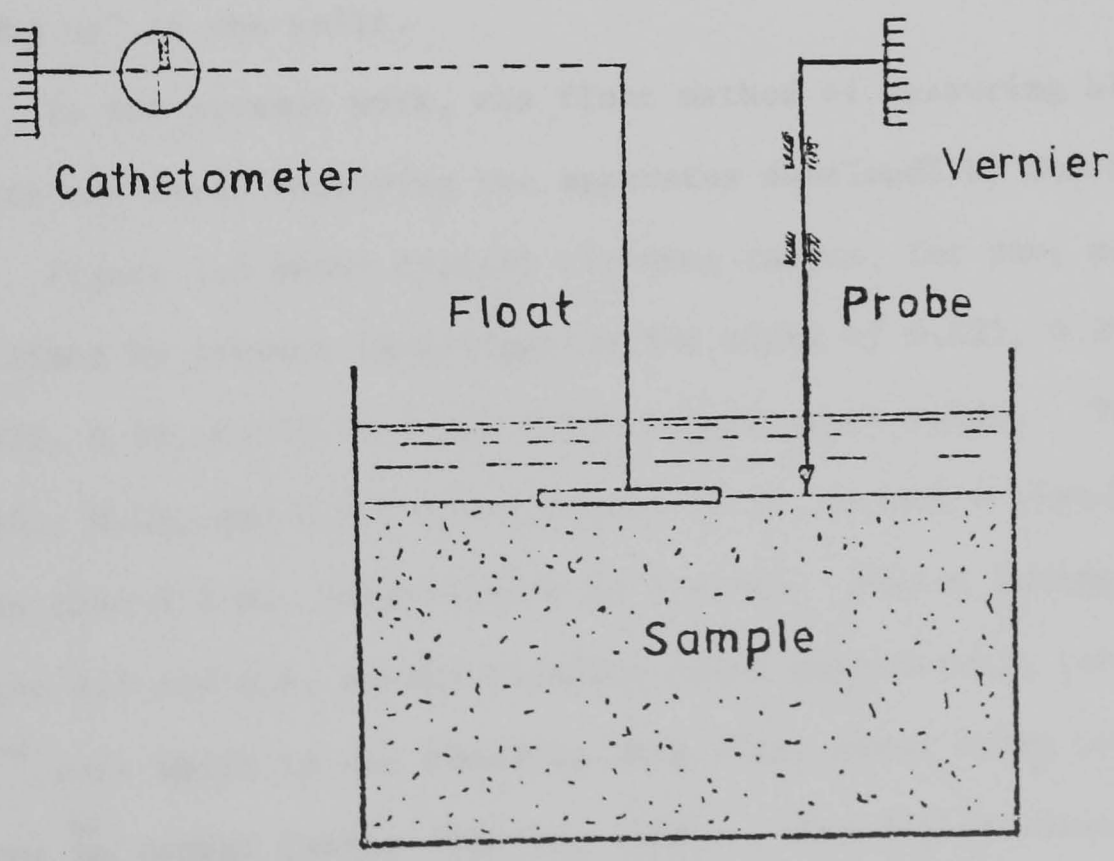

Figure 1.5. Measurement of subsidence of the surface of cement paste.

2. Methods based on the direct measurement of the volume of water accumulated on top of the sample. If the sample is sufficiently stiff, the volume of water can be measured simply by pouring it off into a graduated cylinder. A more accurate method is the "float-siphon method" developed by Powers (1939, 1968) in which the bleeding water is siphoned out into a burette at intervals so as to keep a layer of water of constant thickness above the sample. This method was refined by Valore et al. (1949) who flooded the surface with kerosene withdrawing the water from underneath.

A wall effect can occur when a paste is allowed to settle in a container that is relatively narrow and deep. The rate of settlement at the centre is at first the normal rate for the composition of the mixture, but after a certain time the rate diminishes to the peripheral rate, and this rate is maintained until the end of the dormant period if the sample is sufficiently deep (Powers 1968). The peripheral rate is lower than the rate at the centre because the paste tends to "hang up" at the walls.

In the present work, the float method of measuring bleeding of the paste was used, employing the apparatus developed by Guner (1978).

Figure 1.6 shows typical bleeding curves, for pure cement pastes, obtained by present investigation for mixes of 0.225, 0.25, 0.275, 0.30, 0.325, 0.35, 0.375, 0.4 and 0.425 water/cement ratio. The mixes at 0.225, 0.25, and 0.275 water/cement ratio, showed a bleeding capacity of less than 0.2 mm (stabilizing in $\frac{1}{2}$ hour). Pastes having a water/cement ratio 0.3 and 0.4, showed bleeding rates considerably less than 2.20 x 10^{-4} cm/s which is the bleeding rate limit above which channelling may occur in cement pastes (Powers, 1968). The present investigation is not ultimately concerned with incomplete hydration of the cement nor with cases of excessive bleeding. This led to selecting the values 0.3 and 0.4 as the most useful water/cement ratios to study. Also to be noted is

when the water/cement ratio is as low as 0.225, bleeding is negligible and the cement surface swells and may crack, which would in any case give spurious readings on the bleeding rate equipment.

Figures 1.7 and 1.8 represent the bleeding curves for two water/cement ratios 0.3 and 0.4 and for different percentages of Fly ash replacement of cement. A similar set are presented in Figures 1.9 and 1.10 for different percentages of Blastfurnace slag replacement of cement. Excessive bleeding does not occur at these water/cement ratios.

Significant points can be made about the curves. The bleeding decreases with increasing Fly ash or Blastfurnace slag replacement of cement and with decreasing water/cement ratio from 0.4 to 0.3. Therefore, for slag/cement or Fly ash/cement mixes, a maximum limit for bleeding capacity is probably a sufficient stability criterion, for the corresponding bleeding rate is likely to be low enough not to cause any damage. The apparatus and test procedures for the measurement of bleeding are given in Chapter 3.

In view of the small amount of bleeding at both 0.3 and 0.4 water/cement ratios, the water loss is small and consequently the water/cement ratios can be regarded as remaining constant (2.4% accurate). The set material was found to be homogeneous in this investigation. This was established with electron microscope and electron probe microanalysis. No significant difference in the elemental composition of cement pastes containing Fly ash or Blastfurnace slag within the samples was detected.

Replacement of part of the cement in such mixes with Fly ash or Blastfurnace slag should not increase the bleeding as the specific gravity of both these materials are generally lower than Ordinary Portland cement. There also tends to be less segregation in small test samples.

It is important in assessing the effects of Fly ash or Blastfurnace slag to consider the heat generated during the setting of the cement. This is because characteristics of cement, such as porosity and permeability etc., depend on the development of paste hydration which can result in various rises of temperature. Powers (1968) and Steinour (1945) give data on how the initial rate of bleeding depends on the heat of hydration. In the present work, the temperature was measured using iron-constantan thermo-couples. After casting the temperatures were monitored for 25 hours.

Table 1.1 represents the peak temperature during the progress of reaction of the fresh cement pastes containing varying proportions of Fly ash or Blastfurnace slag within 25 hours after casting.

The results reported in Table 1.1 show the temperature rise of the test sample of the various mixes. It can be seen that the peak temperature reduced and the time to achieve the peak lengthened with increased Fly ash or ground granulated Blastfurnace slag replacement of cement and with increasing water/cement ratio. It may be noted that the lower temperature rise will produce lower thermal expansion; this can improve the durability.

These mixes at water/cement ratios of 0.3 and 0.4 with Fly ash or Blastfurnace slag replacement appeared stable from the point of view of bleeding and were therefore used for the determination of pore size distribution and water permeability.

Table 1.1

Slag/ cement %	Peak temperature °C (time (min) after casting) water/cement ratio			Fly ash/ cement %	Peak temperature °C (time (min) after casting) water/cement ratio	
	0.225	0.3	0.4		0.3	0.4
0	57 (232)	50 (450)	46 (615)	0	50 (450)	46 (615)
5	54 (236)	48 (463)	41 (634)	5	46 (460)	43 (665)
10	53 (258)	48 (492)	40 (690)	10	43 (485)	38 (725)
20	51 (266)	41 (515)	37 (725)	20	37 (505)	32 (820)
40	44 (330)	40 (565)	33 (770)	40	34 (575)	29 (875)
60	40 (360)	35 (580)	33 (815)			
70	37 (363)	33 (590)	32 (825)			
80	35 (380)	31 (635)	30 (830)			
95	31 (392)	30 (660)	29 (850)			

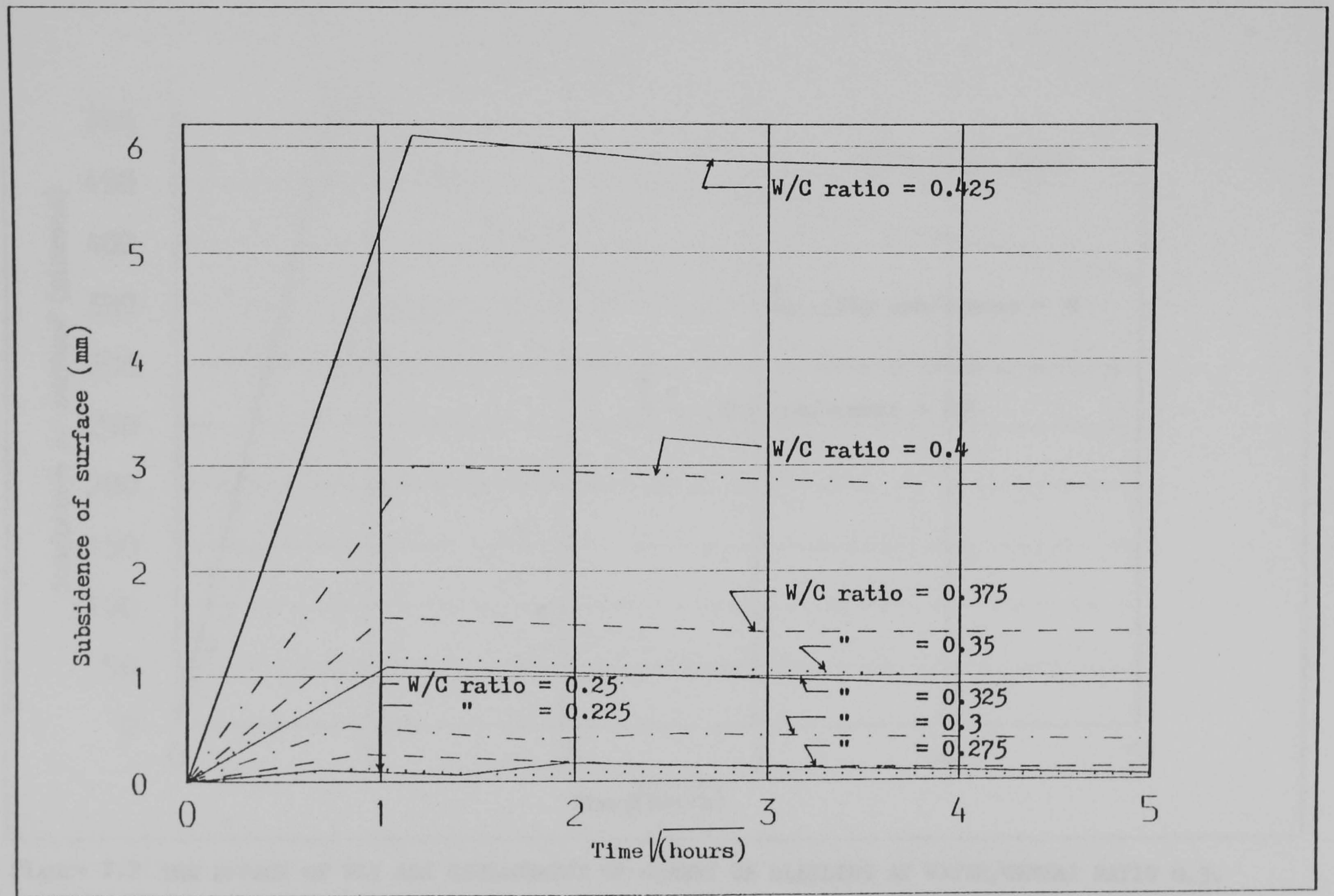

Figure 1.6 THE EFFECT OF WATER/CEMENT RATIO ON PURE CEMENT PASTE BLEEDING

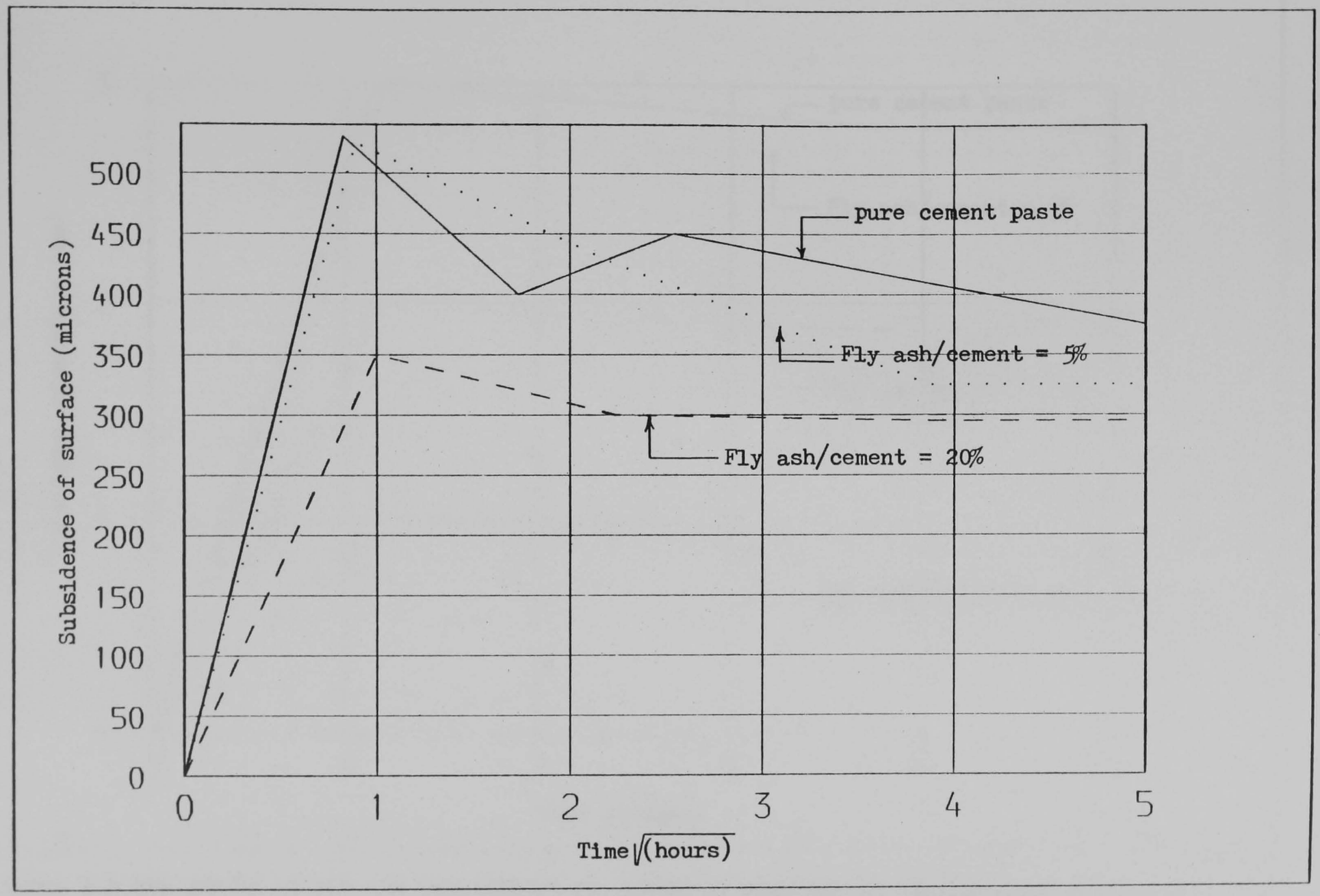

Figure 1.7 THE EFFECT OF FLY ASH REPLACEMENT OF CEMENT ON BLEEDING AT WATER/CEMENT RATIO 0.3.

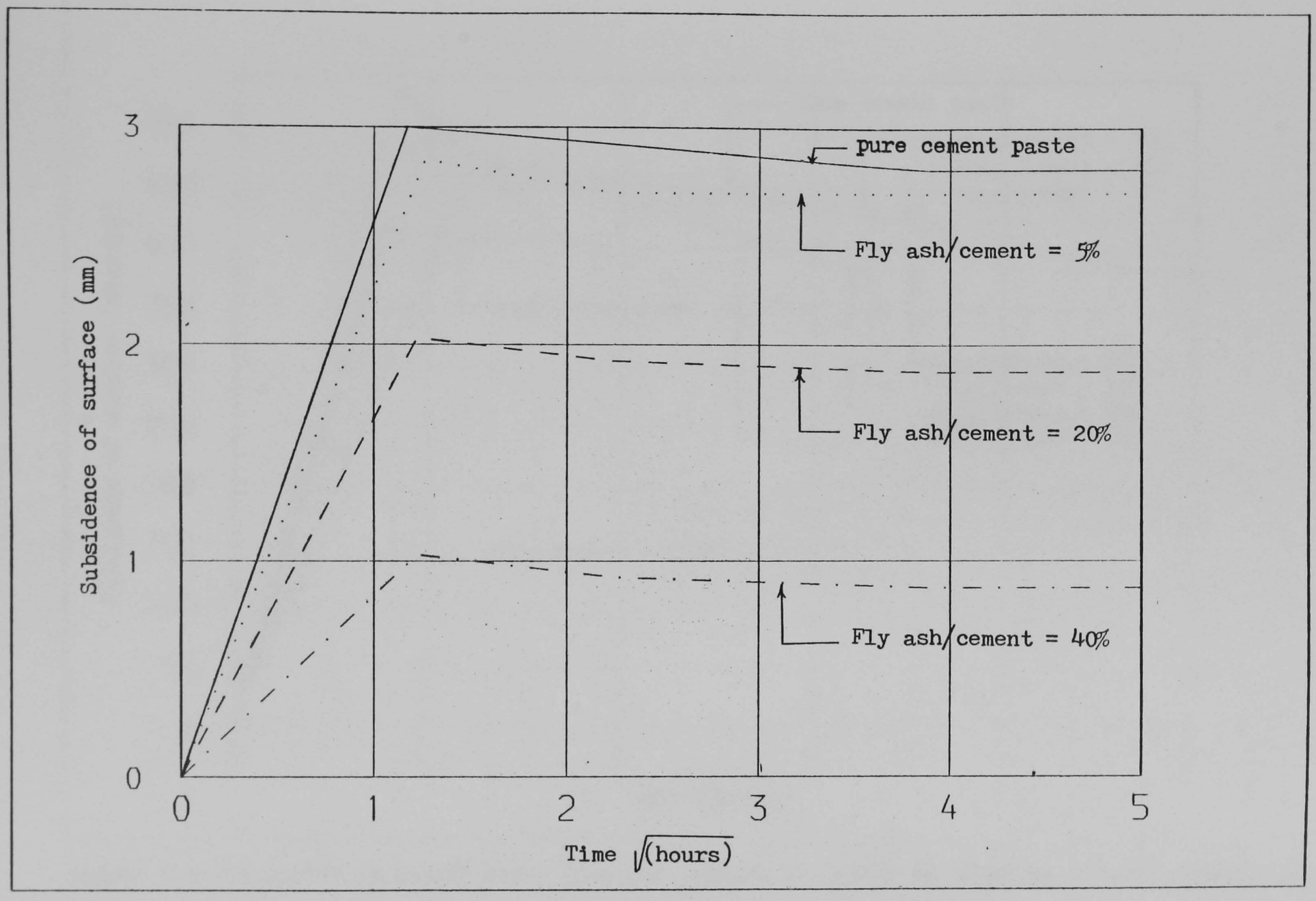

Figure 1.8 THE EFFECT OF FLY ASH REPLACEMENT OF CEMENT ON BLEEDING AT WATER/CEMENT RATIO 0.4.

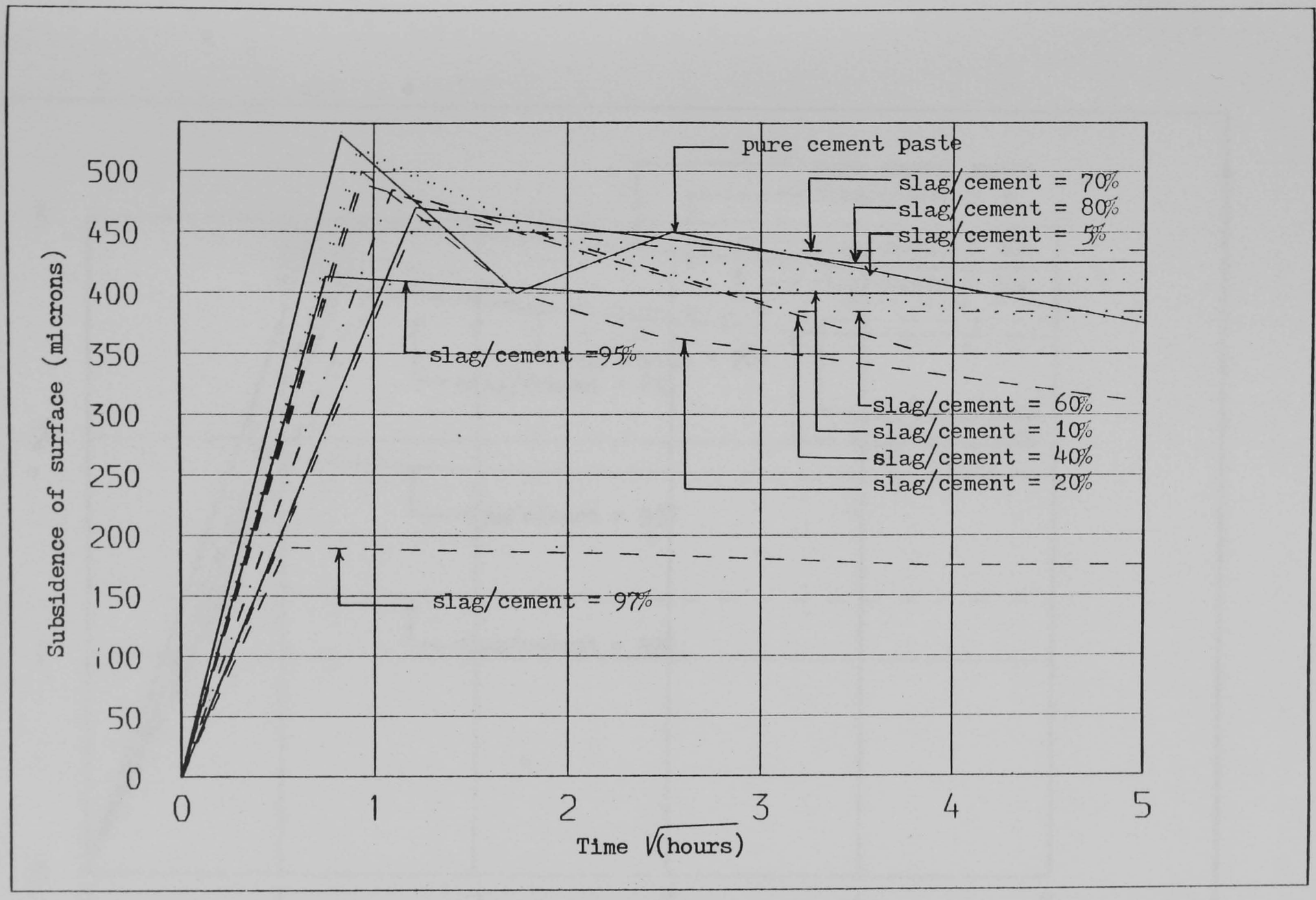

Figure 1.9 THE EFFECT OF BLASTFURNACE SLAG REPLACEMENT OF CEMENT ON BLEEDING AT WATER/CEMENT RATIO 0.3

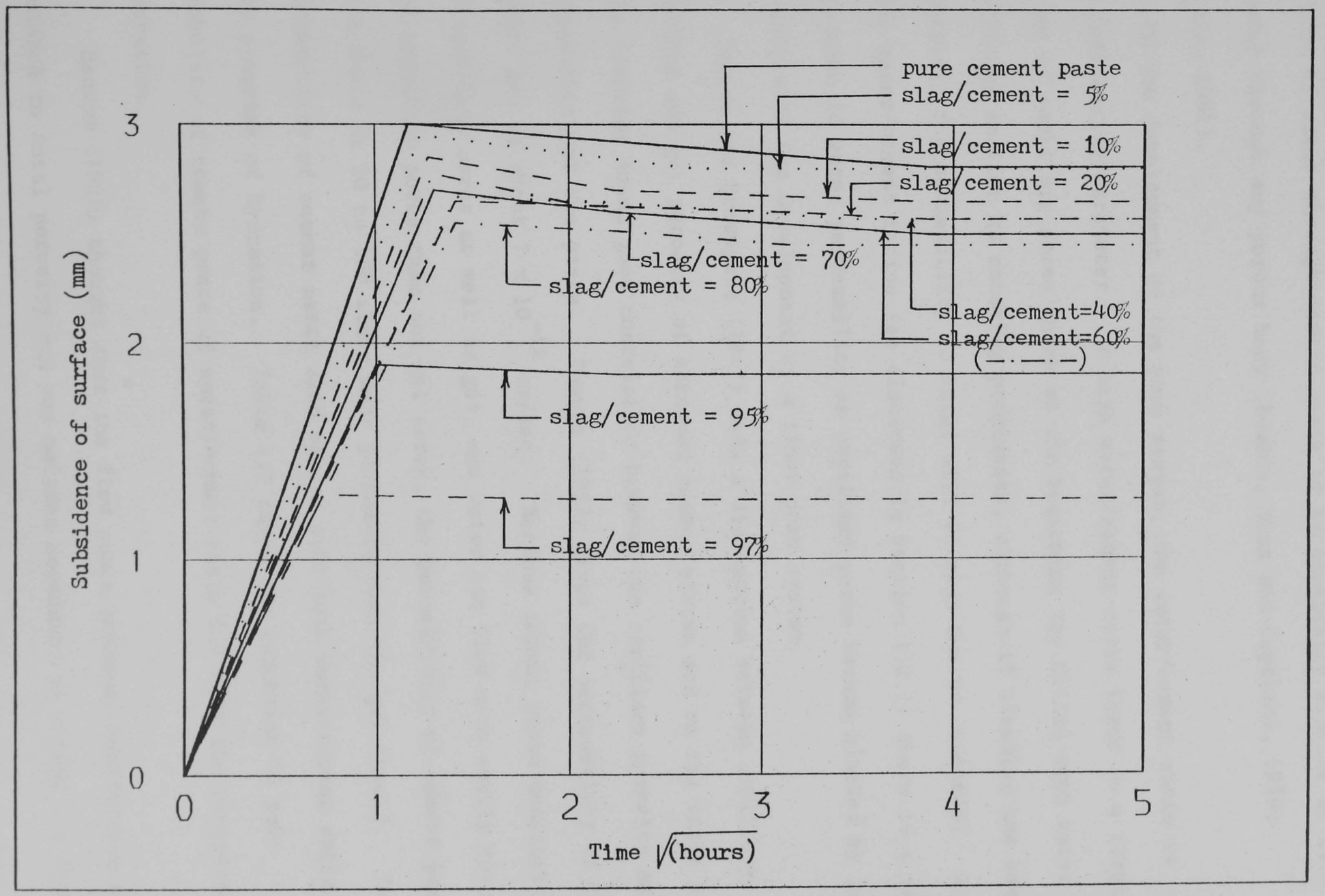

Figure 1.10 THE EFFECT OF BLASTFURNACE SLAG REPLACEMENT OF CEMENT ON BLEEDING AT WATER/CEMENT RATIO 0.4

1.4 WATER PERMEABILITY

The permeability of a porous material to water is a function of the geometry of the boundary between the solid component and the pore space. The flow of water through cement paste is fundamentally similar to flow of water through any porous body (Powers, Mann and Copeland, 1959; Neville, 1981).

In the development of the pore system, the water/cement ratio is the influencing parameter. A high water/cement ratio leads to a large volume of capillary pores which at the beginning are filled with water and become smaller as maturing progresses, although if bleeding has been excessive the permeability to water will be high due to channels. At lower water/cement ratios (as discussed in Section 1.2.1) there is a net reduction in water permeability as capillary pores become blocked by gel product with the development of a finer pore system.

Powers and Brownyard (1947) made a distinction between capillary porosity and gel porosity of hardened cement pastes and on the basis of this division found good correlation between the capillary porosity and permeability of the paste. Powers (1958) gives the permeability of the cement gel as about 7×10^{-14} cm/sec. Because cement paste consists of capillary pores as well as gel, and water can flow more easily through the capillary pores than the gel pores, the permeability of cement paste as a whole is 20 to 100 times more permeable than the gel itself. The permeability of cement paste also varies with both water/cement ratio and progress of hydration. Table 1.2 shows the reduction in permeability of cement paste of water/cement ratio 0.7 with the progress of hydration.

Hancox (1968) thought that the flow space rendered ineffective was related to total porosity and was neither dependent on curing nor type of cement.

Robson (1965) postulated the 'unit pore flow' hypothesis. This involved a calculational procedure requiring repeated subdivision of the measured flow rates through hardened cement pastes, mortars and concretes, and from this deducing average pore flow with newly developed statistics. Robson deduced that permeability depends on the probability of continuous channels developing in mortars and concretes and is not a function of total porosity. But recently Nyame and Illston (1981) defined a porous material as permeable to fluids not because of its porosity but because of the extent of the continuity of the pores within its structure. His results showed the maximum value of dv/dp (mercury intrusion porosimeter) is used to locate a 'threshold radius' and is called the 'primary continuous pore radius', because pores of this radius were primarily responsible for carrying waterflow in hardened cement paste. His results showed the nature of the variation of the primary continuous pore radius with hydration.

Table 1.2 Reduction in permeability of cement paste with the progress of hydration (after Powers et al. 1954 and Neville, 1981).

Age (days)	Coefficient of permeability, k (m/s)
Fresh	2×10^{-6}
5	4×10^{-10}
6	1×10^{-10}
8	4×10^{-11}
13	5×10^{-12}
24	1×10^{-12}
Ultimate	6×10^{-13} (calculated)

1.4.1 MEASUREMENT OF WATER PERMEABILITY

The permeability of cement paste to the flow of water may be determined under small or large head differences in many cases a fairly high water pressure (up to 1400 kNm^2 or more) is used, and the rate at which water passes through the specimen determined (Lea 1980).

Permeability tests at high pressure are most commonly made by a direct method involving cement paste cylinders in an apparatus which permits water under the required pressure to be fed to one side of the specimen and the water percolating through to be collected at the other side and measured. Alternatively, or additionally the rate of inflow of water may be measured.

The specimen is usually sealed into a metal container with suitable watertight caps. The rate of flow is more rapid at the start, but decreases to a steady value after a few days depending on the dimensions of the specimen and other factors (Lea 1980).

In the present work, the permeability of hardened cement pastes was measured with hydrostatic pressures on both sides of the specimen. This has the advantage that in such apparatus the specimen may be subjected to vacuum and any small quantities of air remaining will be compressed thus spurious effects on the permeability will be minimised. The difference between the upstream and downstream pressures was adjusted to give a suitable pressure difference for permeation.

Powers 1947, 1954, 1959, McMillan 1929, Norton 1931, Dunagan et al. 1934, Ruettgers 1935 and Cook 1951,used the direct method to measure permeability. This direct method requires the measurement of steady state inflow or outflow or both. The steady state method of measuring the permeability of hardened cement paste has been more recently described by Nyame and Illston, 1981. The method is based on the measurement of

the quantity of water that flows under a given gradient through a specimen of known length and cross-sectional area in a given time. Inflow rates of water into the specimen were determined and used to calculate the permeability coefficient using Darcy's law. They neglected capillary heads in low pressure tests on specimens (Wiley 1937 and McMillan 1929).

Darcy's law, (see Appendix 1), originally formulated to describe the flow of water through a porous material, such as sand, has also been applied to the flow of gases through porous media (Muskat 1946). Darcy's law has subsequently been found to be valid for a wide variety of materials, including sand, clay, cement paste, mortar and concrete (Muskat 1937, 1947, Hansbo 1960, Olsen 1961 and Nyame 1980). Though Powers (1954, 1958) emphasised that deviations from Darcy's law can occur due to osmotic pressure caused by the difference in calcium hydroxide concentrations within the cement paste. In this work, Darcy's law has been applied to the flow of water through hardened cement pastes with varying proportions of the cement replaced by Fly ash or ground granulated Blastfurnace slag. Obviously, osmotic pressure could affect the values obtained but according to Powers (1954) the effects of calcium hydroxide are probably negligible.

1.5 THEORETICAL ASPECTS OF THE RELATIONSHIP BETWEEN FLOW RATE, COEFFICIENT OF PERMEABILITY AND POROSITY

The problem is to find the value of the coefficient of permeability in Darcy's law in terms of the characteristics of the solid and the liquid. Studies of this problem have been pursued extensively from the theoretical point of view and by the use of models to represent the porous medium (see Appendix 1). Extensive reviews of many of the models have been given by: Scheidegger 1974, Van Brakel 1975, Braester 1972, Slattery 1972, Powers 1968 and Childs et al. 1950.

CHAPTER TWO

THE CHARACTERISTICS OF ORDINARY PORTLAND CEMENT, FLY ASH AND BLASTFURNACE SLAG AND MATERIALS USED IN THE PRESENT WORK

CHAPTER TWO

THE CHARACTERISTICS OF ORDINARY PORTLAND CEMENT, FLY ASH AND BLASTFURNACE SLAG AND MATERIALS USED IN THE PRESENT WORK

2.1 ORDINARY PORTLAND CEMENT

2.1.1 CHEMICAL COMPOSITION

Portland cement is prepared by igniting a mixture of raw materials composed mainly of calcium carbonate and alumina silicates with a smaller proportion of iron oxide. Marls composed of chalk and clay, and shales are also common raw materials (Lea, 1980).

The homogeneous mixture is burnt to form a clinker which is then ground to a powder. The clinker consists mainly of calcium silicates, calcium aluminates and calcium aluminoferrite. The proportions of these materials determines the type of cement produced. B.S.12: 1978 Ordinary Portland cement states that no addition of any other substance other than calcium sulphate or water or the two together may be permitted after formation of the clinker.

The standard chemical analysis for cements are described in B.S. 4550: 1970. The physical properties of Portland cements vary with type and constituents. The specific surface of Ordinary Portland cement is required to be not less than 225 m^2/kg. The specific gravity is usually between 3.05 and 3.15 in paraffin.

There are four major constituents of Ordinary Portland cement (Neville 1981). These are tricalcium silicate ($3CaO.SiO_2$ abbreviation C_3S), Dicalcium Silicate ($2CaO.SiO_2$ abbreviation C_2S), tetracalcium aluminoferrite ($4CaO.Al_2O_3.Fe_2O_3$ abbreviation C_4AF) and

tricalcium aluminate ($3CaO.Al_2O_3$ abbreviation C_3A).

In addition to the major constituents there are minor constituents such as MgO, TiO_2, MnO_2, K_2O and Na_2O. Na_2O and K_2O are known as the alkalis.

Typical proportions of these major constituents obtained by Brunauer and Copeland (1964) using x-ray diffraction analysis on several samples of Ordinary Portland cement are shown in Table 2.1.

Table 2.1: Main compounds of Ordinary Portland cement

(after Brunauer and Copeland 1964)

Name of compound	Oxide Composition	Proportion %
Tricalcium silicate	$3CaO.SiO_2$	53
Dicalcium silicate	$2CaO.SiO_2$	24
Tricalcium aluminate	$3CaO.Al_2O_3$	8
Tetracalcium aluminoferrite	$4CaO.Al_2O_3.Fe_2O_3$	8

The chemical composition of the Ordinary Portland cement used in the present work is given in Table 2.2.

The specification for Ordinary Portland cement is given in B.S.12: 1978. The limitations of chemical composition are: the lime saturation factor is to be not greater than 1.02 and not less than 0.66. The factor is defined as:

$$\frac{(CaO) - 0.7(SO_3)}{2.8(SiO_2) + 1.2(Al_2O_3) + 0.65(Fe_2O_3)}$$

where the symbols in brackets denote the percentage by weight of the given compound present in the cement.

Table 2.2: Chemical composition of Ordinary Portland cement used in present investigation.

Oxide	Content (weight) per cent
CaO	63.2
SiO_2	19.9
Al_2O_3	6.73
Fe_2O_3	2.2
MgO	1.3
K_2O	0.96
Na_2O	0.28
SO_3	3.00
Free lime	0.90

Further requirements of B.S.12: 1978 for the chemical composition of Ordinary Portland cement are that the magnesia content does not exceed 4.0 per cent and that the ratio Al_2O_3/Fe_2O_3 is not less than 0.66. In addition, the insoluble residue, determined by treating with hydrochloric acid,(a measure of the adulteration of the cement, largely arising from impurities in the gypsum) must not exceed 1.5 per cent and the loss on ignition must not exceed 3 per cent in temperate climates or 4 per cent in the tropics. The amount of gypsum added to cement clinker is usually expressed as the weight of SO_3 present, this is limited by B.S.12: 1978 to a maximum of 2.5 per cent when the C_3A content is not more than 7 per cent and 3.0 per cent when the amount of C_3A exceeds 7 per cent. Hence, the Ordinary Portland cement used in this work (Al_2O_3/Fe_2O_3 = 3.05; lime saturation factor = 0.9) was of good quality.

2.1.2 HYDRATION OF ORDINARY PORTLAND CEMENT

Many workers have investigated the hydration of ordinary Portland cement and the process is now well understood and documented (Lea, 1980; Taylor, 1964).

The main cementing components are the two calcium silicate phases, and the calcium aluminate and calcium aluminoferrite phases.

When cement is mixed with water, hydration reactions take place ultimately producing complex hydrates which may form a coherent solid structure and bind the inert components of the cementitious mixture.

During the first few minutes of hydration of Ordinary Portland cement, most of the CaO and $CaSO_4$ dissolve quickly until saturation occurs, and some $Ca(OH)_2$ may precipitate as hexagonal crystals. The $CaO:SiO_2$ ratio of the solid phase at lime solution near saturation is greater than 1.5:1 (Lea, 1980). In the later stages of hydration, $Ca(OH)_2$ and $CaSO_4$ attack silica, alumina and ferric oxide producing complex hydrated compounds such as calcium silicate hydrates, calcium aluminate hydrates, calcium sulpho-aluminate hydrates and calcium sulpho aluminoferrite hydrates. Some free $Ca(OH)_2$ will remain in the hydrated products (Copeland et al. 1964 and Taylor, 1964 , give fuller discussion).

The reactions and rate of reaction during the hydration of Ordinary Portland cement at ordinary temperature are represented schematically in Table 2.3.

2.1.3 PHYSICAL CHARACTERSITICS OF ORDINARY PORTLAND CEMENT

The physical properties of Ordinary Portland Cement used in the present work and obtained from the Association of Portland Cement Manufacturers Limited are given in Table 2.4. The accepted data for the particle size distribution of the cement used in the present work is given in Figure 2.1 (after Card 1981).

Table 2.3: Hydration of Ordinary Portland Cement (After Lea, 1980).

$2CaO.SiO_2$ (β-form) — I — SLOW → $2CaO.SiO_2.aq$

$3CaO.SiO_2$ — Ia — MODERATE → $3CaO.SiO_2.aq$

→ II

$Ca(OH)_2$ + calcium silicate hydrate gel ($CaO:SiO_2$, about 1.5) incorporating some Al_2O_3, Fe_2O_3 and SO_3

→ IIIa

$CaO-SiO_2-H_2O$ ($CaO:SiO_2$, 1.5-1.8) containing Al_2O_3

→ More crystalline product

$3CaO.Al_2O_3$ + $CaSO_4.2H_2O$

IV — immediate → Needles of $3CaO.Al_2O_3.3CaSO_4.aq$

→ Hexagonal plate solid solution $3CaO.Al_2O_3.Ca(SO_4, (OH)_2).aq$

$4CaO.Al_2O_3.Fe_2O_3$ + $CaSO_4.2H_2O$ + $Ca(OH)_2$

IVa — quick → Needles of solid solution $3CaO.(Al_2O_3, Fe_2O_3).3CaSO_4.aq$

V → Hexagonal plate solid solution $3CaO.(Al_2O_3, Fe_2O_3).CaSO_4.aq$

and/or $3CaO.(Al_2O_3, Fe_2O_3).Ca(SO_4,(OH)_2).aq$

→ VI

Hexagonal plate solid solution

$3CaO.(Al_2O_3, Fe_2O_3).Ca(SO_4, (OH)_2, SiO_3).aq$

and possibly

$4CaO.(Al_2O_3, Fe_2O_3).aq$

with also hydrogarnet phase containing alumina, ferric oxide and silica.

Table 2.4: Physical properties of Ordinary Portland cement used in the present investigation. B.S.12 Physical Test Results

Setting Times	
Water %	25.25
Initial (mins)	150
Final (mins)	175
Fineness	
Specific Surface (m^2/kg)	325
Specific Gravity	3.11
Expansion (mm)	Nil
Compressive Strength (MN/m^2)	
B.S.12 concrete 3 days	21.1
7 days	29.9
28 days	41.0

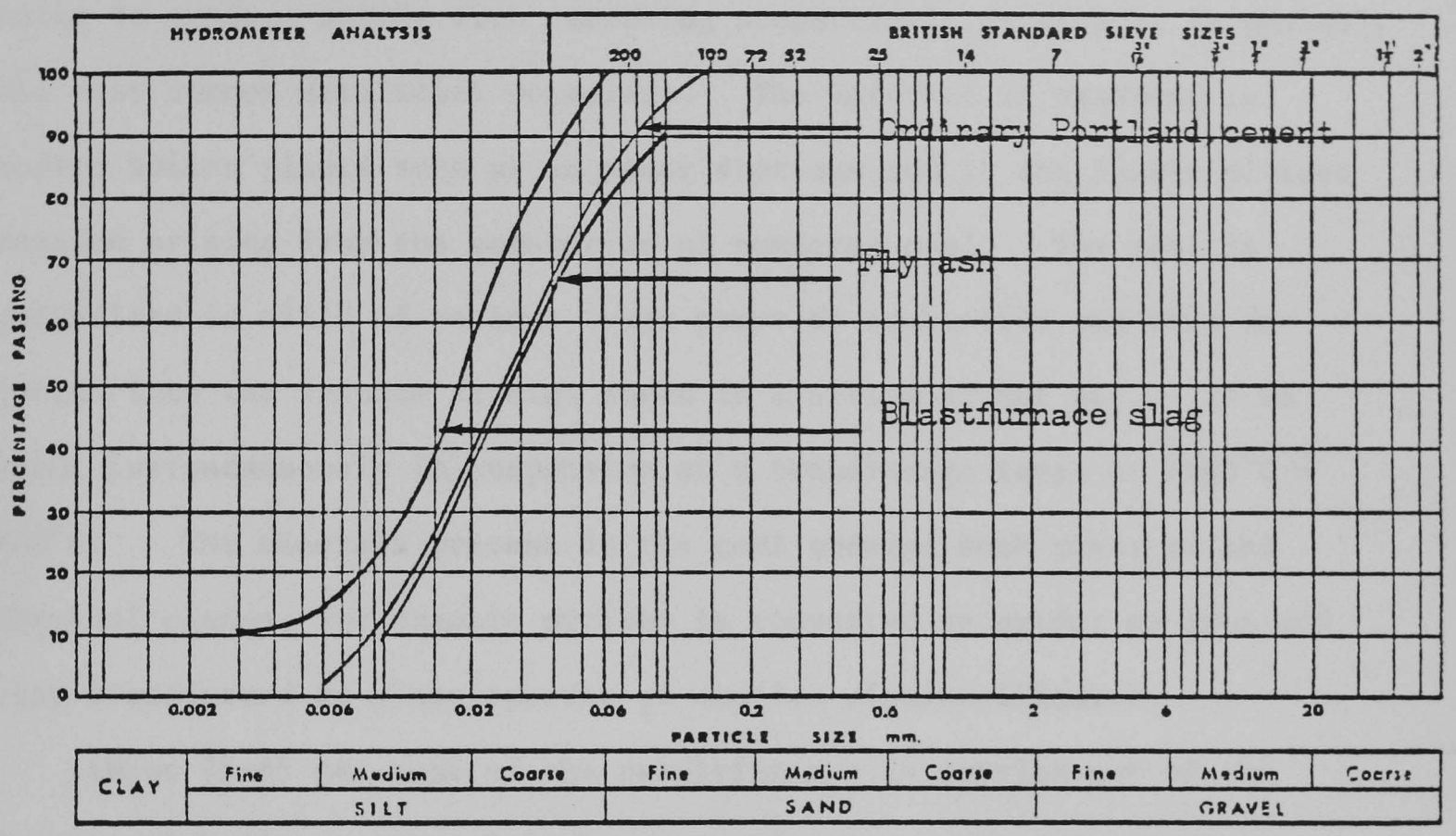

Figure 2.1 The particle size distribution of the cement used in the present investigation (after Guner, 1978 and Card, 1981).

2.2 FLY ASH

2.2.1 DEFINITION

Fly ash mixed with pure water shows no hydration products and virtually no cementing activity. However, it possesses the characteristics of a pozzolana (a substance which combines with lime in the presence of water to produce solids with cementing properties), as such it is probably the most common artificial pozzolana. The material is produced in modern boiler plants such as in power stations and is the finely divided residue arising from the combustion of powdered coal. The coal is pulverised in mills of various types prior to combustion and then injected into the furnace at high speed in a stream of hot air. It is burnt instantaneously in suspension at a temperature range of $1500^{o}C \pm 200^{o}C$. The minerals present in the coal undergo both physical and chemical change, for example pyrites is converted to oxides of iron and clay transformed to glass spheres of complex aluminosilicates.

About 75-85 per cent of the resulting ash is carried out of the furnace with flue gases and is known as Fly ash. The Fly ash is removed by a series of mechanical and electrostatic precipitators before the gas is discharged into the atmosphere. The remaining ash falls to the bottom of the furnace where it sinters to form a coarser material known as furnace bottom ash.

2.2.2 CHEMICAL COMPOSITION OF FLY ASH

The composition and properties of Fly ash depend both on the coal burnt and the efficiency of the combustion process so that the qualities of the material from different power stations or from the same station but at different times can vary widely. The composition of the ash approximates to that of a burnt clay and is high in alumina and iron oxide but can vary widely depending on the type of coal burnt and the

efficiency of the combustion process as illustrated by the data in Table 2.5. The major constituent, some 60 - 90 per cent, is a glass with quartz (SiO_2), mullite ($2SiO_2$, $3\ Al_2O_3$), haematite (Fe_2O_3) and magnetite (Fe_3O_4) as the more important crystalline components. A number of minor constituents including lime (CaO), anhydrite ($CaSO_4$) and gypsum ($CaSO_4.2H_2O$) have also been identified (Simons and Jeffery, 1960).

Table 2.5: Percentage composition of some artificial pozzolanas (Lea, 1980) and the Fly ash used in the present work

Pozzolana	SiO_2	Al_2O_3	Fe_2O_3	CaO	MgO	Na_2O+ K_2O	SO_3	Ignition loss
Burnt clay	58.2	18.4	9.3	3.3	3.9	3.9	1.1	1.6
Burnt clay	60.2	17.7	7.6	2.7	2.5	4.2	2.5	1.3
Spent oil shale	51.7	22.4	11.2	4.3	1.1	3.6	2.1	3.2
Raw gaize	79.6	7.1	3.2	2.4	1.0	-	0.9	5.9
Burnt gaize	88.0	6.4	3.3	1.2	0.8	-	trace	-
Raw moler	66.7	11.4	7.8	2.2	2.1	-	1.4	5.6
Burnt moler	70.7	12.1	8.2	2.3	2.2	-	1.5	-
Raw diatomite (U.S.A.)	86.0	2.3	1.8	trace	0.6	0.4	-	8.3
Burnt diatomite (U.S.A.)	69.7	14.7	8.1	1.5	2.2	3.2	-	0.4
Fly ash (U.S.A.)	47.1	18.2	19.2	7.0	1.1	3.95	2.8	1.2
Fly ash (U.S.A.)	44.8	18.4	11.2	11.6	1.1	3.14	2.0	7.5
Fly ash (Britain)	47.4	27.5	10.3	2.1	2.0	5.7	1.8	0.9
Fly ash (Britain)	45.9	24.4	12.3	3.6	2.5	4.2	0.9	4.1
Fly ash used in tne present work	49.9	28.0	10.1	1.7	1.8	5.1	0.35	2.8

The glass is the active material in Fly ash, the mineral consistuents being mainly inert. The value of the ash as a pozzolana depends therefore on its glass content, though fineness and composition are also important. However, there is no general correlation between these parameters and the ash's contribution to strength development. Increasing SiO_2, or SiO_2 + Al_2O_3 content seems to have a favourable influence on the pozzolanic value. There is a British standard (B.S. 3892:1965) for Fly ash which classifies the material into three fineness zones, 125-275, 275-425, and above 425 m^2/kg. This standard requires that the MgO content is limited to 4 per cent (the Fly ash used in this work had an MgO content of 1.8 per cent). The SO_3 content is limited to 2.5 per cent and the loss on ignition to 7 per cent. The A.S.T.M. specification (C618-78) requires a minimum specific surface of 6500 cm^2/cm^3 and limits the SO_3 content to 5 per cent and the loss on ignition to 12 per cent. The sum of SiO_2 + Al_2O_3 + Fe_2O_3 must be at least 70 per cent. For Fly ash used in this work the sum of SiO_2 + Al_2O_3 + Fe_2O_3 was equal to 88.0. On this basis the Fly ash used was of good quality. Fly ash used in this work was from Fiddlers Ferry source.

2.2.3 SPECIFICATION

Many developed countries have standard specifications for pozzolanas for use in concrete (Smith, 1975), and a good proportion of these standards recognise Fly ash as a useful artificial pozzolana.

Fly ashes often may be cheaper than the Ordinary Portland cement that they may be used to replace but their chief advantage lies in their slow hydration and, therefore, their low rate of heat

development. Other advantages are that addition of Fly ash may improve workability due to the rounded nature of the ash particles and also Fly ash may improve the durability of mixes. A.S.T.M. standard C595-79 describes a Portland-Pozzolana type cement as Type IP, and limits the Fly ash content to between 15 and 40 per cent of the weight of the mixture. In the present work between 5 and 80 per cent of Ordinary Portland cement was replaced by Fly ash.

Partial replacement of Ordinary Portland cement by Pozzolana has to be carefully defined because the specific gravity of Pozzolana is much lower than that of Ordinary Portland cement; for instance, the specific gravity of Fly ash may be 1.9 - 2.7 compared with typically 3.15 for Ordinary Portland cement. Thus replacement on a weight for weight basis results in a considerably greater volume of available cementitious material for a given weight of the mix. Because the continuing formation of hydrates fills the pores and also because of less free lime which could be leached out, partial replacement of Ordinary Portland cement by pozzolana reduces the permeability of paste (Higgison 1966 and Lea 1980). This lower permeability and lack of free lime improve the durability.

The hydration reaction for Fly ash is between the calcium hydroxide produced during Ordinary Portland cement hydration, and the alkali soluble silicates or "glass" content of the Fly Ash. The reaction mainly depends upon the hydration characteristics of the Ordinary Portland cement, its calcium hydroxide content, the temperature during the progress of reaction, the particle size, and the "glass" content of the Fly ash.

As hydration progresses, and this depends on the availability of water and the temperature at which the reaction takes place, the alkaline solution becomes progressively more concentrated, particularly as the hydration is a self-desiccating process. In general terms, the pozzolanic reaction is produced by this progressive concentration of the alkaline solution and the $Ca(OH)_2$ reacting with the "glass" content of the Fly ash to form more gel. Thus the smaller the particles and the greater the "glass" content of Fly ash, the greater will be the volume of gel produced, thereby transforming the weak and soluble $Ca(OH)_2$ into a gel product.

2.2.4 CHARACTERISTICS OF FLY ASH

2.2.4.1 COLOUR

Colour variations within and between different power stations can be from a light grey to black (Dunstan and Mitchell 1976). A method for assessing the colour variation of Fly ash has been developed by Spencer (Owens 1978) using the Munsell/Lovibond coding system.

The Fly ash used in the present work was light grey.

2.2.4.2 CHEMICAL COMPOSITION

In addition to methods of chemical analysis, the actual composition can be determined by microscopic examination of the powder and the identification of species by measurement of the refractive index. Polished and etched sections can also be studied both in reflected and transmitted light. Other methods include the use of X-ray powder diffraction to identify or study the structure of the crystalline

phases, and differential thermal analysis (Lea 1980).

Another development in the present work was the use of the electron microscope and electron probe microanalysis which allows estimation of the composition of the material under examination. This method was used, to estimate the elemental composition of cement pastes containing the various proportions of Fly ash used in the present work, and the results are shown in Table 2.6. The equipment was located at Birkbeck College.

Table 2.6: Elemental composition (% by weight) of cement pastes containing Fly ash.

Component element (*)	per cent Fly ash in mix		
	20	40	60
Si	22.6	31.0	38.0
Ca	60.0	50.0	36.0
Al	8.0	11.0	14.5
Fe	2.3	3.0	4.6
S	2.3	1.5	2.0
K	2.7	2.0	2.5
Mg	2.0	1.4	2.3

(*) only these elements were assumed to be present and figures have been adjusted to total, 100 per cent approximately.

2.2.4.3 PHYSICAL PROPERTIES

The particle size distribution of the Fly ash used is given in Figure 2.1.

Particle shape: Fly ash is a unique powder granulate because of the characteristic spherical shape of the majority of the particles. In the coarser fraction from 300 to 45 microns, most of the particles are porous and black (Owens 1979). Figure 2.2 shows an electron micrograph of a sample of the Fly ash used in this work.

Density: the density of Fly ash varies both with particle size (e.g. residue greater than 45 microns) and loss on ignition (Owens, 1979). The density of the Fly ash used was 2375 kg/m^3.

Figure 2.3 shows the compressive strength of cement pastes at 270 days of hydration prepared by the present investigator at a water/cement ratio of 0.4 as a function of the percentage (by weight) of the cement replaced by Fly ash. Each point represents the average of five results of compressive strength of cylindrical specimens 38.1 mm diameter 80 mm high, reproducibility better than $\pm$ 3 per cent.

This data is in good agreement with Neville (1981) and Lea (1980) and so the Fly ash replaced cement studied in the present investigation was quite normal. The reason for the falling of compressive strength for cement pastes containing more than 40 per cent Fly ash (at all ages) is that the Ordinary Portland cement cannot supply enough lime to allow all the Fly ash to become hydrated.

2.2.4.4 DURABILITY

Fly ash is often used as a pozzolana to improve durability (Lea, 1980); particularly where there are requirements for lower permeability (this will be discussed in more detail in Chapter Five of this work), greater sulphate and acid resistance or reduced alkali aggregate reaction (Lea, 1980).

Figure 2. 2 Representative micrograph of the pure Fly ash.

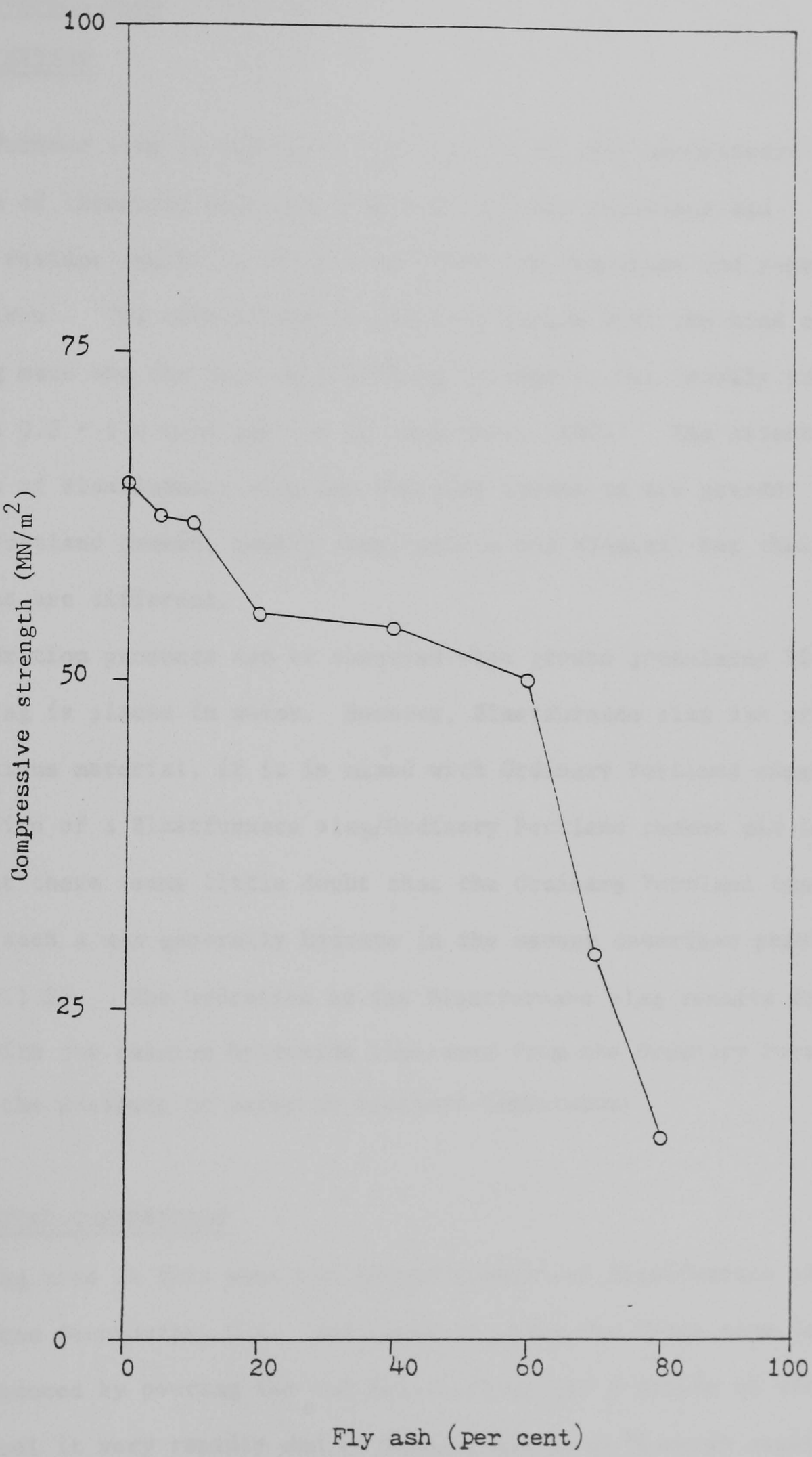

Figure 2.3 Effect of Fly ash replacement of cement on compressive strength of pastes at age 270 days (cured under water) 0.4 water/cement ratio .

2.3 BLASTFURNACE SLAG

2.3.1 DEFINITION

Blastfurnace slag is formed in the process of iron manufacture from the fusion of limestone with ash from coke and the siliceous and aluminous residue remaining in the ore after the reduction and separation of iron. The composition of the slag varies with the kind of iron being made and the type of ore being processed, but usually ranges from about 0.3 - 1.0 tons per ton of iron (Lea, 1980). The essential components of Blastfurnace slag are the same oxides as are present in Ordinary Portland cement, namely lime, silica and alumina, but their proportions are different.

No hydration products can be observed when ground granulated Blastfurnace slag is placed in water. However, Blastfurnace slag can produce a cementitious material, if it is mixed with Ordinary Portland cement. The hydration of a Blastfurnace slag/Ordinary Portland cement mix is complex but there seems little doubt that the Ordinary Portland cement grains in such a mix generally hydrate in the manner described previously (Section 2.1.2). The hydration of the Blastfurnace slag results from a reaction with the calcium hydroxide liberated from the Ordinary Portland cement in the presence of water at ordinary temperature.

2.3.2 CHEMICAL COMPOSITION

The slag used in this work was ground granulated Blastfurnace slag, obtained from Scunthorpe, U.K., and marketed under the trade name Cemsave. This is produced by pouring the hot molten slag into a stream of water so as to cool it very rapidly and is then ground to a fineness similar to that of Ordinary Portland Cement.

The probable assemblages of minerals formed by the four major constituents CaO, SiO_2, Al_2O_3 and MgO in the range of proportions characteristic of slags, cannot be predicted with certainty from phase equilibrium diagrams because the quaternary system has not yet been completely elucidated. Estimates which have been made are, however, in reasonably close agreement with the results of microscopic studies on thin sections, or polished and etched surfaces of slags (Nurse and Midgley 1951).

The composition of slags can vary over a wide range depending on the nature of the ore, the composition of the limestone flux, the coke consumption, and the kind of iron being made (Lee 1974). These variations affect the relative contents of the four major constituents and also the amounts of the minor components, sulphur in the form of sulphide, and ferrous and manganese oxides. The analysis of Blastfurnace slag used in the present work is given in Table 2.7.

Table 2.7: Chemical composition of Blastfurnace slag specified by Scunthorpe U.K. and used in the present investigation

Oxide	Content, (weight) per cent
SiO_2	33.41
Al_2O_3	14.62
CaO	42.80
MgO	5.00
FeO	0.49
SO_3	0.10
K_2O	0.85
Na_2O	0.41
Free lime	0.12

2.3.3 SPECIFICATION

There are various standards for Blastfurnace slag (Lea 1980).

I. DIN 1164 (German Standard): 1967 requires that

$$I = \frac{CaO + MgO + Al_2O_3}{SiO_2} \geq 1$$

II. The Keil index, Ik defined as:

$$Ik = \frac{CaO + CaS + 0.5MgO + Al_2O_3}{SiO_2 + MnO}$$

The Blastfurnace slag is said to be :

'usable' if $Ik \geq 1.5$

'good' if $1.5 < Ik < 1.9$

III. Langavant Index of quality, IL, defined as:

$$IL = 20 + CaO + Al_2O_3 + 0.5MgO - 2SiO_2$$

The quality is :

'inferior' if $IL < 12$

'very good' if $IL > 16$

The Blastfurnace slag used in the present work had values I = 1.87, Ik = 1.82 and IL = 13.1. On this scale of standards it is of good quality.

Standards also exist for Ordinary Portland cement and granulated Blastfurnace slag mixtures depending on the amount of granulated Blastfurnace slag present. Thus B.S. 146 : 1973 Ordinary Portland cement and granulated Blastfurnace slag mixtures, permits the proportion of Blastfurnace slag to be up to 65 per cent of the weight of the mixture. In the U.S.A.(A.S.T.M. C595-79), permits the granulated Blastfurnace slag content to be from 25 to 65 per cent. In Germany two varieties are specified (DIN 1164) namely, Eisenportland cement, containing not more than 40 per cent, and Hochofen cement, from 41 to 85 per cent granulated Blastfurnace slag. In France, Ciment de Fer contains 25 - 35 per cent granulated Blastfurnace slag, Ciment Metallurgique Mite 45 - 55 per cent, Ciment de Haut Fourneau, 65 - 75 per cent, and Ciment de Laitier au Clinker at least 80 per cent (Lea 1980). In the present work, between 20 and 97 per cent of Ordinary Portland cement was replaced by granulated Blastfurnace slag.

2.3.4 CHARACTERISTICS OF BLASTFURNACE SLAG

Slag may be regarded as a mixture of supercooled liquids. It is a characteristic feature of silicate melts that on rapid cooling from the liquid state they tend to form a glass. When a powdered granulated Blastfurnace slag is examined on a microscope slide by transmitted light, the glass is seen to consist of clear isotropic transparent grains (Lea 1980). Figure 2.4 shows an electron micrograph of the Blastfurnace slag used in the present work.

Less perfectly granulated Blastfurnace slags may show brown or black zones of incipient crystallisation or even birefringent

crystalline areas under polarised light (Lee, 1974). The Blastfurnace slag used in the present work was of dove white colour.

Electron probe microanalysis was used to estimate the elemental composition of cement pastes containing varying proportions of the Blastfurnace slag and is shown in Table 2.8.

Table 2.8: Elemental compositions (% by weight) of cement pastes containing Blastfurnace slag used in the present investigation.

Component element (*)	per cent of Blastfurnace slag in mix			
	70	80	95	97
Si	25.0	26.6	31.5	32.2
Ca	57.3	52.9	43.4	41.3
Al	6.6	10.7	12.0	12.6
Fe	1.4	1.7	0.4	0.2
S	0.6	2.1	2.3	2.4
K	2.1	0.6	0.9	0.4
Mg	6.9	5.3	9.4	10.8

(*) Only these elements have been assumed to be present and figures have been adjusted to total, 100 per cent approximately.

The particle size distribution of the Blastfurnace slag supplied by the manufacturer likewise is given in Figure 2.1.

Figure 2.5 shows the compressive strengths of cement pastes prepared at a water/cement ratio 0.4 as function of the percentage of cement replaced by Blastfurnace slag (by weight). As for the Fly ash results represented in Figure 2.3 the plotted points are average of five determination. For replacement levels of Ordinary Portland cement by Blastfurnace slag of less than 20 per cent, there is little effect in the compressive strength. Above 10 per cent the compressive strength increases gradually with increasing Blastfurnace slag replacement up to 70 per cent. Above 80 per cent the compressive strength decreases sharply with increasing Blastfurnace slag replacement. Such a result is to be expected on the basis of Lea (1980).

Density: the density of Blastfurnace slag used in this work was 2900 kg/m^3.

Figure 2.4 Representative micrograph of pure Blastfurnace slag.

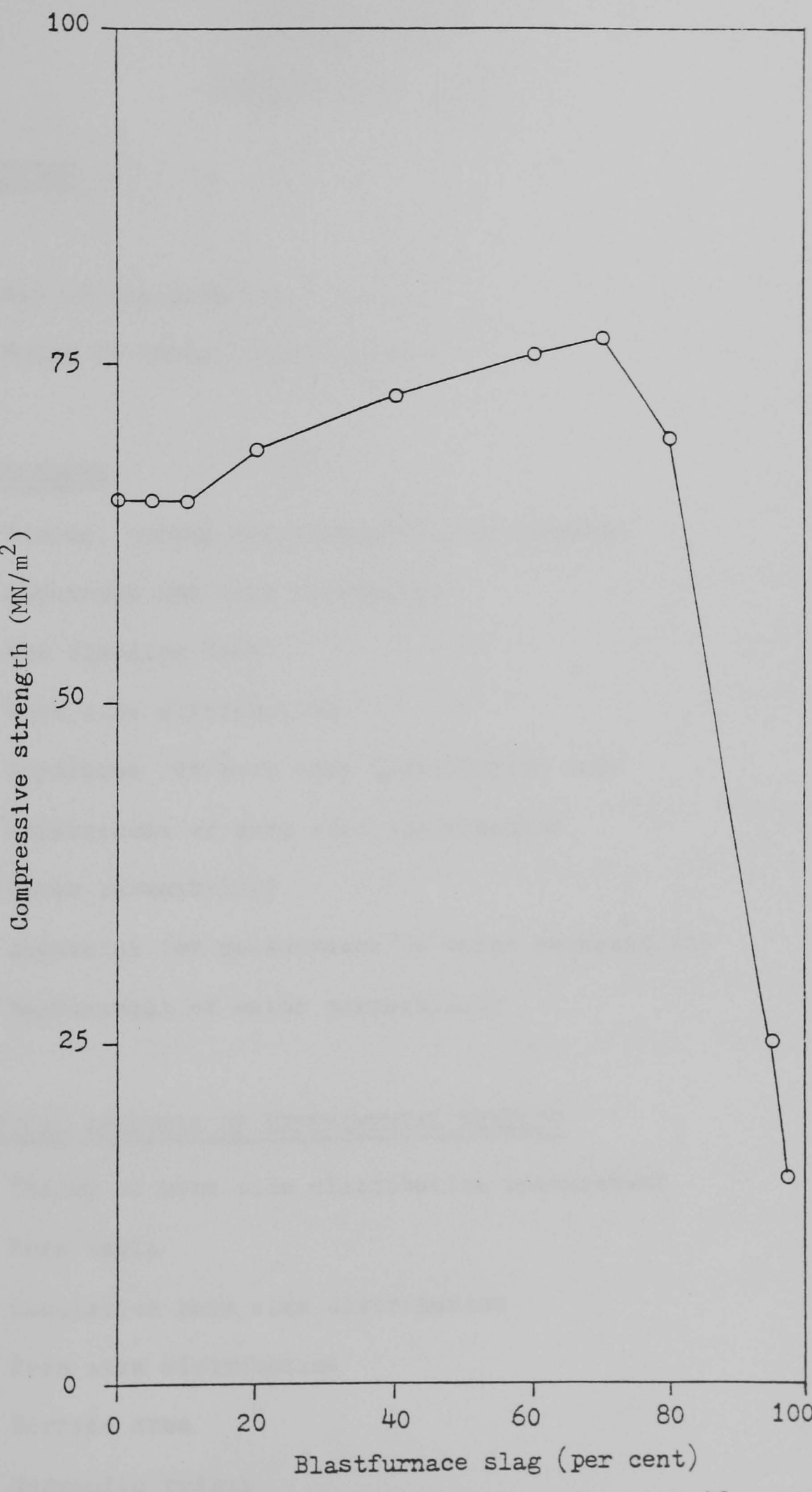

Figure 2.5 Effect of Blastfurnace slag replacement Of cement on compressive strength of pastes at age 270 days (cured under water). 0.4 water/cement ratio .

CHAPTER THREE

EXPERIMENTAL WORK

3.1 INTRODUCTION

3.1.1. Aim of the Experimental work

3.1.2. Range of cement pastes tested

3.2 TEST PROCEDURE

3.2.1 Mixing, curing and preparation of samples

3.2.2 Apparatus and test procedures

3.2.2.1 The Bleeding Test

3.2.2.2 Pore size distribution

3.2.2.2.1 Apparatus for pore size distribution test

3.2.2.2.2 Measurement of pore size distribution

3.2.2.3 Water permeability

3.2.2.3.1 Apparatus for measurement of water permeability

3.2.2.3.2 Measurement of water permeability

3.3 THEORETICAL ANALYSIS OF EXPERIMENTAL RESULTS

3.3.1 Theory of pore size distribution measurement

3.3.1.1 Pore radii

3.3.1.2 Cumulative pore size distribution

3.3.1.3 Pore size distribution

3.3.1.4 Surface area

3.3.1.5 Hydraulic radius

3.3.1.6 Pore surface distribution

3.3.1.7 Total porosity

3.3.2 Theory of flow in porous solids

CHAPTER THREE

EXPERIMENTAL WORK

3.1 INTRODUCTION

3.1.1 AIM OF THE EXPERIMENTAL WORK

The aim of the experimental work was to investigate the effects of varying proportions of Fly ash or Blastfurnace slag replacement of Ordinary Portland cement on total pore volume, pore size distribution and permeability of the resulting pastes.

As discussed in Chapter 1 (Section 1.3) it has been essential to monitor the bleeding characteristics, in order to avoid channel formation and to reach the important decision of employing 0.3 and 0.4 water/cement ratios. Otherwise the porosity could have been seriously affected. The details of the apparatus are given in this chapter.

For the composition and characteristics of the original material (Ordinary Portland cement, Fly ash and Blastfurnace slag) refer to Chapter 2.

Compressive strengtn tests, already discussed in Chapter 2 have been included to ensure comparability between the cement pastes tested in the present investigation and those of other investigations.

Porosity and permeability properties like other properties of cement are affected by the age of samples which implies a considerable amount of data a large proportion of which has been reserved for Chapter 4 or included in Appendix 3.

3.1.2 RANGE OF CEMENT PASTES TESTED

Cement pastes prepared at water/cement ratios of 0.3 and 0.4 with 5-80 per cent Fly ash replacement or 20-97 per cent Blastfurnace slag replacement were tested at ages between 3 and 560 days from mixing.

3.2 TEST PROCEDURE

3.2.1 MIXING, CURING AND PREPARATION OF SAMPLES

Batches of cement paste were mixed and cast at room temperature. A standard amount, 3 kg of cement (Ordinary Portland cement plus Fly ash or Blastfurnace slag) and the required amount of deaired deionized water were weighed to an accuracy of 0.1g. The dry cement powder (Ordinary Portland cement plus Fly ash or Blastfurnace slag) was then mixed in a Hobart AE125 mixer for a standard time of 10 minutes. Water was then added and the standard procedure adopted for all batches was to mix for a further 4 minutes, and then remix the paste after 1 minute to prevent false set.

The mixture was cast into the moulds in two layers whilst they were gently vibrated on a vibrator to allow any trapped air to escape. The period of vibration was standardised as 5 minutes after the mould had been completely filled. Ten specimens were cast from each batch. The moulds was covered with damp paper and kept in high humidity room. The samples were demoulded 24 hours after casting. To facilitate demoulding, the inner surfaces of the moulds were lightly oiled prior to casting. The specimens were then stored under deionised water in sealed boxes or bottles until required for testing.

Samples for pore size distribution and steady state water permeability measurements were cut from the specimens, using a diamond saw. The samples were kept wet throughout the cutting process, by dripping water from a reservoir onto the specimen. The top 20mm of each specimen was discarded and a middle portion 15mm thick was used for the measurements.

The samples tested to determine the total porosities were broken into fragments of approximately 1 gram with sharp hammer. The fragments were surface dried with damp tissue paper, weighed to an accuracy of 0.01g and dried in an oven 105^{o}C. The samples were dried

to constant weight which normally took at least 3 days. The dry densities of the samples were determined from the apparent volume measured (to an accuracy of 0.1 c.c.) using the mercury displacement volumeter.

For the pore size distribution measurements, a portion of the oven dry sample was broken into fragments. A fragment weighing between 0.5-1.0g was selected and weighed to an accuracy of 0.01g and then tested with Carlo Erba 200 mercury intrusion porosimeter.

The compressive strength tests were carried out on 38.1 mm diameter 80mm high specimens obtained from the water cured samples by cutting off the top 20mm with a diamond saw. An INSTRON 1195 testing machine was used for these tests.

3.2.2 APPARATUS AND TEST PROCEDURES

3.2.2.1 THE BLEEDING TEST

The subsidence of the surface of the solids of the setting cement paste was measured using a float which was seated on the subsiding solids surface. The movement of the float was followed using a cathometer and/or a non contacting displacement transducer. The apparatus shown in Figure 3.1 was designed and built in King's College for Jefferis, 1972. The cement paste was poured into the 125mm diameter container of the bleeding apparatus and was trimmed with a straight edge to obtain a level surface. The surface was then flooded with a 10mm layer of water and the float was lowered onto the solids surface. The first reading was taken 2 minutes after the cement paste was placed.

The bleeding apparatus was placed on a horizontal shelf fixed to a solid wall in order to minimise the effects of vibration.

The output from the displacement transducer could be automatically recorded and the surface settlement could be followed to a precision of $\pm$ 10 microns.

The results obtained with this equipment have been given in Section 1.3 of this thesis.

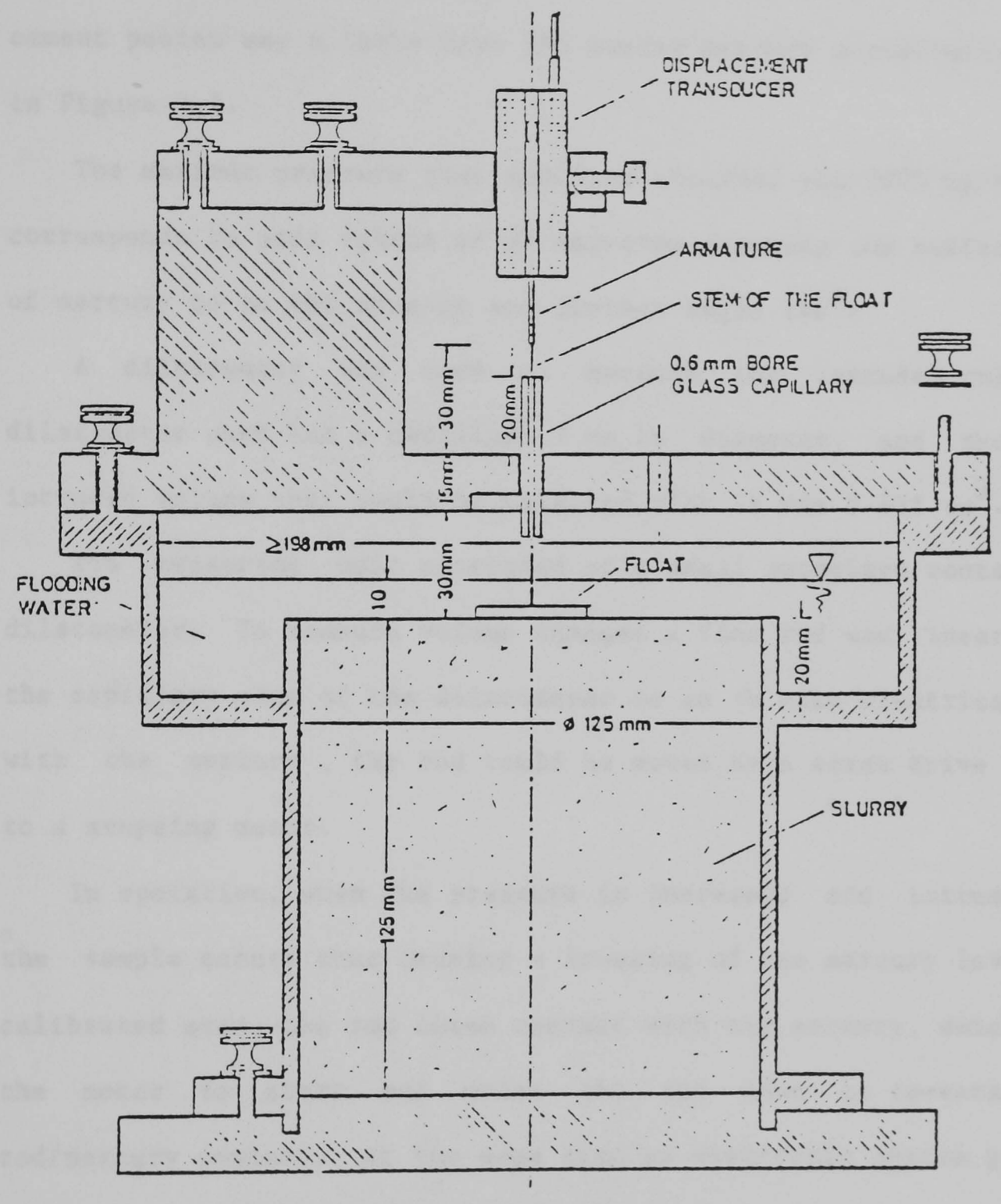

Figure 3.1 The apparatus for the measurement of Bleeding (after Guner, 1978)

3.2.2.2 PORE SIZE DISTRIBUTION

3.2.2.2.1 APPARATUS FOR PORE SIZE DISTRIBUTION TEST

The instrument used to measure the pore size distribution of the cement pastes was a Carlo Erba 200 series mercury porosimeter as shown in Figure 3.2.

The maximum pressure that could be obtained was 2000 kg/cm^2. This corresponds to pore radius of 37 Angstrom assuming the surface tension of mercury to be 480 dyne/cm and contact angle 140^o.

A dilatometer was used to measure the intruded volume. The dilatometer used had a capillary 3 mm in diameter, and the maximum intruded volume that could be measured with it was 0.665 cm^3.

The measuring unit consisted of a small autoclave containing the dilatometer. To measure volume changes a fine rod was inserted into the capillary stem of the dilatometer so as to make electrical contact with the mercury , the rod could be moved by a screw drive connected to a stepping motor.

In operation, when the pressure is increased and intrusion into the sample occurs thus causing a lowering of the mercury level in the calibrated stem, the rod loses contact with the mercury, which causes the motor to start and drive the rod down to re-establish the rod/mercury contact. At the same time an electronic system provides a signal for external recording. The necessary pressure is produced by a pressure multiplier consisting of a differential system with two pistons, a low and a high pressure piston with an area ratio of 100:1 (Figure 3.3). The low pressure piston is actuated by oil, drawn from a reservoir by means of a low pressure pump. The high pressure piston

transfers the pressure to the mercury by means of alcohol as an intermediate fluid.

The instrument is also equipped with two independent safety devices. (i) A pressure indicator stops the pump when the oil pressure rises above a preset pressure value and (ii) an electric contact stops the motor when the mercury level in the dilatometer drops below the maximum displacement of the rod.

The output from the instrument is fed to an electronic chart recorder, which effectively records the mercury level as a function of the pressure in the system.

3.2.2.2.2 MEASUREMENT OF PORE SIZE DISTRIBUTION

For the measurements of the pore size distribution of the cement paste, a weighed fragment from the oven dry sample (see Section 3.2.1) was placed in the dilatometer, mounted on the filling device (a special piece of apparatus used to de-gas the sample and fill the dilatometer with mercury) and evacuated for a minimum of 30 minutes using a Speedivac single stage high vacuum pump (or less than 10^{-2} torr). At the conclusion of the evacuation, the dilatometer was filled with mercury while under vacuum. It was found that air bubbles trapped in the tube linking the mercury reservoir to the dilatometer tended to be drawn by suction into the dilatometer at the initial stage of opening the mercury release valve on the filling device. To overcome this source of error, it was necessary to admit the mercury into the dilatometer in two stages. First, a few drops of mercury were admitted into the dilatometer until a slight kick of the pointer of the vacuum gauge could be observed, which indicated the release of the trapped air into the dilatometer.

The mercury release valve was then closed and the dilatometer evacuated for a further five minutes before the final filling was done. The dilatometer was then placed in the autoclave of the porosimeter, the system assembled filled with alcohol and sealed for the start of the run.

The digital voltmeter (used to indicate the volume of the mercury which penetrates the pores of the sample as a function of pressure) on the instrument and the strip chart recorder were zeroed and calibrated to read an appropriate maximum volume and the full scale pressure of 2000 kg/cm^2 before each run. Once a run was started the printing and plotting of the pressure-volume data were automatic and each run took approximately 90 minutes to complete depending on the porosity of the sample and the delay timer setting (this timer set the interval between the steps in which the pressure was increased).

It was necessary to correct the results for the compressibility of the mercury and the system. A blank run performed without a sample in the 3mm bore dilatometer showed that the change in volume of the mercury and the system reached 0.0339 cm^3 (average of four separate tests) at 2000 kg/cm^2 as shown in Figure 3.4.

Cement pastes are also compressible and a correction should be made for this. However, as there is no accepted way at present of ascertaining the absolute compressibility of the solid part of cement paste no correction could be made. Winslow and Diamond (1970) stated that typical values of the compressibilities of most reasonably strong solids would suggest that the volume change from 0 to 1000 kg/cm^2 would be in fact negligible in comparison with the volume of mercury intruded into cement paste.

For the analysis, the total volume of mercury intruded was divided into 36 intervals corresponding to particular fixed pressures. This method of analysis enables a good resolution of the differential pore size distributions to be obtained at the pore sizes at which substantial amounts of mercury flow into the samples.

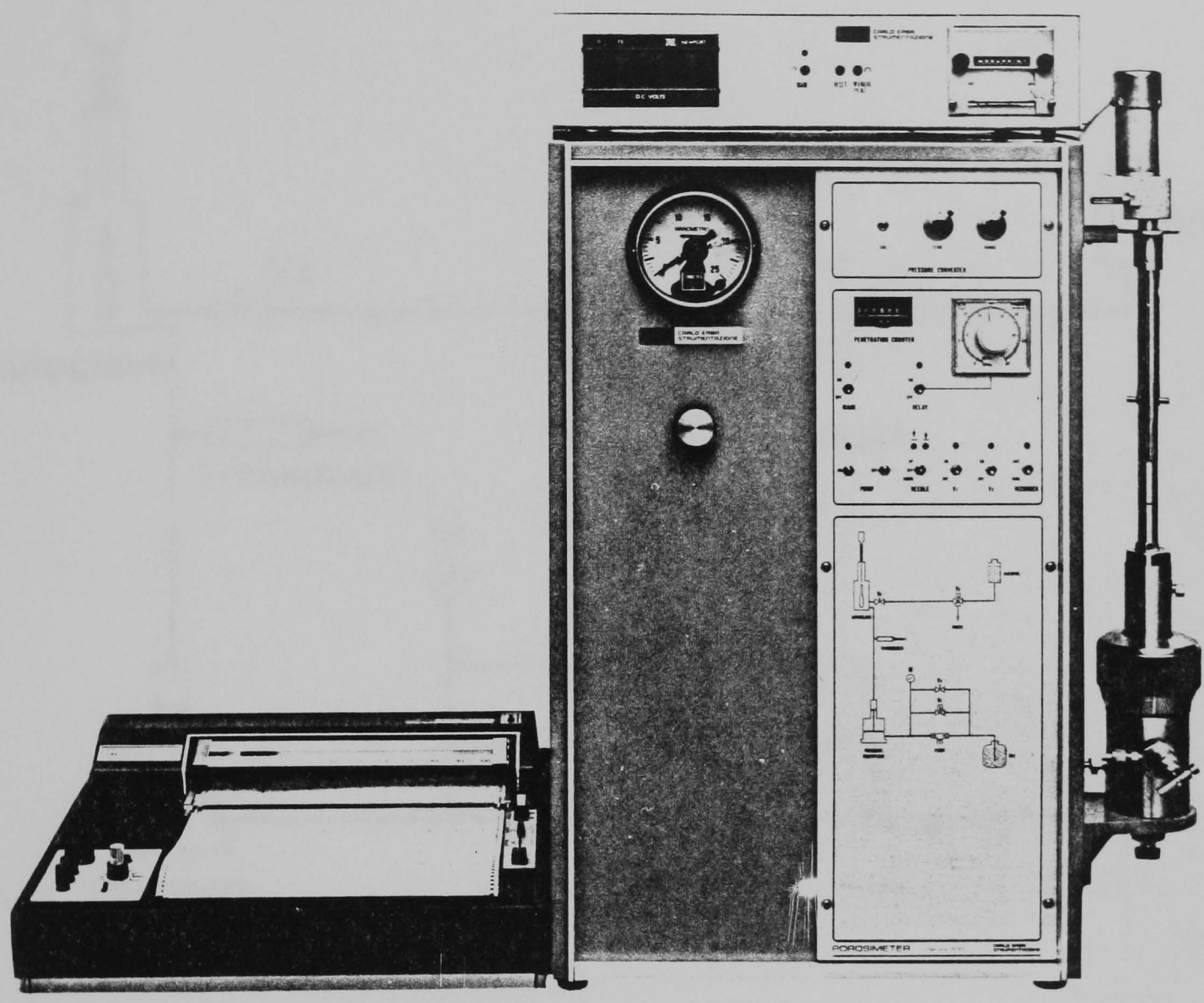

Figure 3.2 Carlo Erba 200 series mercury porosimeter

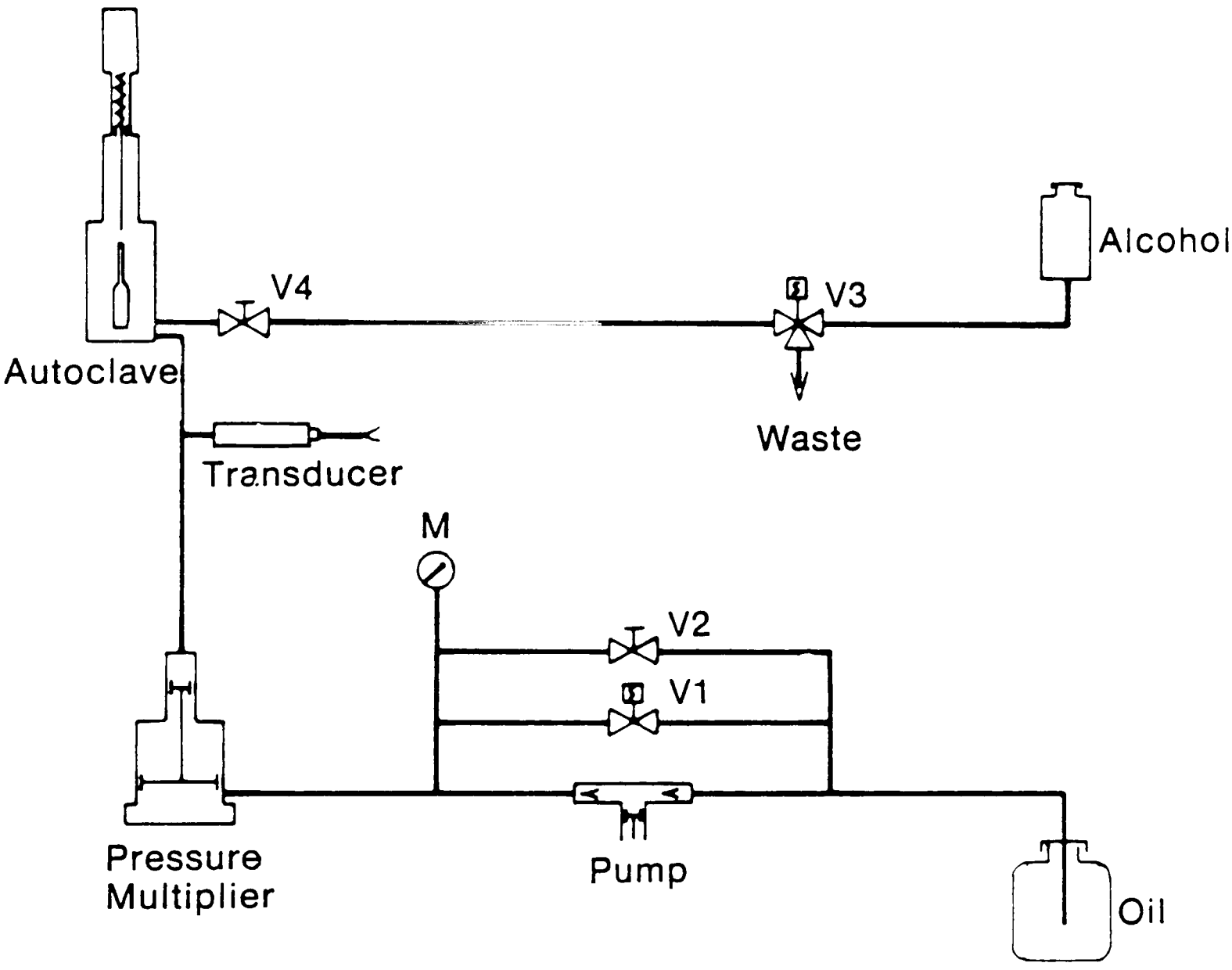

Figure 3.3 Measuring device.

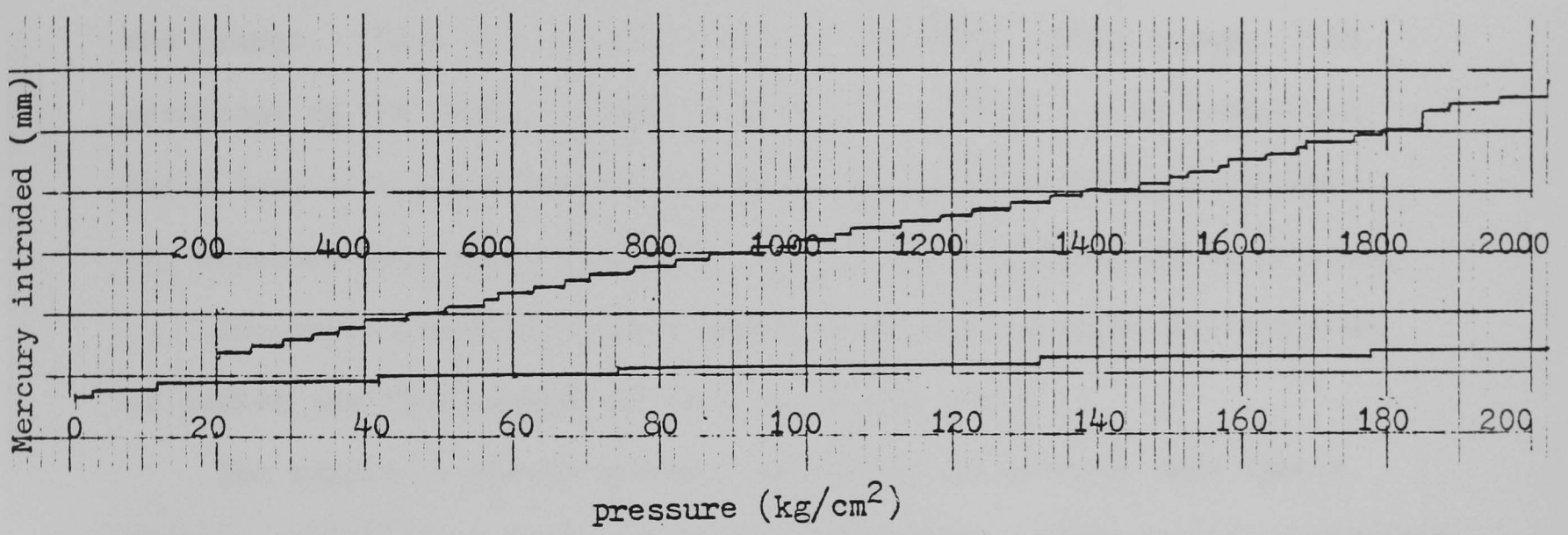

Figure 3.4 Data from a blank run with no sample to investigate the compressibility of the mercury and system.

3.2.2.3 WATER PERMEABILITY

3.2.2.3.1 APPARATUS FOR MEASUREMENT OF WATER PERMEABILITY

The permeameters for this work had to be specially designed as no suitable commercial instruments were available which could cope with the very small permeability of cement paste. The design drawing of the permeameters used are given in Figure 3.5.

The basic cell comprises a brass cylindrical body and two brass end plates. Each cell is fitted with a Urethane rubber jacket. An advantage of the jacket design is that the membrane can be reused and has a long life under operating conditions also the Urethane jackets are standard laboratory equipment used in the triaxial testing of rock.

The brass end plates are clamped on by six tie bars, and the ends of jacket are thus clamped to the top of the cell.

The sample is placed between two porous end platens made from a mortar containing a single sized fine aggregate. When testing a specimen of cement paste for water permeability, it is important to eliminate leakage past the wall of the specimen by applying a sufficiently high confining pressure to the membrane to seal it to the wall of the specimen. To prevent damage of the Urethane membrane, it is essential to ensure the total length of inserted sample is the same as the length of the membrane. Any small gap can result in the membrane tearing due to high pressures with contamination of the system by mercury and hydraulic oil which is extremely inconvenient.

Before assembling the thirteen cells (five cells for 38.1mm diameter specimens and eight for 60.81mm) that were required for the full test programme one cell was made up as a prototype. The cell was connected to a standard laboratory pressure control panel as shown in Figure 3.6 and the flow from the sample monitored with a commercial Kerosene/water volume change gauge as shown in Figure 3.7.

For the first test a 38.1 solid steel cylinder was tested in the cell with deaired deionised water at permeation pressures of 310, 410, and 620 kN/m^2 with a back pressure 100 kN/m^2 and a series of confining pressures. At confining pressures of 930 kN/m^2 and above no flow was measured and it was concluded that a pressure of at least this magnitude would be required to prevent leakage at the wall of the sample when testing the cement pastes.

A general view of the permeameters and flow control system is shown in Figures 3.8 and 3.9. Because of the very sensitive volume measurements that were to be made the apparatus was installed in a temperature controlled room set at 20°C. All pressures are gauge pressures above atmospheric.

3.2.2.3.2 MEASUREMENT OF WATER PERMEABILITY

For the measurements of the water permeability of the cement pastes, saturated samples 15 mm thick were placed in the permeability cells.

To make a permeability test, the system was first emptied of all water by opening all outlet valves. A vacuum was then applied to the vacuum connection and the entire system was subjected to vaccum for 8 hours using a Speedivac single stage high vacuum pump. When the system was exhausted the vacuum connection valve was closed, and the system was filled with deaired deionized water. The constant hydrostatic pressure was then applied, 410 kN/m^2 as loading pressure and 100 kN/m^2 as back pressure. The back pressure was used to minimize the effect of any trapped air bubbles. The tests were usually continued until the inflow and outflow were approximatly equal. During the period of observation the rate of flow was measured for at least two weeks with 4-5 readings made during this period.

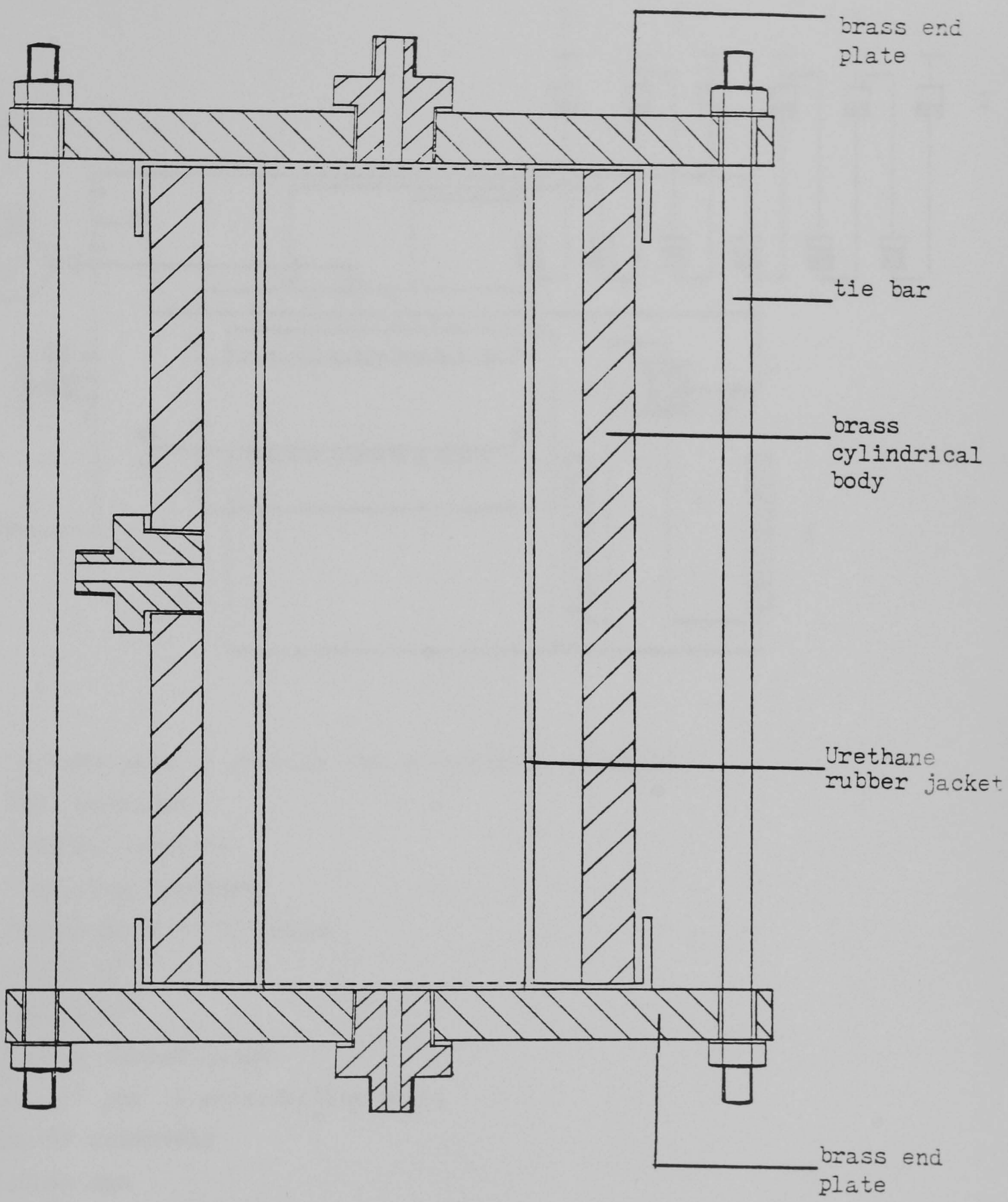

Figure 3.5 Diagram of the permeameter

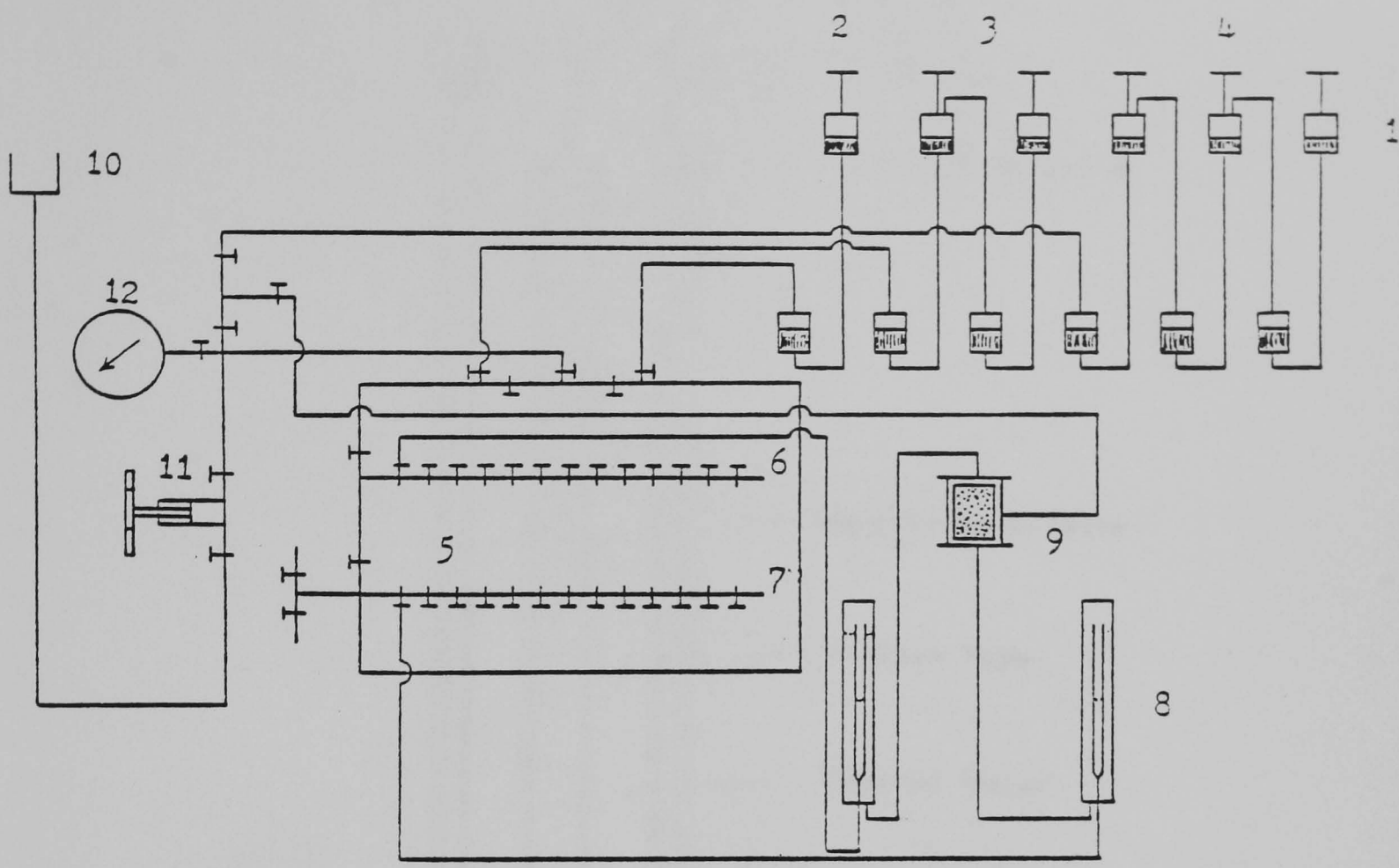

1. Mercury pots to provide the hydrostatic pressure
2. Back pressure
3. Loading pressure
4. Confining pressure
5. Connections to 13 cells
6. 410 kN/m^2
7. 100 kN/m^2
8. Volume change gauge
9. One of the 13 permeability cells
10. Water reservoir
11. Screw ram
12. pressure gauge

Figure 3.6 Central pressure control panel.

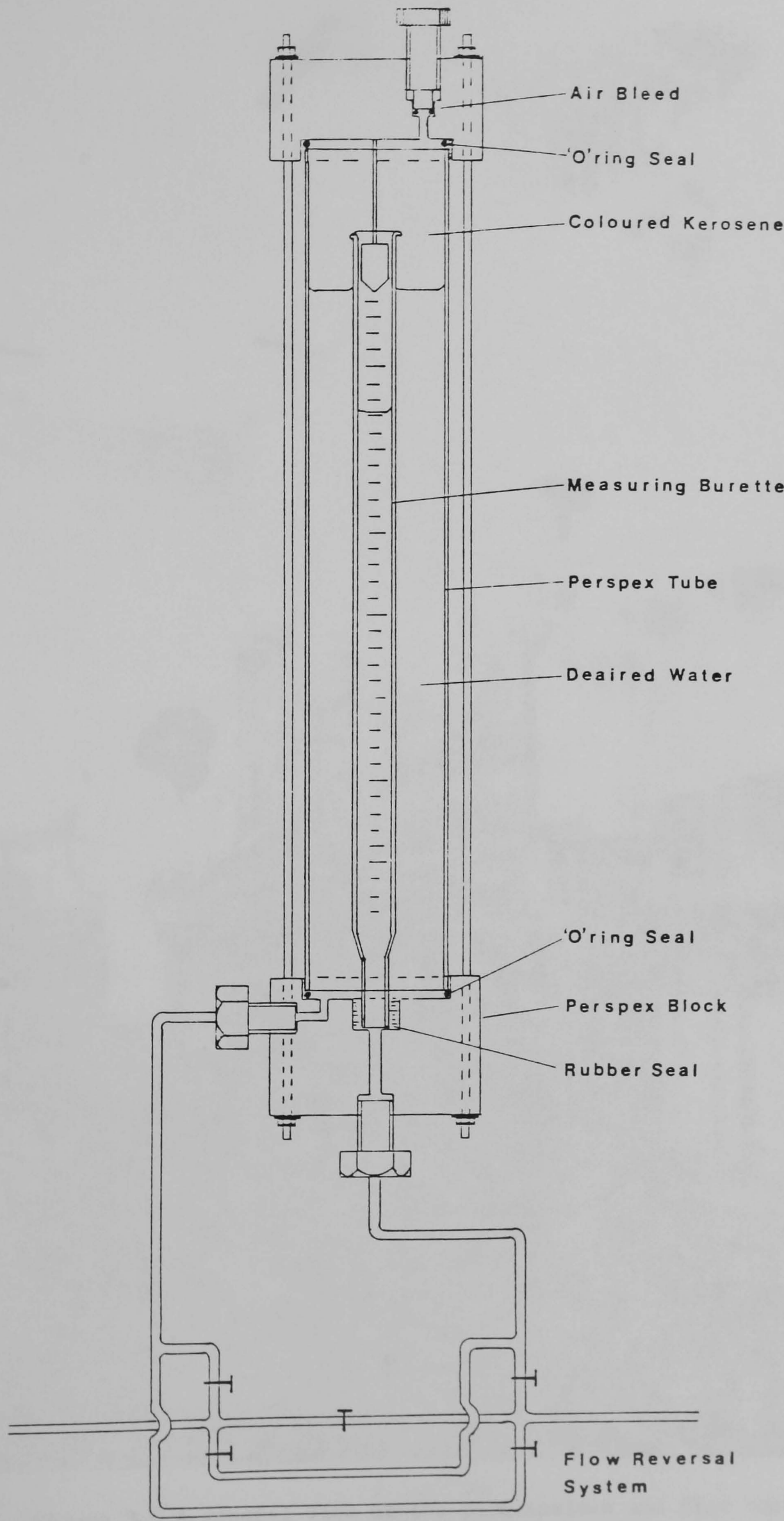

Figure 3.7 Diagram of the Kerosene/Water volume change gauge.

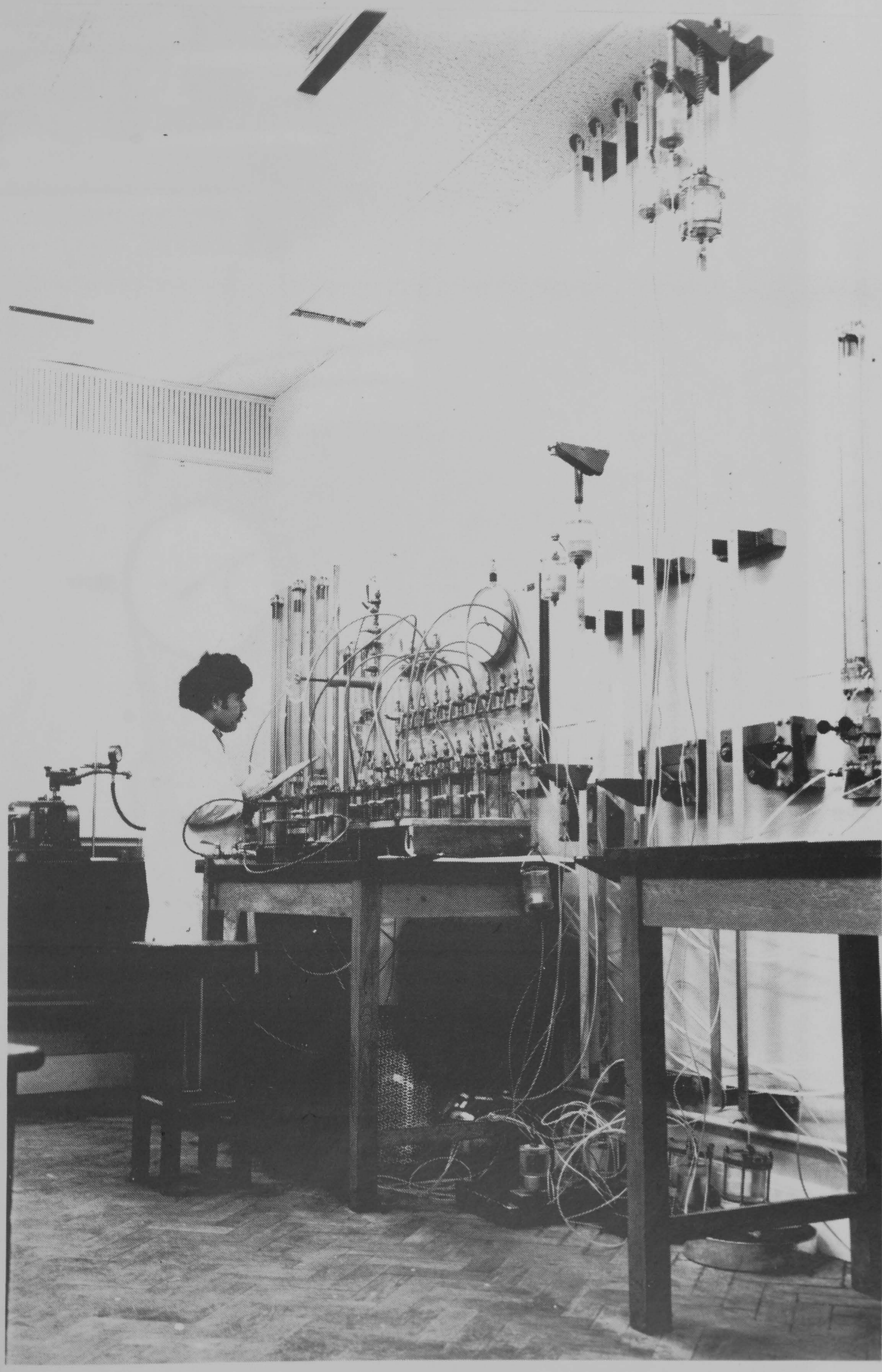

Figure 3.8 A general view of the permeameters and flow control system.

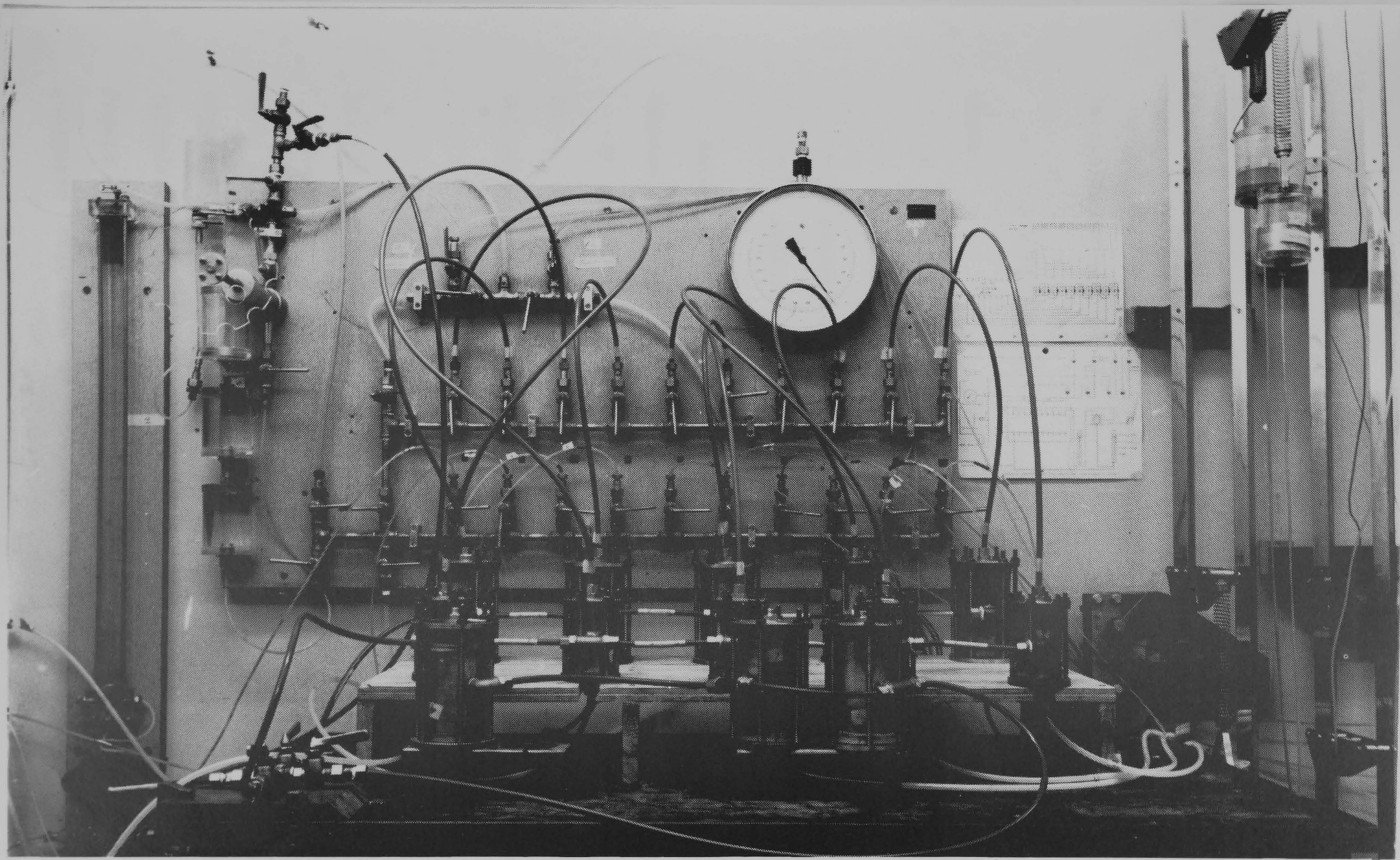

Figure 3.9 A general view of the permeameters and flow control system.

3.3 THEORETICAL ANALYSIS OF EXPERIMENTAL RESULTS

3.3.1 THEORY OF PORE SIZE DISTRIBUTION MEASUREMENT

3.3.1.1 PORE RADII

The principle of the measurement of pore radii by mercury intrusion is based on the Washburn equation:

$$r = -2\gamma \cos \theta / P \qquad (3.1)$$

where

r = pore radius

γ = surface tension of mercury

θ = contact angle between the mercury and the wall of pore

P = applied pressure.

Reported values of the contact angle and the mercury surface tension are given in Section 1.2.2.1.

If the applied pressure is P (kg/cm^2) and the radius of the pore is r in Angstrom then assuming the mercury surface tension to be 480 dyne/cm and the contact angle to be 140°, it can be shown that:

$$r = 75000/P \qquad (3.2)$$

3.3.1.2 CUMULATIVE PORE SIZE DISTRIBUTION

The total intruded pore volume that can be measured with the Carlo Erba 200 system is that at 2000 kg/cm^2, the maximum applied pressure. For analysis this total volume of mercury intruded after correction for the compressibility of mercury (using the data in Figure 3.4) was divided into 36 volumes at a series of standard pressures suggested by Midgley, 1979. This range of pressure was

selected to enable good resolution of the pressure-volume data when determining the pore size distribution of typical cement pastes.

The cumulative pore size distribution is the sum of all volumes intruded at pressures up to a given pressure. The volume intruded at the maximum pressure of the instrument is referred to as the total intruded pore volume. For convenience the cumulative pore size distribution is generally plotted as a function of log r.

Typical plots of pressure-volume data are given in Figures 3.10 and 3.11. These were obtained directly from the strip chart recorder. The vertical axis represents the volume penetrated and the horizontal axis, the pressure at which penetration occurs. The pressure scales have two ranges; 0-200 kg/cm^2 on the lower portion of the plot and 200-2000 kg/cm^2 on the upper portion of the plot.

A typical plot of a cumulative pore size distribution is given in Figures 3.12 and 3.13. The summation to give the cumulative volume is logically carried out from the largest radius (intruded under the least pressure), downward to the smallest that can be intruded. The minimum size is set by the maximum pressure capacity of the instrument. The volumes are usually expressed as volumes per gram of dry material tested. In order to convert the experimental data to a suitable form, each cumulative intruded volume measurement was divided by the total intruded pore volume of the sample concerned. The data is thus expressed as the percentage cumulative pore size distribution, normalized to 100 percent of the volume present.

3.3.1.3 PORE SIZE DISTRIBUTION

Ritter and Dark 1945 and Orr 1970, plotted the pore size

distribution function given below:

$$Dv(r) = dV/dr \qquad (3.3)$$

where

The total volume of all pores having radii between r and r+dr is dV, and Dv(r) is volume pore size distribution function defined as the pore volume per unit interval of radius.

Differentiation of Equation 3.1, assuming constant γ and θ gives :

$$Pdr + rdP = 0 \qquad (3.4)$$

Eliminating r and dr from Equation 3.1, 3.3 and 3.4 gives

$$dV = Dv(r) \frac{2\gamma\cos\theta}{P^2} \cdot dP \qquad (3.5)$$

$$dV = -Dv(r) \frac{r}{P} dP \qquad (3.6)$$

$$\text{Then} \quad Dv(r) = \frac{-P}{r} \cdot \frac{dV}{dP} \qquad (3.7)$$

In the experimental data, the total volume measured by the dilatometer is the total intruded pore volume Vt which must be corrected for the compressibility of the mercury and the system Vc. Equation 3.7 may then be rewritten in the form

$$Dv(r) = \frac{-P}{r} \cdot \frac{d(Vt-Vc)}{dP} = \frac{d(Vt-Vc)}{dr} \qquad (3.8)$$

Because there is a wide range of pore sizes in cement paste, it is convenient to plot the distributions on logarithmic pore radius basis (logarithms to base 10 are the most convenient for data presentation),

hence the volume pore size distribution function must be transformed from an equal radius basis to an equal logarithmic pore radius. Using the identity

$$d \log r = 2.303 \; dr/r \qquad (3.9)$$

d(Vt-Vc)/dr can be transformed to d(Vt-Vc)/dlogr by multiplying Equation 3.8 by r/2.303.

Hence

$$Dv(r) \frac{r}{2.303} = Dv^{*}(r) = \frac{r}{2.303} \cdot \frac{d(Vt-Vc)}{dr} = \frac{d(Vt-Vc)}{d\log r} \qquad (3.10)$$

Plotting $Dv^{*}(r)$ against a logarithmic scale of r gives the required pore size distribution. It is, however, somewhat tedious to obtain the pore size distribution function curve, and the precise shape of the curve will depend upon the interval between slope measurements. Also, it is not readily possible from the distribution curve to estimate the pore volume in any range of pore sizes (Auskern and Horn 1973).

3.3.1.4 SURFACE AREA

Orr 1970 and Rootare 1966, used the mercury porosimetry for surface area determination.

The surface area of all pores and voids filled up to pressure P is calculated using Equation 3.1 as follows.

$$-2\gamma \cos\theta = Pr$$

Hence $$-2\pi rL\gamma \cos\theta = P\Delta V \qquad (3.11)$$

assumming that the pores are open ended cylinders of radius r and length L so that $\Delta V = \pi r^2 L$ and the pore surface area S is $2\pi rL$ gives:

$$S\gamma\cos\theta = -P\Delta V \qquad (3.12)$$

Then the area, dS of pores in the range r to r+dr which have volume dV is given by

$$dS = -\frac{PdV}{\gamma\cos\theta} \qquad (3.13)$$

The area of pores filled up to radius r is given by integration of Equation 3.13 which gives

$$S = -\frac{1}{\gamma\cos\theta}\int_0^V P\,dV \qquad (3.14)$$

assuming constant surface tension and angle of contact.

An alternative way to obtain the total surface area is as follows:

For cylindrical pores

$$dS = \frac{2\,dV}{r} \qquad (3.15)$$

If it is assumed that there are several such cylindrical pores interconnected within the porous network then the contributions to the total surface area of the solid phases can be assumed to be dS_i for each of the volume steps dV_i, thus the total surface area is given by

$$S_t = \sum_{i=1}^{n} \frac{2\,dV_i}{r_i} \qquad (3.16)$$

where

S_t = total measurable surface area, and

n = number of volume steps used.

3.3.1.5 HYDRAULIC RADIUS

The hydraulic radius (mean pore radius) of a pore system may be defined as the ratio of the total intruded pore volume to surface area of pores.

$$m = \frac{\text{Volume of pores}}{\text{Surface of pores}}$$

For cylindrical pores m equals half the radius of the cylinder, since:

$$m = \frac{V}{S} = \frac{\pi r^2 L}{2\pi rL} = r/2 \qquad (3.17)$$

3.3.1.6 PORE SURFACE DISTRIBUTION

The pore surface distribution Ds(r) is the surface area per unit pore radius.

$$Ds(r) = \frac{dS}{dr} \qquad (3.18)$$

Equation 3.18 can be written as:

$$Ds(r) = \frac{dS}{dV} \cdot \frac{dV}{dr}$$

if the pores are cylinders, then

$$\frac{dS}{dV} = \frac{2}{r} \quad \text{and} \quad Dv(r) = \frac{dV}{dr}$$

Hence

$$Ds(r) = \frac{2}{r} Dv(r) \qquad (3.19)$$

3.3.1.9 TOTAL POROSITY

For water saturated cement pastes the total porosity may be calculated from Equation 3.22 below

$$e = W \rho_s / \rho_w \qquad (3.20)$$

where

e = total porosity (cm^3/cm^3)

W = weight lost on heating to 105°C (grams per gram of dry paste)

ρ_s = apparent dry density (g/cm^3)

ρ_w = density of water (1.0 g/cm^3)

3.3.2 THEORY OF FLOW IN POROUS SOLIDS

Darcy's law may be applied over a differential distance dx along in the direction of flow to give:

$$Q = \frac{K A}{\rho g} (dP/dx) \qquad (3.21)$$

where Q = volume rate of flow (m^3/s) measured at any point x in the medium and where the total pressure gradient is dP/dx

P = total pressure at point x (N/m^2)

ρ = unit weight of permeant (kg/m^3)

g = acceleration due to gravity (N/kg)

x = length coordinate in direction of flow (m)

A = cross sectional area of the porous material (m^2)

K = coefficient of permeability (m/s)

In subsequent discussions it will be convient to use Darcy's law in the following form.

$$Q = K A (H/L) \qquad (3.22)$$

where Q = rate of flow (m^3/s)

H = hydraulic head, m ($H=P/\rho g$)

L = length of the sample (m)

and thus $H/L = i$ = hydraulic gradient across sample in the direction of flow.

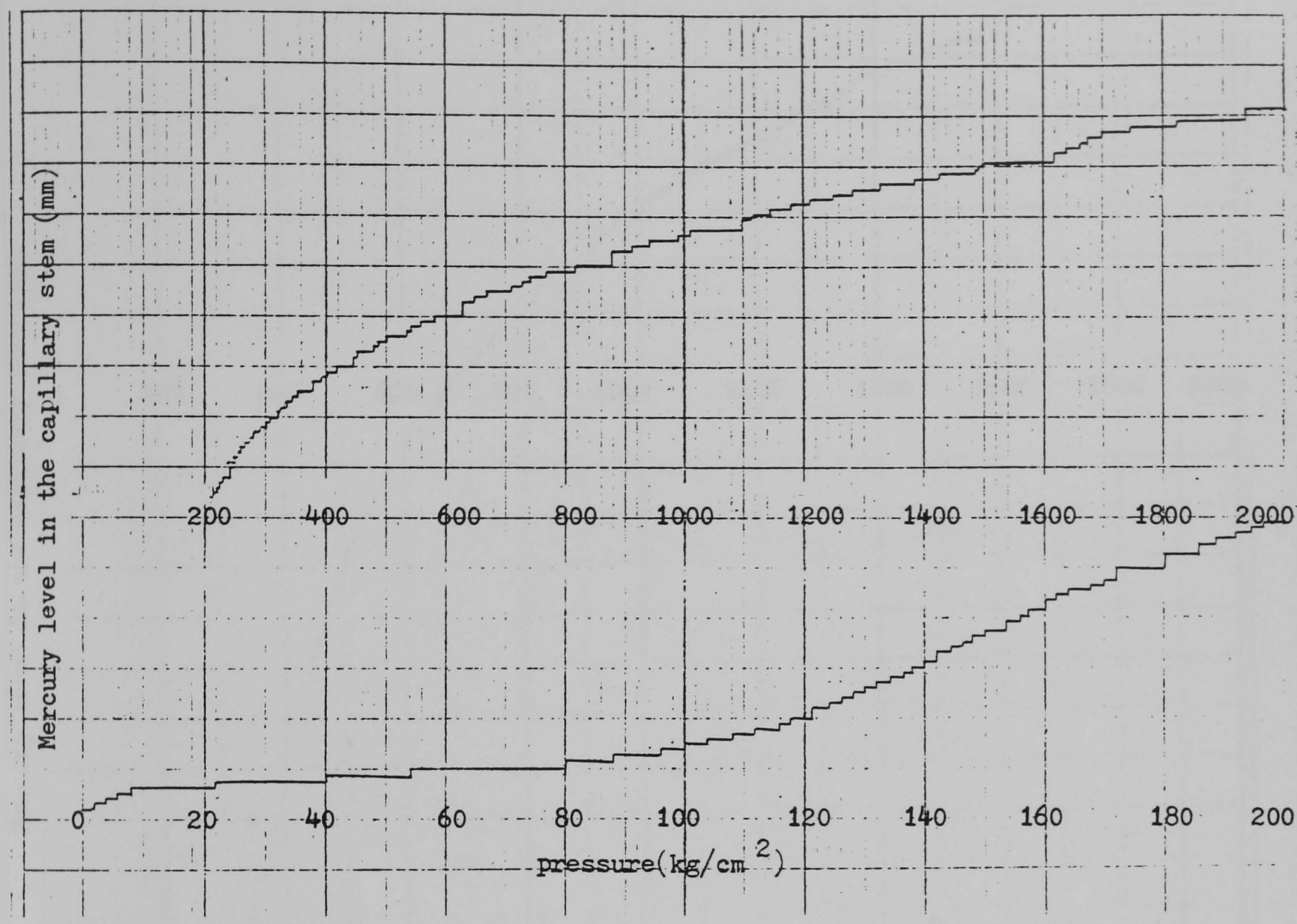

Figure 3.10 plots pressure-volume for pure hardened cement paste at age 560 days (cured under water),0.4 water/cement ratio.

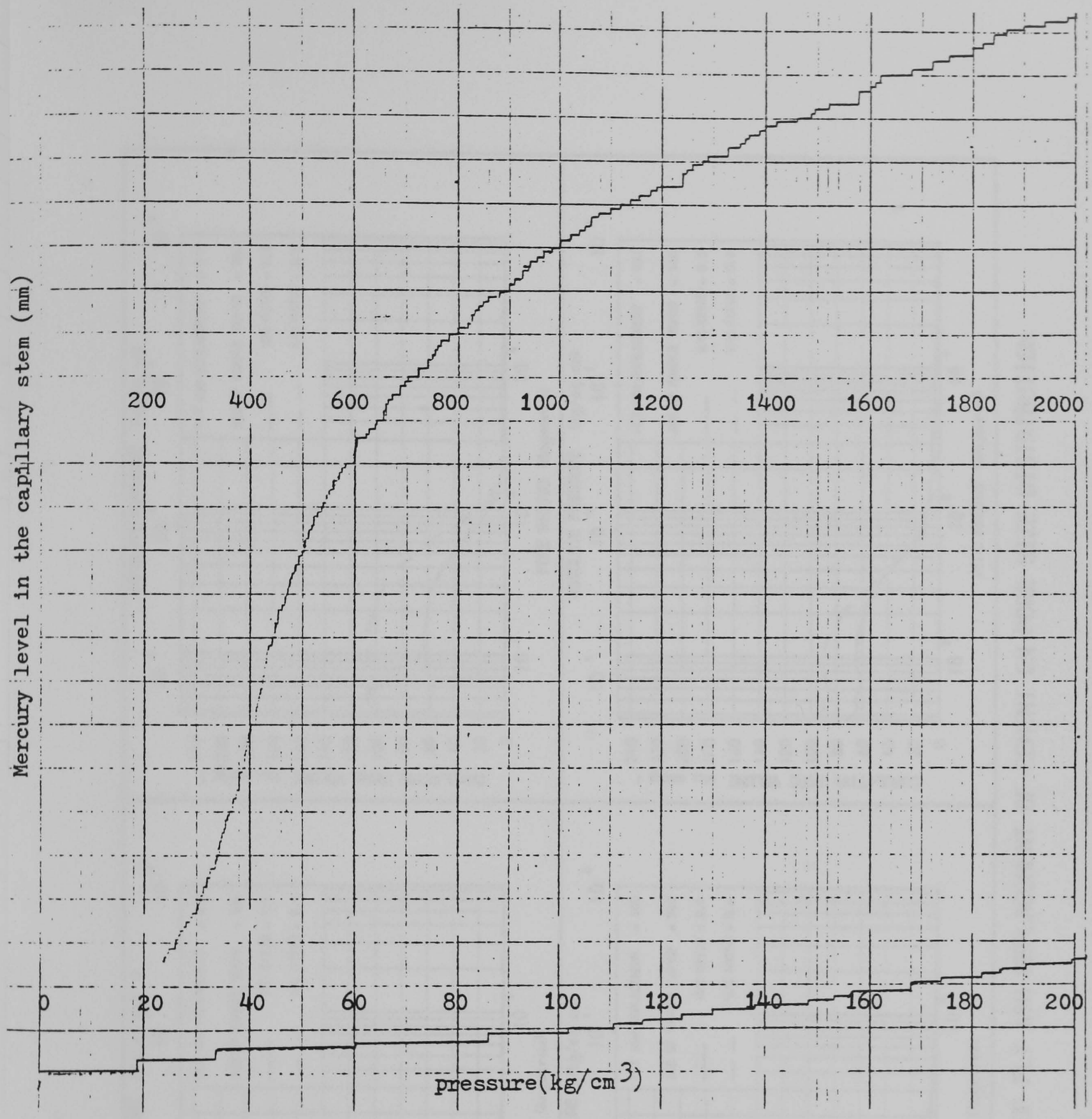

Figure 3.11 plots pressure-volume for hardened cement paste replaced cement by 60 per cent Fly ash at 560 days (cured under water),0.4 water/cement ratio.

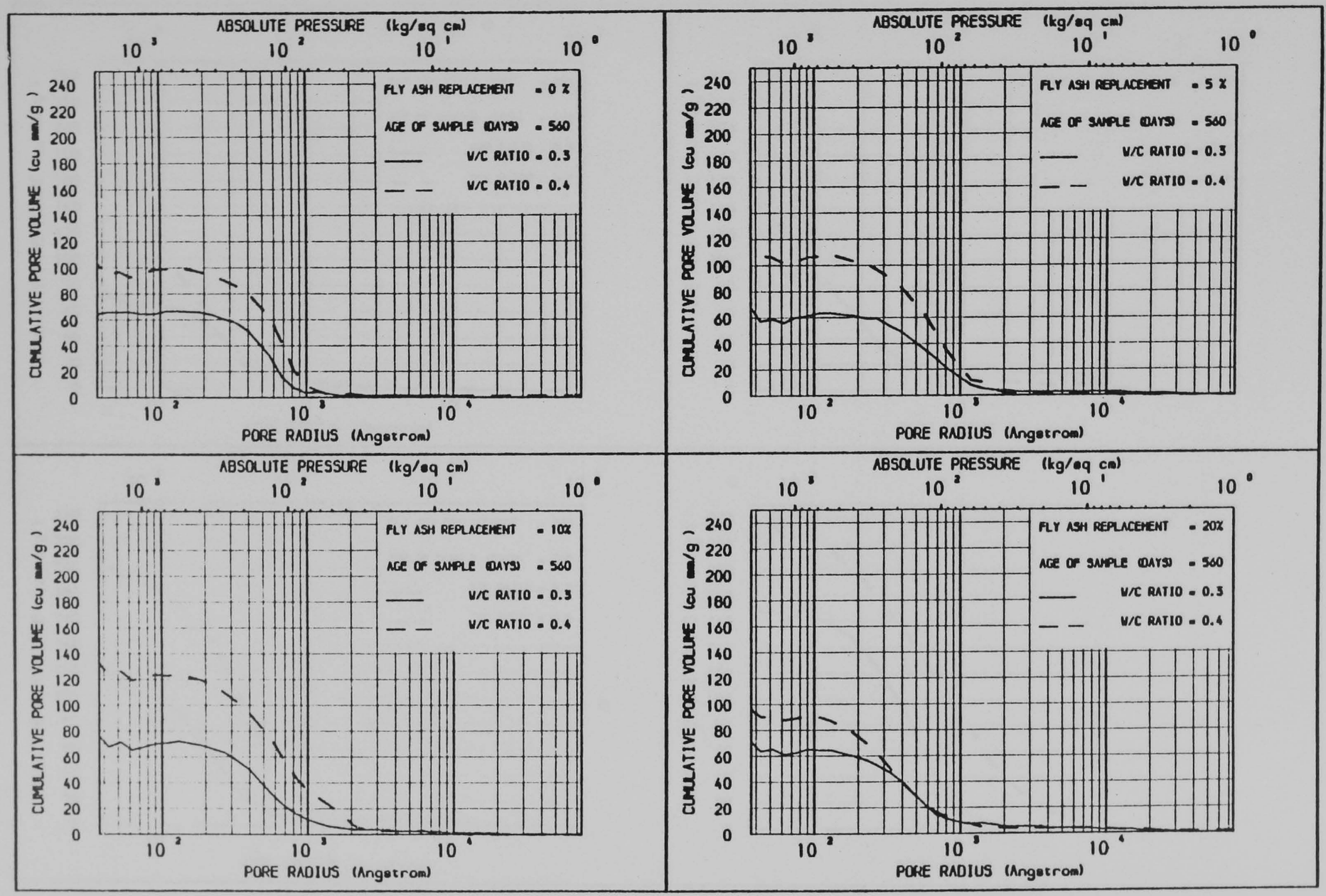

Figure 3.12 THE EFFECT OF FLY ASH REPLACEMENT OF CEMENT ON PORE SIZE DISTRIBUTION

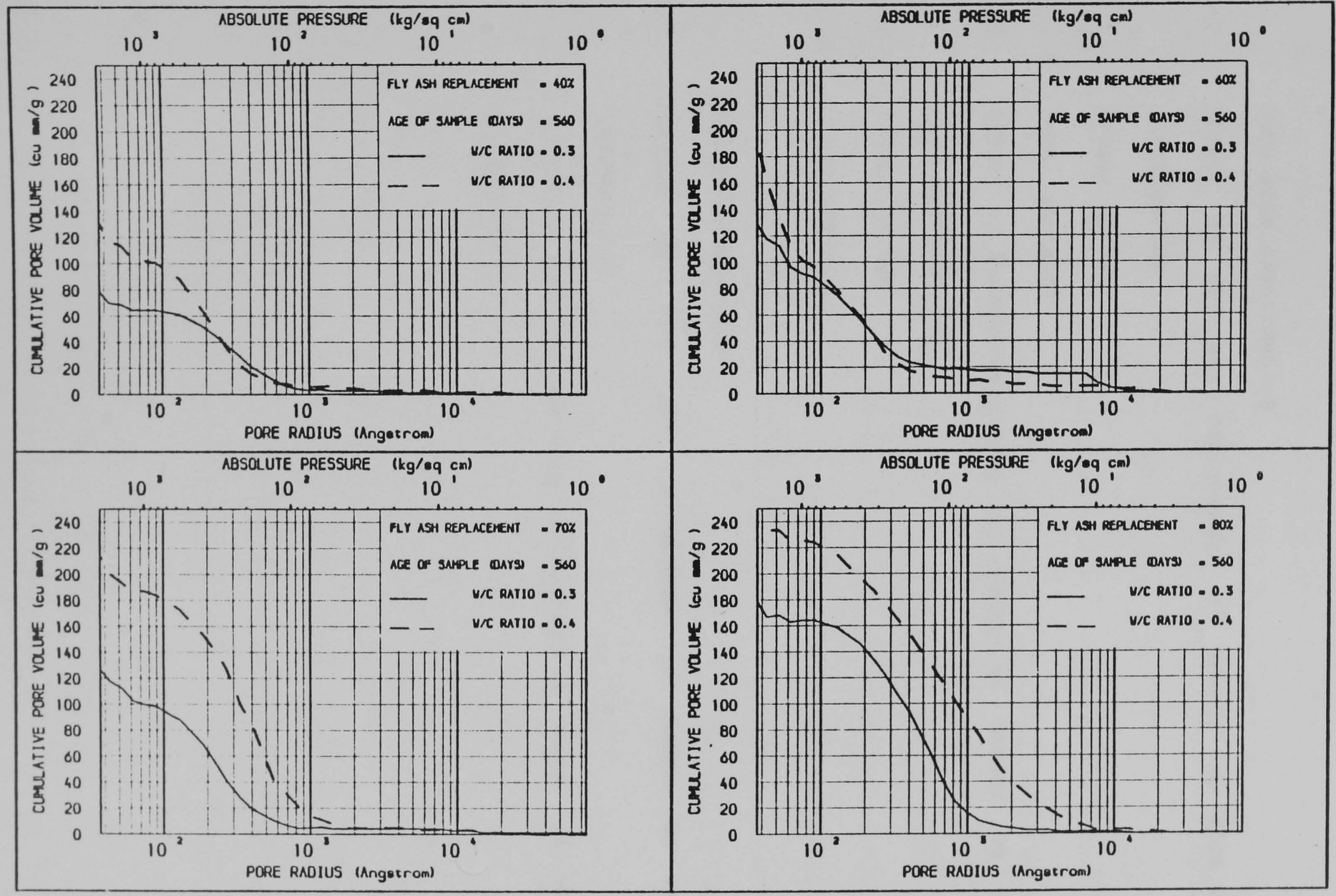

Figure 3.13 THE EFFECT OF FLY ASH REPLACEMENT OF CEMENT ON PORE SIZE DISTRIBUTION

CHAPTER FOUR

EXTENSIVE EXPERIMENTAL RESULTS AND ANALYSIS

CHAPTER FOUR

EXTENSIVE EXPERIMENTAL RESULTS AND ANALYSIS

4.1 PORE SIZE DISTRIBUTION

Pore size distribution were determined by mercury intrusion porosimetry on 240 samples. 240 samples arises from 0.3 and 0.4 water/cement ratios for Fly ash and Blastfurnace slag replaced cement pastes of various replacement levels, at ages of 3, 7, 28, 90, 270 and 560 days. The pore size distributions were determined for cement pastes containing varying proportions of Fly ash or Blastfurnace slag and prepared at water/cement ratios of 0.3 and 0.4. Due to the large amount of data accumulated, the analysis of the distributions was made using the computer programme which is listed in Appendix 2. The experimental pore size distribution curves are presented as the cumulative pore size distribution curves (or the percentage cumulative pore size distribution curves). The pore volume parameter being expressed in cubic millimetres of pore space per gram of oven dry sample.

In the cumulative distribution curves the cumulative pore volume of mercury intruded is plotted as the ordinate; the abscissa is marked in logarithmic scales of pore radius and absolute pressure.

The volume pore size distribution function is plotted as pore size distribution against a logarithmic scale of pore radius.

Due to the large amount of data and to make comparison between samples as simple as possible, cumulative pore volume and pore size distribution functions of the data are plotted on one graph for each sample.

The mean values of total porosity obtained from the oven dried weight losses are given as the total measurable pore volume per gram of oven dried weight of the sample. Oven drying was also selected as the standard technique for drying the samples for porosimetry.

4.1.1 EFFECT OF FLY ASH REPLACEMENT OF CEMENT ON PORE SIZE DISTRIBUTION

The pure Fly ash showed almost no cementitious properties in itself in the presence of pure water. When Ordinary Portland cement and Fly ash are mixed little tendency to set is observed at Fly ash levels of greater than 80 per cent.

Typical pore size distribution curves are presented in Figures 4.1-4.4 for cement pastes of two water/cement ratios after 560 days of hydration.

Figures 4.1 and 4.2 represent the cumulative pore size distribution curves for a water/cement ratio of 0.3 and for eight percentages of Fly ash replacement of the cement. In each pair of figures replacements of 0,5,10,20,40,60,70 and 80 per cent are shown in Frames A,B,C,D,E,F,G and H respectively. A similar set of results are presented in Figures 4.3 and 4.4 for the corresponding water/cement ratio 0.4.

Figures 4.5 and 4.6 represent the percentage cumulative pore volume curves for the two water/cement ratios, 0.3 and 0.4, and for the eight percentages of Fly ash replacement at 560 days of hydration.

Figures 4.7, 4.8, 4.9 and 4.10 represent the total intruded pore volume plotted against the percentage of Fly ash in the cement, for pore size ranges 37-1000 Angstrom, over 400 Angstrom and for pore sizes in the range 37-400 Angstrom respectively for the two water/cement ratios 0.3 and 0.4 at 270 days of hydration.

This data will be discussed in Chapter 5.

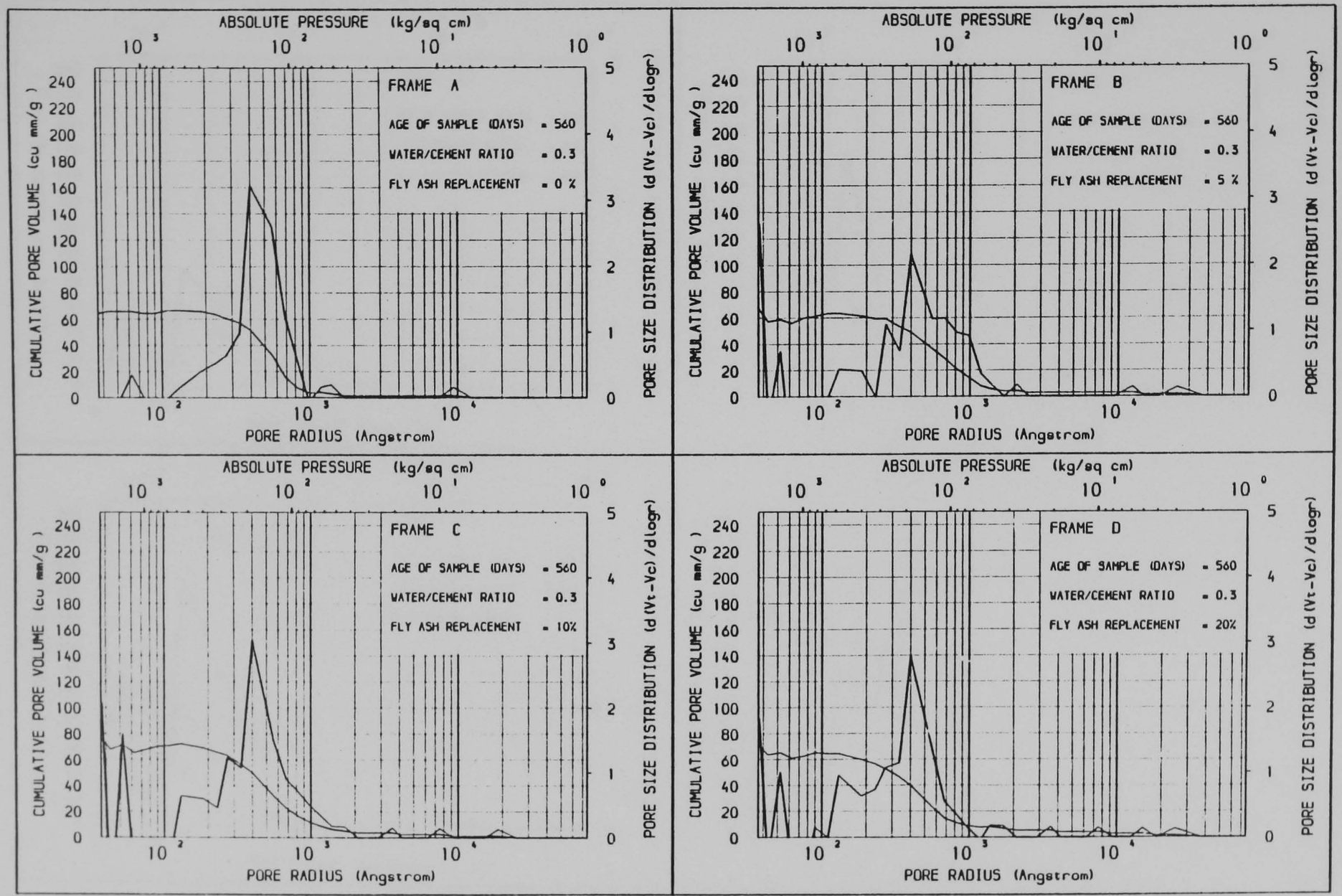

Figure 4.1 THE EFFECT OF FLY ASH REPLACEMENT OF CEMENT ON PORE SIZE DISTRIBUTION

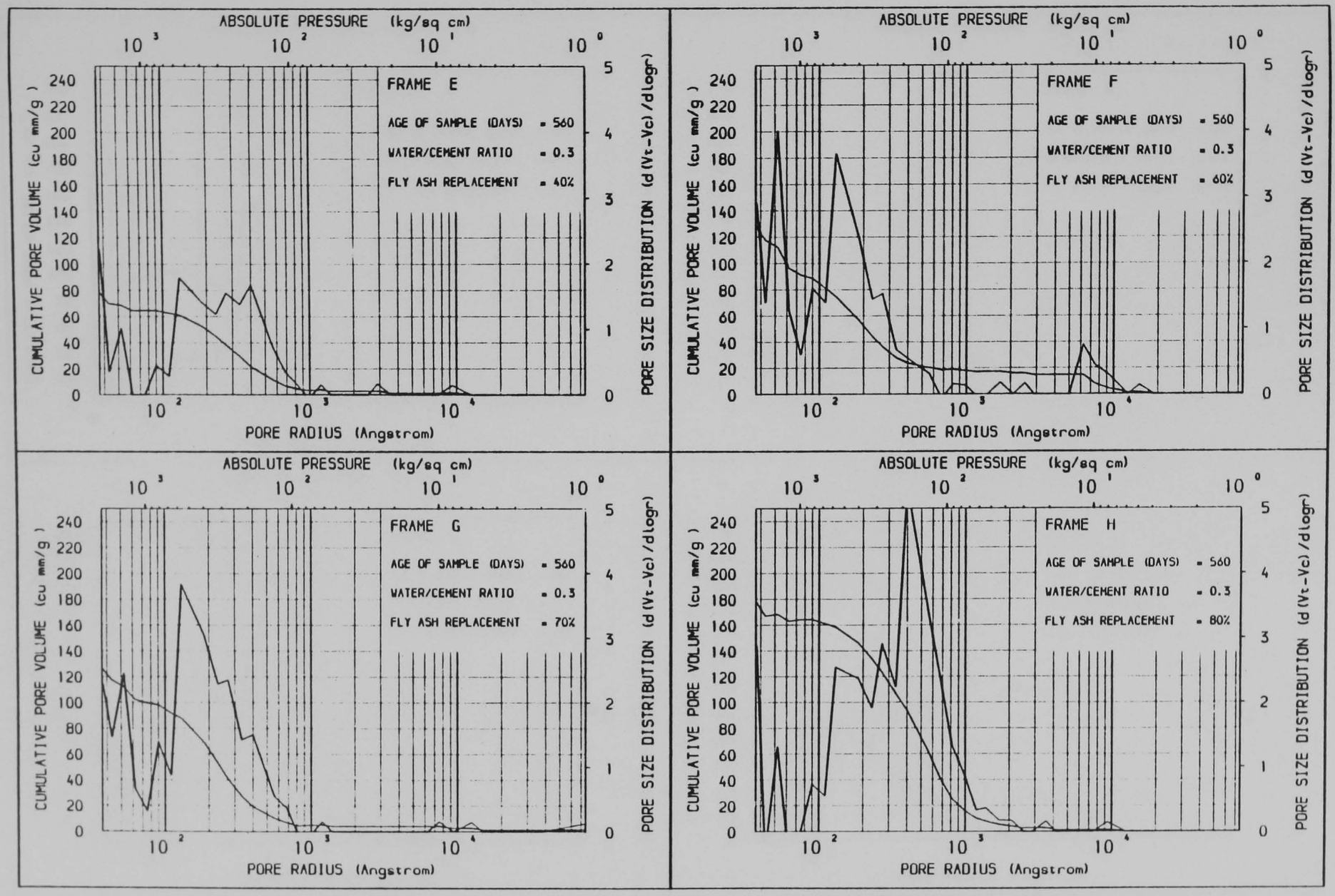

Figure 4.2 THE EFFECT OF FLY ASH REPLACEMENT OF CEMENT ON PORE SIZE DISTRIBUTION

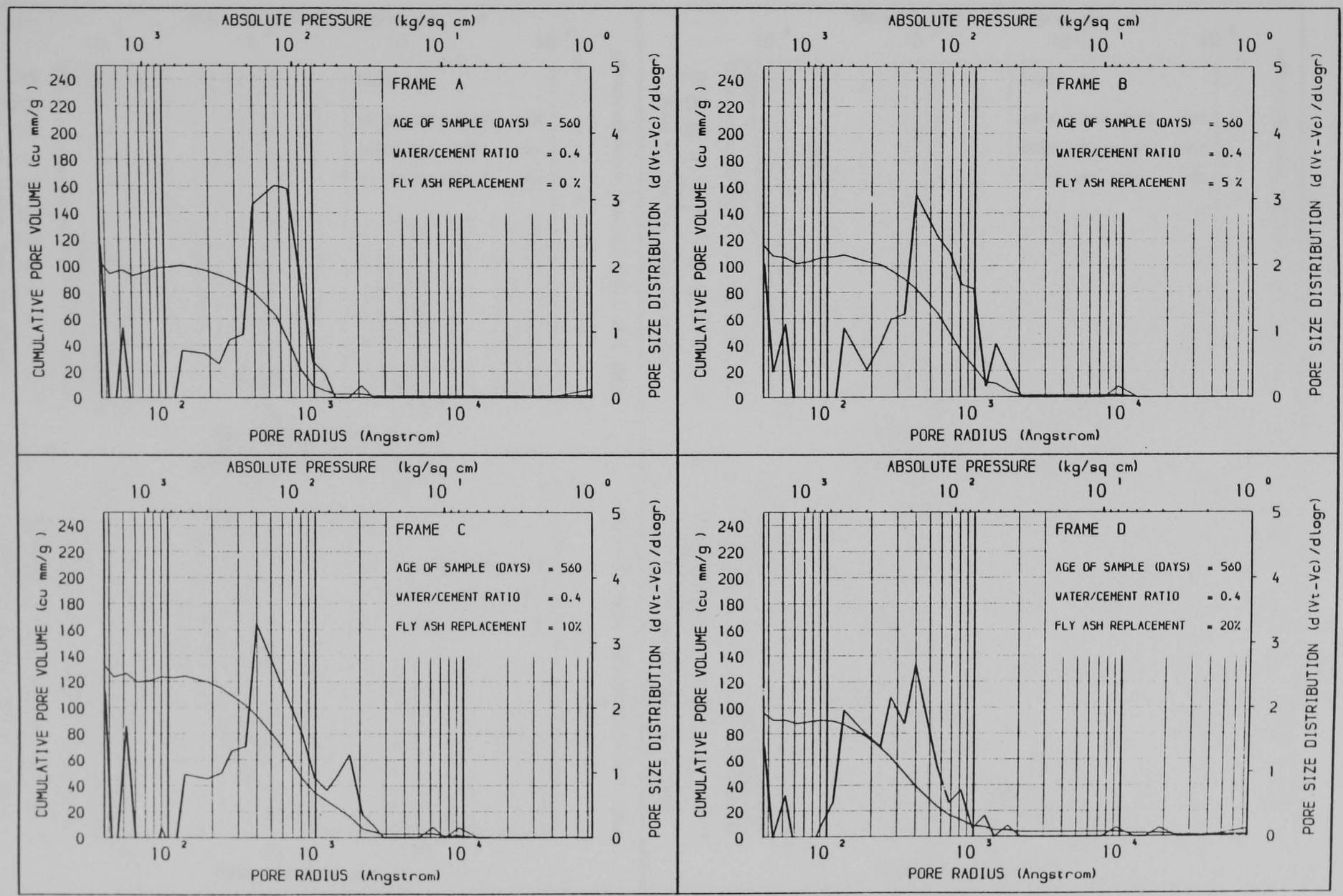

Figure 4.3 THE EFFECT OF FLY ASH REPLACEMENT OF CEMENT ON PORE SIZE DISTRIBUTION

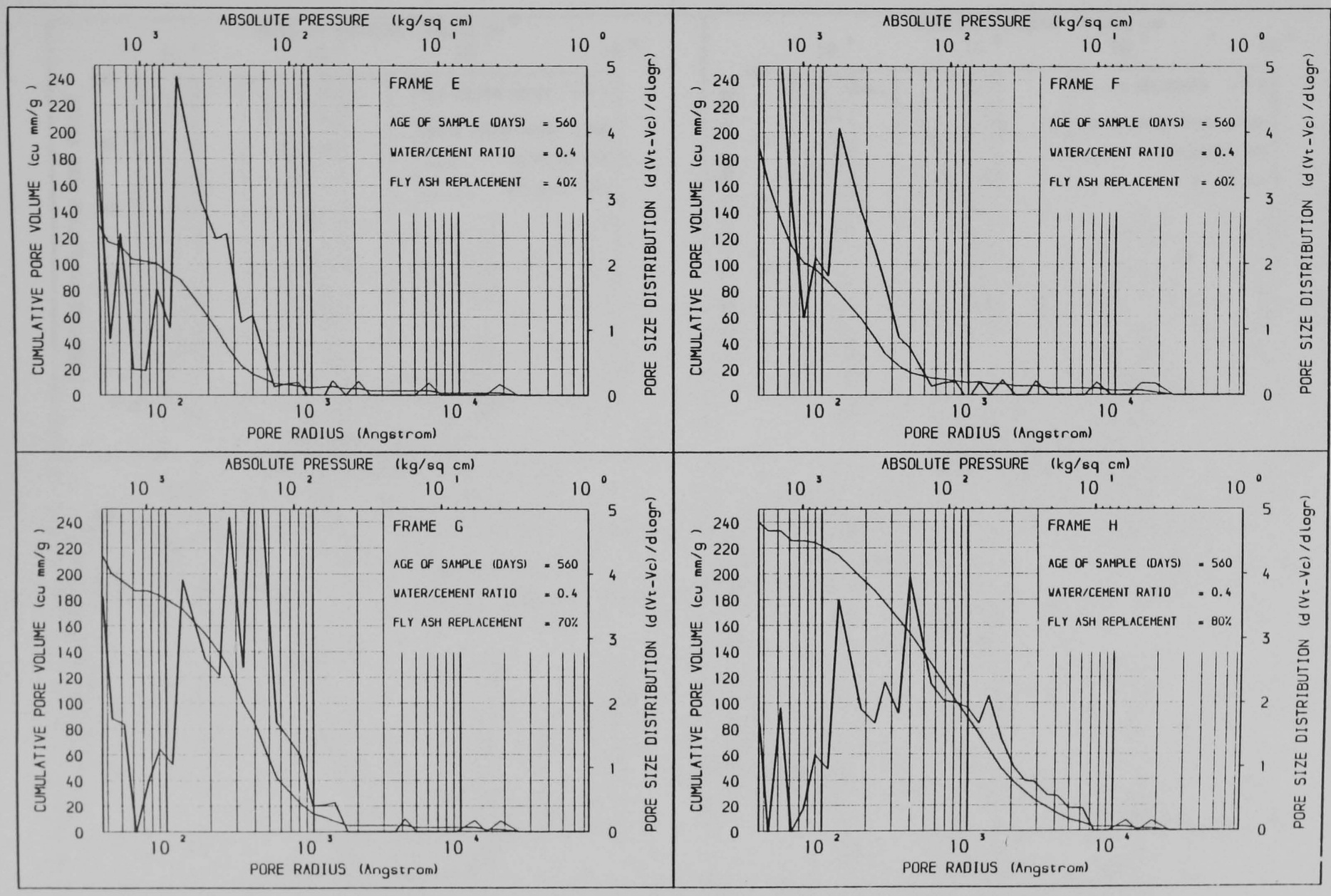

Figure 4.4 THE EFFECT OF FLY ASH REPLACEMENT OF CEMENT ON PORE SIZE DISTRIBUTION

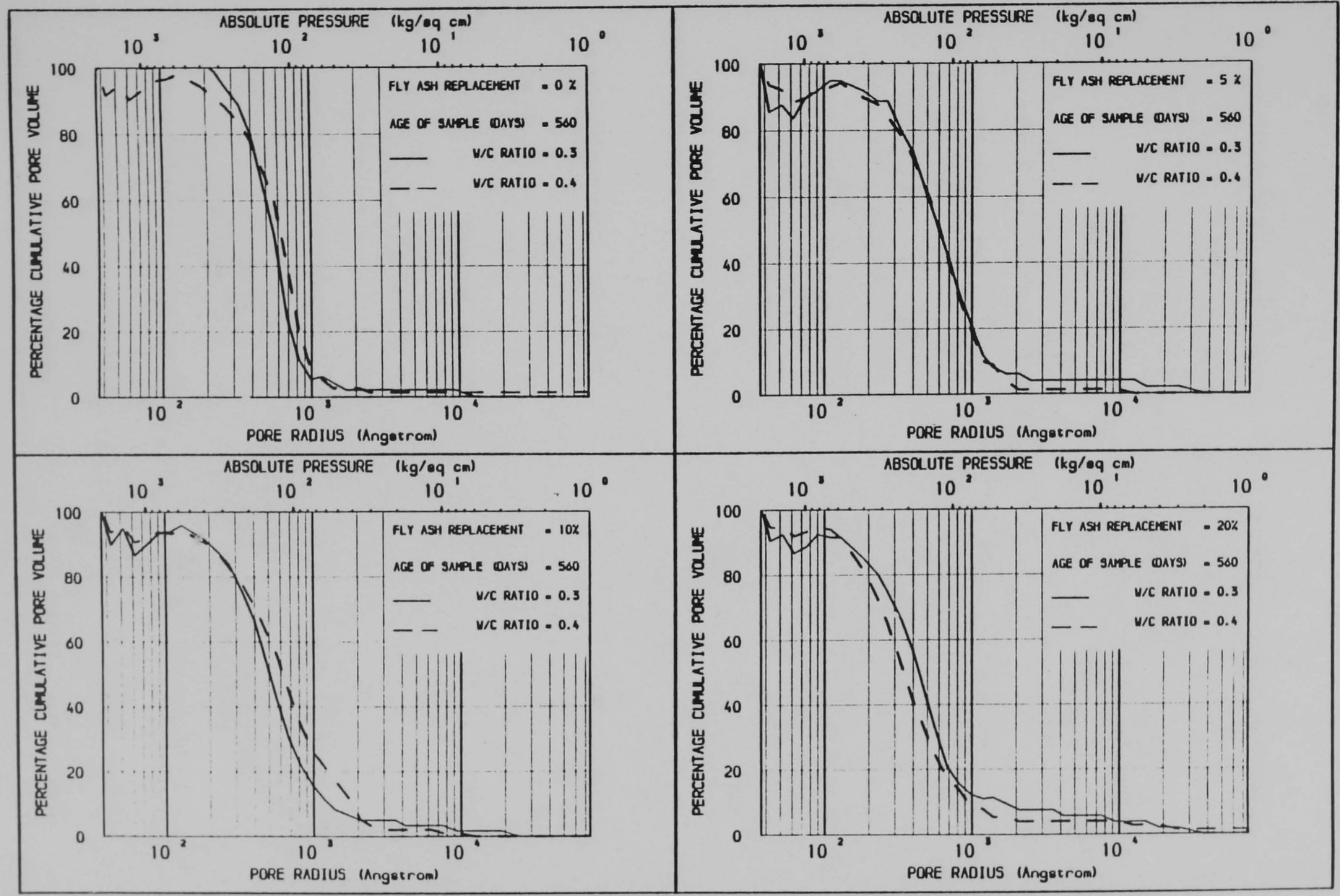

Figure 4.5 THE EFFECT OF FLY ASH REPLACEMENT OF CEMENT ON PORE SIZE DISTRIBUTION

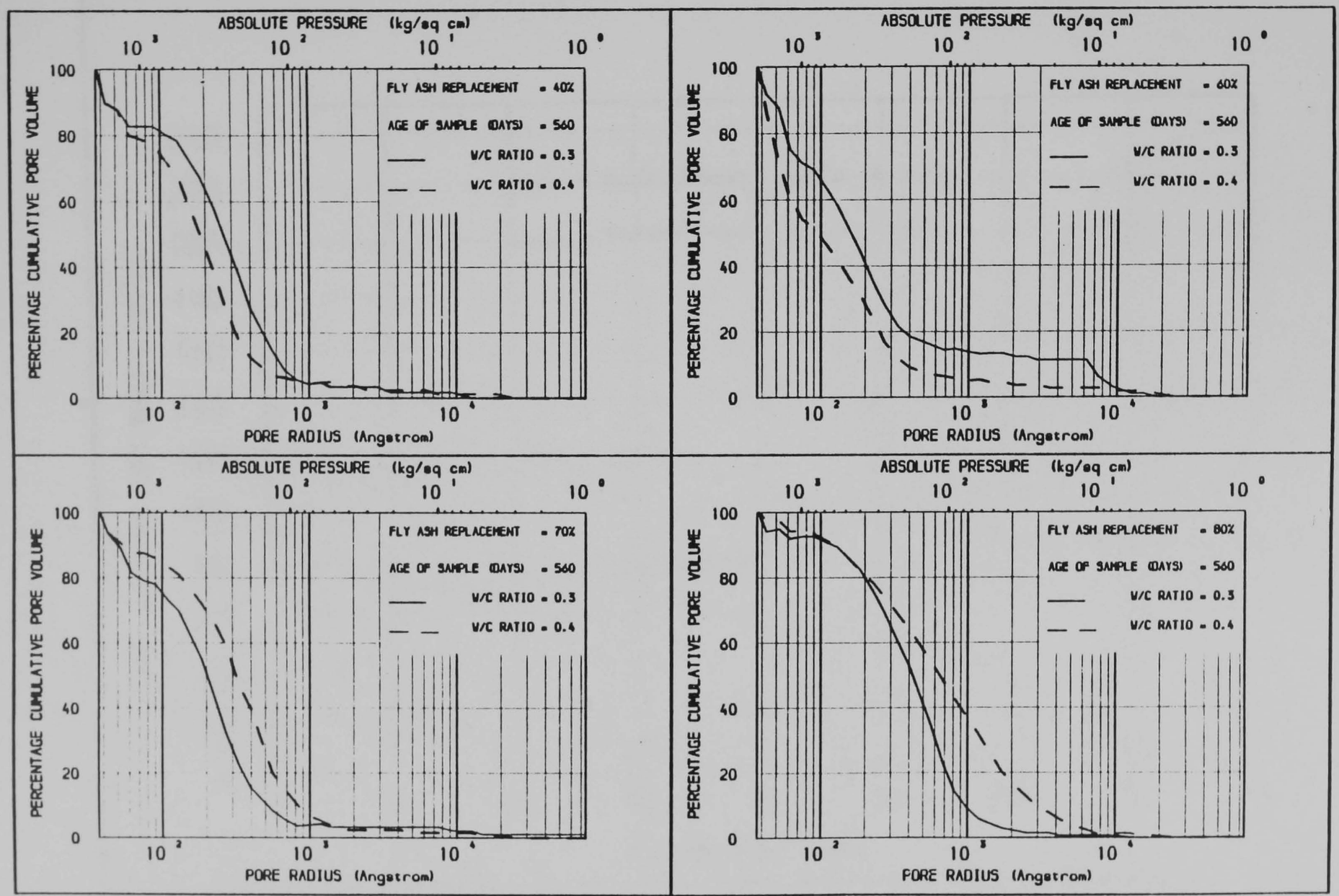

Figure 4.6 THE EFFECT OF FLY ASH REPLACEMENT OF CEMENT ON PORE SIZE DISTRIBUTION

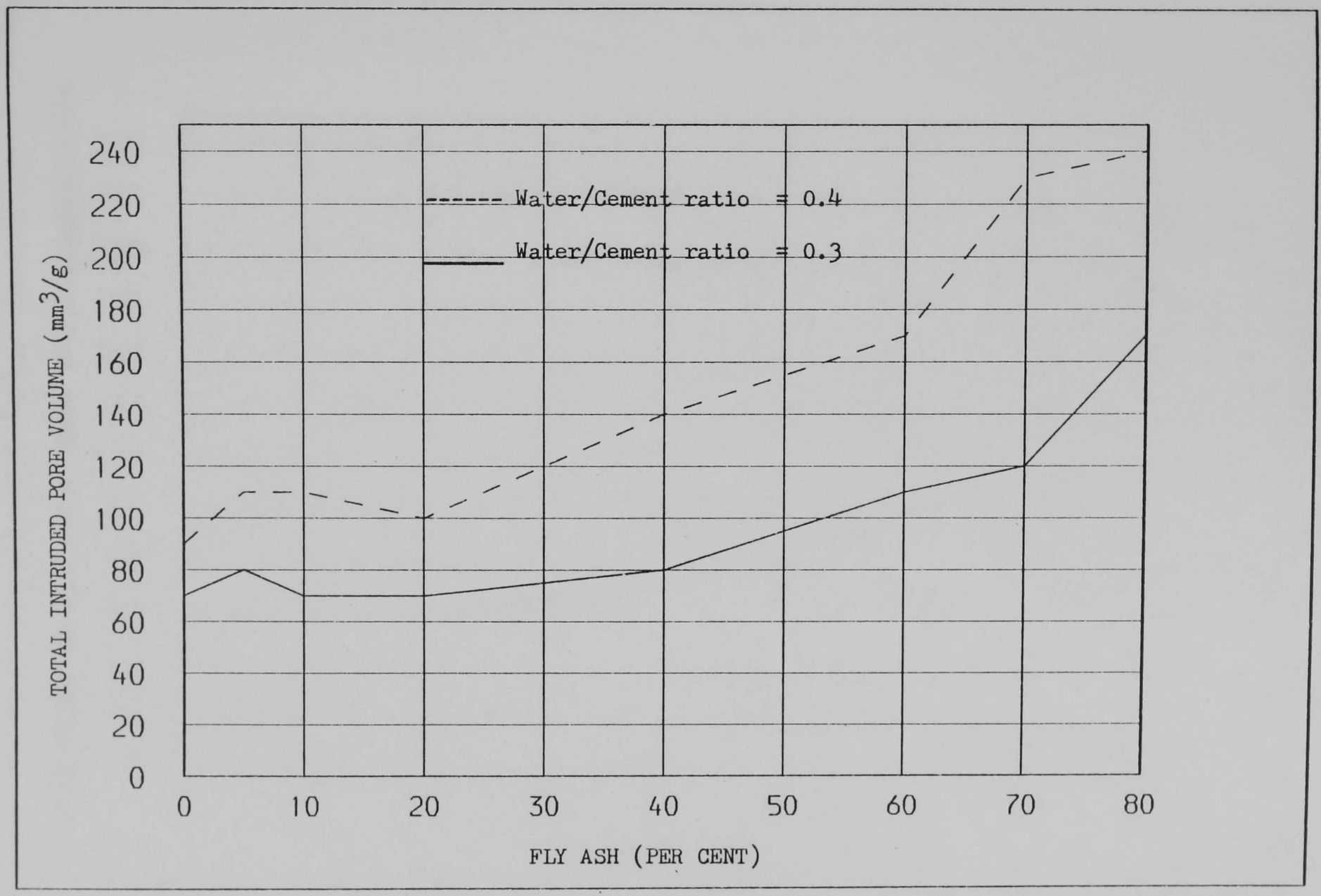

Figure 4.7 Effect of Fly ash replacement of cement on total intruded pore volume at age 270 days.

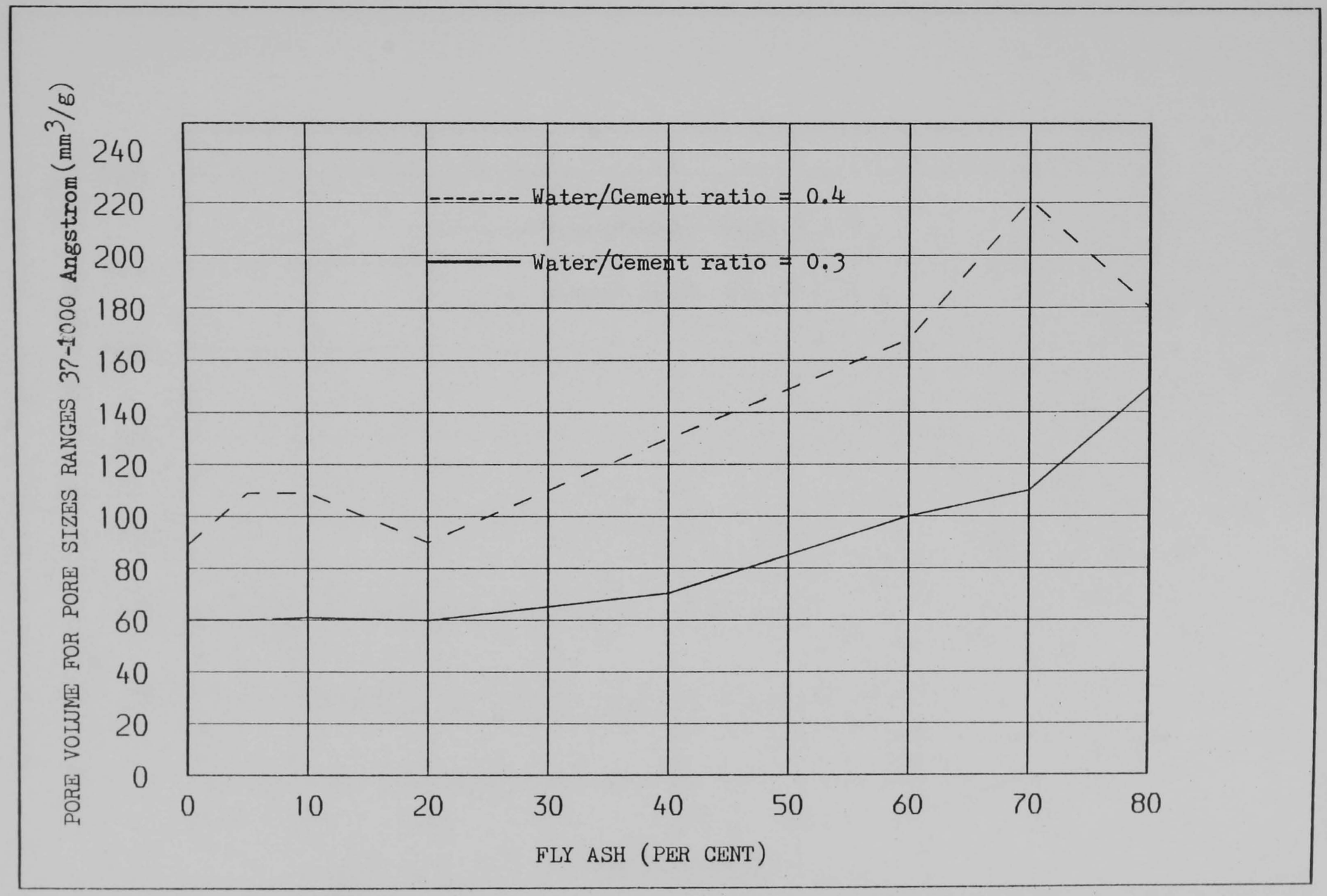

Figure 4. 8 Effect of Fly ash replacement of cement on pore volume for pore sizes ranges 37-1000 Angstrom at age 270 days.

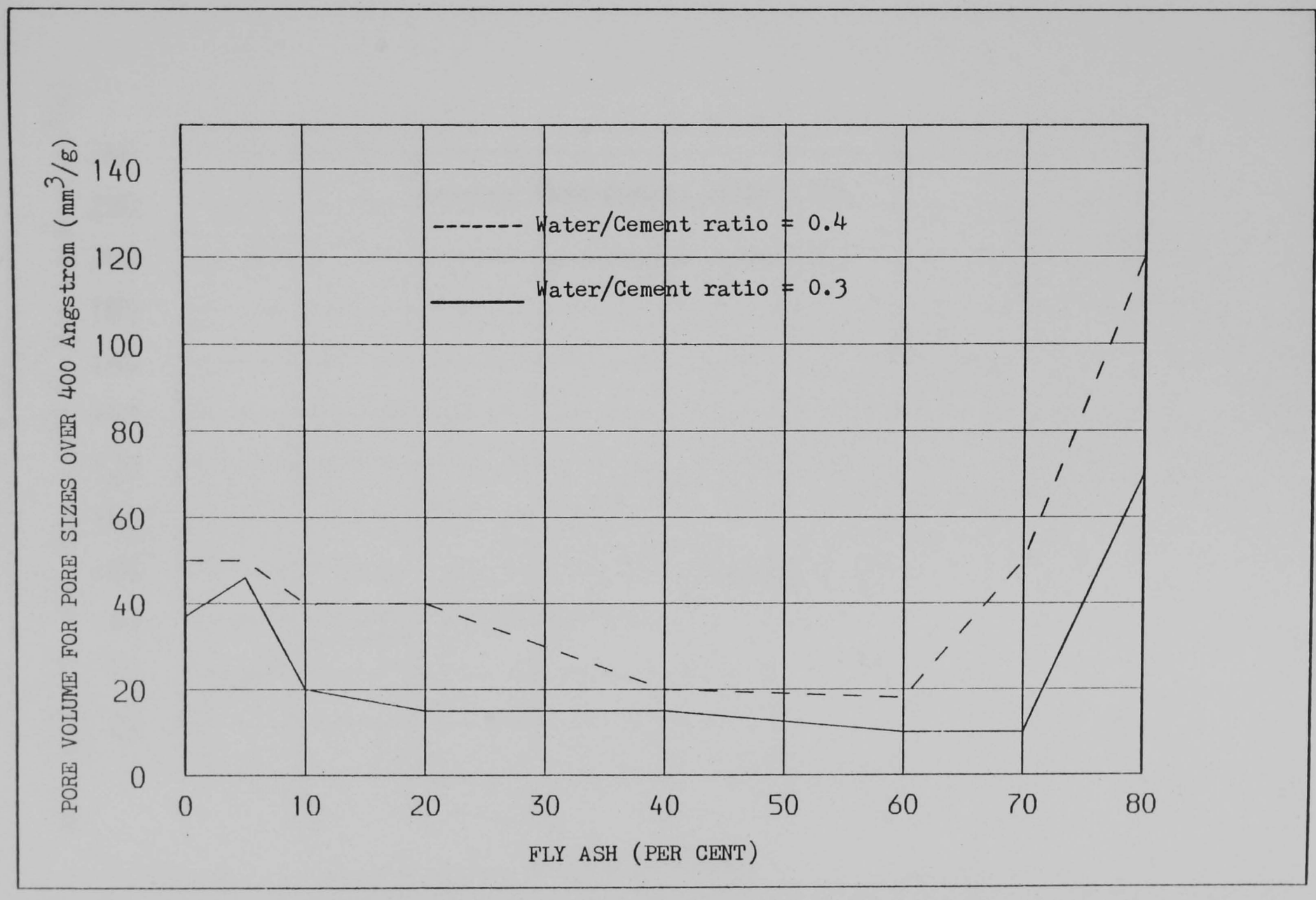

Figure 4.9 Effect of Fly ash replacement of cement on pore volume for pore sizes over 400 Angstrom at age 270 days.

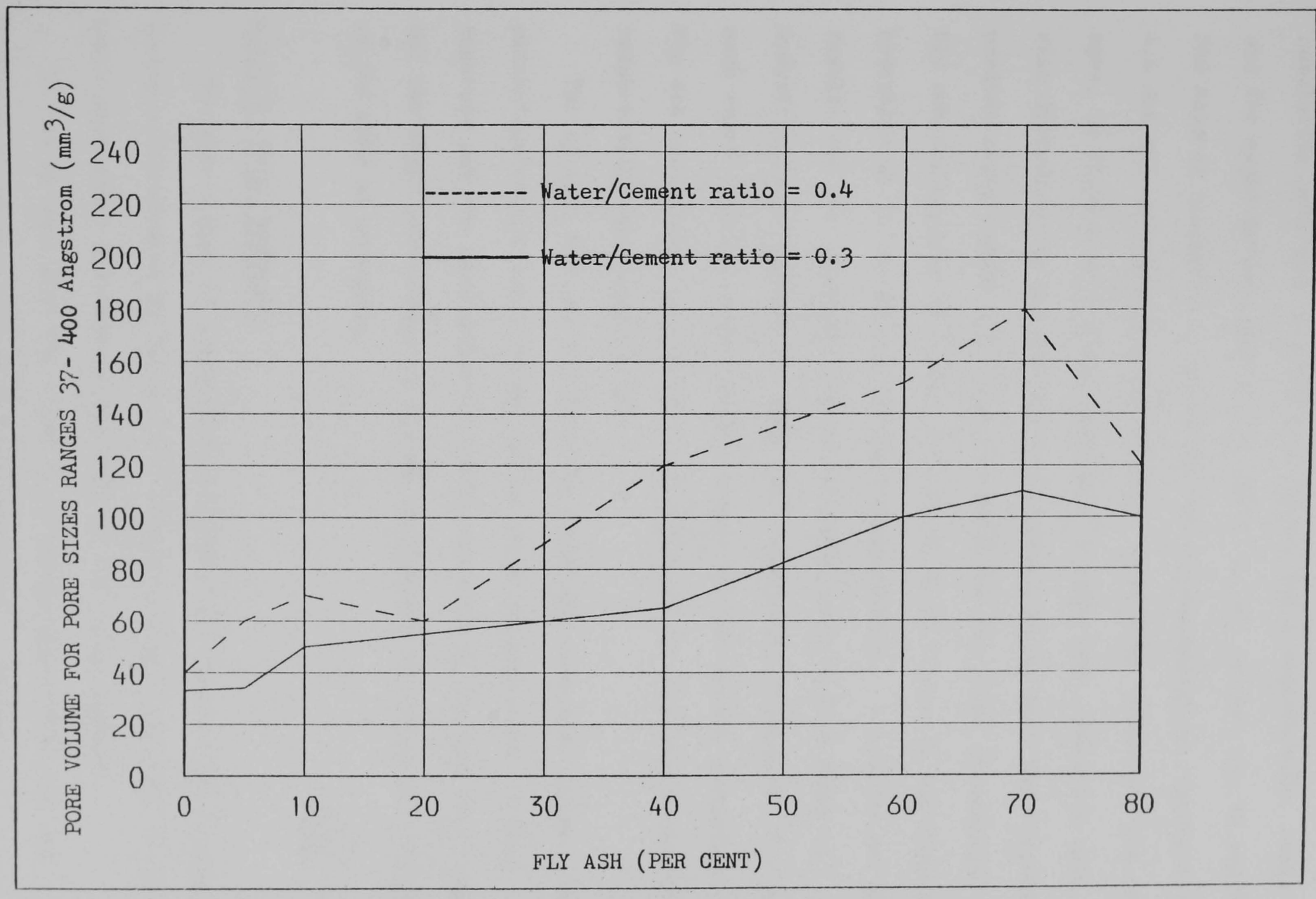

Figure 4.10 Effect of Fly ash replacement of cement on pore volume for pore sizes ranges 37- 400 Angstrom at age 270 days.

4.1.1.1 EFFECT OF AGE

In the previous section Figures 4.1 and 4.2 represent the cumulative pore size distribution curves for a water/cement ratio 0.3 and for eight percentages of Fly ash 0, 5, 10, 20, 40, 60, 70 and 80 at 560 days of hydration. A similar set are presented in Figures 4.3 and 4.4 for the corresponding water/cement ratio 0.4. Data for the other ages, in Figures A3.1-A3.10 (Appendix 3) give the cumulative pore size distributions for the 0.3 water/cement ratio, each two figures present eight frames A,B,C,D,E,F,G and H for the eight percentages of Fly ash replacement of cement, 0,5,10,20,40,60,70 and 80 and times of hydration at 3,7,28,90 and 270 days respectively. A similar set of results for the corresponding water/cement ratio 0.4 at times of hydration 3,7,28,90 and 270 days are presented in Figures A3.11 - A3.25, each three figures present twelve frames for the twelve percentages of Fly ash replacement of cement 0,5,10,20,30,35,40,45,50,60,70 and 80 respectively (see Appendix 3).

Tables 4.1, 4.2 and 4.3 give the total intruded pore volume, the percentage of the total volume in the range of pore radii 37-1000 Angstrom and the mean hydraulic radius for each of the two water/cement ratios and the eight percentages of Fly ash replacement of cement as a function of the time of hydration.

4.1.1.2 TOTAL POROSITY

The mean values of porosities obtained from the oven dried weight losses are presented in Table 4.4. The porosities are given as the total measurable pore volume per gram of oven dried sample.

It can be seen that the total porosity increases with Fly ash replacement and decreases with increasing time of hydration.

Table 4.4 also lists the total intruded pore volume for each paste with a water/cement ratio of 0.4. This is in all cases less than the total porosity . The actual percentage of total pore volume intruded is also quoted. This percentage represents the percentage of accessible capillary pores as a percentage of the total pores (Auskern and Horn 1973). The difference between the total porosity and the total intruded pore volume has been suggested to represent gel pores (Winslow and Dimond 1970, Auskern and Horn 1973).

Time of hydration days		3	7	28	90	270	560
Fly ash (per cent)	W/C ratio	Total intruded pore volume (mm^3/g)					
0	0.3	140	120	90	80	70	60
	0.4	180	160	130	130	90	100
5	0.3		110	100	80	80	70
	0.4	180	160	140	130	110	110
10	0.3		120		90	70	80
	0.4	200	180	140	120	110	130
20	0.3		140	110	80	70	70
	0.4	230	200	170	130	100	100
40	0.3		140		100	80	80
	0.4	240	240	190	170	140	130
60	0.3		170		140	110	130
	0.4	310	250	240	220	170	190
70	0.3		180		140	120	130
	0.4	320	280	270	250	230	210
80	0.3		220		220	170	180
	0.4	330	320	300	290	240	240

Table 4.1 Effect of Fly ash replacement of cement on total intruded pore volume

Time of hydration days		3	7	28	90	270	560
Fly ash (per cent)	W/C ratio	(Sizes lower than 1000 Angstrom / total intruded pore volume) %					
0	0.3	64	83	89	88	86	95
	0.4	61	75	70	77	99	91
5	0.3		73	90	99	75	80
	0.4	67	69	86	70	99	80
10	0.3		83		89	87	85
	0.4	65	72	70	67	99	74
20	0.3		71	79	88	86	88
	0.4	57	80	70	77	90	91
40	0.3		64		99	88	96
	0.4	42	67	84	94	93	96
60	0.3		76		93	91	86
	0.4	29	68	60	95	99	95
70	0.3		78		93	92	96
	0.4	25	36	59	92	96	99
80	0.3		55		64	88	91
	0.4	21	41	47	55	75	63

Table 4.2 Effect of Fly ash replacement of cement on substantial pore volume (sizes lower than 1000 Angstrom).

Time of hydration days		3	7	28	90	270	560
Fly ash (per cent)	W/C ratio	Mean hydraulic radius (Angstrom)					
0	0.3	20472	9287	9295	12229	10169	9195
	0.4	20320	14180	14165	13748	8658	8359
5	0.3		27302	19862	12520	12664	10927
	0.4	17175	20943	16892	13920	8534	10074
10	0.3		12687		11617	5633	8680
	0.4	15794	14694	12929	15626	6740	8368
20	0.3		12330	20648	10352	5736	9922
	0.4	18332	11978	11486	10524	8676	10131
40	0.3		10547		9377	5918	6598
	0.4	27177	11923	11029	7740	6195	5419
60	0.3		7423		7824	5028	6043
	0.4	27156	13587	13003	6479	5684	3715
70	0.3		8921		5215	4080	5743
	0.4	21702	20383	15619	6941	7802	7789
80	0.3		11435		11261	8209	10338
	0.4	31153	18349	14449	14180	10583	13121

Table 4.3 Effect of Fly ash replacement of cement on mean hydraulic radius

Fly ash (per cent)	Total pore volume: time of hydration days	dry density kg/m^3	water porosity: per cent	mm^3/g	Hg intruded: mm^3/g	capillary porosity % of total porosity
0	28	1663	30.9	186	130	69.8
	270	1663	26.1	157	90	57.3
5	28	1647	32.9	200	140	69.9
	270	1647	31.5	191	110	57.6
10	28	1617	33.3	206	140	68.0
	270	1617	31.9	197	110	55.8
20	28	1591	41.7	262	170	64.8
	270	1591	30.1	189	100	52.9
30	28	1543	40.0	259	170	65.6
	270	1543	37.8	245	130	53.1
35	28	1541	41.6	270	190	70.4
	270	1541	39.0	253	140	55.3
40	28	1502	39.8	265	190	71.6
	270	1502	36.8	245	140	57.1
45	28	1451	40.5	279	200	71.7
	270	1451	36.4	251	150	59.8
50	28	1433	41.7	291	210	72.2
	270	1433	37.7	263	160	60.8
60	28	1380	41.3	299	240	80.3
	270	1380	36.0	261	170	65.2
70	28	1357	44.6	329	270	82.0
	270	1357	41.9	309	230	74.4
80	28	1312	46.3	353	300	84.9
	270	1312	42.0	320	240	75.0

Table 4.4 Effect of Fly ash replacement of cement on total and capillary porosities at 0.4 water/cement ratio.

4.1.2 EFFECT OF BLASTFURNACE SLAG REPLACEMENT OF CEMENT ON PORE SIZE DISTRIBUTION

No hydration products were observed when granulated slag was mixed with pure water. When Ordinary Portland cement and Blastfurnace slag are mixed little tendency to set is observed at slag levels of greater than 97 per cent.

Typical pore size distribution curves are presented in Figures 4.11 - 4.14 for pastes of different water/cement ratio at 360 days of hydration.

Figures 4.11 and 4.12 represent the cumulative pore size distribution curves for a water/cement ratio of 0.3 and for eight percentages of Blastfurnace 0,20,40,60,70,80,95 and 97 per cent shown respectively in Frames A,B,C,D,E,F,G and H. A similar set of results are presented in Figures 4.13 and 4.14 for the corresponding water/cement ratio 0.4.

Figures 4.15 and 4.16 represent the percentage cumulative pore volume curves for the two water/cement ratios, 0.3 and 0.4 and for the eight percentages of Blastfurnace slag replacement at 360 days of hydration.

Figures 4.17, 4.18, 4.19 and 4.20 show the total intruded pore volume plotted against the percentage of Blastfurnace slag in the cement, for pore sizes in the ranges 37-1000 Angstrom, over 400 Angstrom and for pore sizes in the ranges 37- 400 Angstrom respectively for the two water/cement ratios 0.3 and 0.4 at 270 days of hydration.

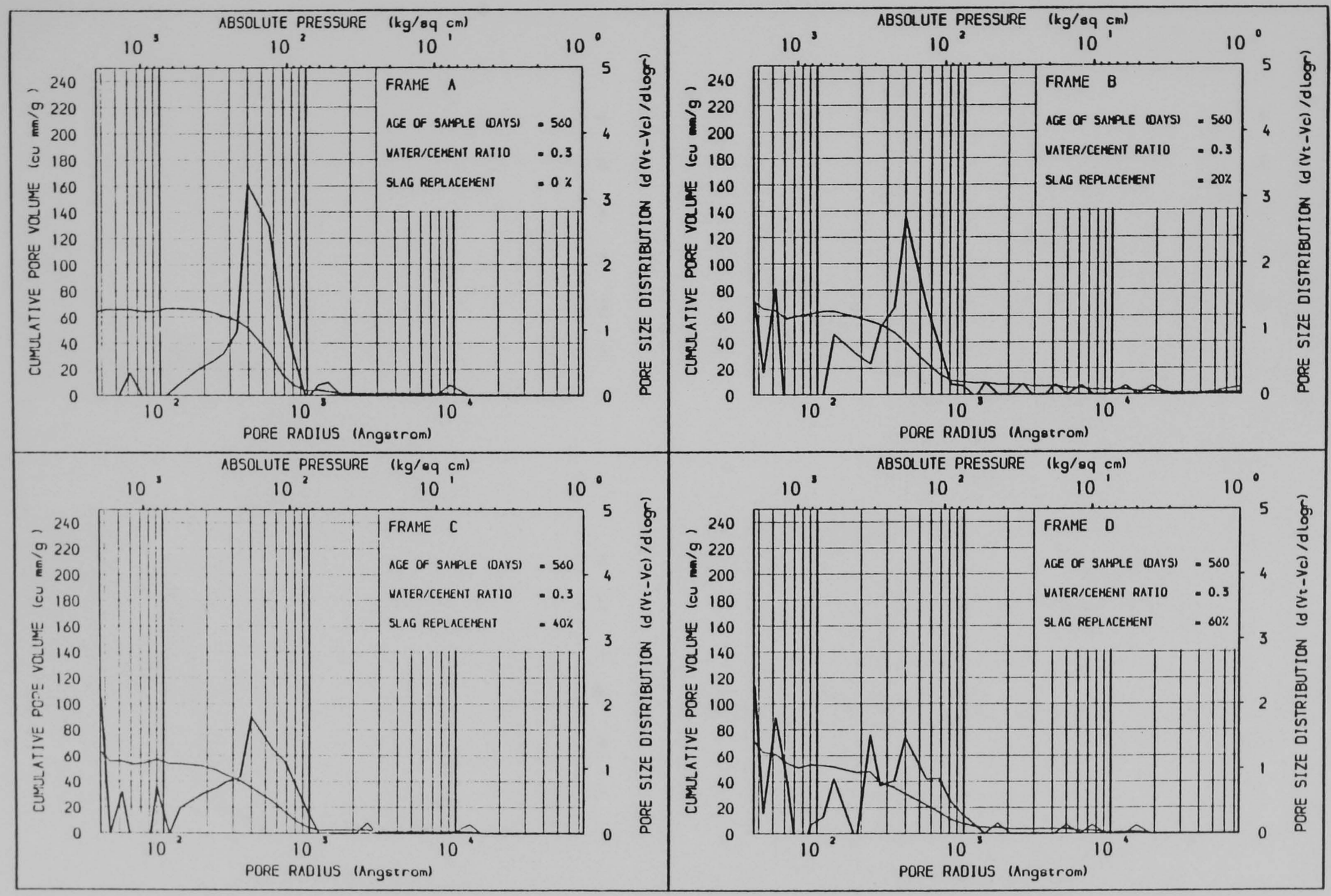

Figure 4.11 THE EFFECT OF BLASTFURNACE SLAG REPLACEMENT OF CEMENT ON PORE SIZE DISTRIBUTION

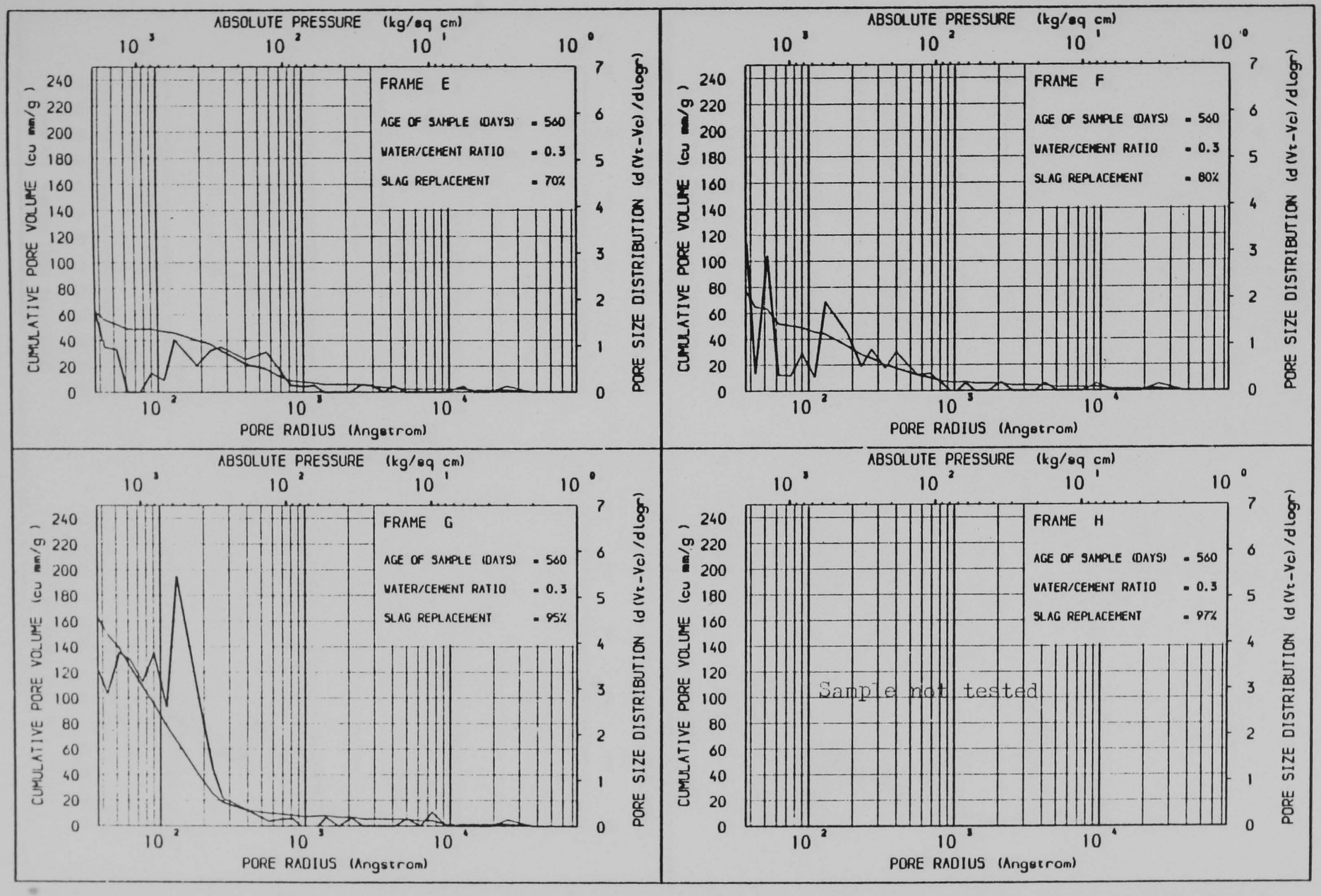

Figure 4.12 THE EFFECT OF BLASTFURNACE SLAG REPLACEMENT OF CEMENT ON PORE SIZE DISTRIBUTION

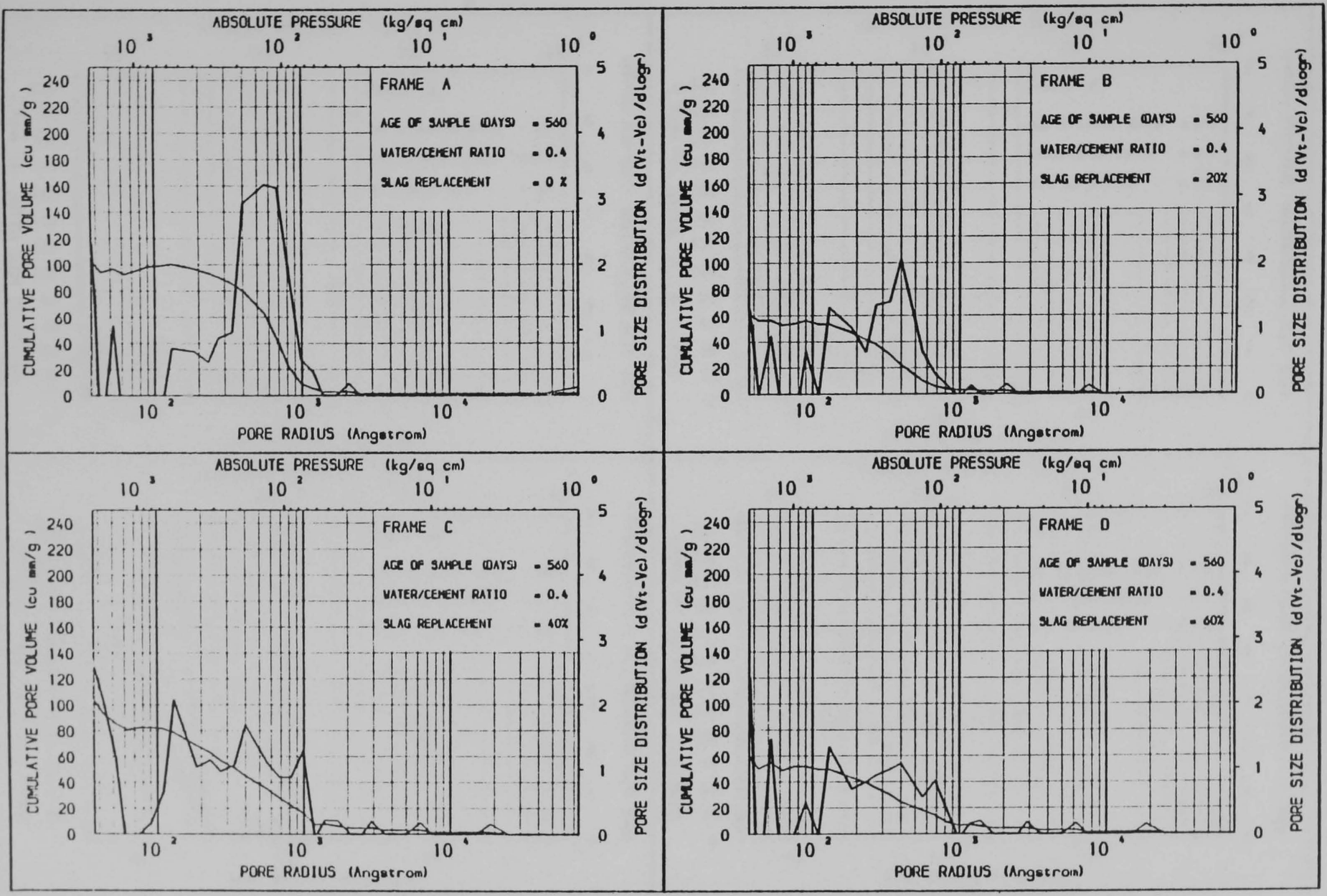

Figure 4.13 THE EFFECT OF BLASTFURNACE SLAG REPLACEMENT OF CEMENT ON PORE SIZE DISTRIBUTION

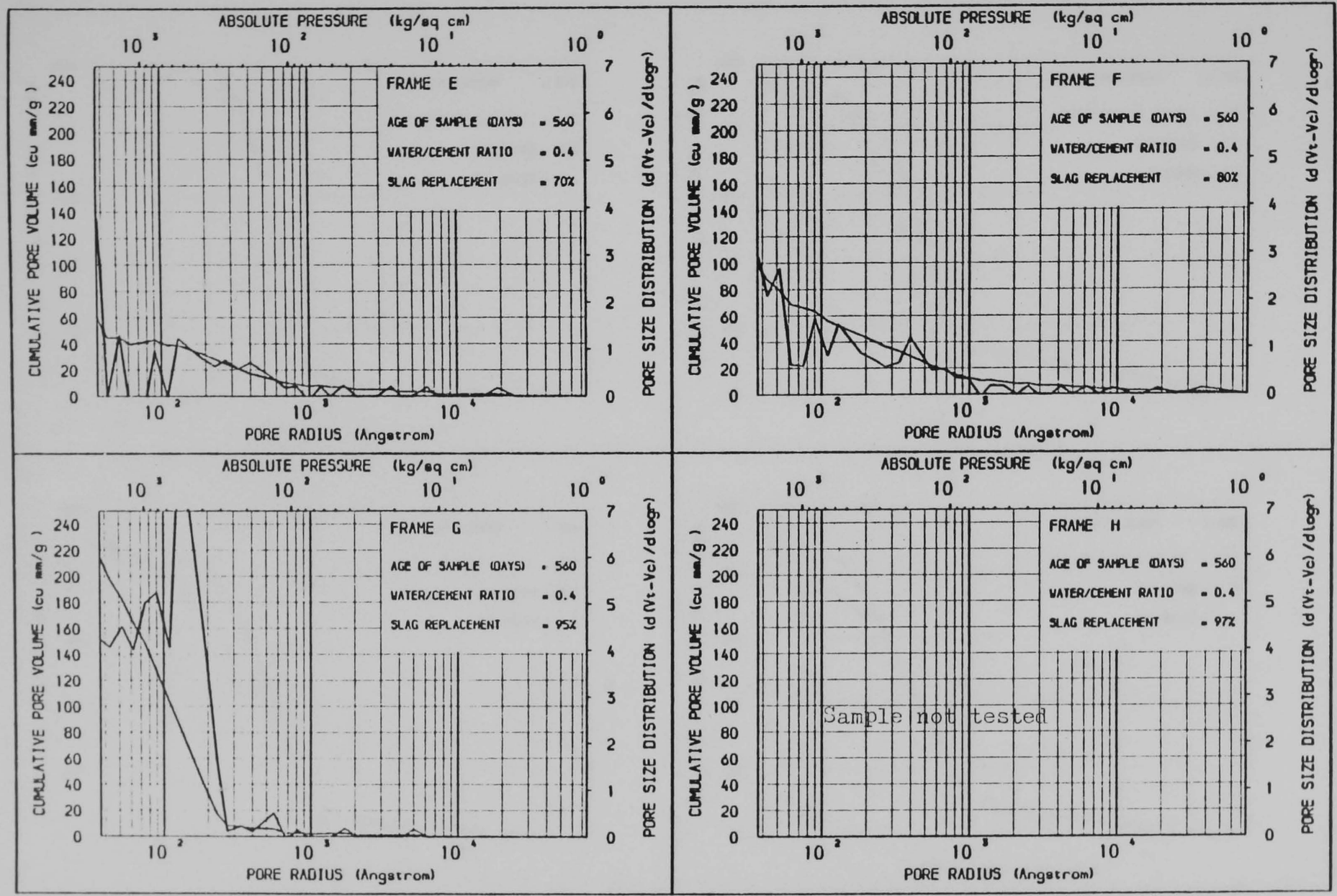

Figure 4.14 THE EFFECT OF BLASTFURNACE SLAG REPLACEMENT OF CEMENT ON PORE SIZE DISTRIBUTION

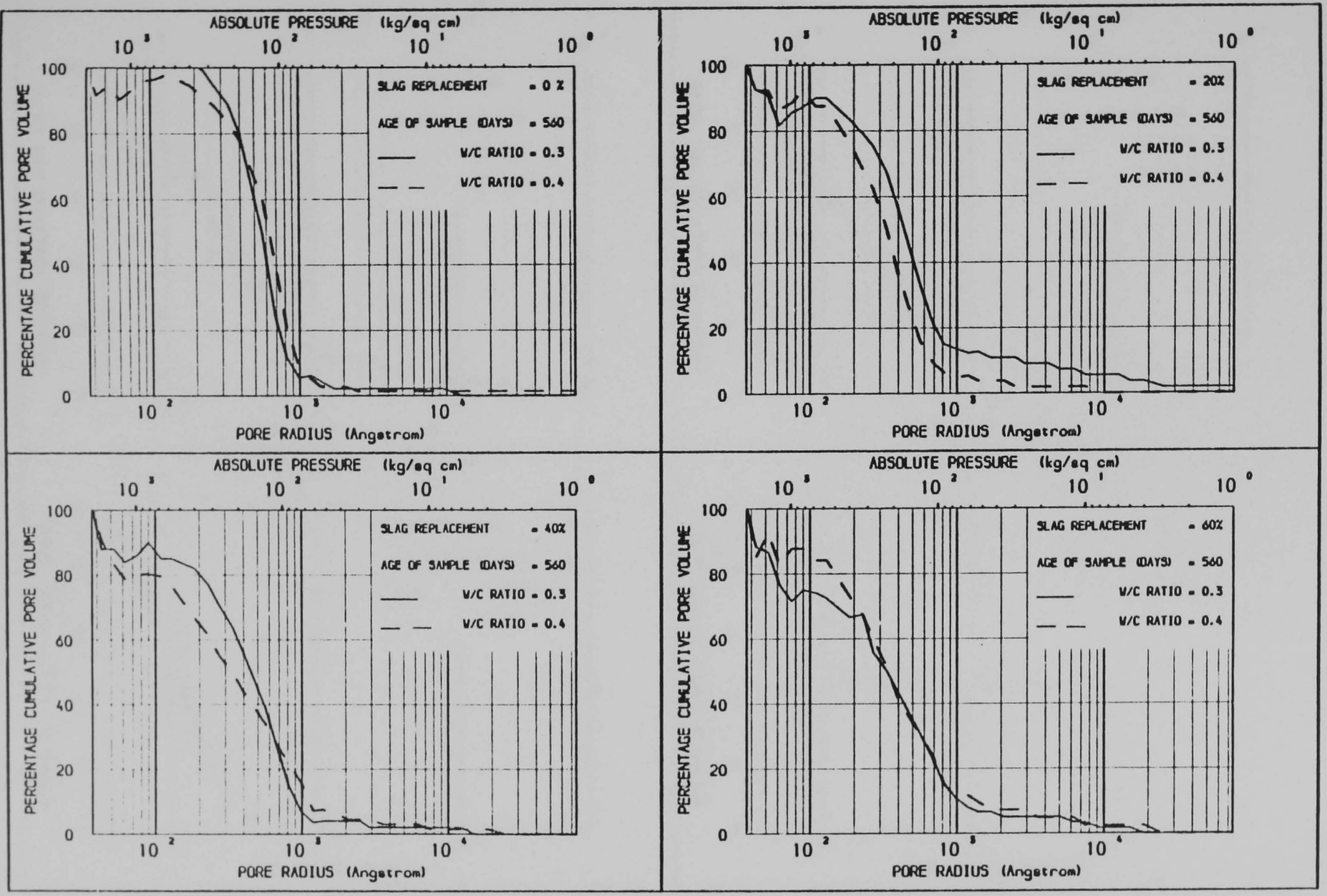

Figure 4.15 THE EFFECT OF BLASTFURNACE SLAG REPLACEMENT OF CEMENT ON PORE SIZE DISTRIBUTION

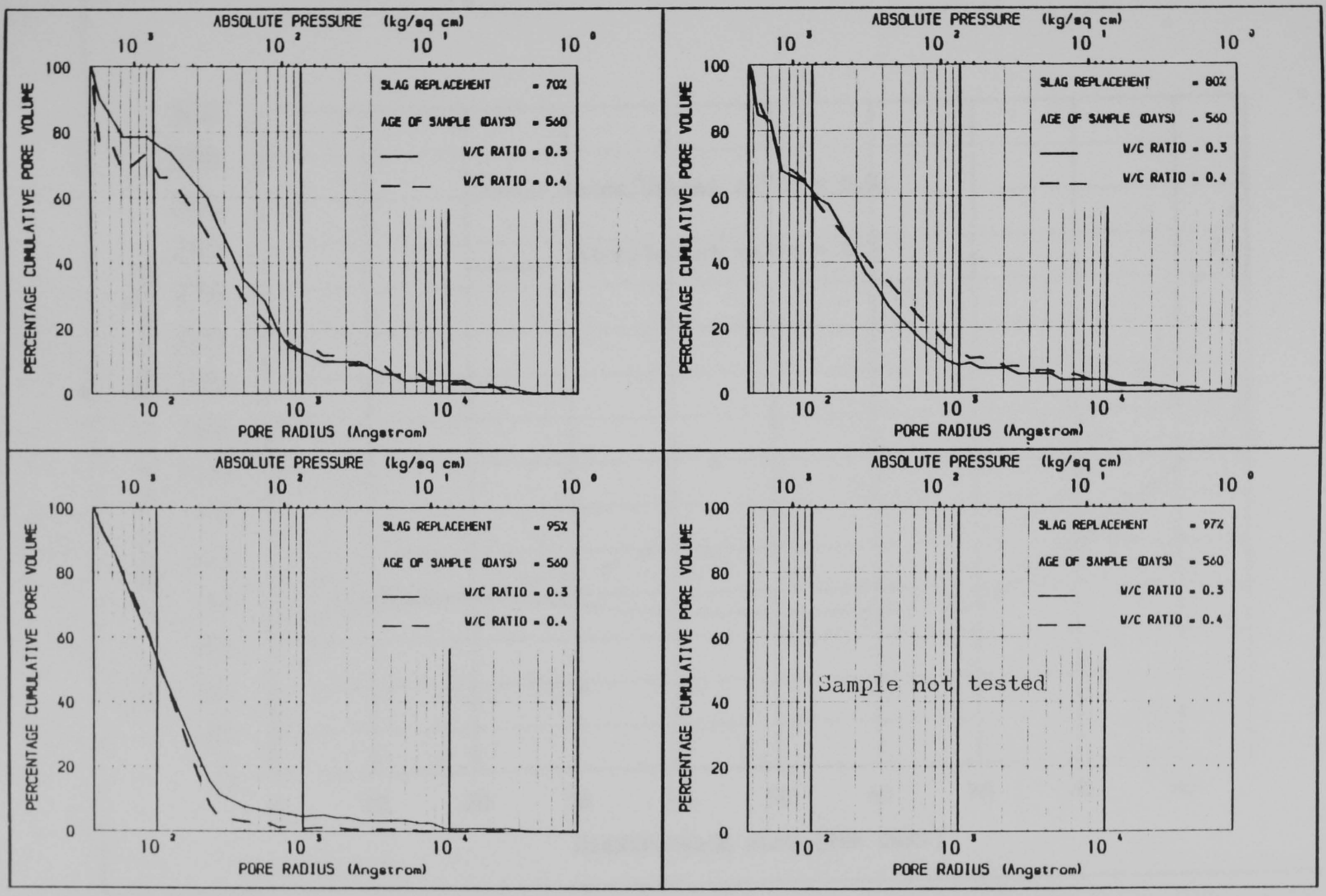

Figure 4.16 THE EFFECT OF BLASTFURNACE SLAG REPLACEMENT OF CEMENT ON PORE SIZE DISTRIBUTION

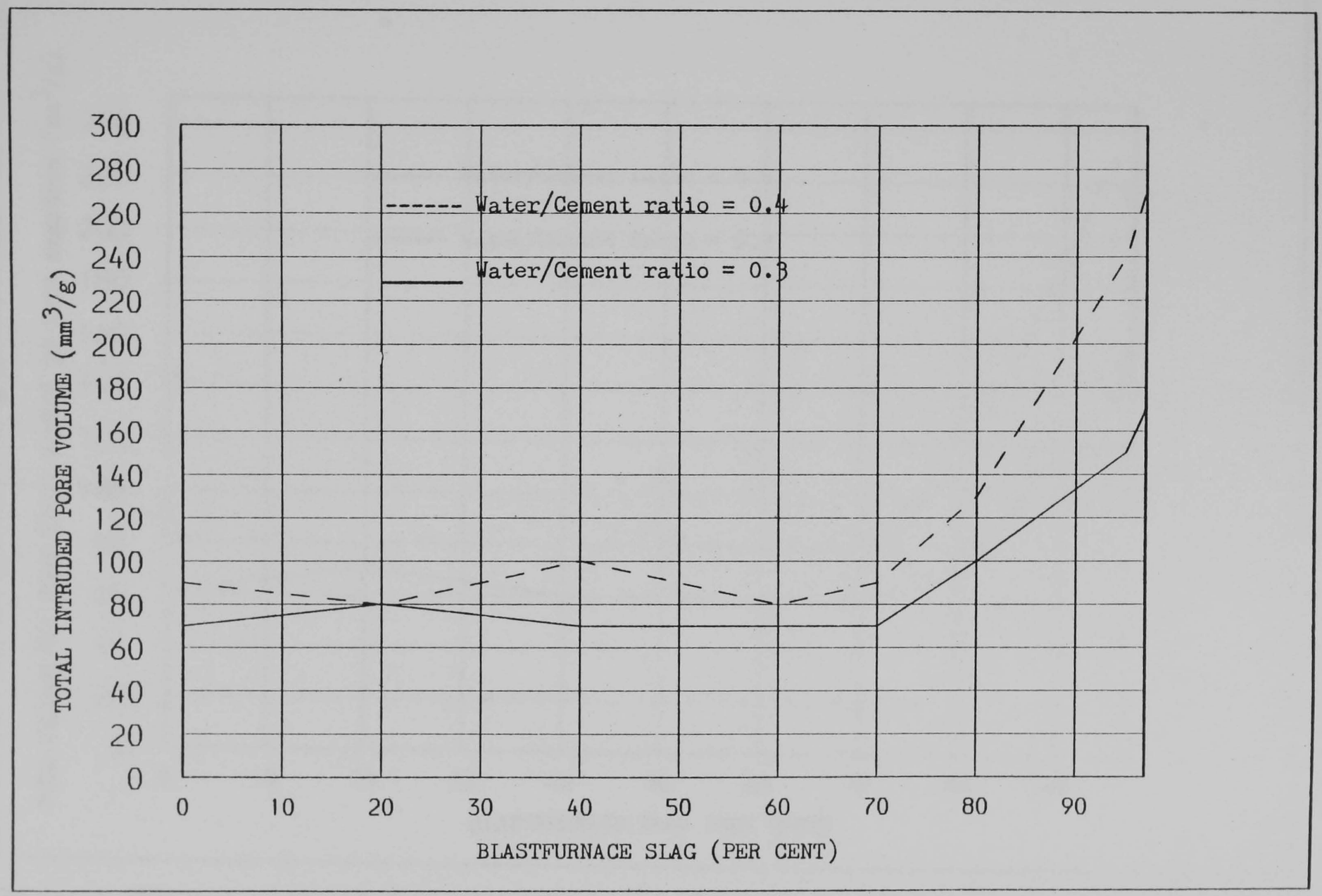

Figure 4.17 Effect of Blastfurnace slag replacement of cement on total intruded pore volume at age 270 days.

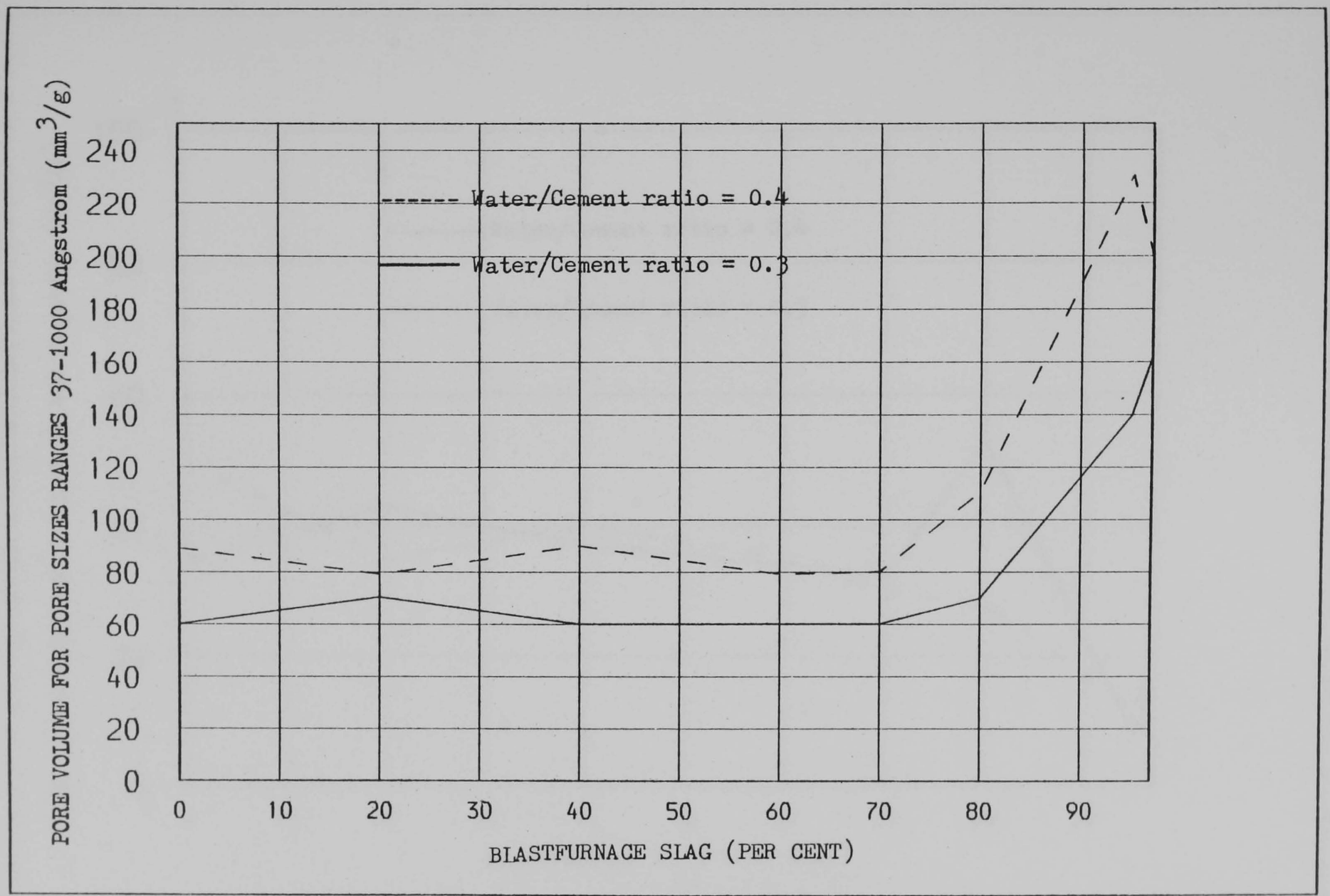

Figure 4. 18 Effect of Blastfurnace slag replacement of cement on pore volume for sizes ranges 37-1000 Angstrom at 270 days.

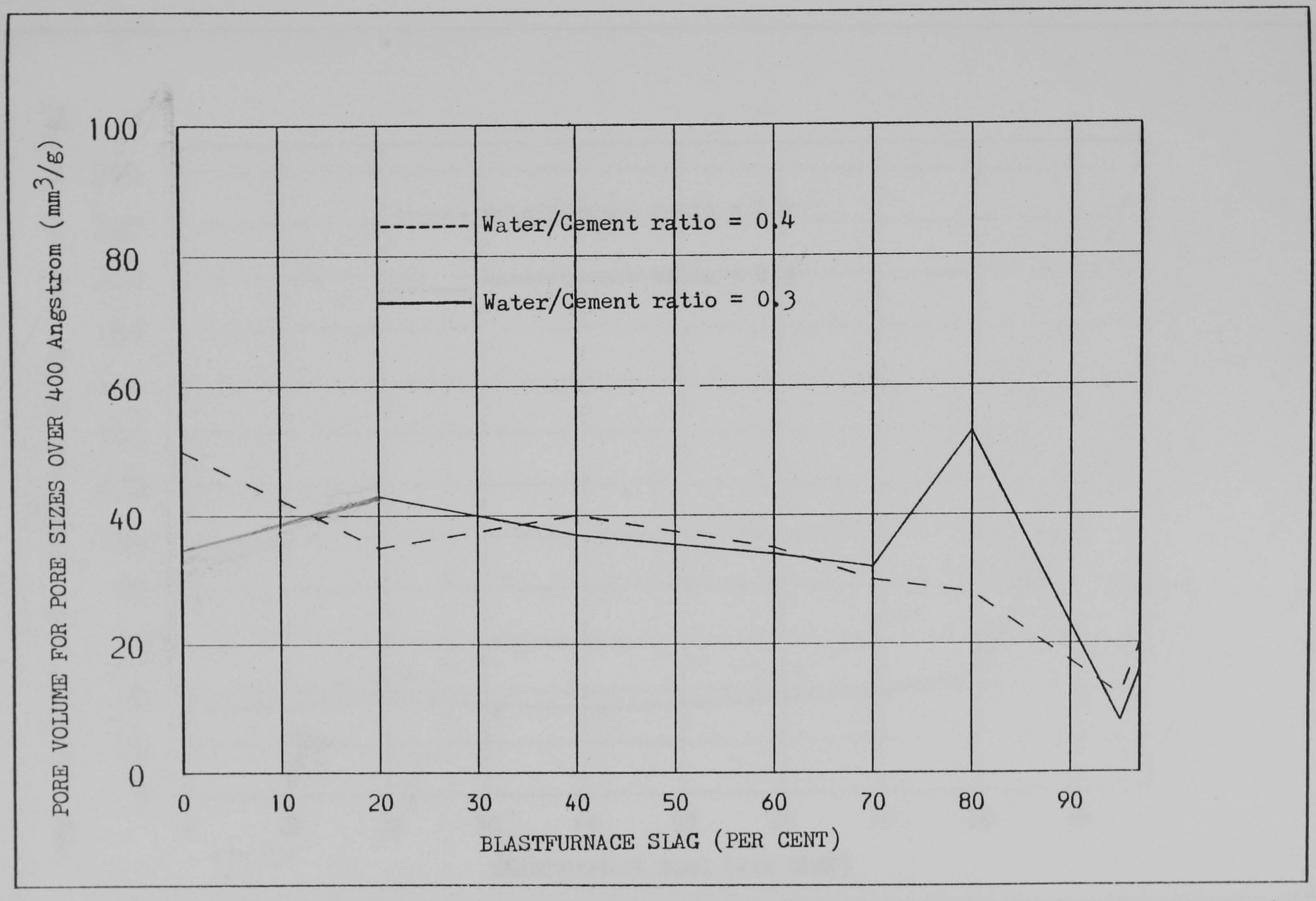

Figure 4.19 Effect of Blastfurnace slag replacement of cement on pore volume for pore sizes over 400 Angstrom at age 270 days.

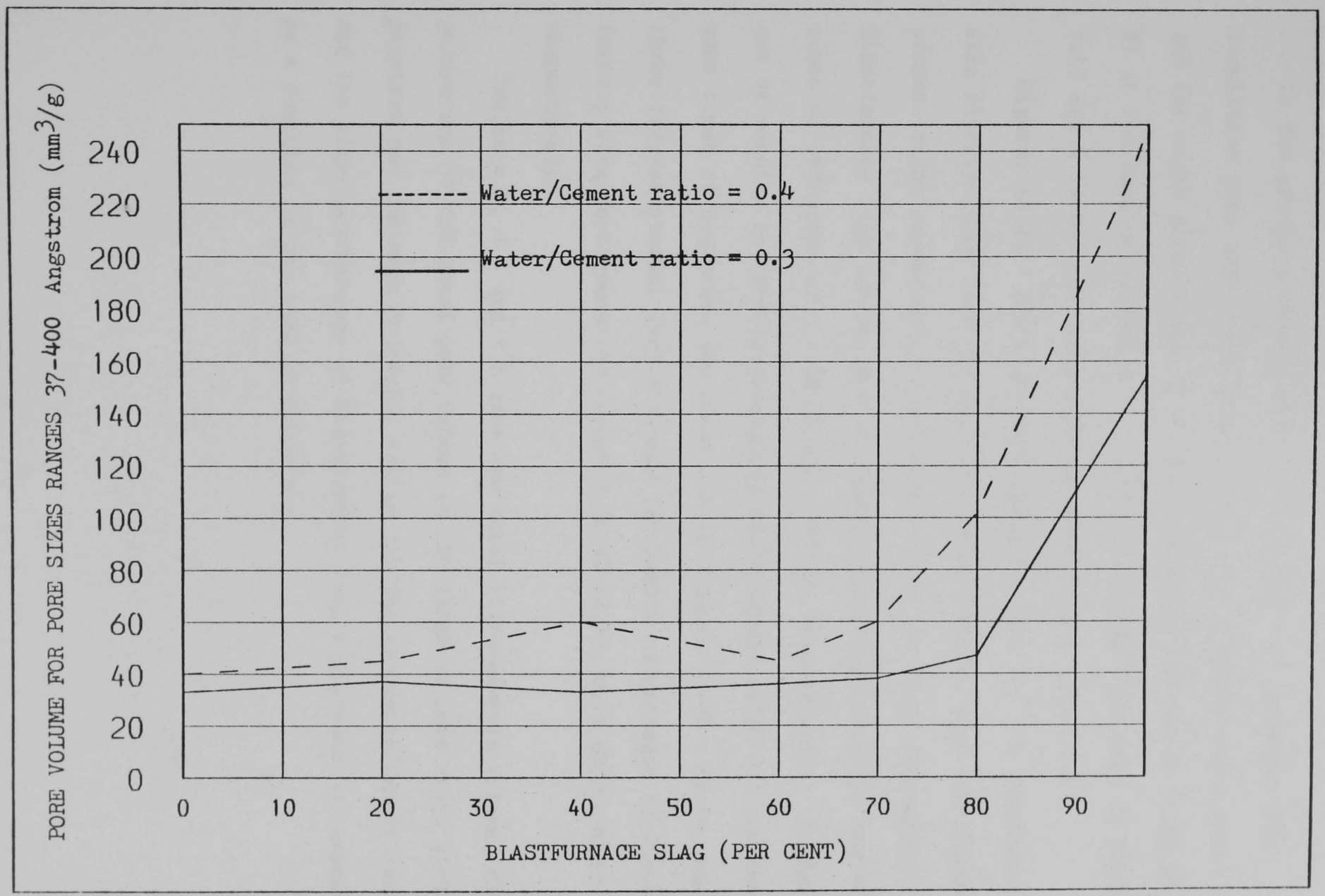

Figure 4.20 Effect of Blastfurnace slag replacement of cement on pore volume for pore sizes ranges 37- 400 Angstrom at age 270 days.

4.1.2.1 EFFECT OF AGE

In the previous section Figures 4.11 and 4.12 represent the cumulative pore size distribution curves for a water/cement ratio 0.3 and for eight percentages of Blastfurnace slag 0,20,40,60,70,80,95 and 97 at 560 days of hydration. A similar set is presented in Figures 4.13 and 4.14 for the corresponding water/cement ratio 0.4.

Figures A3.26 - A3.35 present remaining data for the cumulative pore size distributions for the 0.3 water/cement ratio, each two figures present eight frames A,B,C,D,E,F,G and H for the eight percentages of Blastfurnace slag replacement of cement, 0,20,40,60,70,80,95 and 97 and times of hydration of 3,7,28,90 and 270 days respectively. A similar set of results for the corresponding water/cement ratio 0.4 and the same times of hydration are presented in Figures A3.36 - A3.50, each three figures present twelve frames for twelve percentages of Blast-furnace slag replacement of cement 0,20,40,60,65,70,75,80,85,90,95 and 97 respectively.

Tables 4.5, 4.6 and 4.7 give the total intruded pore volume, the percentage of the total pore volume in the range of pore radii 37-1000 Angstrom and the mean hydraulic radius for the two water/cement ratios and the eight percentages of Blastfurnace slag replacement of cement as a function of the time of hydration.

4.1.2.2. TOTAL POROSITY

The mean values of porosities obtained from the oven dried weight losses are presented in Table 4.8. The porosities are given as the total measurable pore volume per gram of oven dried sample.

It can be seen that the total porosity increases with Blastfurnace slag replacement and decreases with increasing time of hydration.

Table 4.8 gives the total intruded pore volume for each paste. Once again this is in all cases less than the total porosity. The total intruded pore volume expressed as a percentage of the total porosity is also given and again this percentage could be regarded as the percentage of capillary pores to total pores and the difference between the total porosity and the total intruded pore volume could be regarded as gel pores. The data is discussed in more detail in the next chapter.

Time of hydration days		3	7	28	90	270	560
slag (per cent)	W/C ratio	Total intruded pore volume (mm^3/g)					
0	0.3	140	120	90	80	70	60
	0.4	180	160	130	130	90	100
20	0.3	150	130	90	80	80	70
	0.4	180	180	140	120	80	60
40	0.3	160	130	90	70	70	60
	0.4	230	170	130	130	100	100
60	0.3	160	150	80	70	70	70
	0.4	250	190	180	120	80	60
70	0.3	170	130	90	80	70	60
	0.4	270	150	170	130	90	60
80	0.3	180	170	120	110	100	80
	0.4	290	220	210	180	130	100
95	0.3	210	210	200	180	150	160
	0.4	300	270	280	260	240	210
97	0.3	250	230	220	210	170	
	0.4	310	300	300	280	270	

Talbe 4.5 Effect of Blastfurnace slag replacement of cement on total intruded pore volume

Time of hydration days		3	7	28	90	270	560
slag (per cent)	W/C ratio	(Sizes lower than 1000 Angstrom / total intruded pore volume) %					
0	0.3	64	83	89	88	86	95
	0.4	61	75	70	77	99	91
20	0.3	87	88	89	88	88	87
	0.4	67	78	72	67	99	95
40	0.3	69	92	90	86	86	93
	0.4	43	53	77	70	90	84
60	0.3	99	80	99	86	86	89
	0.4	36	58	78	99	99	89
70	0.3	47	79	67	65	86	87
	0.4	41	73	82	77	89	87
80	0.3	56	56	92	91	70	92
	0.4	35	99	90	89	85	87
95	0.3	86	93	95	89	93	95
	0.4	40	52	54	54	96	99
97	0.3	72	90	95	95	95	
	0.4	45	60	67	61	74	

Table 4.6 Effect of Blastfurnace slag replacement of cement on substantial pore volume (sizes lower than 1000 Angstrom).

Time of hydration days		3	7	28	90	270	560
slag (per cent)	W/C ratio	Mean hydraulic radius (Angstrom)					
0	0.3	20472	9287	9295	12229	10169	9196
	0.4	20320	14180	14165	13748	8658	8359
20	0.3	16130	11902	9953	10119	10169	9196
	0.4	17761	16090	12885	12414	8539	8360
40	0.3	18379	13236	9457	12197	11265	8491
	0.4	18829	23578	10829	8426	7539	6671
60	0.3	10251	7369	8820	8849	11265	6227
	0.4	19629	13927	10383	9559	7182	7809
70	0.3	11918	10343	8772	6849	7735	4610
	0.4	22260	15743	8929	7049	6045	5737
80	0.3	8774	16611	5275	5844	8975	6955
	0.4	16029	14633	7392	7057	4747	5320
95	0.3	8813	6999	5661	6952	5064	4188
	0.4	14544	12812	13199	11712	4853	4271
97	0.3	10724	8759	7349	5695	6297	
	0.4	18387	15302	12711	13224	6977	

Table 4.7 Effect of Blastfurnace slag replacement of cement on mean hydraulic radius.

Total pore volume			water porosity		Hg intruded	
slag (per cent)	time of hydration days	dry density kg/m^3	per cent	mm^3/g	mm^3/g	capillary porosity % of total porosity
0	28	1663	30.9	186	130	69.8
	270	1663	26.1	157	90	57.3
20	28	1610	32.6	202	140	69.3
	270	1610	25.4	158	80	50.6
40	28	1552	32.8	211	130	61.6
	270	1552	28.2	182	100	54.9
60	28	1513	43.4	287	180	62.7
	270	1513	27.8	184	80	43.5
65	28	1507	43.9	291	160	55.0
	270	1507	28.2	187	90	48.1
70	28	1499	46.8	312	170	54.5
	270	1499	28.6	191	90	47.1
75	28	1493	44.8	300	190	63.3
	270	1493	29.9	200	100	50.0
80	28	1492	47.7	320	210	65.6
	270	1492	32.5	218	130	59.6
85	28	1485	47.8	322	220	68.3
	270	1485	39.5	266	170	63.9
90	28	1468	48.3	329	250	76.0
	270	1468	45.5	310	210	67.7
95	28	1446	49.2	340	280	82.4
	270	1446	44.8	310	240	77.4
97	28	1442	50.8	352	300	85.2
	270	1442	48.7	338	270	80.0

Table 4.8 Effect of Blastfurnace slag replacement of cement on total and capillary porosities at 0.4 water/cement ratio.

4.2 WATER PERMEABILITY

Water permeability was determined for the cement pastes containing the varying proportions of Fly ash or Blastfurnace slag. Water/cement ratios of 0.3 and 0.4 were used and times of hydration of 28 and 270 days.

4.2.1 EFFECT OF FLY ASH REPLACEMENT OF CEMENT ON WATER PERMEABILITY

Figure 4.21 shows the coefficients of permeability for water/cement ratios of 0.3 and 0.4 for Fly ash replacement levels of 0,5,10,20,40, 60,70 and 80 per cent at 28 days of hydration. A similar set of results is presented in Figure 4.22 for 270 days of hydration. Table 4.9 presents the same data but enables a comparison between the coefficients of water permeability at 28 and 270 days of hydration to be made. Each point is the average of at least 3 tests. Occasionally some test results were found to show a very high or very low permeabilities. These were assumed to be due to leakage past the sample or blockage of the flow lines respectively. In calculating average permeabilities such results have been ignored with the exception of these results permeabilities from duplicate runs varies by a maximum of $\sim$ 10 per cent.

A general observation that can be made on the appearance of the curves is that there is little effect on the permeability below 10 per cent Fly ash replacement. Above this level the coefficient of permeability decreases gradually with increasing Fly ash replacement of cement up to 40 per cent. Above 60 per cent the permeability sharply increases with increasing Fly ash replacement for 28 and 270 days of hydration and for both the water/cement ratios.

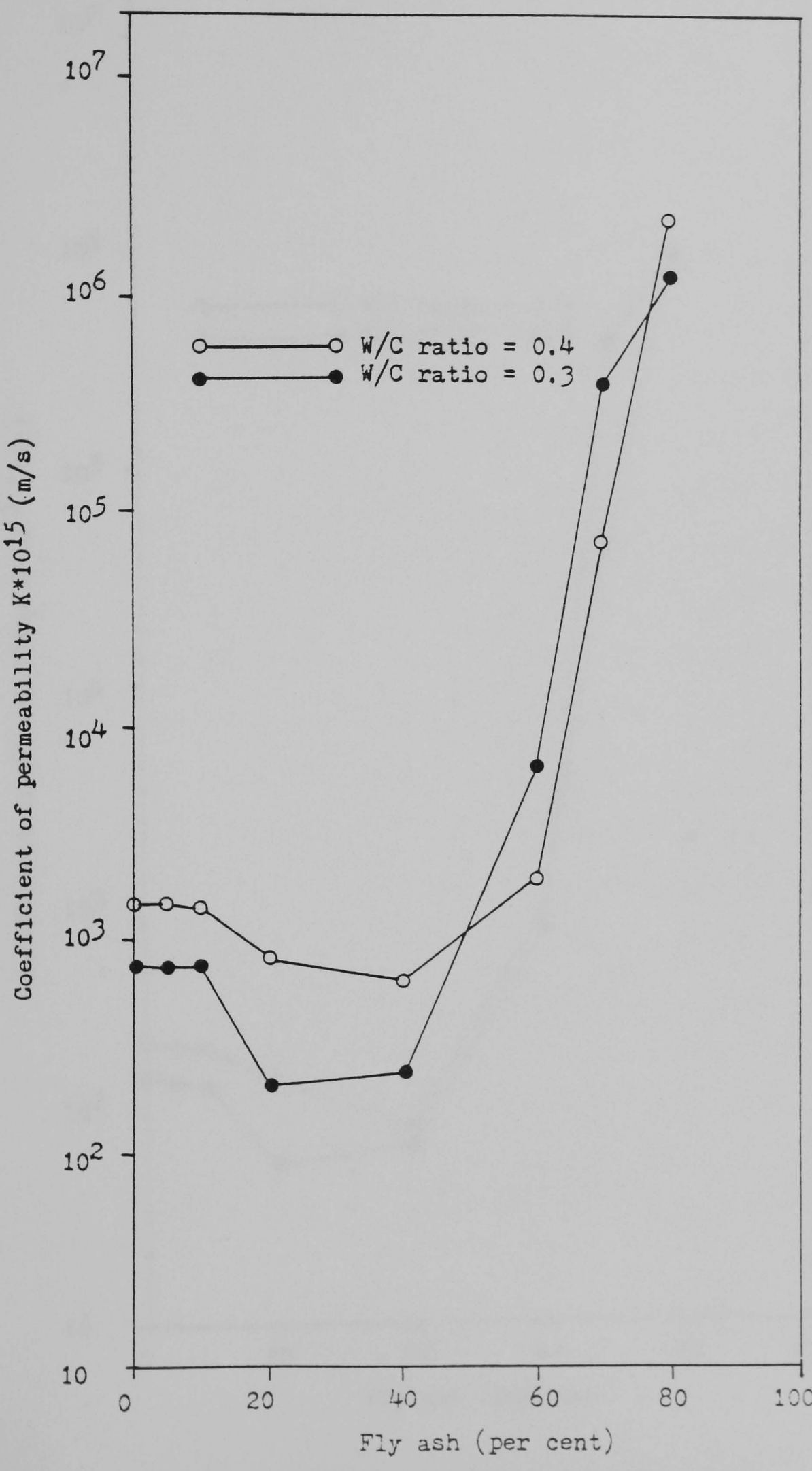

Figure 4.21 Effect of Fly ash replacement of cement on coefficient of permeability at age 28 days.

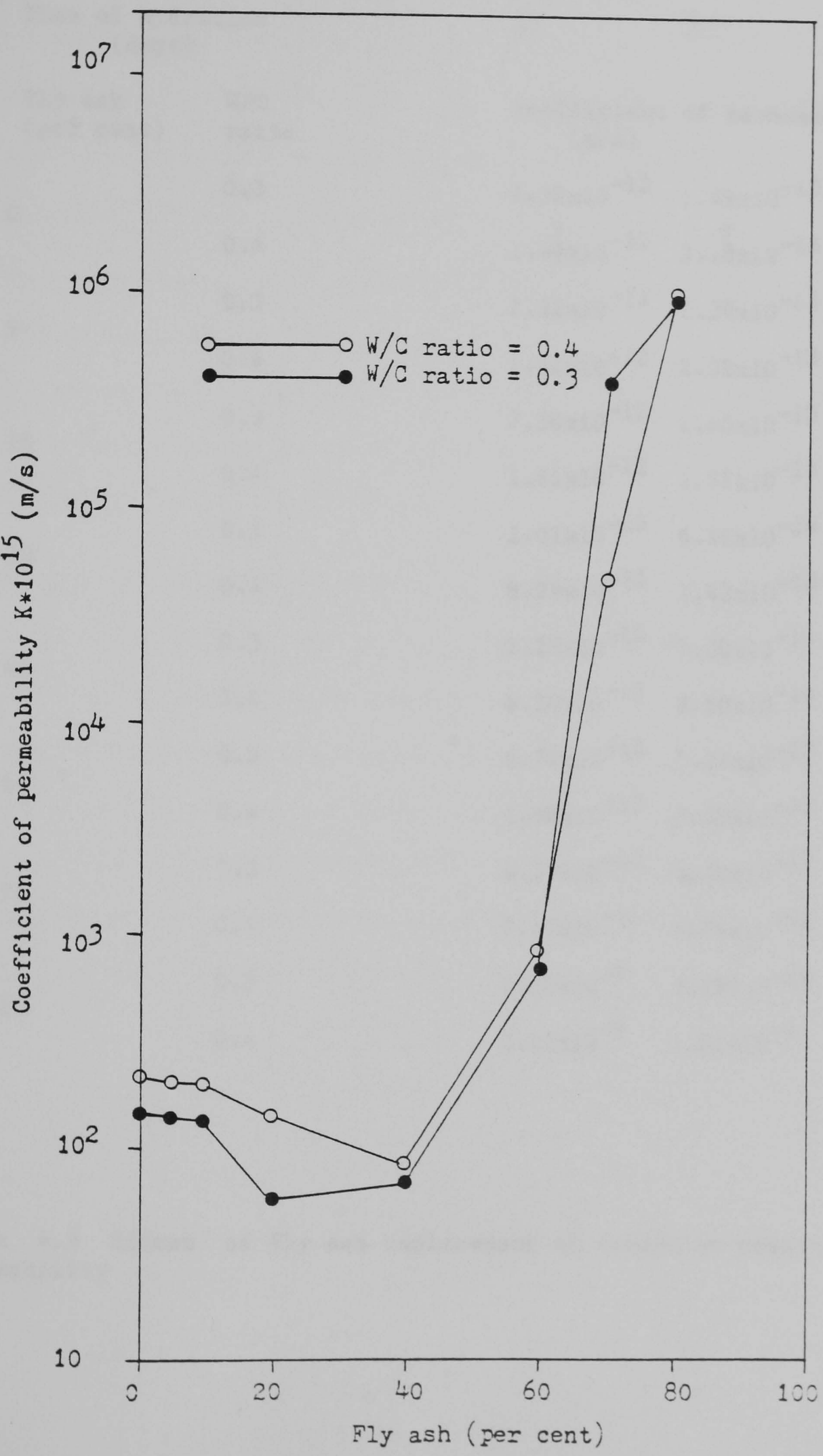

Figure 4.22 Effect of Fly ash replacement of cement on coefficient of permeability at age 270 days.

Time of hydration (days)		28	270
Fly ash (per cent)	W/C ratio	coefficient of permeability (m/s)	
0	0.3	7.32×10^{-13}	1.49×10^{-13}
	0.4	1.49×10^{-12}	2.16×10^{-13}
5	0.3	7.31×10^{-13}	1.39×10^{-13}
	0.4	1.52×10^{-12}	2.02×10^{-13}
10	0.3	7.30×10^{-13}	1.40×10^{-13}
	0.4	1.41×10^{-12}	1.97×10^{-13}
20	0.3	2.01×10^{-13}	6.10×10^{-14}
	0.4	8.24×10^{-13}	1.42×10^{-13}
40	0.3	2.23×10^{-13}	7.00×10^{-14}
	0.4	6.24×10^{-13}	8.50×10^{-14}
60	0.3	6.71×10^{-12}	7.21×10^{-13}
	0.4	1.98×10^{-12}	8.33×10^{-13}
70	0.3	4.39×10^{-10}	4.02×10^{-10}
	0.4	7.11×10^{-11}	4.74×10^{-11}
80	0.3	1.22×10^{-9}	9.99×10^{-10}
	0.4	2.17×10^{-9}	1.01×10^{-9}

Table 4.9 Effect of Fly ash replacement of cement on coefficient of permeability

4.2.2 EFFECT OF BLASTFURNACE SLAG REPLACEMENT OF CEMENT ON WATER PERMEABILITY

Figure 4.23 shows the coefficients of permeability for the two water/cement ratios and the eight percentages of Blastfurnace slag replacement 0,20,40,60,70,80,95 and 97, at 28 days of hydration. A similar set of results are presented in Figure 4.24 for the corresponding 270 days of hydration.

Again the data is also presented in Table 4.10 for comparison purposes between the two ages.

As for the Fly ash results represented in Section 4.2.1. The plotted points are average of at least 3 determination and exclude any obviously high or low results.

The general observations that can be made on the appearance of the curves are that there is little effect on the permeability below 40 per cent Blastfurnace slag replacement. The coefficient of permeability decreases gradually with increasing Blastfurnace slag replacement between 40 and 80 per cent. Above 80 per cent the permeability increases with increasing Blastfurnace slag replacement for 28 and 270 days of hydration and for the two water/cement ratios. Again the data is discussed in detail in Chapter Five.

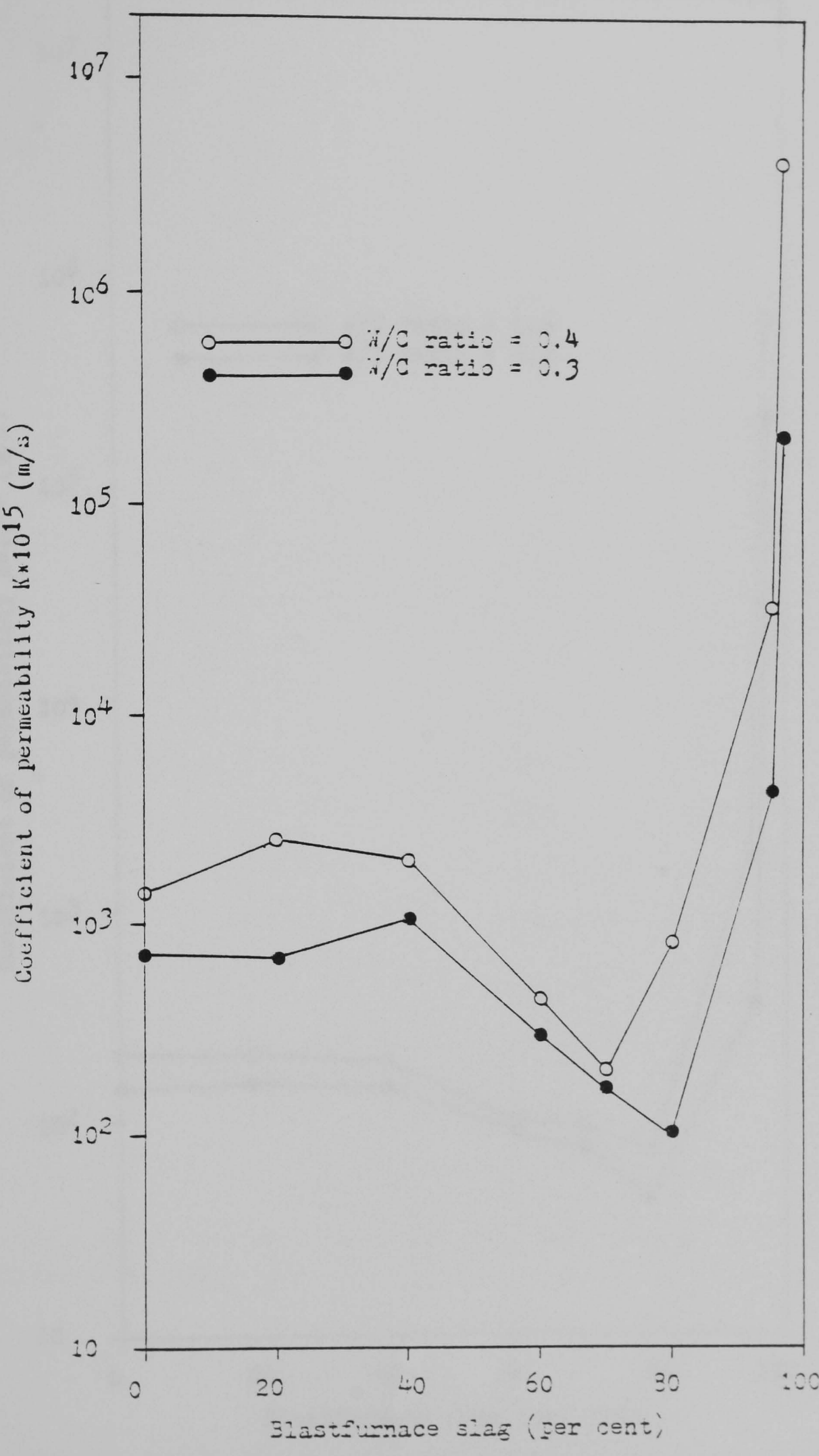

Figure 4.23 Effect of Blastfurnace slag replacement of cement on coefficient of permeability at age 28 days.

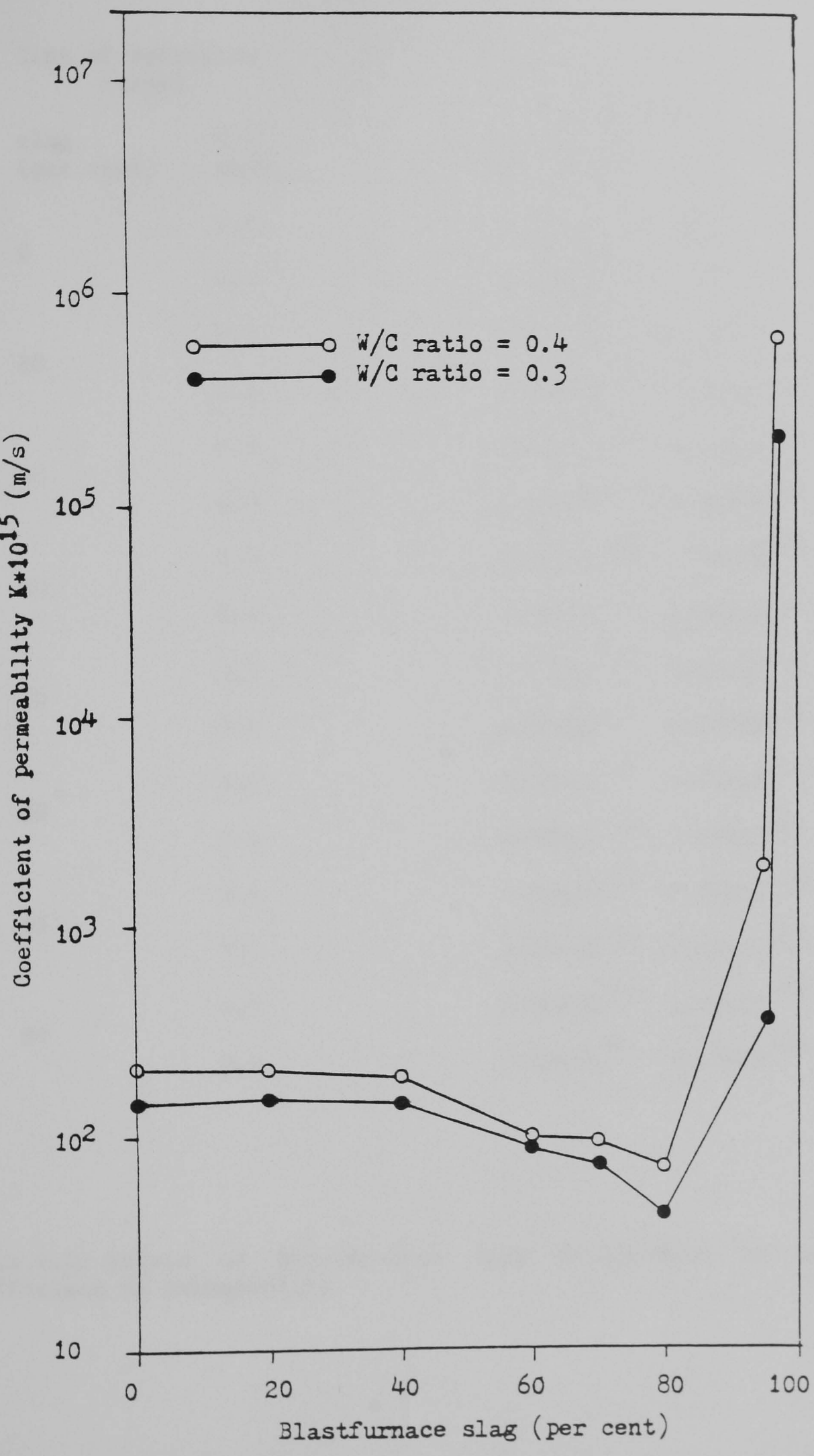

Figure 4.24 Effect of Blastfurnace slag replacement of cement on coefficient of permeability at age 270 days.

Time of hydration (days)		28	270
slag (per cent)	W/C ratio	Coefficient of permeability (m/s)	
0	0.3	7.32×10^{-13}	1.49×10^{-13}
	0.4	1.48×10^{-12}	2.14×10^{-13}
20	0.3	7.01×10^{-13}	1.57×10^{-13}
	0.4	2.69×10^{-12}	2.12×10^{-13}
40	0.3	1.01×10^{-12}	1.50×10^{-13}
	0.4	2.06×10^{-12}	2.06×10^{-13}
60	0.3	4.42×10^{-13}	9.70×10^{-14}
	0.4	4.46×10^{-13}	1.00×10^{-13}
70	0.3	1.65×10^{-13}	8.00×10^{-14}
	0.4	2.05×10^{-13}	9.80×10^{-14}
80	0.3	1.07×10^{-13}	4.70×10^{-14}
	0.4	8.63×10^{-13}	7.60×10^{-14}
95	0.3	4.45×10^{-12}	1.36×10^{-12}
	0.4	3.26×10^{-11}	2.08×10^{-12}
97	0.3	2.00×10^{-10}	2.24×10^{-10}
	0.4	4.36×10^{-9}	6.49×10^{-10}

Table 4.10 Effect of Blastfurnace slag replacement of cement on coefficient of permeability.

CHAPTER FIVE

DISCUSSION, CONCLUSIONS AND FURTHER WORK

CHAPTER FIVE

DISCUSSION, CONCLUSIONS AND FURTHER WORK

5.1 DISCUSSION

The effects on the pore volume, pore size distribution and water permeability of hardened cement pastes of replacing varying proportions of the cement by Fly ash or ground granulated Blastfurnace slag have been presented in the previous chapters. In the following section a general discussion and the main implications of the results will be given.

5.1.1. GENERAL DISCUSSION

The pure Fly ash showed almost no tendency to set when mixed with pure water and possessed virtually no cementing activity, a result in accordance with Lea (1980) and Neville (1981). Furthermore, above 80 per cent replacement by Fly ash, there was little cementing activity of the mix. The rate of initial hydration reactions was higher when pure Ordinary Portland cement was used than a mix containing Fly ash. The Fly ash was also found to cause a decrease in the compressive strength of hardened cement pastes with water/cement ratio 0.4 at 270 days of hydration (Figure 2.3); such results are again in accordance with Lea (1980) and Neville (1981). The latter investigators considered that the lower temperature reached during hydration retarded the development of strength at ages up to about a year, and also observed the loss in strength of mixes with high replacement levels, over 40 per cent Fly ash replacement giving a reduction of strength at all ages.

For replacement levels of Ordinary Portland cement by Fly ash of less than 10 per cent the physical properties of the resulting cement

paste were little altered (Yoshil et al.1958). In the present research when the cement has been replaced by Fly ash it has been over the range 5 to 80 per cent by weight of the mixture.

Just as for Fly ash, no hydration products can be observed when ground granulated Blastfurnace slag is mixed with pure water. This lack of cementitious properties agrees with the data of Lea (1980) and Lee (1974). A mix containing more than 97 per cent Blastfurnace slag showed hardly any cementing activity and again the rate of initial hydration reactions was higher when pure cement was used, results again agreeing with the data cited. Figure 2.5 shows the compressive strength increases gradually with increasing Blastfurnace slag replacement up to 70 per cent. Above 80 per cent the compressive strength reduced sharply for samples cured under water for 270 days. The effect of the fineness of ground granulated Blastfurnace slag possibly leads to a reduction of the water/solid ratio and hence to increase of compressive strengths at replacement levels up to 80 per cent.

Replacing Portland cement by less than 20 per cent of Blastfurnace slag had little effect on compressive strength of mortars Lea (1980) and similar results were found here (Figure 2.5) for cement pastes. Consequently, in the present investigation, where the permeability and porosity characteristics of Blastfurnace slag replaced cement have been studied, the replacement has been over the range 20 to 97 per cent by weight of the mixture.

Bleeding data for the various mixes is given in Figures 1.6, 1.7, 1.8, 1.9 and 1.10 for cement pastes having water/cement ratios of 0.3 and 0.4. These show that the bleeding rate decreases with increasing Fly ash or ground granulated Blastfurnace slag replacement by weight of the cement. Bleeding rate also decreases with reduction of water/cement ratio from 0.4 to 0.3. The specific gravity of both these materials are generally lower than Ordinary Portland Cement, and hence for a given water/cement ratio more solids are available on a volumetric basis in comparison

to the water in the replaced cements. Other effects operate which may reduce the bleeding rates: Blastfurnace slag is finer than Ordinary Portland cement and so a greater surface area is available to absorb water,and the spherulitic material in Fly ash which improves the workability often contains spheres which are hollow thus presenting the water with a large surface area for hydration reactions. The improved bleeding of the replaced cements reported here agrees with the discussion of Lea 1980.

Powers (1968) quotes 2.20×10^{-4} cm/sec bleeding rate as the limit above which channelling may occur in cement paste; bleeding rate is the slope of the initial linear part of the bleeding versus time curve. From the present data it can be seen that for a Fly ash or Blastfurnace slag replaced cement mix, the maximum limit of bleeding rate quoted above was not exceeded and so the bleeding rates employed in the present investigation were low enough not to cause any damage by channelling.

Table 1.1 shows the temperature rise during the first 25 hours of hydration of the test samples of the various mixes. The peak temperature is reduced and the time elapsing between placing the cement and achieving the peak increased with increasing Fly ash or Blastfurnace slag replacement of the cement and with increasing water/cement ratio. It may be noted that the lower temperature rise produces a lower thermal expansion. In addition the thermal expansion of pure cement pastes is about $8\text{-}10 \times 10^{-6}$ per ^{o}F, whereas Fly ash or Blastfurnace slag, have expansions as low as $1\text{-}3 \times 10^{-6}$ per ^{o}F, which can further improve the durability of the mix (Lea 1980).

From the point of view of bleeding, mixes at water/cement ratios 0.3 and 0.4 with 5-80 per cent Fly ash replacement or 20-97 per cent Blastfurnace slag replacement appeared stable. Such mixes were therefore used for the determination of pore volume, pore size distribution and water permeability in the present investigation.

5.1.2 PORE VOLUME AND PORE SIZE DISTRIBUTION

In order to calculate the true volume intrusion of mercury into the pores of the sample, a correction was made for the compressibility of the mercury and the system (see Section 3.2.2.2.2 and Figure 3.4). In theory a correction ought to be made to the observed intrusion to account for the compressibility of the solid component of the sample excluding the pores, but at present a method has not been developed so far for doing this. Winslow and Diamond (1970) stated that typical values of the compressibility of most reasonably strong solids would suggest that the volume change from zero to 1000 kg/cm^2 would in fact be negligible in comparison with the volume of mercury intruded into the cement paste; interpretation of the present data requires some allowance for this effect above pressures of 1000 kg/cm^2 and is discussed later, although for the purpose of comparing one sample with another in this investigation the effect has been neglected.

In the investigation by Ritter and Drake (1945), the pore radius was limited to a minimum of 100 Angstroms, because in their view neither the concept of surface tension nor of contact angle is strictly applicable to smaller pore sizes. As hydrated cement is so heterogenous a single contact angle for all the phases present is probably not valid, further it is possible that the contact angle changes with the pressure. Using a value of contact angle of 140 degrees (Ritter and Drake, 1945) as a reasonable average for most materials, it can be seen that a 1 degree error in this contact angle leads to 1.5 per cent error in the pore radius value calculated since:

$$Pr = -2\gamma \cos\Theta$$

$$Pdr = 2\gamma \sin\Theta \, d\Theta$$

$$\frac{Pdr}{P} = \frac{2\gamma \sin\Theta \, d\Theta}{-2\gamma \cos\Theta / r}$$

$$\frac{dr}{r} = -d\Theta \tan\Theta$$

therefore

$$\frac{\Delta r}{r} = -\Delta\Theta \tan\Theta$$

For the apparatus used in this investigation the maximum pressure attainable was 2000 kg/cm^2 corresponding to a pore radius of 37 Angstrom. The various effects which might cast doubt on the validity of pore size measurements less than 100 Angstrom are discussed in more detail later in this chapter.

Mikhail et al. (1975) mentioned that the high pressures used in mercury porosimetry could lead to deformation or even destruction of the pores. Thus in the high pressure region there may be errors due to crushing of the sample or possibly changes in the contact angle. In some curves in the present investigation the mercury was found to enter the sample rather rapidly at high pressure giving rise to the idea that the sample contained many fine pores of small radius, see for example Figures 4.6 and 4.16; this phenomenon could be explained, however, by a sudden flow of mercury into an internal cavity previously empty, whose walls have been broken by the mercury pressure. Additionally another effect is considered under Section 5.3.

In contrast to a sudden increase in the mercury intruded volume as the pressure is increased, it is quite possible to observe a negative intruded volume, ie. as the pressure is increased above a certain value mercury is actually expelled from the sample. This is seen in most of the Figures 4.1-4.4, A3.1-A3.25 for Fly ash replaced cement, and in most of the Figures 4.11-4.14, A3.26-A3.50 for Blastfurnace slag replaced cement. It might be the case that such an effect reduces the

total intruded pore volume if it is due to the destruction of pores. The exact mechanism of what is taking place is difficult to understand. If the radius of a pore is r and its length be L a small decrease in radius Δr, may squeeze out a volume $2\pi r\Delta rL$ of mercury with little overall change in volume; more drastically a decrease in the radius of a pore would increase the pressure required to keep the mercury within the pore, and if this rises above the external applied pressure then all the mercury of volume $\pi r^2 L$ might flow back out of the pore with a consequent increase in overall volume. The problems of non-cylindrical pores adds to the difficulties and are considered later under Section 5.3

If a negative intrusion of mercury is indicative of a mechanical weakness of the pore structure, the figures listed above, in particular Figures A3.9, A3.10, A3.23, A3.24, A3.25, A3.34, A3.35, A3.48, A3.49 and A3.50 show that the strength of the pore systems (which is evidently not related to the compressive strengths) generally increases with increasing Fly ash or Blastfurnace slag replacement. This is possibly due to the hydration reaction of Fly ash or Blastfurnace slag with the calcium hydroxide produced during Ordinary Portland cement hydration as these reactions transform the weak and soluble calcium hydroxide into a gel product, which otherwise could be leached out during curing to leave a voided structure.

The effect of increasing time of hydration upon total intruded pore volume was always to decrease the latter, irrespective of the level of replacement by Fly ash or by Blastfurnace slag and applied for both the water/cement ratios of 0.3 and 0.4. Data for Fly ash and Blastfurnace slag replacements is given in Tables 4.1 and 4.5 respectively. In the later stages of hydration from 270 to 560 days the change in total intruded volume is not very great, the decrease being more marked in the earlier stages of hydration. Increasing the water/cement ratio from 0.3 to 0.4 increased the total intruded pore volume in all cases. These

results are expected on the general consideration that the hydration products occupy more volume than that occupied by the cement grains they replace and thus they tend to fill the space originally filled with water.

Generally the total intruded pore volume increased with increasing Fly ash or Blastfurnace slag replacement although the increase became more pronounced at the higher levels of replacement. Figure 4.7 indicates that as the Fly ash replacement is increased, the total pore volume increased for the two water/cement ratios at 270 days of hydration, the total intruded pore volume increasing more sharply beyond 60 per cent replacement. Data for Blastfurnace slag, given in Figure 4.17, indicates little change in the total intruded pore volume up to replacement levels of 70 per cent, but greater than 70 per cent replacement resulted in a sharp increase in the total intruded pore volume. At high replacement levels it is possible that the lime produced by the hydration of the Ordinary Portland cement is not sufficient to react with the excessive quantity of replacement material, giving rise to an increase in the total intruded pore volume observed (Lea 1980).

Auskern and Horn (1973) observed that the pore sizes with radii less than a 1000 Angstrom in pure cement pastes represented the substantial pore volume at all ages. A similar effect was observed in the Fly ash and Blastfurnace slag replaced cements studied here, particularly at the greater ages. Data for Fly ash is presented in Table 4.2 and Figure 4.8. The ratio of cumulative pore volume with pore sizes less than 1000 Angstrom to the total pore volume is substantial at all ages, but while this ratio decreases with high levels of Fly ash replacement (which accompanies the decrease in compressive strength) at early ages of a few days, the fine pore sizes soon increase as a percentage of total porosity as the hydration proceeds. The major pore volume in all Fly ash cement pastes is due to pores of less than 1000 Angstrom.

Similar trends for Blastfurnace slag replaced cement can be seen in Table 4.6 and Figure 4.18. At 3 days of hydration there are some fluctuations in the ratio of cumulative pore size volume below 1000 Angstrom to the total intruded pore volume but as hydration proceeded, this ratio was heading into the upper eighty and ninety percents. Hence, Blastfurnace slag replacement results in fine pore development.

The interparticle spaces present within a fixed volume of cement paste were observed to decrease in size as the proportion of hydration products increased with age at any percentage of Fly ash or Blastfurnace slag replacement. This general trend can be judged from the large amount of data illustrated quantitatively in Tables 4.3 and 4.7, where mean hydraulic radius as a function of time of hydration for the two water cement ratios and eight percentages of Fly ash or Blastfurnace slag replacements are presented. Mean hydraulic radius is a measure of average interparticle space. It is this kind of data which would be useful for making estimates of the coefficient of water permeability from theoretical considerations; for example, if it were assumed that no pores are sealed off and that they were of uniform size, the Carman-Kozeny type of equation might be applied (see Appendix 1, equation A1.10). However, it has already been indicated by Nyame (1980), the mean hydraulic radius of pure cement pastes has certain limitations because it was found to be less sensitive to differences in water/cement ratios and times of hydration than the pore size distribution. A difficulty with the mean hydraulic radius is this concept can take into account pores which are blocked but which cannot contribute to water permeability.

As already shown, the pore sizes reduce with increasing Fly ash or Blastfurnace slag replacement and with increasing hydration. The overall distribution is a shift towards the finer pore sizes when the water/cement ratio is reduced from 0.4 to 0.3, and the mercury porosimetry results, Figures 4.1-4.4, A3.1-A3.25 show that the pore volume

is concentrated in pore sizes in the range 37-400 Angstrom. These pores generally increase with increasing Fly ash replacement of the cement up to 60 per cent and with increasing time of hydration, whereas the pores larger than 400 Angstrom show a decrease in number. This trend is shown for the eight percentages of Fly ash and the two water/cement ratios at 270 days hydration in Figures 4.9 and 4.10. Examining Figure 4.9 it is clear that the pore volume over 400 Angstrom reduces with Fly ash replacement up to 60 or 70 per cent depending on water/cement ratio, above which it increases. The reverse effect is observed for pores in the range 37-400 Angstrom, which increases up to 70 per cent replacement by Fly ash for both water/cement ratios. Above a figure in the region of 60 to 70 per cent replacement by Fly ash the rapid reduction in compressive strength which occurs is possibly due not only to insufficient cement present to allow hydration of the excessive Fly ash but also to a lack of sufficient chemical reaction to homogenize the mix resulting in a gross increase in the number of pores greater than 400 Angstrom.

Figures 4.11-4.14, A3.26-A3.50 show that the pore size range 37-400 Angstrom increases with increasing percentage of Blastfurnace slag replacement of the cement and with increasing time of hydration. This typical trend is illustrated for the two water/cement ratios at 270 days of hydration in Figures 4.19 and 4.20.

Figure 4.19 shows that there is a small reduction in pore volume over 400 Angstrom with Blastfurnace slag replacement up to 70 per cent. Figure 4.20 shows that there is little change in pore volume in the range 37-400 Angstrom up to 70 per cent Blastfurnace slag replacement, above which it sharply increases.

Auskern and Horn (1973) suggested that "the gel porosity is given by the difference between the total water porosity and the mercury porosity". The general observation in the present research is that the capillary porosity decreases with increasing age of hydration and increases with increasing water/cement ratio. Such a result should be expected on the basis of the Powers model (1949) for pure cement paste who considered that as hydration proceeds, the amount and the distribution of porosity

between capillary and gel pores changes considerably. Initially all the pores are capillary pores; as hydration proceeds most of the capillary pores become filled with gel and the capillary pore volume is reduced. This trend is illustrated quantitatively in Tables 4.4 and 4.8 for the Fly ash and the Blastfurnace slag replaced cements respectively, the percentage of capillary pores to total pores decreased with increasing age of hydration for all levels of replacement. This means that the relative percentage of the gel pores increases with increasing age of hydration.

5.1.3 WATER PERMEABILITY

In order to measure the water permeability of hardened cement paste prepared at water/cement ratios 0.3 and 0.4 with 5-80 per cent Fly ash replacement or 20 - 97 per cent ground granulated Blastfurnace slag replacement at ages 28 and 270 days, a saturated sample 15 mm thick was placed between two porous end platens and then placed in the permeability cell. The specimen was sealed into a brass container with a urethane rubber jacket and two brass end plates. To eliminate leakage past the wall of the specimen a sufficiently high confining pressure was applied to the membrane to seal it to the wall of the specimen.

The water permeability of hardened cement pastes was measured with hydrostatic pressures on both sides of the specimen. This has the advantage that any trapped air, which might remain after initial evacuation, will be compressed and thus its effect on the permeability will be minimised. The difference between the upstream and downstream pressures were adjusted to give a suitable pressure difference for permeation. Also because of the very sensitive volume measurements and to ensure reproducibility of results, the apparatus was installed in a temperature controlled room set at $20^{o}C$.

As in other investigations Darcy's law has been applied to the flow of water through hardened cement pastes. Obviously, osmotic pressure could affect the values obtained but according to Powers et al. (1954) it was negligible for pure cement pastes. For Fly ash or Blastfurnace slag replaced cement the effect will again be negligible because the quantity of calcium hydroxide present is even less.

The coefficient of permeability for pure cement paste was found to decrease with increasing time of hydration and increase with water/cement ratio (Tables 4.9 and 4.10). Again such results are expected both on the basis of the Powers model for pure cement paste (1954) and on the general consideration that the chemical reactions between the constituents of cement and water progressively replace the original cement minerals with hydration products, principally cement gel. The volume the hydration products occupy is greater than that originally occupied by the cement grains they replace, and thus they tend to fill the capillary pores originally filled with water. Also according to Powers, Copeland and Mann (1959) who considered the permeability of paste in terms of capillary pores, hydration of cement increases the solid content of the paste, the original capillaries becoming blocked by gel, producing the effect of closing capillary pores within the hydration product.

To evaluate the permeability data obtained in the present investigation (Tables 4.9 and 4.10 for Fly ash and Blastfurnace slag replaced cement for water/cement ratios 0.3 and 0.4 at ages 28 and 270 days) it is useful to compare the values of permeabilities obtained for pure cement pastes with the new apparatus used here, with the data of Powers. This data (Table 1.2), is quite comparable. The general trend observed of decreasing permeability with increasing time of hydration has been explained in the previous paragraph. The ultimate values at age 270 days of the coefficient of permeability for water/cement ratios 0.3 and 0.4 were about one quarter and one third respectively of Powers'

ultimate value. His larger value of permeability is expected because of his water/cement ratio of 0.7 which develops more pores.

The experimental results also seem to give good correlation at age 270 days with the Kozeny-Carman equation (see Appendix 1, Equation A1.10). Application of the Kozeny-Carman equation to cement paste may be simplified by inserting the values of the constants. Thus for the coefficient of water permeability at 20°C the equation becomes:

$$k = (2.409\ \varepsilon m^2) \times 10^{-23} \qquad (5.1)$$

where

k = coefficient of water permeability (m/s)

ε = total intruded pore volume (mm^3/g)

m = mean hydraulic radius (Angstrom)

Data summarised in Tables 4.1 and 4.5 shows the variation of the total intruded pore volume, mm^3/g, for hardened cement pastes prepared at two water/cement ratios and hydrated for different ages. A similar set of data is presented in Tables 4.3 and 4.7 for the mean hydraulic radius, in Angstrom. The calculated values of water permeability k for the pure cement pastes can be found from these radii by using equation 5.1. A typical set of calculated k values and their correlation with measured values are presented in Table 5.1.

Table 5.1: Correlation between measured water permeabilities and values calculated from the Kozeny-Carman equation for pure hardened cement pastes.

	Age (days)			
	28		270	
w/c ratio	calculated $k \times 10^{-13}$ (m/s)	Correlation calculated k ÷ measured k	calculated $k \times 10^{-13}$ (m/s)	Correlation calculated k ÷ measured k
0.3	1.873	0.256	1.744	1.170
0.4	6.284	0.425	1.625	0.759

Tables 4.9 and 4.10 also show the coefficient of permeability for 28 and 270 days of hydration for two water/cement ratios and eight percentages of Fly ash and Blastfurnace slag replacement of cement respectively and are discussed as follows:-

The coefficient of permeability decreases gradually with increasing Fly ash replacement of cement between 20 and 40 per cent, there is little effect on the permeability below 10 per cent. The permeability sharply increases with increasing Fly ash replacement above 60 per cent for 28 and 270 days of hydration and for the two water/cement ratios. For simple comparison this data is shown in Figures 4.21 and 4.22. In the development of the pore system, the permeability should be less with increasing time of hydration, which was found to be the case for 0 to 60 per cent Fly ash replacement; however the increase in permeability of the cement for 60-80 per cent Fly ash replacement did not show any significant reduction as the age of the sample increased from 28 to 270 days. Evidently the increase in pores brought about by high levels of Fly ash replacement do not become sealed or reduced during the further hydration which occurs. On the basis of work on pure cement pastes permeability is expected to be greater, the greater the water/cement ratio. This behaviour is also exhibited by Fly ash replaced cement up to a value of 50 per cent (Figure 4.21); above this value at 28 days of hydration, the permeability was found to be less for the Fly ash replaced cement with 0.4 water/cement ratio than 0.3 water/cement ratio, a result which is rather unexpected. Perhaps the additional water assists the hydration which is limited at these high values of Fly ash replacement. However when the age 270 days is reached the substance behaves more as expected with the 0.3 water/cement ratio developing a lower ultimate permeability than the 0.4 water/cement ratio up to a Fly ash replacement level of 60 per cent. The data indicates a useful decrease of

permeability up to 40 per cent Fly ash replacement, a figure which happens to coincide with the normal upper limit of permitted Fly ash replacement which has been determined on the basis of compressive strengths (A.S.T.M. C595-79).

It is useful to compare the water permeability data for Fly ash replacement cement with the mercury intrusion porosimetry data. Apart from slight 'humps' in the curves at low percentage Fly ash replacement, the curves for pore volume for size ranges 37-400 Angstrom and 37-1000 Angstrom show a general tendency to increase for Fly ash replacement 0 - 70 per cent (Figures 4.8 and 4.10); in contrast, the pore volume for sizes greater than 400 Angstrom generally decreases from 0 to 60 or 70 per cent Fly ash replacement (Figure 4.9). It can be concluded then, that the reason for the decrease in water permeability as Fly ash replacement is increased from 0-40 per cent (seen in Figure 4.21) is due to the decrease in pores of sizes greater than 400 Angstrom which offsets the increase in finer pores which occurs. Over the range 40-60 per cent, large pore size (greater than 400 Angstrom) is still decreasing, whereas the water permeability is increasing (Figure 4.22); hence this must be due to the finer pores beginning to make a significant contribution to the water permeability. The sharp increase in water permeability which occurs as Fly ash is increased above 60 per cent must correspond, however, to increased large pores (greater than 400 Angstrom) which at this stage suddenly show a rapid increase in numbers (Figure 4.9). Additionally to these arguments there is a good correlation between water permeability of Fly ash replaced cement and the ratio of capillary to total porosity (Table 4.4).

The coefficient of permeability decreases gradually with increasing ground granulated Blastfurnace slag replacement of cement between 40 - 80 per cent, there is little effect lower than 40 per cent of Blastfurnace slag replacement. Above 80 per cent the permeability increases with increasing

Blastfurnace slag replacement of cement for 28 and 270 days of hydration and for the two water/cement ratios. This data is shown in Figures 4.23 and 4.24.

It is not easy to relate water permeability with porosity data for Blastfurnace slag replaced cement. For an age of 270 days and 0-40 per cent Blastfurnace slag, the variations in large pore size (greater than 400 Angstrom)seen in Figure 4.19 have virtually no effect upon the water permeability seen in Figure 4.24. It is possible that the finest particles in the Blastfurnace slag, of the order of 20,000 Å, play a role in blocking the largest pores (up to 75,000 Å). This mechanism might also explain the decrease in water permeability from 40-80 per cent Blastfurnace slag replacement (Figure 4.24). The very sharp increase in water permeability (Figure 4.24) as the Blastfurnace slag replacement is increased from 80-97 per cent is accompanied by a general decrease in the larger pore sizes (greater than 400 Å, Figure 4.19) and could therefore only be explained by the rapid increase in pore sizes in the ranges 37-400 Angstrom (Figure 4.20) which occurs. The choices of range of pore size to plot are somewhat arbitrary and perhaps studies of other pore size ranges would show a closer correlation with water permeability data. In spite of the lack in relationship, however, there is a correlation between water permeability of Blastfurnace slag replaced cement and the ratio of capillary porosity to total porosity; the latter ratio is tabulated (Table 4.8) and follows the same general trend as the water permeability curve for ages 28 and 270 days at 0.4 water/cement ratio. In respect of this particular correlation the Blastfurnace slag replaced cement behaves similarly to Fly ash replaced cement.

The constancy of water permeability over the range 0-40 per cent Blastfurnace slag replacement (Figure 4.24) merits further comment for it is rather unexpected on physical grounds; one might expect the fine

particles of Blastfurnace slag to reduce the permeability of the cement; possibly, however, they become hydrated first being of greatest surface area to mass ratio.

The present investigator is of the opinion that very complex chemical effects, in particular the vastly larger quantity of CaO present in Blastfurnace slag (Table 2.7) than the trace amounts in Fly ash (Table 2.5) certainly must be taken into consideration when trying to match theory with observation.

5.2 CONCLUSIONS

Fly ash and Blastfurnace slag produce significant changes in pore volume, pore size distribution and water permeability. They generally cause an increase in the total porosity but reduce the ratio of capillary to total porosity, for limits of up to 50 per cent Fly ash and 80 per cent Blastfurnace slag replacement respectively. The water permeability generally shows a reduction up to the same limits above. These substances also reduce bleeding. More detailed conclusions follow:-

1. The interparticle spaces present within the fixed volume of cement paste decrease in size as the content of hydration products increases with increasing age at any given percentage of Fly ash or Blastfurnace slag replacement.

2. At all percentages of Fly ash or Blastfurnace slag replacements the total pore volume intruded by mercury (the capillary pore volume) decreased with increasing time of hydration up to 270 days, showing little further change with age up to 560 days. The total intruded pore volume also increased with increasing water/cement ratio.

3. Fly ash replacement of cement up to 40 per cent by weight is suitable in practice because within this range, the water permeability is reduced although the compressive strength at less than one year may be lower.

4. For Fly ash replaced cement there was a good correlation between water permeability and the ratio of capillary to total pores. From 0-10 per cent replacement there was little effect on water permeability, but it decreased thereafter to a minimum from 20-40 per cent, thereafter increasing in value to approximately equal to pure cement paste around 50 per cent replacement. Above 60 per cent replacement the permeability increased sharply. The ratio of capillary to total pores shows a very similar trend with an initial constancy (at replacement 0-10 per cent) followed by a minimum, and then sharp increase above 60 per cent replacement, showing a close correlation with the water permeability.

5. For Blastfurnace slag replaced cement there was little effect on the water permeability from 0-40 per cent replacement. Thereafter it decreased gradually with increasing Blastfurnace slag replacement from 40-80 per cent. Above 80 per cent replacement the water permeability increased very rapidly. Although this data was difficult to correlate with pore size data, in particular the large increase in permeability at high replacement was not accompanied by increasing number of large capillary pores, yet the ratio of capillary porosity to total porosity showed a similar trend as the water permeability data with increasing replacement.

6. Data which has been obtained in the investigation covers the range of pore sizes 37 Å - 75,000 Å, which is outside the normal range of 100 Å - 1000 Å normally given in other research; the investigation of large pore sizes has been of particular interest for high replacement levels of Fly ash and Blastfurnace slag. The small pore sizes

raise certain questions involving physical interpretation of data. The phenomenon, not fully understood, of negative mercury intrusion has often been observed for pressures greater than 1000 kg/cm^2 and the effect reduces at later stages of hydration and at high replacement levels of Fly ash or Blastfurnace slag.

7. For a pure hardened cement paste the coefficient of permeability decreased with increasing time of hydration and increased with increasing water/cement ratio.

8. There was some discrepancy between the present data on porosities of pure cement, and the data given by Powers (1964) and Neville (1981). They stated that for water/cement ratios of 0.38, fully hydrated cement paste would have no capillary porosity and would have only gel pores occupying about 28 per cent of the gel volume; at higher water/cement ratios and complete hydration, there would be about 28 per cent gel pores plus additional capillary pores due to excess water.

However, in the present work, pure cement paste (water/cement ratio 0.4) at 270 days hydration had a capillary volume of 14.9 per cent, considerably higher than expected on the Powers model (near zero), and the gel porosity was 11.2 per cent, less than half the value expected on the same model. Even if allowance is made for the uncertain distinction between gel pores and capillary pores, the sum of gel and capillary pores (14.9 per cent + 11.2 per cent = 26.1 per cent) gives a value less than the 28 per cent expected on the Powers model.

9. The Kozeny-Carman equation which enables an estimate of water permeability to be made using data on mean hydraulic radius and total intruded mercury porosity (capillary porosity) was found to give reasonable agreement with the measured water permeability of pure cement pastes, (0.3 and 0.4 water/cement ratio, age 270 days).

However the equation clearly cannot be applied to Fly ash or Blastfurnace slag replaced cements because as the level of replacement increases (up to 40 per cent Fly ash or 70 per cent Blastfurnace slag) the total pore volume increases while the water permeability decreases, which is at variance with the equation. This departure from the Kozeny-Carmen equation implies that the pore structure of Fly ash or Blastfurnace slag replaced cements is considerably different from that of pure cement paste. On a unit weight basis the replaced cements contain more capillary pores according to mercury intrusion than the pure cement paste. Since the water permeability is reduced, however, it is clear that these capillaries do not transport water and are probably blocked by the greater quantity of gel product which is available in the replaced cement paste.

10. The bleeding rate decreased with increasing Fly ash or Blastfurnace slag replacement of the cement and decreased with decreasing water/cement ratio, and is probably due to a decrease in water/solid ratio.

11. The rate of heat development during early stages of hydration was slowed down with increasing Fly ash or Blastfurnace slag replacement of the cement and with increasing water/cement ratio.

12. It is of interest to note that for high replacement levels of both Fly ash (> 40 per cent) and Blastfurnace slag cements (> 80%) the rapid decrease in compressive strength is evidently correlated with the rapid increase in water permeability.

5.3 FURTHER WORK

The data obtained in the present investigation has been restricted to one composition of Fly ash and Blastfurnace slag respectively. This was in the interest of obtaining consistent experimental data so the permeability and porosity characteristics could be related to the varying levels of replacement of the concrete. While the Fly ash and Blast-

furnace slag used in this investigation were typical it is not known how much the data obtained would be influenced by the large variations in the chemical and physical properties that can occur in practice. Nor is it known how the permeability and porosity characteristics would develop in mass concrete as opposed to small test samples. Only additional extensive experimental work could help to elucidate.

Permeability apparatus and measurements raise a number of problems which suggest further work in this area is required. It takes several weeks to obtain results from the sample, apart from being very inconvenient, young samples must age significantly during the tests. The samples are also subjected to high pressure which influences hydration and leaching of calcium hydroxide. There is an absence of suitable commercial equipment to measure the permeability of concrete which leads to difficulties in comparing data between different laboratories. There is no standard concrete for calibration or for assessing equipment, leakages and so on. Increasing the temperature which reduces the water viscosity or increasing the cross-sectional area of the samples with the same thickness might speed up the obtaining of data, at the same time reducing the proportion of leakage at the circumference in relation to the total flow. Additionally the confining pressure required to suppress leakage may be lower because of the larger radius of curvature of the specimen.

The interpretation of porosity data obtained with mercury intrusion apparatus raises a number of questions. Firstly it would be useful to develop the physical theories of mercury intrusion, especially at high pressures; the diameter of the mercury molecule being around 3 Angstrom then a simple surface tension theory is possibly inadequate when pores only some 10 times bigger diameter are being considered. The concept of a continuous surface possessing geometric parameters such as radius of curvature or contact angle becomes questionable. Secondly the pores cannot be assumed to be cylindrical or even of constant cross-section. To some extent this problem is resolved when data between different laboratories is compared using the same equipment. However, if the

pressure is great enough to cause mechanical failure of the sample and upset the close packing of the particles greater voidage will be created and give the erroneous idea that the sample contains many fine pores. This area of physics requires further research.

It may be possible to measure the compressibility of the cement matrix simply by saturating the sample fully with water so the pores are filled, and measuring the compressibility in normal mercury intrusion apparatus. From the known characteristics of water, its quantity and the weight of the dry sample, the compressibility of the cement matrix may be calculable. However,the existence of encapsulated pores suggested by Diamond and Dolch 1972 may raise some difficulties with such a proposal.

The phenomenon of negative mercury intrusion at high pressures, observed in the present research needs further study. Increasing Fly ash causes decrease of compressive strength, therefore it may be expected that more negative mercury intrusion would appear at lower pressures than observed for the pure cement paste. This does not happen therefore the negative mercury intrusion is not apparently associated with fracture of the material under the high pressures. On the basis of energy, mercury is forced out of the sample as the pressure is increased and so the hardened cement sample performs work on the surroundings. This implies a reduction of 'stored energy' in the sample, which may be associated with surface energy of the pore, decreasing when the pore diameter is reduced. It may be that at certain critical pressures the work done in forcing mercury into a pore, which is a mechanism for storing energy, leads to instability,the sytem becoming more stable if mercury is expelled and a pore shrinks taking up a state of lower stored energy. To develop an adequate theory especially since the pores are not cylindrical, is an area which requires further research.

In the present investigation it was observed that while the total porsity increased the water permeability decreased for increasing Fly ash or Blastfurnace slag replacement up to certain limits. This

represented a departure from the Kozeny-Carman equation. This was due partly to the geometry of the pores in the replaced cements, in particular the reduction in ratio of large pores to total pores during hydration and partly to chemical effects, with gel product blocking the capillary pores. The Kozeny-Carman equation is more applicable to a sand system with continuous pores, therefore to develop a theory which applies to the cement pastes so that water permeabilities can be predicted on the basis of porosity characteristics is an area requiring further work.

Bleeding characteristics for Fly ash or Blastfurnace slag replaced cements for both water/cement ratios of 0.3 and 0.4 were found to be improved in this research, but this data needs to be extended in several respects. Segregation of cement during setting depends on specific gravity of constituents; the replacement by Fly ash or Blastfurnace slag, having lower specific gravities than the pure cement, might possibly lead to less segregation. The effects on mass concrete setting need to be evaluated as opposed to the small test samples (100 mm length and 38.1 mm diameter cylinder) used in research which tend to remain homogenous. Data on segregation, bleeding and water gain for higher water/cement ratios also need to be obtained, and in relation to rich and lean mixes.

No data has been obtained here on the effects of replacing cement by various combinations of Fly ash and Blastfurnace slag together, apparently such pozzolana cements have not been developed. Fly ash contains less CaO than Blastfurnace slag. The influence of the CaO upon the pore system is uncertain but, perhaps the permeability of Fly ash replaced cement might be further reduced by adding varying proportions of Blastfurnace slag, as well as increasing the compressive strength.

APPENDICES

APPENDIX 1 Relationship between permeability and porosity including Darcy's law and Kozeny-Carman model.

APPENDIX 2 Computer Program

APPENDIX 3 Pore size distribution data additional to Chapter Four.

APPENDIX ONE

THEORETICAL ASPECTS OF THE RELATIONSHIP BETWEEN FLOW RATE, COEFFICIENT OF PERMEABILITY AND POROSITY

The starting point of the analysis in Darcy's law, is the assumption that the velocity of flow of a liquid through a porous medium due to difference in pressure is proportional to the pressure gradient in the direction of flow. This assumption is supported by experiment. When the macroscopic flow is unidirectional, the law may be stated as follows:

$$q = K\,H/L \qquad (A1.1)$$

where q = volume of liquid passing through a unit area of the porous medium in a unit of time (m/s)

K = coefficient of permeability of the porous medium to a specified liquid at a given temperature (m/s)

H = hydraulic head across the thickness of the permeable body (m)

L = thickness of the permeable body (m)

The problem is to find the value of K in terms of the characteristics of the solid and the liquid, and their relative proportions. The problem has been studied by many workers. The most successful development is the Kozeny - Carman equation, the history of which was reviewed by Kozeny, 1927. There has been much discussion of the details of the development and the physical significance of the parameters of the equation. The equation is derived from the Poiseuille equation.

1.1 ANALYSIS BASED ON POISEUILLE'S LAW

The flow of liquid through a permeable body composed of particles and interstices is considered to be analogous to the flow through a solid body which is pierced by a number of identical, parallel, cylindrical capillaries. The coefficient of permeability of such a body for laminar flow in the direction of the capillaries can readily be calculated in terms of Poiseuille's Law.

According to Poiseuille's law, the rate of flow of a liquid through a tube is directly proportional to, the difference in liquid pressure at the ends of the tube, and the fourth power of the radius of the tube, and is inversely proportional to the viscosity of the liquid.

The quantitative relationship between rate of flow and pressure drop may be expressed as follows :

$$Q = \frac{\pi R^4}{8\eta} \rho_f \, g \, \frac{H}{Le} \qquad \text{(A1.2)}$$

where Q = volume efflux from the capillary (m^3/s)

R = radius of the capillary (m)

Le = length of the capillary (m)

ρ_f = density of the fluid (kg/m^3)

η = viscosity of the fluid ($N \cdot s/m^2$)

g = acceleration due to gravity (m/s^2)

H = hydraulic head (m)

Since the total flow per unit area of the plug is the flow from N capillary openings in area A, it follows that

$$q = \frac{N}{A} Q \qquad \text{(A1.3)}$$

and

$$\frac{N}{A} = \frac{v}{A} \cdot \frac{1}{\pi R^2} = \frac{\varepsilon}{\pi R^2} \qquad \text{(A1.4)}$$

where q = flow per unit total area

v = total volume of the capillary per unit length

R = radius of the capillary

πR^2 = capacity of the capillary

ε = porosity of the system of capillaries, that is porous volume/total volume

Since H is the same for the plug as a whole as it is for a single capillary, the expression for flow through the plug can be written

$$q = \frac{\rho_f g}{8\eta} \frac{\pi R^4}{\pi R^2} \varepsilon \cdot \frac{H}{Le} = \frac{\rho_f g R^2}{8\eta} \varepsilon \cdot \frac{H}{Le} \qquad \text{(A1.5)}$$

Equations A1.1 and A1.5 may be combined to give,

$$K = \frac{R^2 \rho_f g}{8\eta} \cdot \varepsilon \qquad \text{(A1.6)}$$

which gives the coefficient of permeability of the plug in terms of

its porosity, pore size and the viscosity of the liquid. Since viscosity is a function of temperature, K will also vary with temperature. Hence when quoting values of K for a medium it is necessary to quote both the fluid used (that is ρ_f and η) and the temperature.

1.1.1 THE KOZENY - CARMAN MODEL

It is obvious that Equation A1.6 is not directly applicable to a permeable body composed of particles and interstices. However, there is a certain similarity between a granular bed and a system of parallel capillaries with respect to permeability. Specifically, if the porous medium is uniform and isotropic, the area for flow in the direction of the pressure gradient may be assumed to be the fraction ε of unit volume, as in Equation A1.6. However, although the area for flow in any plane normal to the direction of flow may be ε, the openings in that plane will not be circular, nor all of the same size. Also it is apparent that the flow paths through the interstitial spaces will not be parallel straight lines in the direction of flow. Nevertheless, Kozeny (1927) showed that the Poiseuille model can be adapted to it.

The derivation of Kozeny's equation, as presented by Powers 1968, is as follows: For a noncircular conduit, the radius of the conduit may be considered as the mean hydraulic radius m, defined as the volume (capacity) of the conduit divided by the wetted surface area.

For example, a circular section.

$$m = \frac{\pi R^2 L}{2\pi RL} = \frac{R}{2} \qquad \text{(A1.7)}$$

Substituting 2m for R in Equation A1.5, gives

$$\frac{q}{\varepsilon} = \frac{\rho_f g}{2\eta} m^2 \cdot \frac{H}{Le} \qquad \text{(A1.8)}$$

For a section other than circular, the factor 2 is replaced by a shape factor Ko. For ellipses, Ko is between 2 and 2.5, depending on the ratio of major to minor axis length, for a square section, it is 1.78, and for various rectangles having different ratios of width to height it ranges upward from that value to 3.0 for infinite ratio. Carman (1937) found that the value for the openings in granular beds may be taken as 2.5.

The pressure drop in the conduit depends on the actual velocity and on the effective length of the flow path. For the Poiseuille model, the effective macroscopic velocity was simply q/ε, and the factor of Le/L must be included where Le is the actual distance of flow in transversing thickness L. Hence Equation A1.8 must be modified as follows:

$$\frac{q\ Le}{\varepsilon\ L} = \frac{\rho_f g}{Ko\eta} m^2 \cdot \frac{H}{Le}$$

which gives:

$$q = \frac{\rho_f g}{Ko(Le/L)^2 \eta} \cdot \varepsilon\, m^2 \frac{H}{L} = K\frac{H}{L} \qquad (A1.9)$$

Equations A1.1 and A1.9 are then combined to give,

$$K = \frac{\rho_f g}{Ko(Le/L)^2 \eta} \cdot \varepsilon\, m^2 \qquad (A1.10)$$

Carman (1937) observed coloured streams passing through beds of particles and concluded that on the average their direction was inclined at 45^o to the general direction of flow. Hence the ratio $(Le/L) = 2^{1/2}$ or $(Le/L)^2=2$, this being called the tortuosity factor.

It follows that $Ko(Le/L)^2 = Kc = 2.5 \times 2 = 5$, which was Carman's constant, but which may be also called the Kozeny constant.

Studies by Wyllie et al(1952) have shown that Kc is not the same for all systems and that in a given system it may take on different values if ε is varied. Though, according to Powers 1968, Kc = 5 has become widely used. Steinor (1945) found Kc=4.06 for Portland cement pastes.

APPENDIX TWO

COMPUTER PROGRAM

COMPUTER PROGRAM

The computer program used in this work consists of the main program with a series of plotting routines and an input data subroutine.

The plotting routines are standard routines for graphical results used in London University Computer Centre. For further information on the plotting routine used in this work, DIMFILM manual (Kingś College London) must be consulted.

The basic program structure is shown in program flowchart. In the first section X_L,X_R,X_L,X_U factors controlling the final printed slide size are evaluated. In section two,the following data are read in and control the limits for the plots;

NPROB = identification number of problem,

N = frequency intervals of pore radius,

K = maximum value on pore radius scale,75000 Angstrom,at lower x-axis and pressure scale,2000 kg/cm^2,at upper x-axis,

YAMAX = maximum value on cumulative pore volume scale (mm^3/g),

YBMAX = maximum value on pore size distribution ($d(V_t-V_c)/dlogr$),

A(IJ) = total intruded pore volume (cm^3/g) for sample for which data is to be plotted.

In section three,the data from the previous sections is based to set the plotter camera in the configuration required for the plots. Section four is the data entry routine for the experimental data in Subroutine Datain for frame 1 of the plot one. In section five , the results calculated in section four are printed and plotted as frame 1 of the final plot.

In the subsequent sections (6-11) the repeated calls to Datain and graph plot the remaining 3 frames to complete the figure.

PROGRAM FLOWCHART

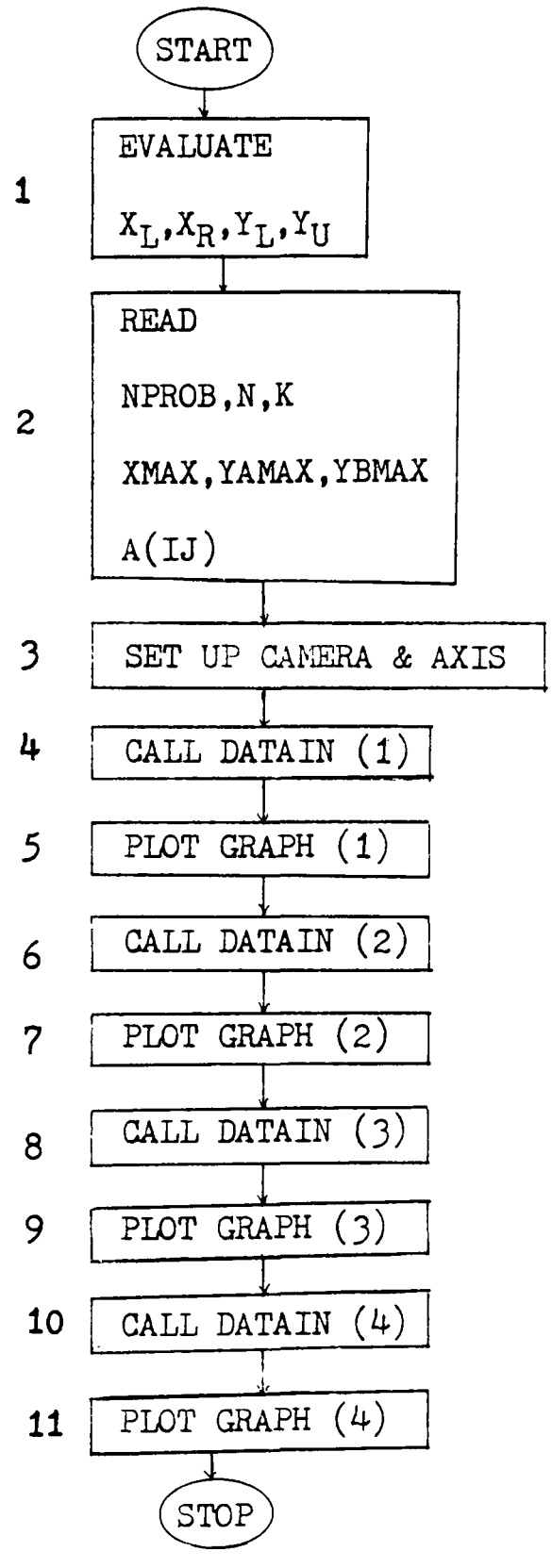

SUBROUTINE DATAIN

The experimental data results of cumulative pore volume etc. are read in this Subroutine. The structure of this Subroutine is shown in DATAIN FLOWCHART, and the arrays which have been used in this Subroutine are as follows:-

P(I) = Applied pressure (kg/cm^2).

HG(I) = Compressibility of the mercury and the system at P(I), mercury level in the capillary stem in millimeter data from blank run.

S(I) = Mercury level in the capillary stem intruded the sample at P(I), millimeter.

X(1) = 75000 Angstrom (maximum pore radius).

Initial values,
YA(1) = 0.0, YB(1) = 0.0, V(1) = 0.0, and SA = 0.0 .

X(I) = 75000./P(I) (pore radius in Angstrom).

V(I) = (S(I)-HG(I))/(S(N)-HG(N)), Temporary variables

YA(I) = V(I)*1000.*A(IJ), (cumulative pore volume, mm^3/g) .

YB(I) = (YA(I)-YA(I-1))/ALOG(X(I)), (pore size distribution) .

SA = SA+(YA(I)-YA(I-1))/X(I)*0.2 (surface area, m^2/g).

RH = (A(IJ)/SA)*10000. (mean hydrulic radius, Angstrom)

DATAIN FLOWCHART

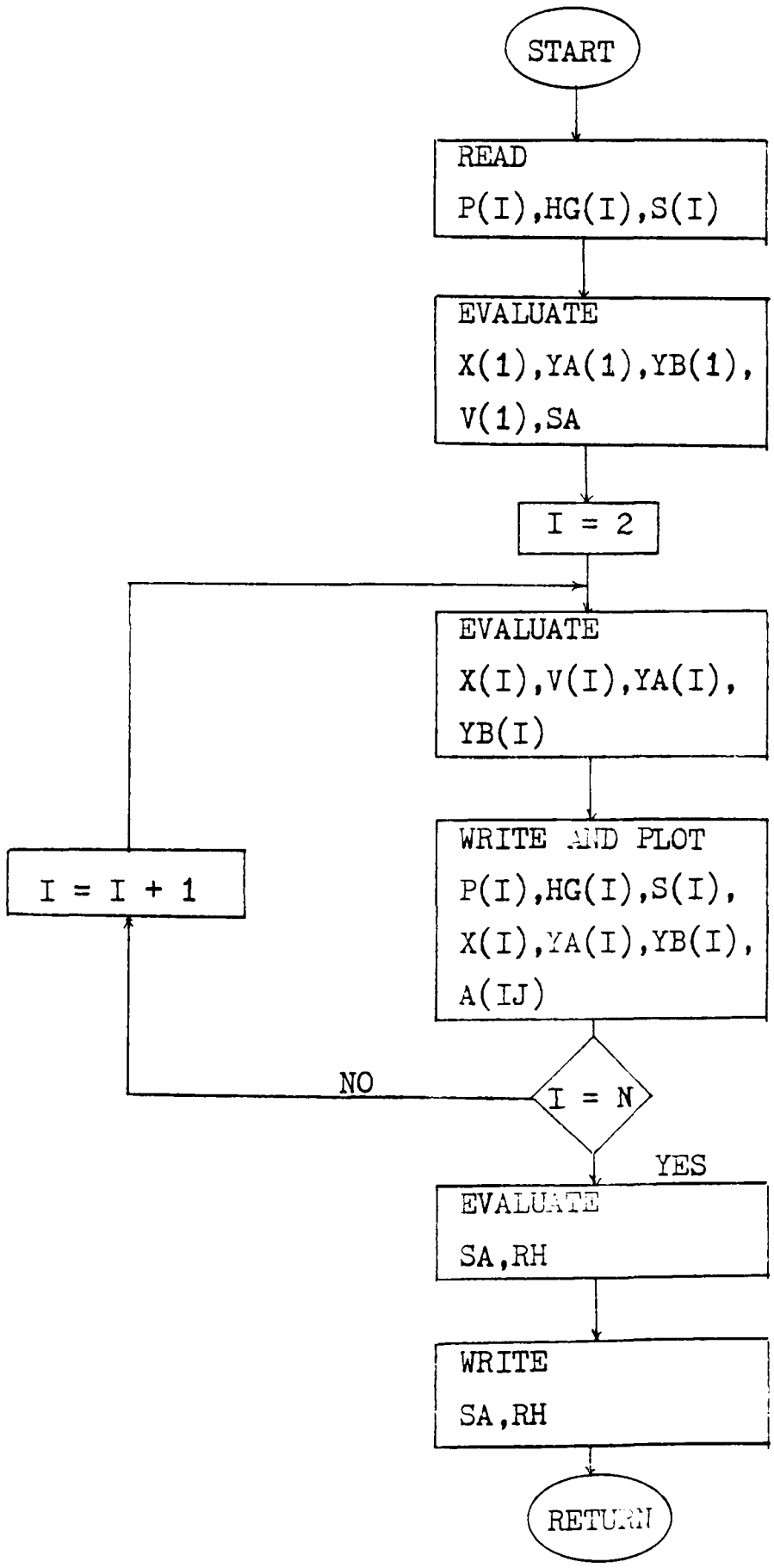

COMPUTER PROGRAM

```
PROGRAM MANSOU

      PROGRAM MANSOU(INPUT,OUTPUT,TAPE5=INPUT,TAPE6=OUTPUT,TAPE27)
      DIMENSION X(40),YA(40),YB(40),A(40)
      DATA IALT/1R*/
      DATA DELTA/0.17/
      XL=-36.0*DELTA
      XR=36.0*(1.0+DELTA)
      YL=-25.0*DELTA
      YU=25.0*(1.0+DELTA)
      CALL CAM35MM
      CALL GRAFCON(0.74,0.01,0.01,0.04,0.8,0.10,0.005,0.78,0.54,0.01,0.0
     [175)
      CALL IXAX
      CALL IYAX
      CALL SLIDE(XL,XR,YL,YU)
      CALL IBACK(8)
      CALL LOGLIM(2.0,5.0)
      READ(5,501) NPROB,N,K
  501 FORMAT (3I10)
      READ(5,502) XMAX,YAMAX,YBMAX
  502 FORMAT (3F10.4)
      READ(5,503) (A(IJ),IJ=1,K)
  503 FORMAT(8F10.8)
      CALL HVYTYPE
      CALL WINDOW(0.0,36.0,-1.3,0.0)
      CALL SYMHT(0.633)
      CALL OFFTOXY(0.0,-1.1)
      CALL CASEALT(1R&)
      CALL SYMTEXT(94HF&IGURE& A3.26 THE EFFECT OF BLASTFURNACE SLAG REP
     LACEMENT OF CEMENT ON PORE SIZE DISTRIBUTION,94)
      CALL NRMTYPE
      CALL WINDOW(0.0,18.0,0.0,12.0)
      CALL OFFTOXY(6.34,0.35)
      CALL SYMHT(0.40)
      CALL SYMTEXT(24HPORE RADIUS (A&NGSTROM&),24)
      CALL SYMHT(0.40)
      CALL OFFTOXY(5.7,11.5)
      CALL SYMTEXT(31HABSOLUTE PRESSURE  (&KG/SQ CM&),31)
      CALL SYMANGL(90.0)
      CALL SYMHT(0.40)
      CALL OFFTOXY(0.80,2.10)
      CALL SYMTEXT(35HCUMULATIVE PORE VOLUME (&CU MM/G& ),35)
      CALL SYMHT(0.40)
      CALL OFFTOXY(17.55,1.55)
      CALL SYMTEXT(47HPORE SIZE DISTRIBUTION (&D&(V&T&-V&C&)/&DLOGR&),47
     C)
      CALL SYMANGL(0.0)
      CALL DATAIN(X,YA,YB,N,NPROB,1,A)
      CALL WINDOW(0.0,18.0,0.0,12.0)
      CALL LOGX
      CALL XAXIS(37.,75000.)
      CALL YAXIS(0.0,YBMAX)
      CALL INTSTY(16)
      CALL GRAPHIC(X,YB,N)
      CALL RYOPPT
      CALL RYVAL
      CALL YAXIS(0.0,YAMAX)
      CALL GRAPHIC(X,YA,N)
```

```
      PROGRAM MANSOU

                  CALL LYVAL
                  CALL LXVAL
60                CALL BLANK(10.05,18.0,6.60,12.0)
                  CALL INTSTY(10)
                  CALL XGRID
                  CALL INTSTY(6)
                  CALL YGRID
65                CALL ENDBLNK
                  CALL LOGX
                  CALL XAXIS(2000.0,1.0)
                  CALL UXVAL
                  CALL INTSTY(22)
70                CALL UXOPPT
                  CALL INTSTY(10)
                  CALL GRFRAME
                  CALL OFFTOXY(10.3,9.8)
                  CALL SYMHT(0.4)
75                CALL SYMTEXT(8HFRAME  C,8)
                  CALL OFFTOXY(10.3,8.8)
                  HT=24.0*0.45/34.5
                  CALL SYMHT(HT)
                  CALL SYMTEXT(27HAGE OF SAMPLE (DAYS)  = 3  ,27)
80                CALL OFFTOXY(10.3,8.0)
                  HT=24.0*0.45/34.5
                  CALL SYMHT(HT)
                  CALL SYMTEXT(27HWATER/CEMENT RATIO    = 0.3,27)
                  CALL OFFTOXY(10.3,7.2)
95                HT=24.0*0.45/34.5
                  CALL SYMHT(HT)
                  CALL ROMGRK(1R*)
                  CALL SYMTEXT(28HSLAG REPLACEMENT      = 40*$,28)
                  CALL WINDFRM
90                CALL DATAIN(X,YA,YB,N,NPROB,2,A)
                  CALL WINDOW(18.0,36.0,0.0,12.0)
                  CALL SYMHT(0.40)
                  CALL OFFTOXY(24.34,0.35)
                  CALL SYMTEXT(24HPORE RADIUS (A&NGSTROM&),24)
95                CALL SYMHT(0.40)
                  CALL OFFTOXY(23.7,11.5)
                  CALL SYMTEXT(31HABSOLUTE PRESSURE  (&KG/SQ CM&),31)
                  CALL SYMANGL(90.0)
                  CALL SYMHT(0.40)
100               CALL OFFTOXY(18.80,2.10)
                  CALL SYMTEXT(35HCUMULATIVE PORE VOLUME (&CU MM/G& ),35)
                  CALL SYMHT(0.40)
                  CALL OFFTOXY(35.55,1.55)
                  CALL SYMTEXT(47HPORE SIZE DISTRIBUTION (&D&(V&T&-V&C&)/&DLOGR&),47
105               C)
                  CALL SYMANGL(0.0)
                  CALL LOGX
                  CALL XAXIS(37.,75000.)
                  CALL YAXIS(0.0,YBMAX)
110               CALL INTSTY(16)
                  CALL GRAPHIC(X,YB,N)
                  CALL RYOPPT
                  CALL RYVAL
                  CALL YAXIS(0.0,YAMAX)
```

```
      PROGRAM MANSOU

115               CALL GRAPHIC(X,YA,N)
                  CALL LYVAL
                  CALL LXVAL
                  CALL BLANK(28.05,36.0,6.60,12.0)
                  CALL INTSTY(10)
120               CALL XGRID
                  CALL INTSTY(6)
                  CALL YGRID
                  CALL ENDBLNK
                  CALL LOGX
125               CALL XAXIS(2000.0,1.0)
                  CALL UXVAL
                  CALL INTSTY(22)
                  CALL UXOPPT
                  CALL INTSTY(10)
130               CALL GRFRAME
                  CALL OFFTOXY(28.3,9.8)
                  CALL SYMHT(0.4)
                  CALL SYMTEXT(8HFRAME  D,8)
                  CALL OFFTOXY(28.3,8.8)
135               HT=24.0*0.45/34.5
                  CALL SYMHT(HT)
                  CALL SYMTEXT(27HAGE OF SAMPLE (DAYS)  = 3  ,27)
                  CALL OFFTOXY(28.3,8.0)
                  HT=24.0*0.45/34.5
140               CALL SYMHT(HT)
                  CALL SYMTEXT(27HWATER/CEMENT RATIO    = 0.3,27)
                  CALL OFFTOXY(28.3,7.2)
                  HT=24.0*0.45/34.5
                  CALL SYMHT(HT)
145               CALL SYMTEXT(28HSLAG REPLACEMENT      = 60*$,28)
                  CALL WINDFRM
                  CALL DATAIN(X,YA,YB,N,NPROB,3,A)
                  CALL WINDOW(0.0,18.0,12.0,24.0)
                  CALL SYMHT(0.40)
150               CALL OFFTOXY(6.34,12.35)
                  CALL SYMTEXT(24HPORE RADIUS (A&NGSTROM&),24)
                  CALL SYMHT(0.40)
                  CALL OFFTOXY(5.7,23.5)
                  CALL SYMTEXT(31HABSOLUTE PRESSURE  (&KG/SQ CM&),31)
155               CALL SYMANGL(90.0)
                  CALL SYMHT(0.40)
                  CALL OFFTOXY(0.8,14.10)
                  CALL SYMTEXT(35HCUMULATIVE PORE VOLUME (&CU MM/G& ),35)
                  CALL SYMHT(0.40)
160               CALL OFFTOXY(17.55,13.55)
                  CALL SYMTEXT(47HPORE SIZE DISTRIBUTION (&D&(V&T&-V&C&)/&DL3GR&),47
                 C)
                  CALL SYMANGL(0.0)
                  CALL LOGX
165               CALL XAXIS(37.,75000.)
                  CALL YAXIS(0.0,YBMAX)
                  CALL INTSTY(16)
                  CALL GRAPHIC(X,YB,N)
                  CALL RYOPPT
170               CALL RYVAL
                  CALL YAXIS(0.0,YAMAX)
```

```
      PROGRAM MANSOU

                  CALL GRAPHIC(X,YA,N)
                  CALL LYVAL
                  CALL LXVAL
175               CALL BLANK(10.05,18.0,18.60,24.0)
                  CALL INTSTY(10)
                  CALL XGRID
                  CALL INTSTY(6)
                  CALL YGRID
180               CALL ENDBLNK
                  CALL LOGX
                  CALL XAXIS(2000.0,1.0)
                  CALL UXVAL
                  CALL INTSTY(22)
185               CALL UXOPPT
                  CALL INTSTY(10)
                  CALL GRFRAME
                  CALL SYMHT(0.4)
                  CALL OFFTOXY(10.3,21.8)
190               CALL SYMTEXT(8HFRAME  A,8)
                  CALL OFFTOXY(10.3,20.8)
                  HT=24.0*0.45/34.5
                  CALL SYMHT(HT)
                  CALL SYMTEXT(27HAGE OF SAMPLE (DAYS)  = 3  ,27)
195               CALL OFFTOXY(10.3,20.0)
                  HT=24.0*0.45/34.5
                  CALL SYMHT(HT)
                  CALL SYMTEXT(27HWATER/CEMENT RATIO    = 0.3,27)
                  CALL OFFTOXY(10.3,19.2)
200               HT=24.0*0.45/34.5
                  CALL SYMHT(HT)
                  CALL SYMTEXT(28HSLAG REPLACEMENT      = 0 *$,28)
                  CALL WINDFRM
                  CALL DATAIN(X,YA,YB,N,NPROB,4,A)
205               CALL WINDOW(18.0,36.0,12.0,24.0)
                  CALL SYMHT(0.40)
                  CALL OFFTOXY(24.34,12.35)
                  CALL SYMTEXT(24HPORE RADIUS (A&NGSTROM&),24)
                  CALL SYMHT(0.40)
210               CALL OFFTOXY(23.7,23.5)
                  CALL SYMTEXT(31HABSOLUTE PRESSURE  (&KG/SQ CM&),31)
                  CALL SYMANGL(90.0)
                  CALL SYMHT(0.40)
                  CALL OFFTOXY(18.80,14.10)
215               CALL SYMTEXT(35HCUMULATIVE PORE VOLUME (&CU MM/G& ),35)
                  CALL SYMHT(0.40)
                  CALL OFFTOXY(35.55,13.55)
                  CALL SYMTEXT(47HPORE SIZE DISTRIBUTION (&D&(V&T&-V&C&)/&DLOGR&),47
                 C)
220               CALL SYMANGL(0.0)
                  CALL LOGX
                  CALL XAXIS(37.,75000.)
                  CALL YAXIS(0.0,YBMAX)
                  CALL INTSTY(16)
225               CALL GRAPHIC(X,YB,N)
                  CALL RYOPPT
                  CALL RYVAL
                  CALL YAXIS(0.0,YAMAX)
```

```
      PROGRAM MANSOU

                  CALL GRAPHIC(X,YA,N)
230               CALL LYVAL
                  CALL LXVAL
                  CALL BLANK(28.05,36.0,18.60,24.0)
                  CALL INTSTY(10)
                  CALL XGRID
235               CALL INTSTY(6)
                  CALL YGRID
                  CALL ENDBLNK
                  CALL LOGX
                  CALL XAXIS(2000.0,1.0)
240               CALL UXVAL
                  CALL INTSTY(22)
                  CALL UXOPPT
                  CALL INTSTY(10)
                  CALL GRFRAME
245               CALL OFFTOXY(28.3,21.8)
                  CALL SYMHT(0.4)
                  CALL SYMTEXT(8HFRAME  8,8)
                  CALL OFFTOXY(28.3,20.8)
                  HT=24.0*0.45/34.5
250               CALL SYMHT(HT)
                  CALL SYMTEXT(27HAGE OF SAMPLE (DAYS)  = 3  ,27)
                  CALL OFFTOXY(28.3,20.0)
                  HT=24.0*0.45/34.5
                  CALL SYMHT(HT)
255               CALL SYMTEXT(27HWATER/CEMENT RATIO    = 0.3,27)
                  CALL OFFTOXY(28.3,19.2)
                  HT=24.0*0.45/34.5
                  CALL SYMHT(HT)
                  CALL SYMTEXT(28HSLAG REPLACEMENT      = 20*$,28)
260               CALL WINDFRM
                  CALL WINDOW(0.0,36.0,0.0,24.0)
                  CALL WINDFRM
                  CALL END FILM
                  STOP
265               END
```

SUBROUTINE DATAIN

```
      SUBROUTINE DATAIN(X,YA,YB,N,NPROB,IJ,A)
      DIMENSION X(N),YA(N),YB(N)
      DIMENSION S(40),P(40),HG(40),A(40),V(40)
      READ(5,20) (P(I),HG(I),S(I),I=1,N)
20    FORMAT(8F10.5)
      X(1) = 75000.
      YA(1)=0.0
      YB(1)=0.
      V(1)=0.0
      SA=0.0
      DO 21 I=2,N
      X(I)=75000.0/P(I)
      V(I)=(S(I)-HG(I))/(S(N)-HG(N))
      YA(I)=V(I)*1000.*A(IJ)
      YB(I)=(YA(I)-YA(I-1))/ALOG(X(I))
      SA=SA+(YA(I)-YA(I-1))/X(I)
21    WRITE(6,600) P(I),HG(I),S(I),X(I),YA(I),YB(I),A(IJ)
600   FORMAT(20X,7E14.7)
      SA=SA*0.20
      RH=(A(IJ)/SA)*10000.
      WRITE(6,601) SA,RH
601   FORMAT(1X,2E14.7)
      RETURN
      END
```

DATA

```
      .1000000E+01 0.            .1000000E+00  .7500000E+05  .1253971E+01  .1117099E+00  .1605083E+00
      .2000000E+01 0.            .1000000E+00  .3750000E+05  .1253971E+01 0.            .1605083E+00
      .3000000E+01 0.            .1000000E+00  .2500000E+05  .1253971E+01 0.            .1605083E+00
      .4000000E+01 0.            .1000000E+00  .1875000E+05  .1253971E+01 0.            .1605083E+00
      .5000000E+01 0.            .2000000E+00  .1500000E+05  .2507942E+01  .1304073E+00  .1605083E+00
      .6000000E+01 0.            .3000000E+00  .1250000E+05  .3761913E+01  .1329277E+00  .1605083E+00
      .8000000E+01 0.            .4000000E+00  .9375000E+04  .5015884E+01  .1371089E+00  .1605083E+00
      .1000000E+02 0.            .5000000E+00  .7500000E+04  .6269855E+01  .1405378E+00  .1605083E+00
      .1200000E+02 0.            .5000000E+00  .6250000E+04  .6269855E+01 0.            .1605083E+00
      .1500000E+02 0.            .6000000E+00  .5000000E+04  .7523827E+01  .1472282E+00  .1605083E+00
      .1800000E+02 0.            .6000000E+00  .4166667E+04  .7523827E+01 0.            .1605083E+00
      .2100000E+02 0.            .7000000E+00  .3571429E+04  .8777798E+01  .1532837E+00  .1605083E+00
      .2600000E+02 0.            .8000000E+00  .2884615E+04  .1003177E+02  .1573927E+00  .1605083E+00
      .3000000E+02 0.            .8000000E+00  .2500000E+04  .1003177E+02 0.            .1605083E+00
      .3600000E+02 0.            .9000000E+00  .2083333E+04  .1128574E+02  .1640953E+00  .1605083E+00
      .4400000E+02 0.            .1200000E+01  .1704545E+04  .1504765E+02  .5055619E+00  .1605083E+00
      .5400000E+02 0.            .1700000E+01  .1388889E+04  .2131751E+02  .8664498E+00  .1605083E+00
      .6300000E+02  .2000000E-01  .2500000E+01  .1190476E+04  .3109848E+02  .1381082E+01  .1605083E+00
      .7600000E+02  .5000000E-01  .4200000E+01  .9868421E+03  .5203980E+02  .3037390E+01  .1605083E+00
      .9200000E+02  .7000000E-01  .6300000E+01  .8152174E+03  .7812240E+02  .3890919E+01  .1605083E+00
      .1100000E+03  .1000000E+00  .7600000E+01  .6818182E+03  .9404783E+02  .2440768E+01  .1605083E+00
      .1340000E+03  .1500000E+00  .8600000E+01  .5597015E+03  .1059606E+03  .1882719E+01  .1605083E+00
      .1880000E+03  .3000000E+00  .9800000E+01  .3989362E+03  .1191273E+03  .2198553E+01  .1605083E+00
      .2240000E+03  .4000000E+00  .1060000E+02  .3348214E+03  .1279051E+03  .1509874E+01  .1605083E+00
      .2780000E+03  .5500000E+00  .1130000E+02  .2697842E+03  .1348019E+03  .1232102E+01  .1605083E+00
      .3260000E+03  .6500000E+00  .1190000E+02  .2300613E+03  .1410717E+03  .1152897E+01  .1605083E+00
      .4050000E+03  .9000000E+00  .1270000E+02  .1851852E+03  .1479686E+03  .1320891E+01  .1605083E+00
      .5770000E+03  .1350000E+01  .1380000E+02  .1299827E+03  .1561194E+03  .1674572E+01  .1605083E+00
      .6820000E+03  .1750000E+01  .1430000E+02  .1099707E+03  .1573734E+03  .2667902E+00  .1605083E+00
      .8340000E+03  .2200000E+01  .1480000E+02  .8992806E+02  .1580004E+03  .1393608E+00  .1605083E+00
      .1000000E+04  .2800000E+01  .1540000E+02  .7500000E+02  .1580004E+03 0.            .1605083E+00
      .1210000E+04  .3500000E+01  .1580000E+02  .6198347E+02  .1542384E+03 -.9115662E+00  .1605083E+00
      .1442000E+04  .3800000E+01  .1640000E+02  .5201110E+02  .1580004E+03  .9520319E+00  .1605083E+00
      .1744000E+04  .4600000E+01  .1690000E+02  .4300459E+02  .1542384E+03 -.1000161E+01  .1605083E+00
      .2000000E+04  .4800000E+01  .1760000E+02  .3750000E+02  .1605083E+03  .1729930E+01  .1605083E+00
.8733056E-01  .1837940E+05
      .1000000E+01 0.            0.            .7500000E+05 0.            0.            .1635587E+00
      .2000000E+01 0.            .1000000E+00  .3750000E+05  .1837738E+01  .1744893E+00  .1635587E+00
      .3000000E+01 0.            .1000000E+00  .2500000E+05  .1837738E+01 0.            .1635587E+00
```

.4000000E+01	0.	.1000000E+00	.1875000E+05	.1837738E+01	0.	.1635587E+00
.5000000E+01	0.	.1000000E+00	.1500000E+05	.1837738E+01	0.	.1635587E+00
.6000000E+01	0.	.2000000E+00	.1250000E+05	.3675476E+01	.1948101E+00	.1635587E+00
.8000000E+01	0.	.2000000E+00	.9375000E+04	.3675476E+01	0.	.1635587E+00
.1000000E+02	0.	.2000000E+00	.7500000E+04	.3675476E+01	0.	.1635587E+00
.1200000E+02	0.	.2000000E+00	.6250000E+04	.3675476E+01	0.	.1635587E+00
.1500000E+02	0.	.3000000E+00	.5000000E+04	.5513215E+01	.2157681E+00	.1635587E+00
.1800000E+02	0.	.3000000E+00	.4166667E+04	.5513215E+01	0.	.1635587E+00
.2100000E+02	0.	.3000000E+00	.3571429E+04	.5513215E+01	0.	.1635587E+00
.2600000E+02	0.	.3000000E+00	.2884615E+04	.5513215E+01	0.	.1635587E+00
.3000000E+02	0.	.5000000E+00	.2500000E+04	.9188691E+01	.4697667E+00	.1635587E+00
.3600000E+02	0.	.9000000E+00	.2083333E+04	.1653964E+02	.9619495E+00	.1635587E+00
.4400000E+02	0.	.2800000E+01	.1704545E+04	.5145667E+02	.4692484E+01	.1635587E+00
.5400000E+02	0.	.2900000E+01	.1388889E+04	.5329441E+02	.2539625E+00	.1635587E+00
.6300000E+02	.2000000E-01	.3700000E+01	.1190476E+04	.6762877E+02	.2024024E+01	.1635587E+00
.7600000E+02	.5000000E-01	.4200000E+01	.9868421E+03	.7626614E+02	.1252789E+01	.1635587E+00
.9200000E+02	.7000000E-01	.4800000E+01	.8152174E+03	.8692502E+02	.1590058E+01	.1635587E+00
.1100000E+03	.1000000E+00	.5200000E+01	.6818182E+03	.9372465E+02	.1042127E+01	.1635587E+00
.1340000E+03	.1500000E+00	.5700000E+01	.5597015E+03	.1019945E+03	.1306985E+01	.1635587E+00
.1880000E+03	.3000000E+00	.6400000E+01	.3989362E+03	.1121020E+03	.1687743E+01	.1635587E+00
.2240000E+03	.4000000E+00	.6700000E+01	.3348214E+03	.1157775E+03	.6322207E+00	.1635587E+00
.2780000E+03	.5500000E+00	.7200000E+01	.2697842E+03	.1222096E+03	.1149074E+01	.1635587E+00
.3260000E+03	.6500000E+00	.7700000E+01	.2300613E+03	.1295605E+03	.1351689E+01	.1635587E+00
.4050000E+03	.9000000E+00	.8300000E+01	.1851852E+03	.1359926E+03	.1231880E+01	.1635587E+00
.5770000E+03	.1350000E+01	.9200000E+01	.1299827E+03	.1442624E+03	.1699022E+01	.1635587E+00
.6820000E+03	.1750000E+01	.9600000E+01	.1099707E+03	.1442624E+03	.1935007E-12	.1635587E+00
.8340000E+03	.2200000E+01	.1010000E+02	.8992806E+02	.1451813E+03	.2042381E+00	.1635587E+00
.1000000E+04	.2800000E+01	.1060000E+02	.7500000E+02	.1433436E+03	-.4256499E+00	.1635587E+00
.1210000E+04	.3500000E+01	.1110000E+02	.6198347E+02	.1396681E+03	-.8906213E+00	.1635587E+00
.1442000E+04	.3800000E+01	.1180000E+02	.5201110E+02	.1470191E+03	.1860314E+01	.1635587E+00
.1744000E+04	.4600000E+01	.1240000E+02	.4300459E+02	.1433436E+03	-.9771807E+00	.1635587E+00
.2000000E+04	.4800000E+01	.1370000E+02	.3750000E+02	.1635587E+03	.5577599E+01	.1635587E+00

.1595608E+00	.1025056E+05					
	.1000000E+01	0.	0.	.7500000E+05	0.	0.	.1422587E+00
	.2000000E+01	0.	0.	.3750000E+05	0.	0.	.1422587E+00
	.3000000E+01	0.	.1000000E+00	.2500000E+05	.1635157E+01	.1614710E+00	.1422587E+00
	.4000000E+01	0.	.1000000E+00	.1875000E+05	.1635157E+01	0.	.1422587E+00
	.5000000E+01	0.	.1000000E+00	.1500000E+05	.1635157E+01	0.	.1422587E+00
	.6000000E+01	0.	.1000000E+00	.1250000E+05	.1635157E+01	0.	.1422587E+00
	.8000000E+01	0.	.1000000E+00	.9375000E+04	.1635157E+01	0.	.1422587E+00
	.1000000E+02	0.	.1000000E+00	.7500000E+04	.1635157E+01	0.	.1422587E+00
	.1200000E+02	0.	.1000000E+00	.6250000E+04	.1635157E+01	0.	.1422587E+00
	.1500000E+02	0.	.2000000E+00	.5000000E+04	.3270315E+01	.1919831E+00	.1422587E+00
	.1800000E+02	0.	.2000000E+00	.4166667E+04	.3270315E+01	0.	.1422587E+00
	.2100000E+02	0.	.2000000E+00	.3571429E+04	.3270315E+01	0.	.1422587E+00
	.2600000E+02	0.	.3000000E+00	.2884615E+04	.4905472E+01	.2052375E+00	.1422587E+00
	.3000000E+02	0.	.6000000E+00	.2500000E+04	.9810944E+01	.6269738E+00	.1422587E+00
	.3600000E+02	0.	.1400000E+01	.2083333E+04	.2289220E+02	.1711820E+01	.1422587E+00
	.4400000E+02	0.	.2000000E+01	.1704545E+04	.3270315E+02	.1318489E+01	.1422587E+00
	.5400000E+02	0.	.2600000E+01	.1388889E+04	.4251409E+02	.1355803E+01	.1422587E+00
	.6300000E+02	.2000000E-01	.2900000E+01	.1190476E+04	.4709253E+02	.6464799E+00	.1422587E+00
	.7600000E+02	.5000000E-01	.3500000E+01	.9868421E+03	.5641293E+02	.1351858E+01	.1422587E+00
	.9200000E+02	.7000000E-01	.4300000E+01	.8152174E+03	.6916716E+02	.1902635E+01	.1422587E+00
	.1100000E+03	.1000000E+00	.5000000E+01	.6818182E+03	.8012271E+02	.1679073E+01	.1422587E+00
	.1340000E+03	.1500000E+00	.5900000E+01	.5597015E+03	.9402155E+02	.2196610E+01	.1422587E+00
	.1880000E+03	.3000000E+00	.7600000E+01	.3989362E+03	.1193665E+03	.4232055E+01	.1422587E+00
	.2240000E+03	.4000000E+00	.8200000E+01	.3348214E+03	.1275423E+03	.1406321E+01	.1422587E+00
	.2780000E+03	.5500000E+00	.8800000E+01	.2697842E+03	.1349005E+03	.1314524E+01	.1422587E+00
	.3260000E+03	.6500000E+00	.9100000E+01	.2300613E+03	.1381708E+03	.6013436E+00	.1422587E+00
	.4050000E+03	.9000000E+00	.9600000E+01	.1851852E+03	.1422587E+03	.7829179E+00	.1422587E+00
	.5770000E+03	.1350000E+01	.1010000E+02	.1299827E+03	.1430763E+03	.1679703E+00	.1422587E+00
	.6820000E+03	.1750000E+01	.1040000E+02	.1099707E+03	.1414411E+03	-.3478900E+00	.1422587E+00
	.8340000E+03	.2200000E+01	.1070000E+02	.8992806E+02	.1389884E+03	-.5451724E+00	.1422587E+00
	.1000000E+04	.2800000E+01	.1110000E+02	.7500000E+02	.1357181E+03	-.7574577E+00	.1422587E+00
	.1210000E+04	.3500000E+01	.1160000E+02	.6198347E+02	.1324477E+03	-.7924448E+00	.1422587E+00
	.1442000E+04	.3800000E+01	.1220000E+02	.5201110E+02	.1373532E+03	.1241434E+01	.1422587E+00

	.1744000E+04	.4600000E+01	.1280000E+02	.4300459E+02	.1340829E+03	-.8694624E+00	.1422587E+00
	.2000000E+04	.4800000E+01	.1350000E+02	.3750000E+02	.1422587E+03	.2255800E+01	.1422587E+00
.6948852E-01	.2047226E+05						
	.1000000E+01	0.	0.	.7500000E+05	0.	0.	.1471283E+00
	.2000000E+01	0.	0.	.3750000E+05	0.	0.	.1471283E+00
	.3000000E+01	0.	.1000000E+00	.2500000E+05	.2263512E+01	.2235208E+00	.1471283E+00
	.4000000E+01	0.	.1000000E+00	.1875000E+05	.2263512E+01	0.	.1471283E+00
	.5000000E+01	0.	.1000000E+00	.1500000E+05	.2263512E+01	0.	.1471283E+00
	.6000000E+01	0.	.2000000E+00	.1250000E+05	.4527025E+01	.2399445E+00	.1471283E+00
	.8000000E+01	0.	.2000000E+00	.9375000E+04	.4527025E+01	0.	.1471283E+00
	.1000000E+02	0.	.2000000E+00	.7500000E+04	.4527025E+01	0.	.1471283E+00
	.1200000E+02	0.	.2000000E+00	.6250000E+04	.4527025E+01	0.	.1471283E+00
	.1500000E+02	0.	.2000000E+00	.5000000E+04	.4527025E+01	0.	.1471283E+00
	.1800000E+02	0.	.2000000E+00	.4166667E+04	.4527025E+01	0.	.1471283E+00
	.2100000E+02	0.	.2000000E+00	.3571429E+04	.4527025E+01	0.	.1471283E+00
	.2600000E+02	0.	.3000000E+00	.2884615E+04	.6790537E+01	.2841058E+00	.1471283E+00
	.3000000E+02	0.	.3000000E+00	.2500000E+04	.6790537E+01	0.	.1471283E+00
	.3600000E+02	0.	.3000000E+00	.2083333E+04	.6790537E+01	0.	.1471283E+00
	.4400000E+02	0.	.3000000E+00	.1704545E+04	.6790537E+01	0.	.1471283E+00
	.5400000E+02	0.	.4000000E+00	.1388889E+04	.9054049E+01	.3128014E+00	.1471283E+00
	.6300000E+02	.2000000E-01	.4000000E+00	.1190476E+04	.8601347E+01	-.6392199E-01	.1471283E+00
	.7600000E+02	.5000000E-01	.6000000E+00	.9868421E+03	.1244932E+02	.5581210E+00	.1471283E+00
	.9200000E+02	.7000000E-01	.1000000E+01	.8152174E+03	.2105066E+02	.1283121E+01	.1471283E+00
	.1100000E+03	.1000000E+00	.2200000E+01	.6818182E+03	.4753376E+02	.4058859E+01	.1471283E+00
	.1340000E+03	.1500000E+00	.3400000E+01	.5597015E+03	.7356415E+02	.4113914E+01	.1471283E+00
	.1880000E+03	.3000000E+00	.5100000E+01	.3989362E+03	.1086486E+03	.5858341E+01	.1471283E+00
	.2240000E+03	.4000000E+00	.5800000E+01	.3348214E+03	.1222297E+03	.2336088E+01	.1471283E+00
	.2780000E+03	.5500000E+00	.6500000E+01	.2697842E+03	.1346790E+03	.2224037E+01	.1471283E+00
	.3260000E+03	.6500000E+00	.6800000E+01	.2300613E+03	.1392060E+03	.8324267E+00	.1471283E+00
	.4050000E+03	.9000000E+00	.7300000E+01	.1851852E+03	.1448648E+03	.1083776E+01	.1471283E+00
	.5770000E+03	.1350000E+01	.7900000E+01	.1299827E+03	.1482601E+03	.6975526E+00	.1471283E+00
	.6820000E+03	.1750000E+01	.8200000E+01	.1099707E+03	.1459965E+03	-.4815765E+00	.1471283E+00
	.8340000E+03	.2200000E+01	.8600000E+01	.8992806E+02	.1448648E+03	-.2515567E+00	.1471283E+00
	.1000000E+04	.2800000E+01	.9100000E+01	.7500000E+02	.1426013E+03	-.5242660E+00	.1471283E+00
	.1210000E+04	.3500000E+01	.9500000E+01	.6198347E+02	.1358107E+03	-.1645446E+01	.1471283E+00
	.1442000E+04	.3800000E+01	.1000000E+02	.5201110E+02	.1403378E+03	.1145660E+01	.1471283E+00
	.1744000E+04	.4600000E+01	.1070000E+02	.4300459E+02	.1380743E+03	-.6017888E+00	.1471283E+00
	.2000000E+04	.4800000E+01	.1130000E+02	.3750000E+02	.1471283E+03	.2498123E+01	.1471283E+00
.9121170E-01	.1613042E+05						

APPENDIX THREE

FIGURES A3.1 - A3.50

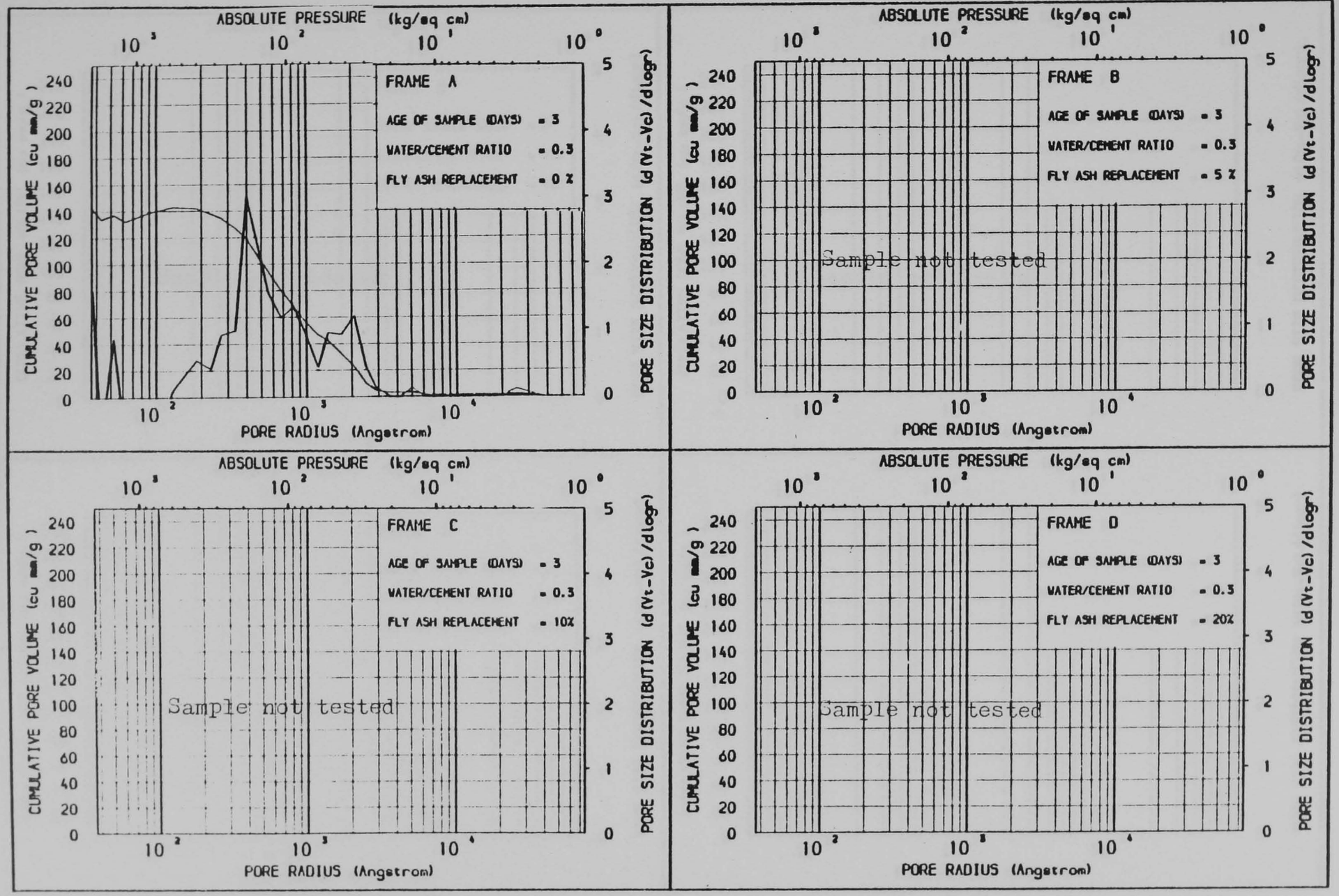

Figure A3.1 THE EFFECT OF FLY ASH REPLACEMENT OF CEMENT ON PORE SIZE DISTRIBUTION

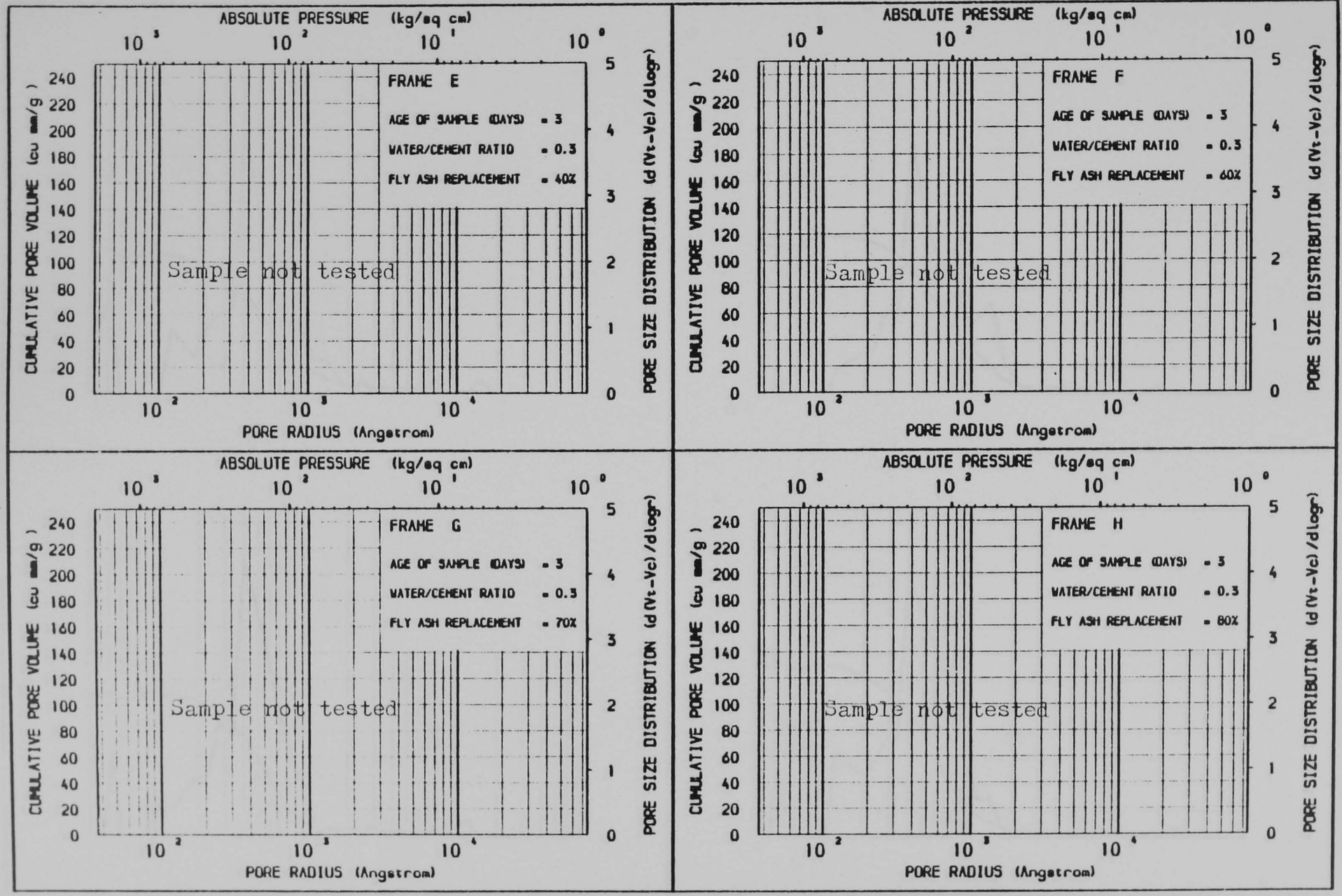

Figure A3.2 THE EFFECT OF FLY ASH REPLACEMENT OF CEMENT ON PORE SIZE DISTRIBUTION

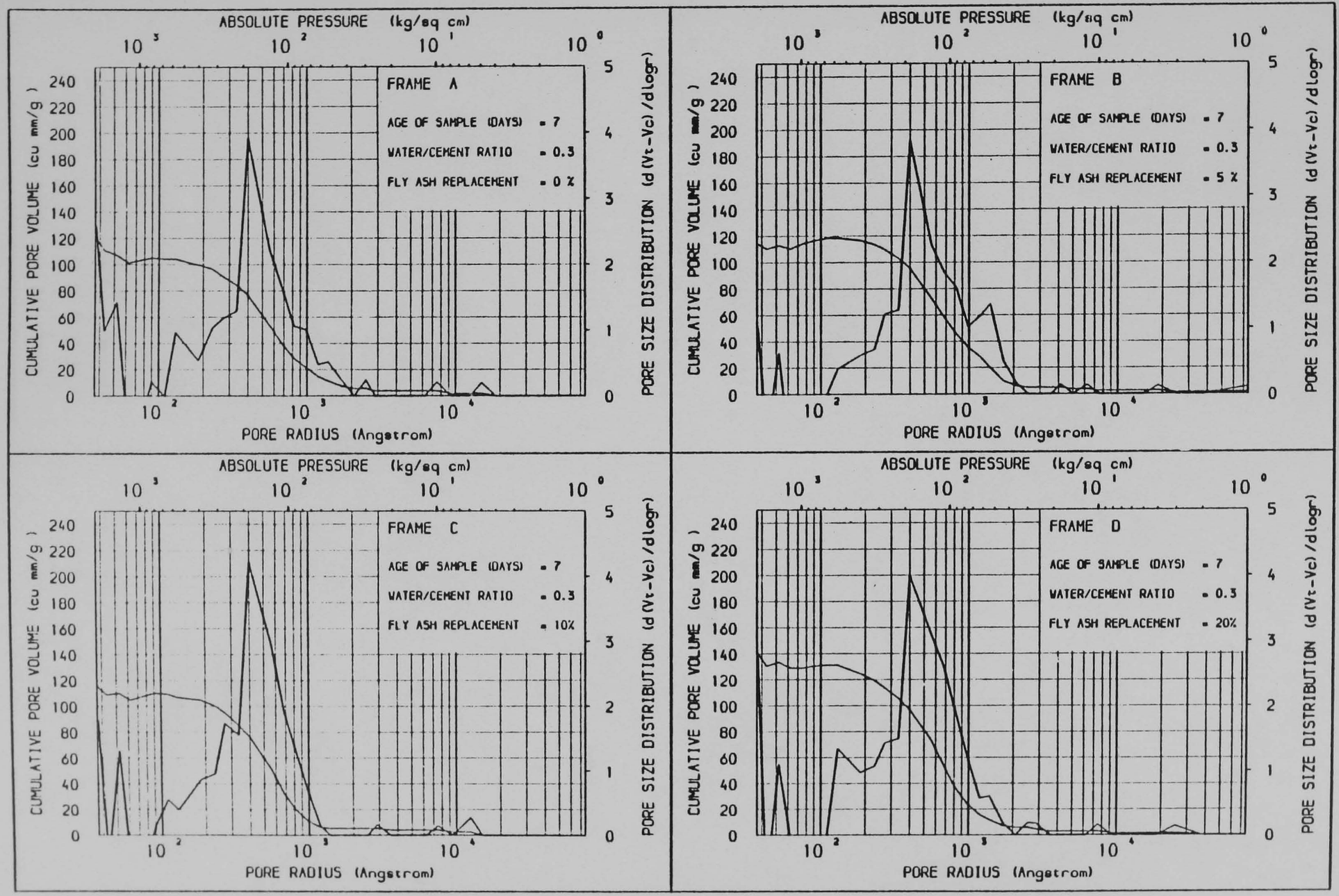

Figure A3.3 THE EFFECT OF FLY ASH REPLACEMENT OF CEMENT ON PORE SIZE DISTRIBUTION

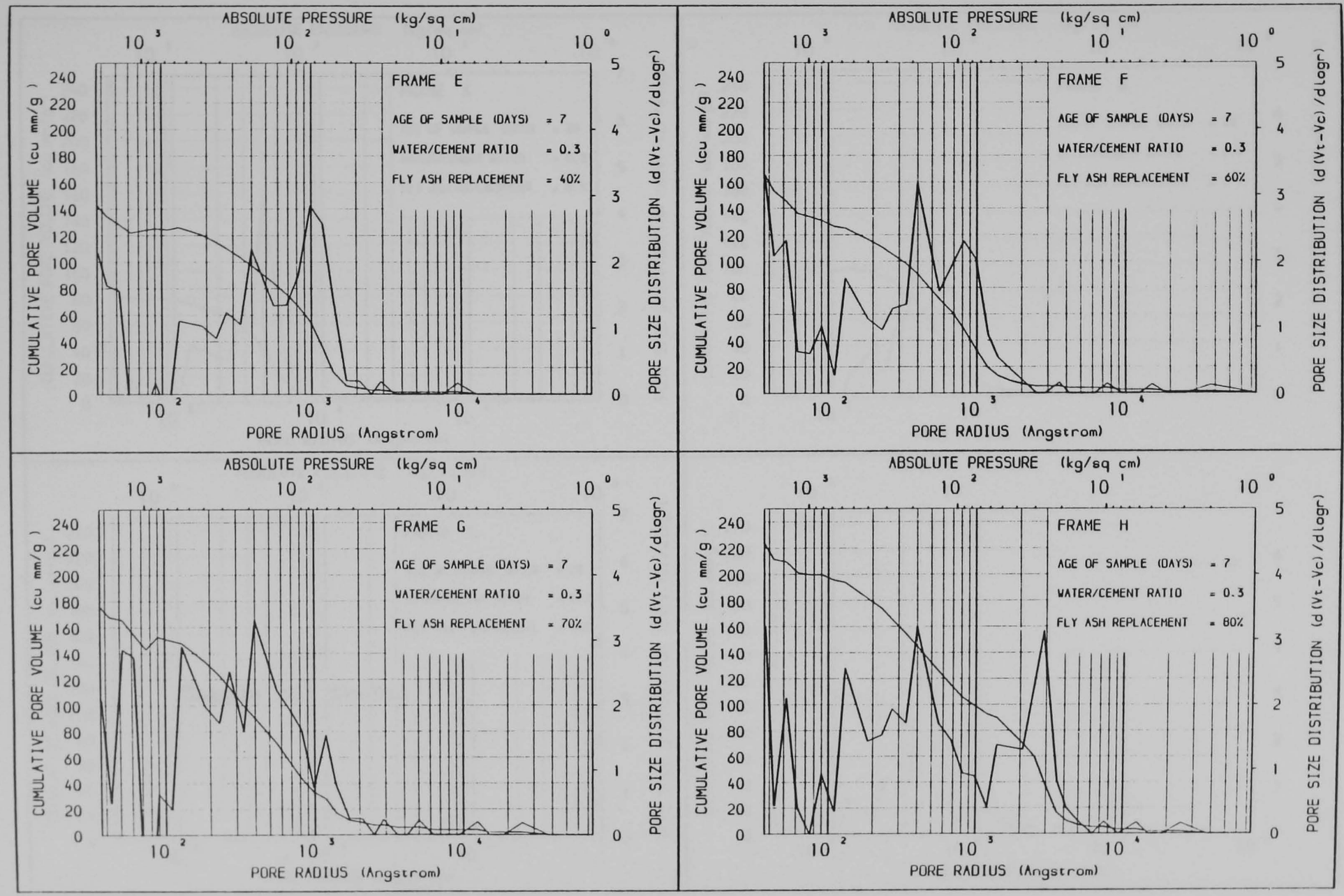

Figure A3.4 THE EFFECT OF FLY ASH REPLACEMENT OF CEMENT ON PORE SIZE DISTRIBUTION

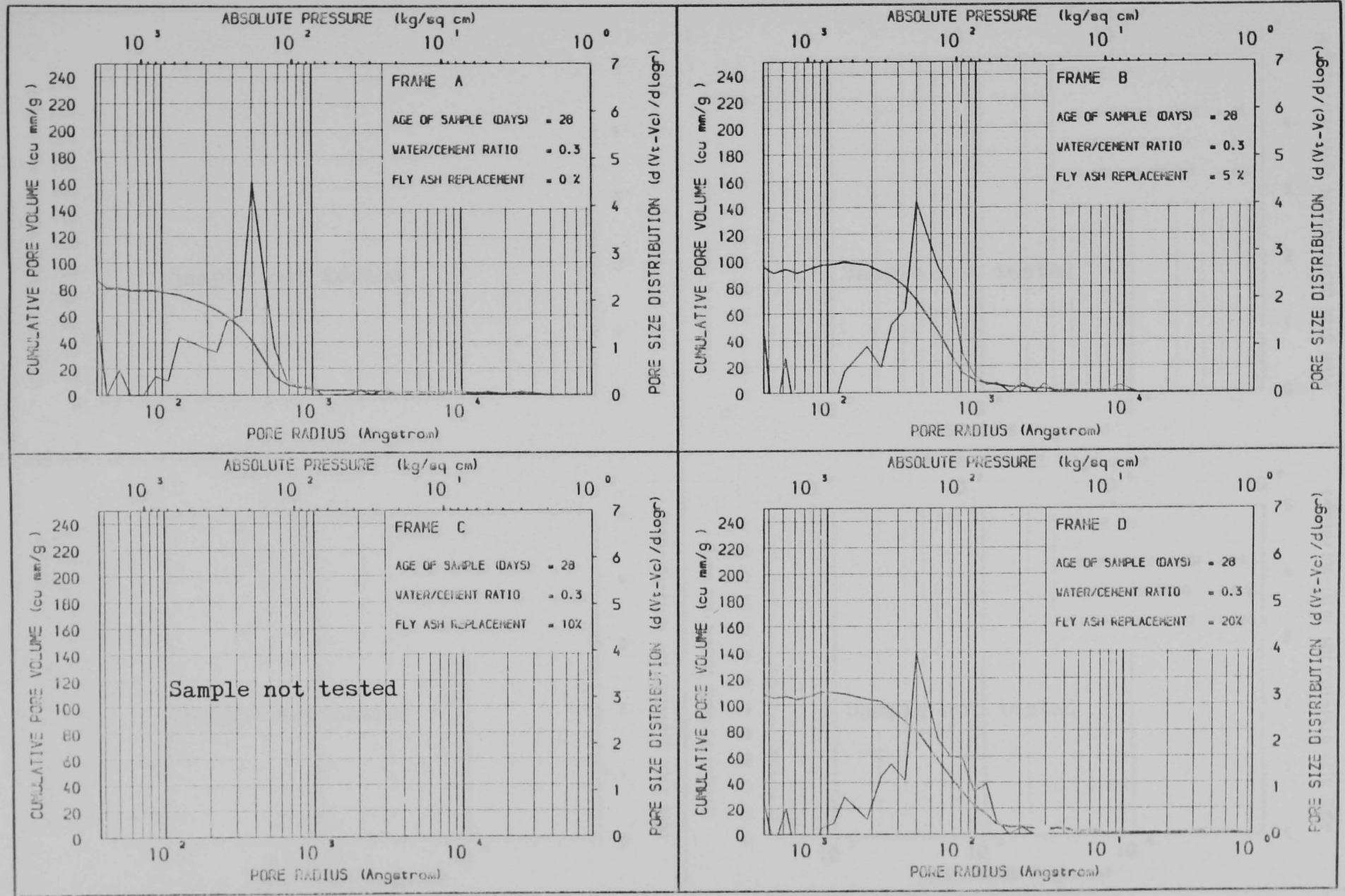

Figure A3.5 THE EFFECT OF FLY ASH REPLACEMENT OF CEMENT ON PORE SIZE DISTRIBUTION

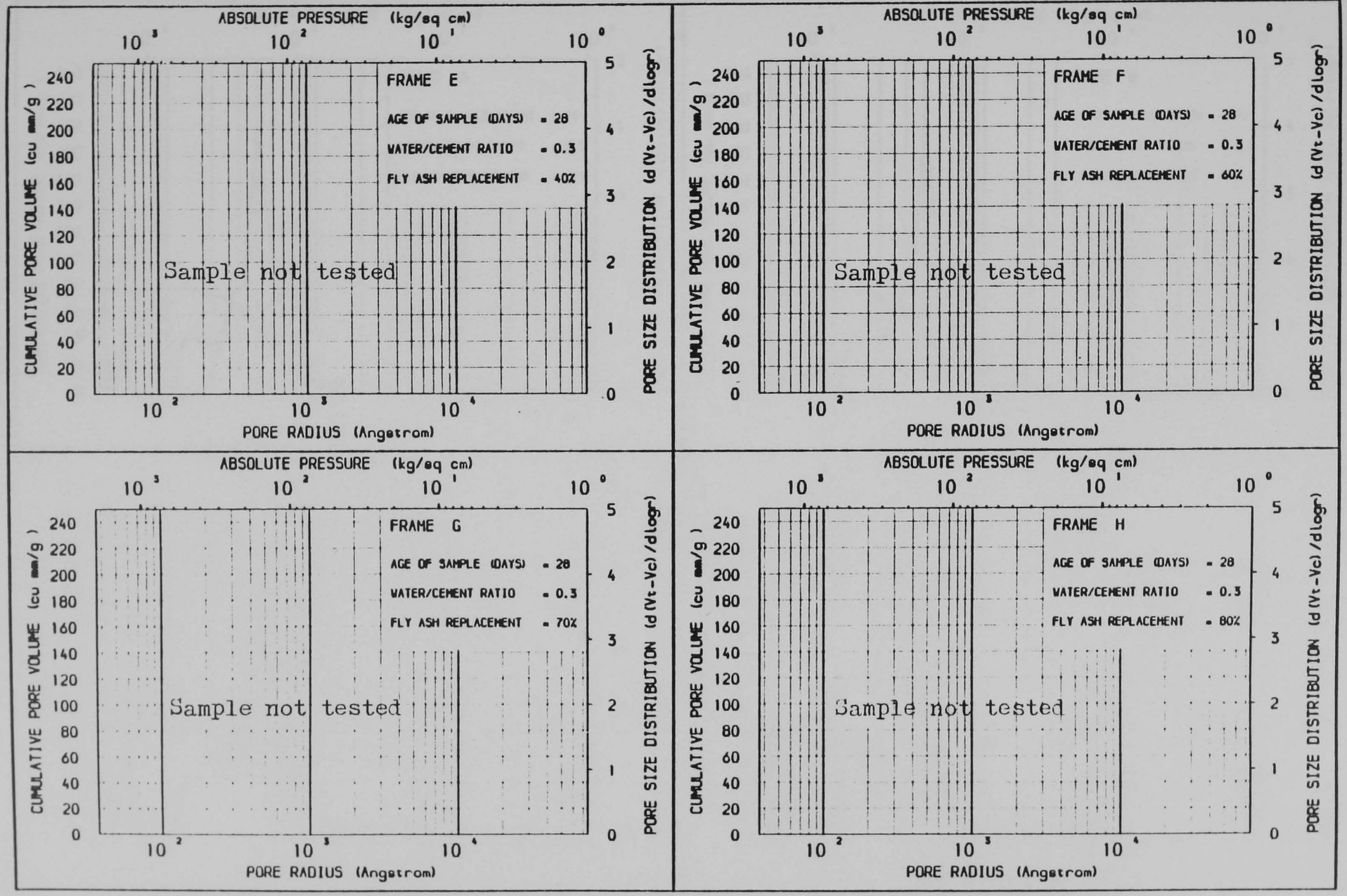

Figure A3.6 THE EFFECT OF FLY ASH REPLACEMENT OF CEMENT ON PORE SIZE DISTRIBUTION

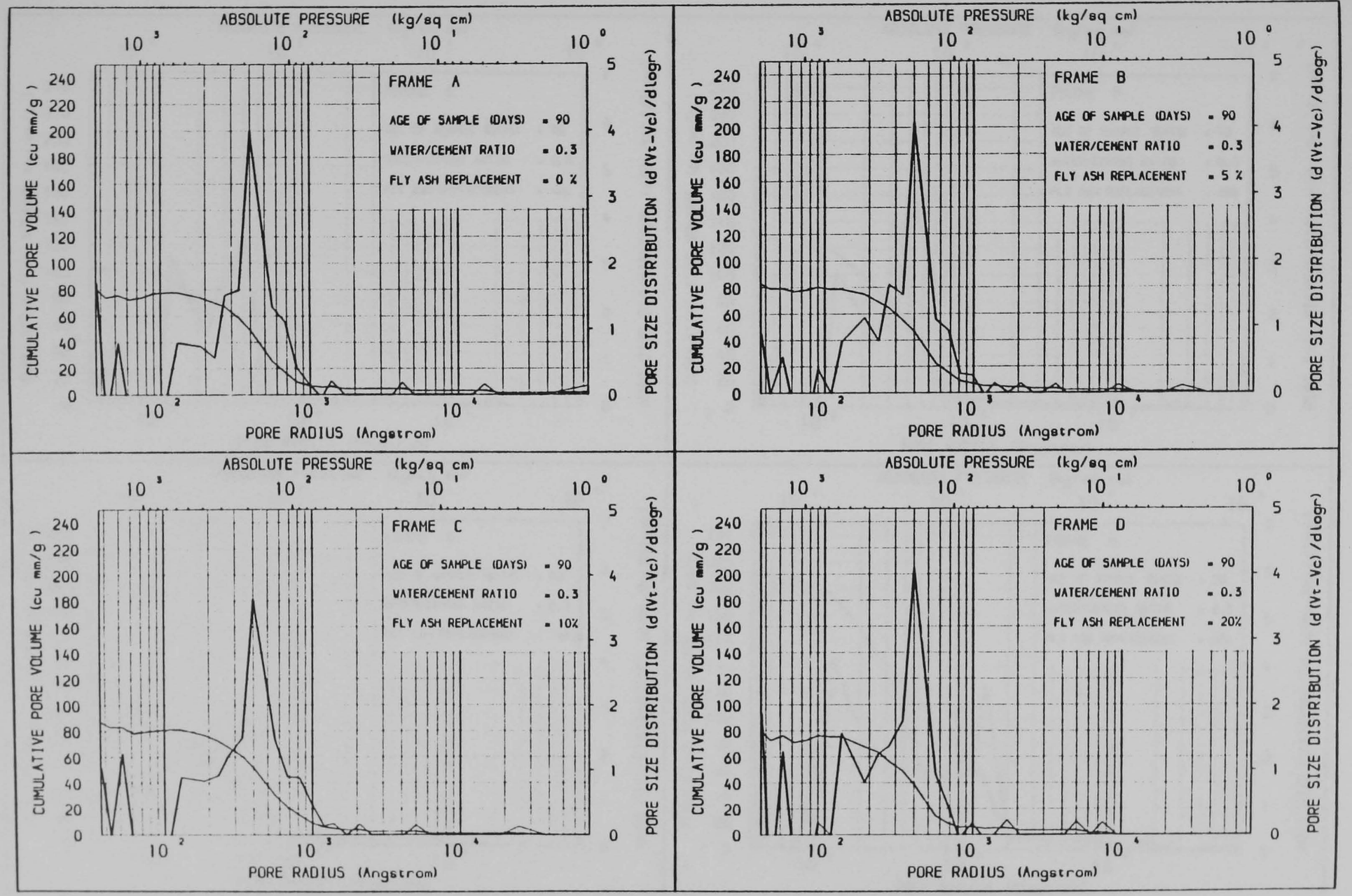

Figure A3.7 THE EFFECT OF FLY ASH REPLACEMENT OF CEMENT ON PORE SIZE DISTRIBUTION

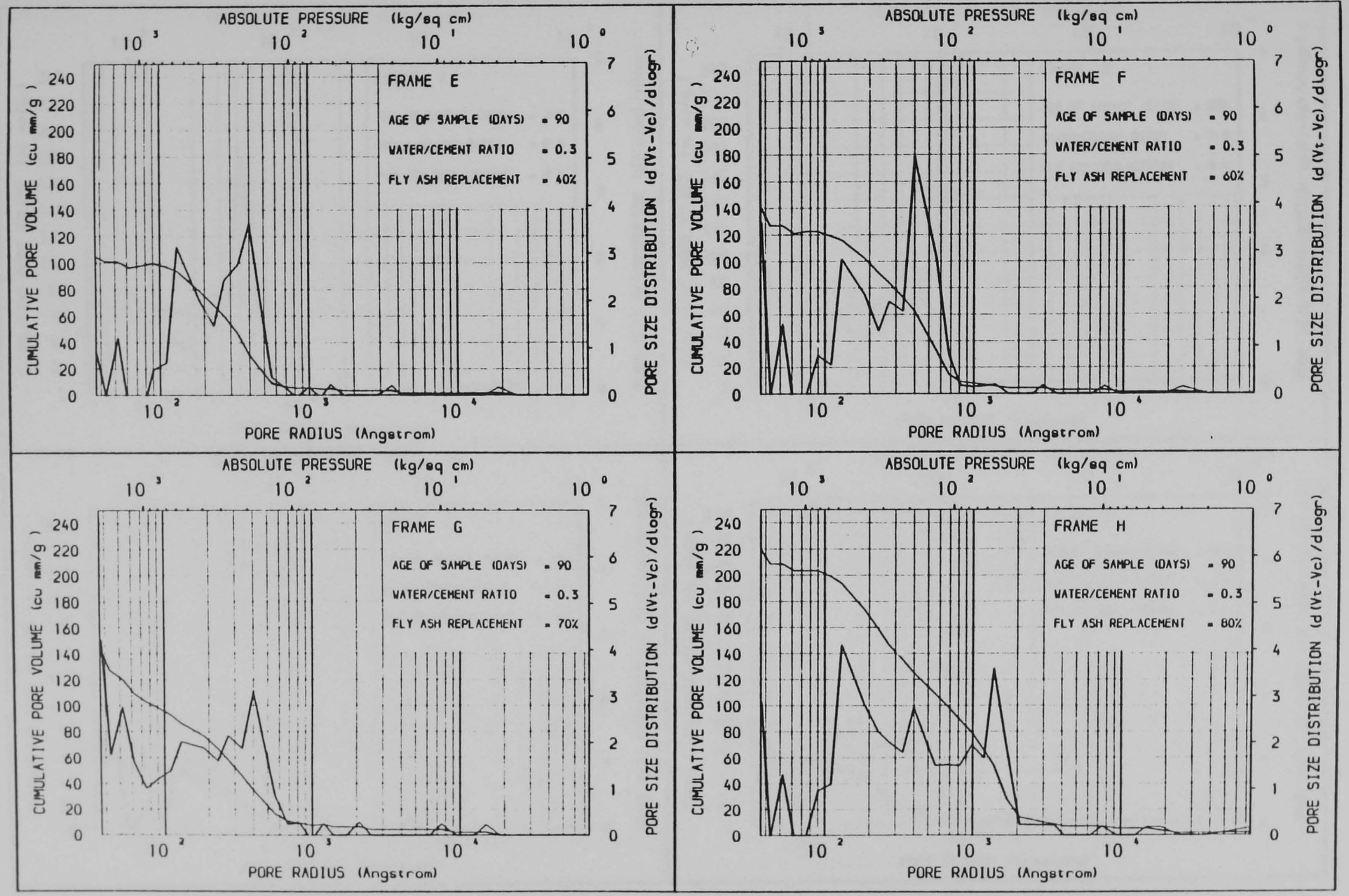

Figure A3.8 THE EFFECT OF FLY ASH REPLACEMENT OF CEMENT ON PORE SIZE DISTRIBUTION

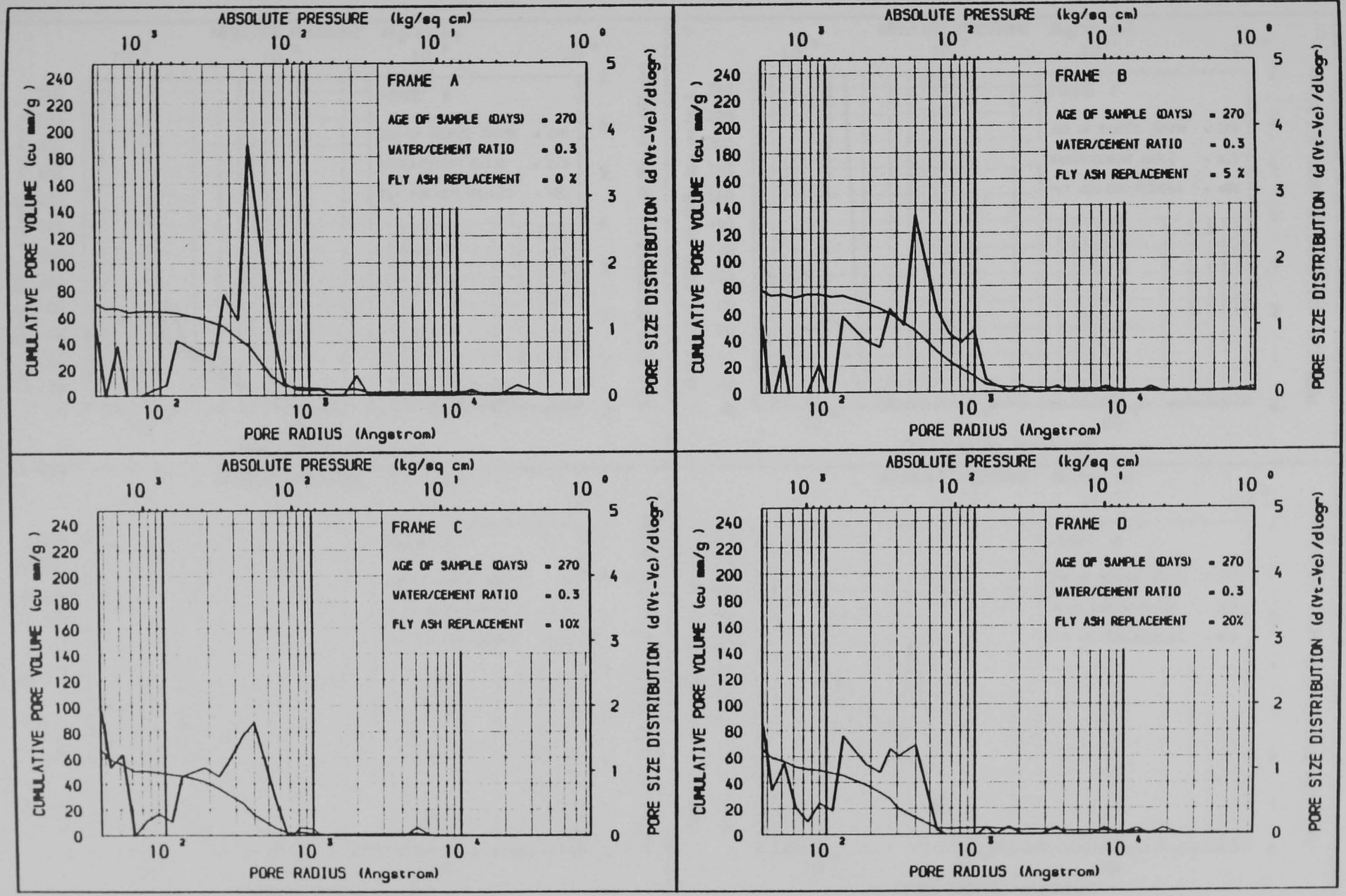

Figure A3.9 THE EFFECT OF FLY ASH REPLACEMENT OF CEMENT ON PORE SIZE DISTRIBUTION

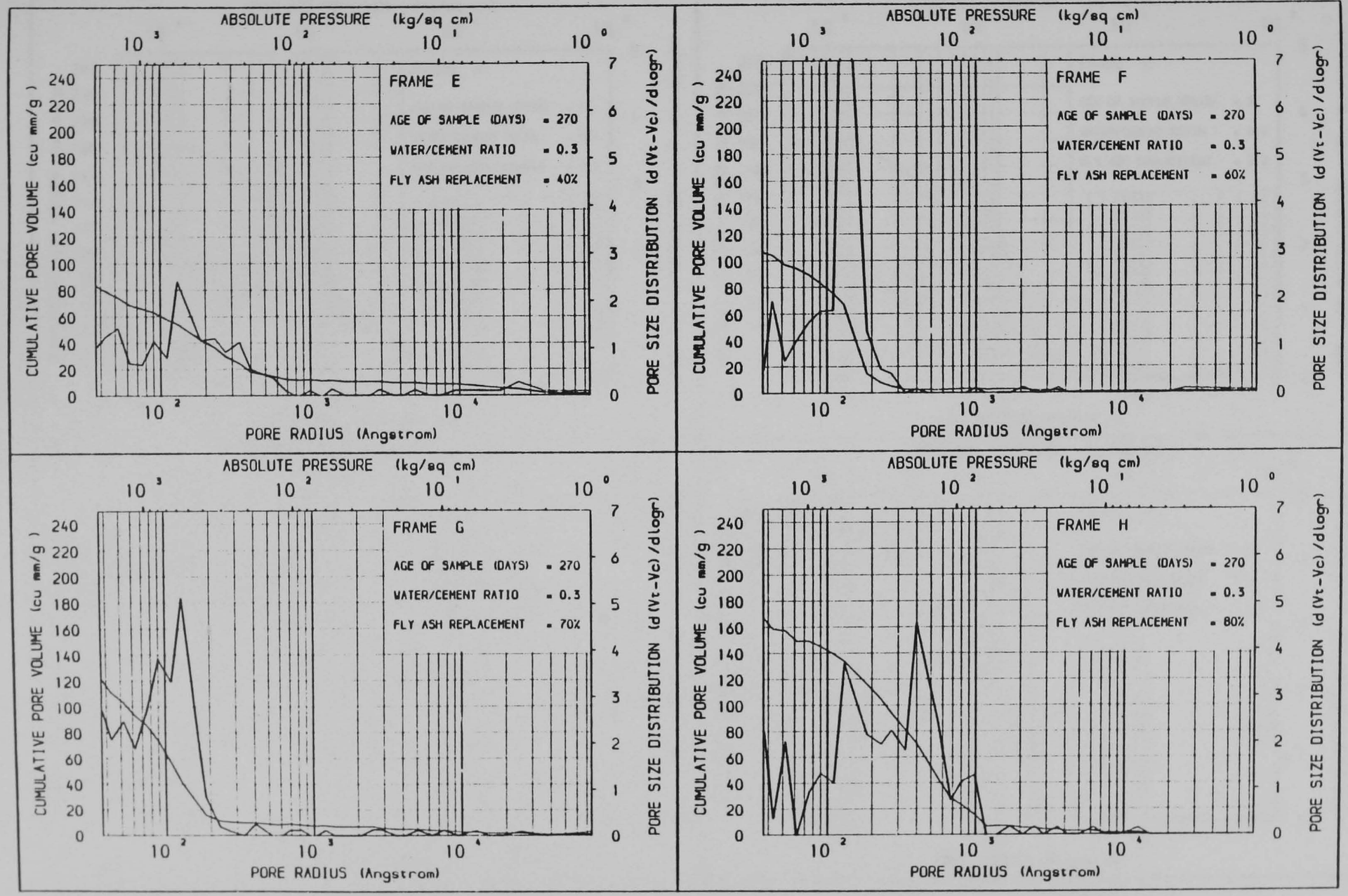

Figure A3.10 THE EFFECT OF FLY ASH REPLACEMENT OF CEMENT ON PORE SIZE DISTRIBUTION

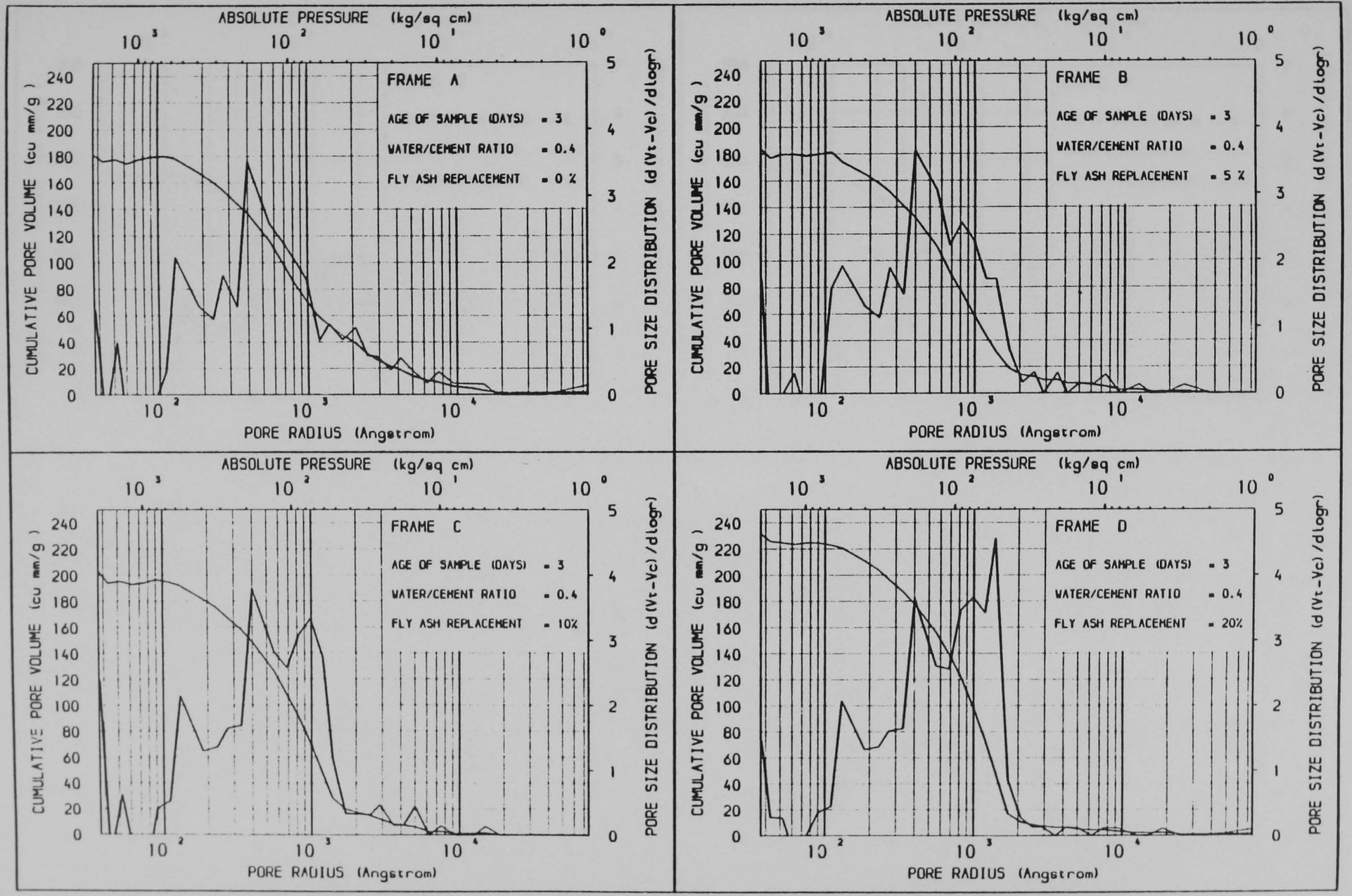

Figure A3.11 THE EFFECT OF FLY ASH REPLACEMENT OF CEMENT ON PORE SIZE DISTRIBUTION

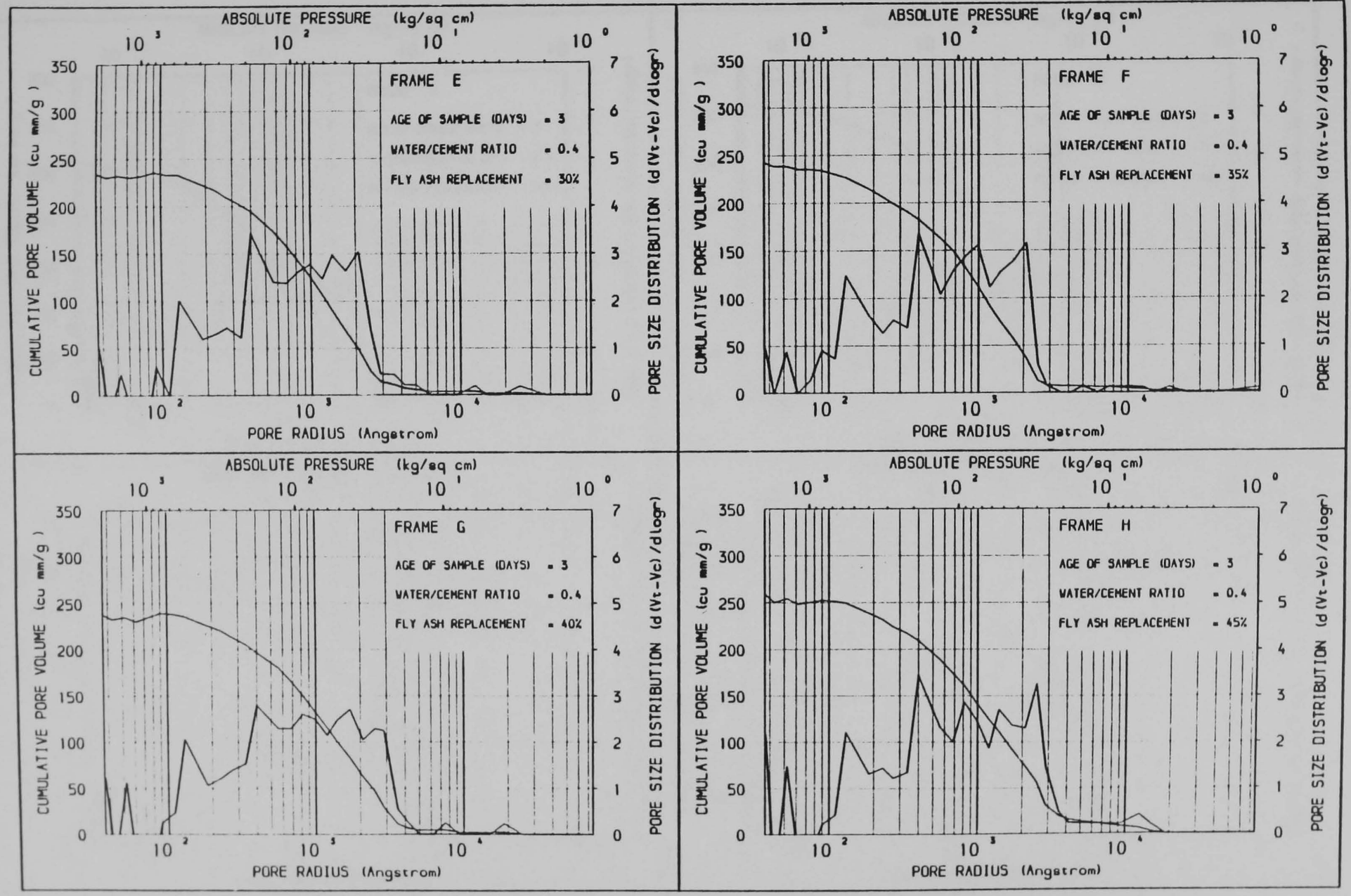

Figure A3.12 THE EFFECT OF FLY ASH REPLACEMENT OF CEMENT ON PORE SIZE DISTRIBUTION

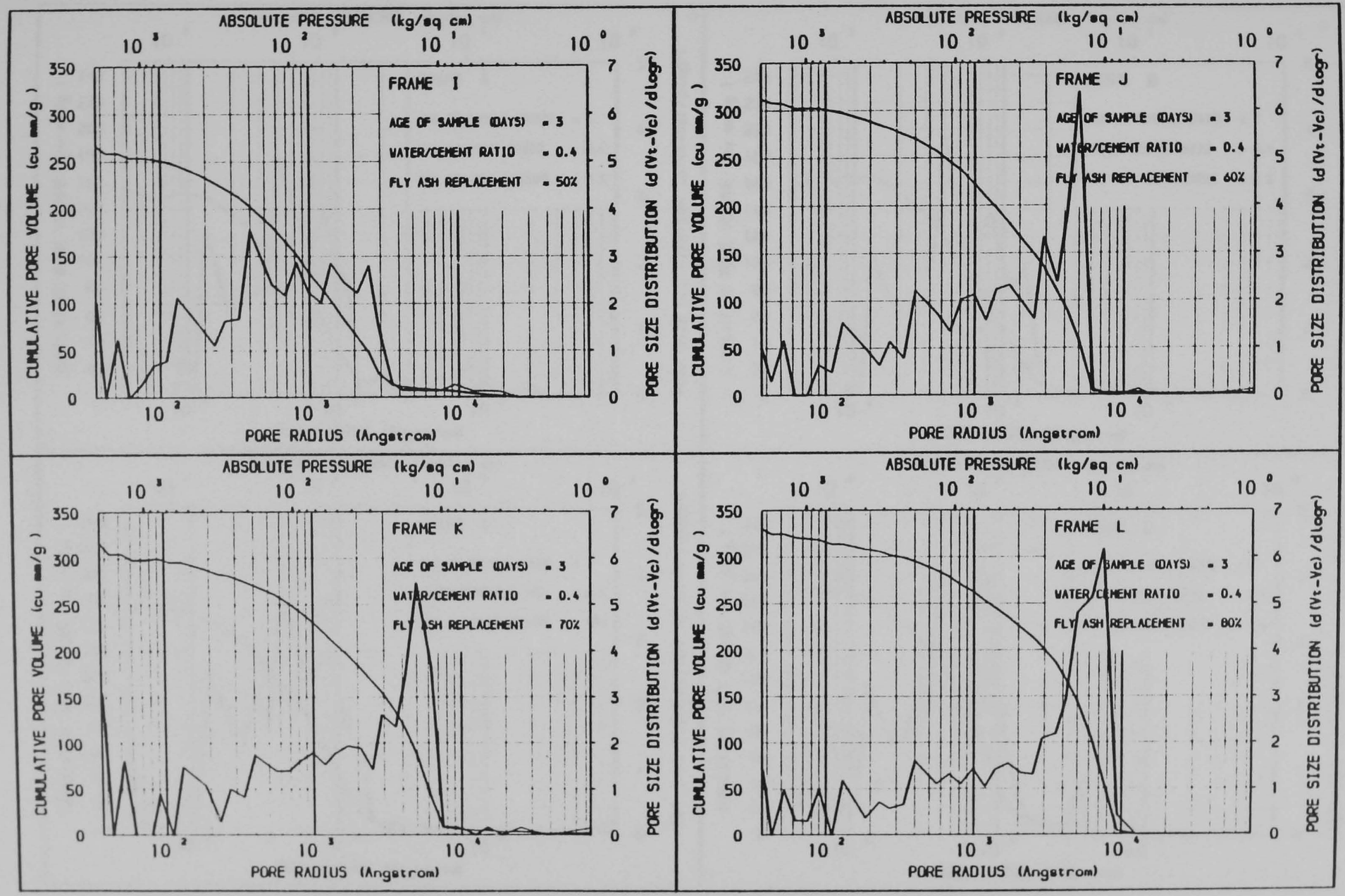

Figure A3.13 THE EFFECT OF FLY ASH REPLACEMENT OF CEMENT ON PORE SIZE DISTRIBUTION

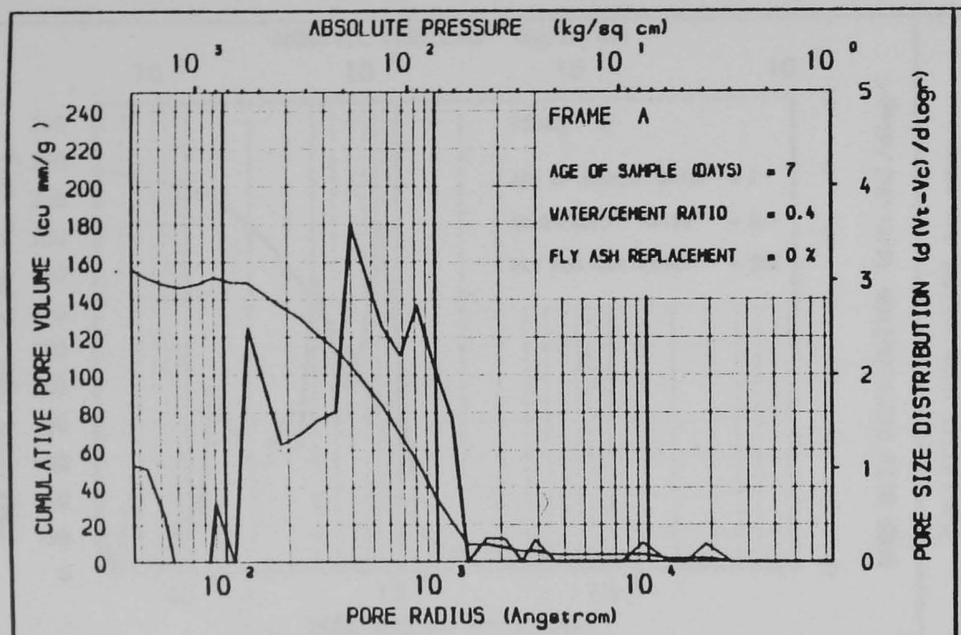

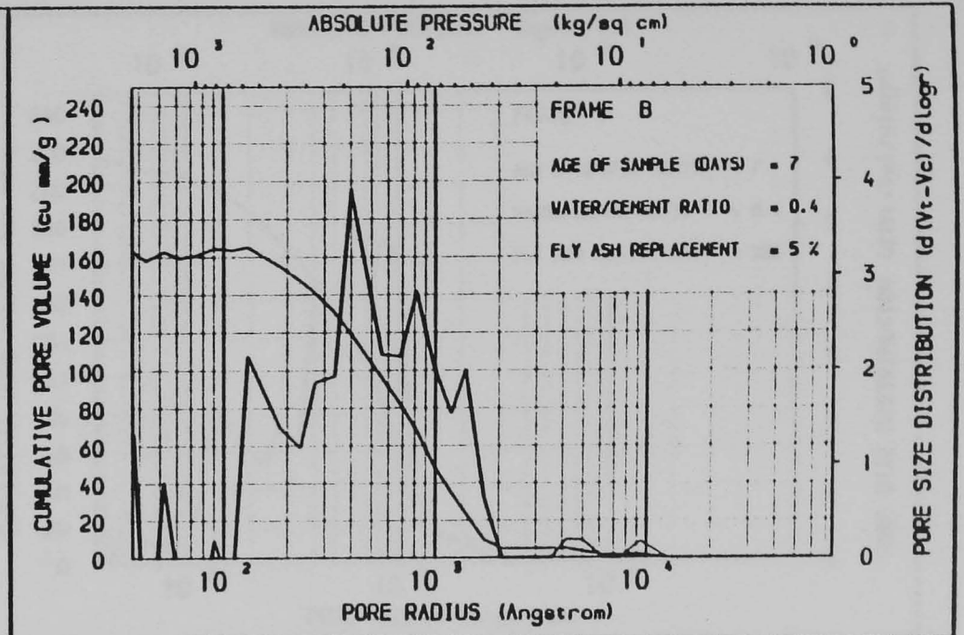

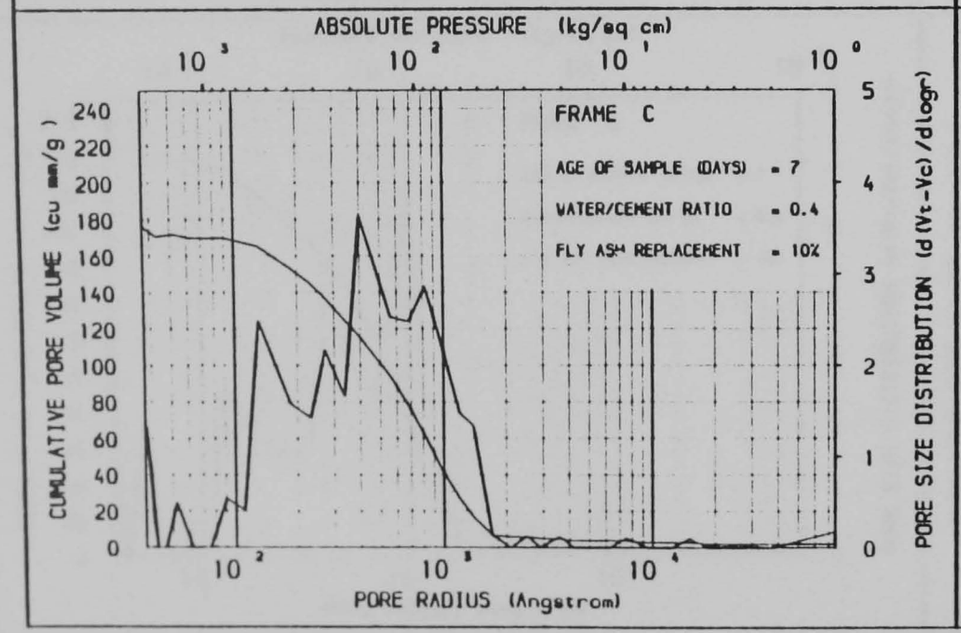

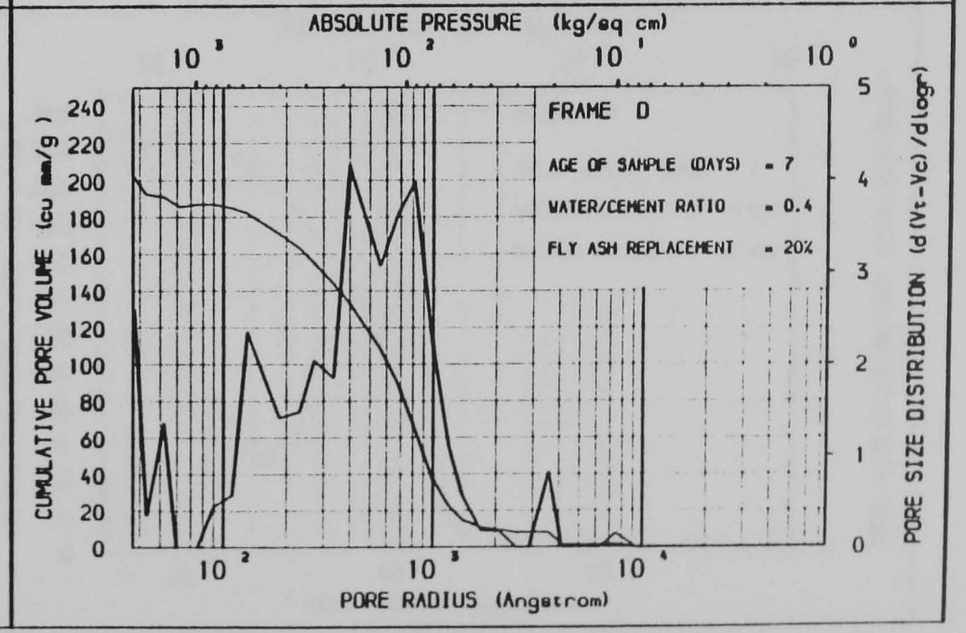

Figure A3.14 THE EFFECT OF FLY ASH REPLACEMENT OF CEMENT ON PORE SIZE DISTRIBUTION

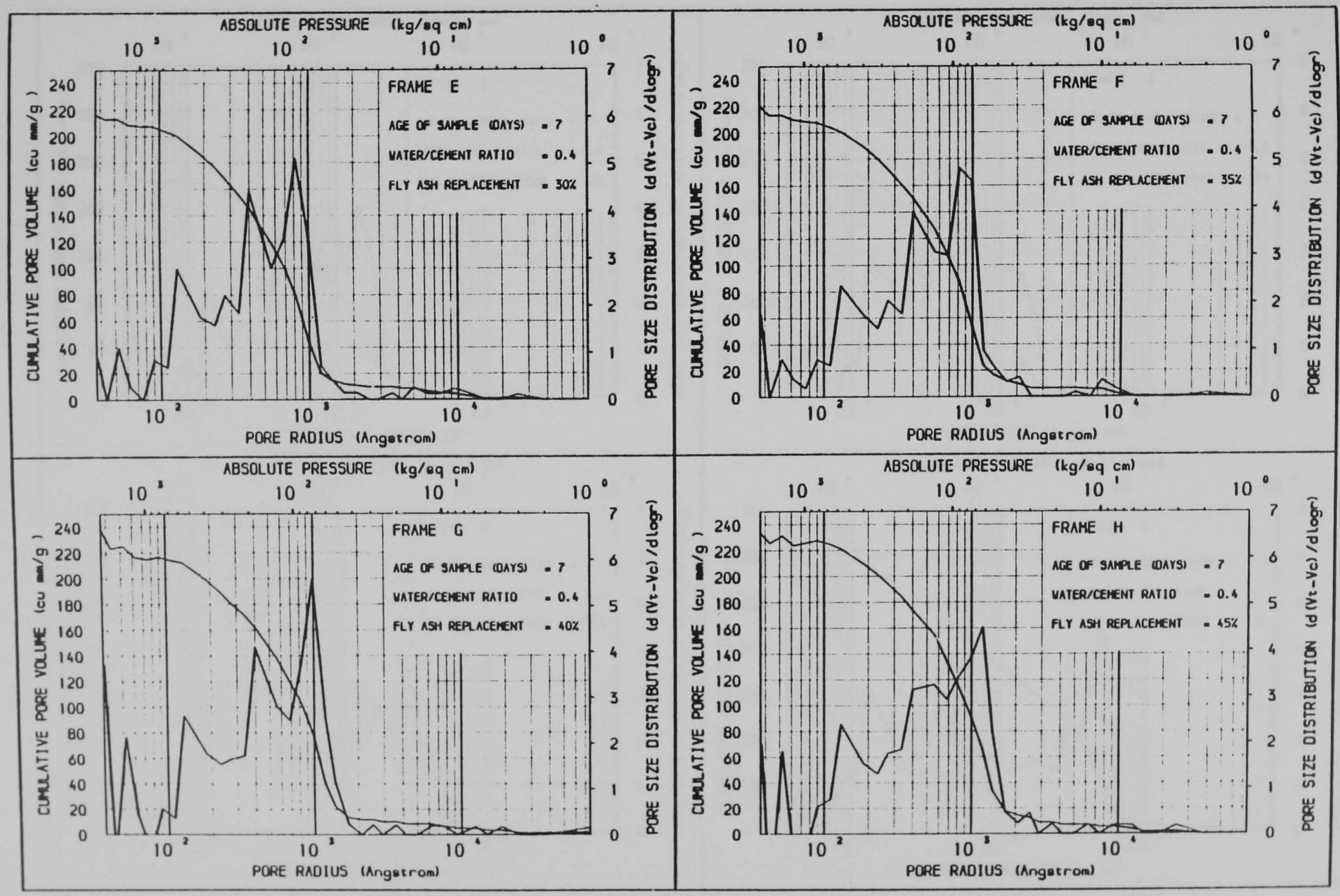

Figure A3.15 THE EFFECT OF FLY ASH REPLACEMENT OF CEMENT ON PORE SIZE DISTRIBUTION

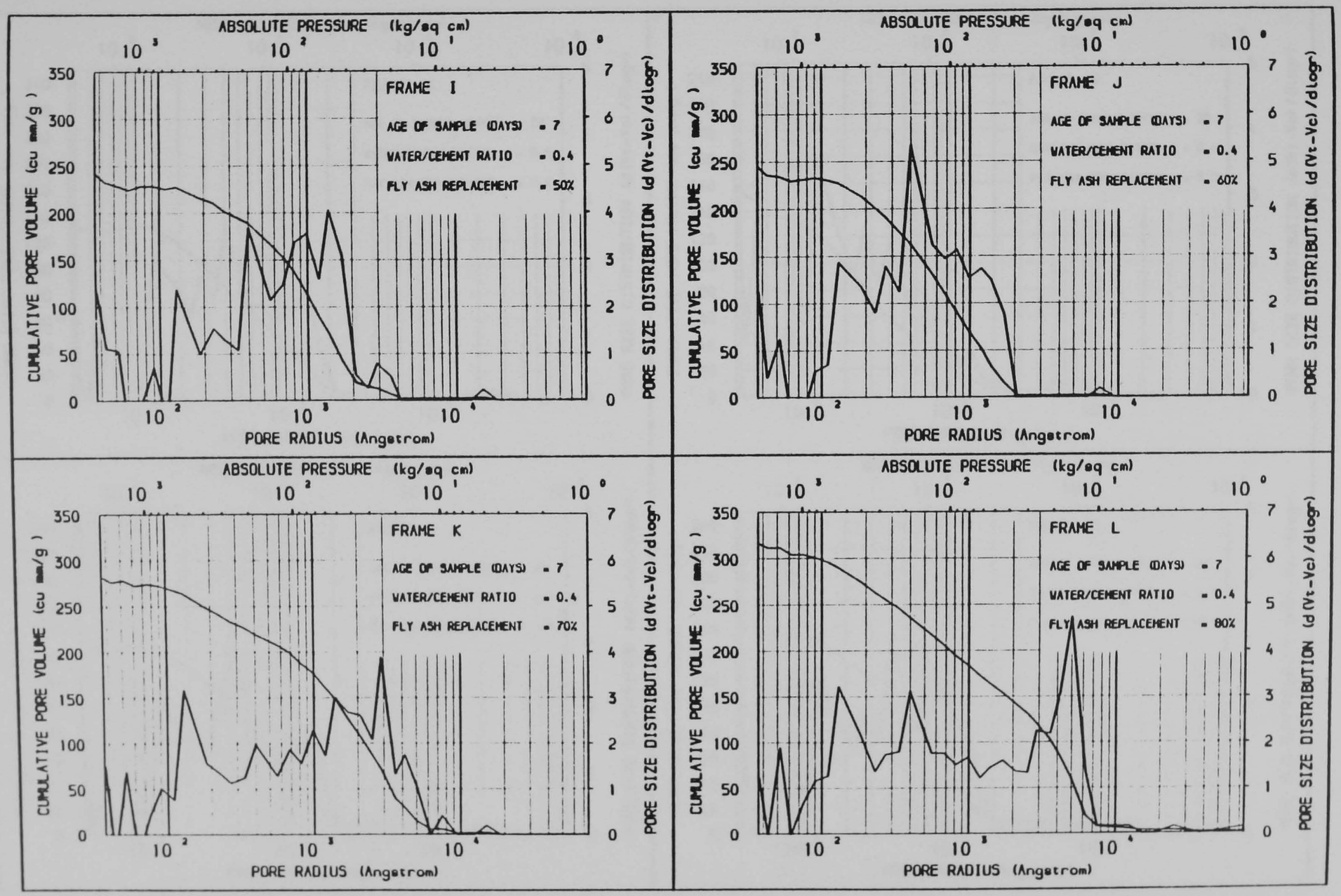

Figure A3.16 THE EFFECT OF FLY ASH REPLACEMENT OF CEMENT ON PORE SIZE DISTRIBUTION

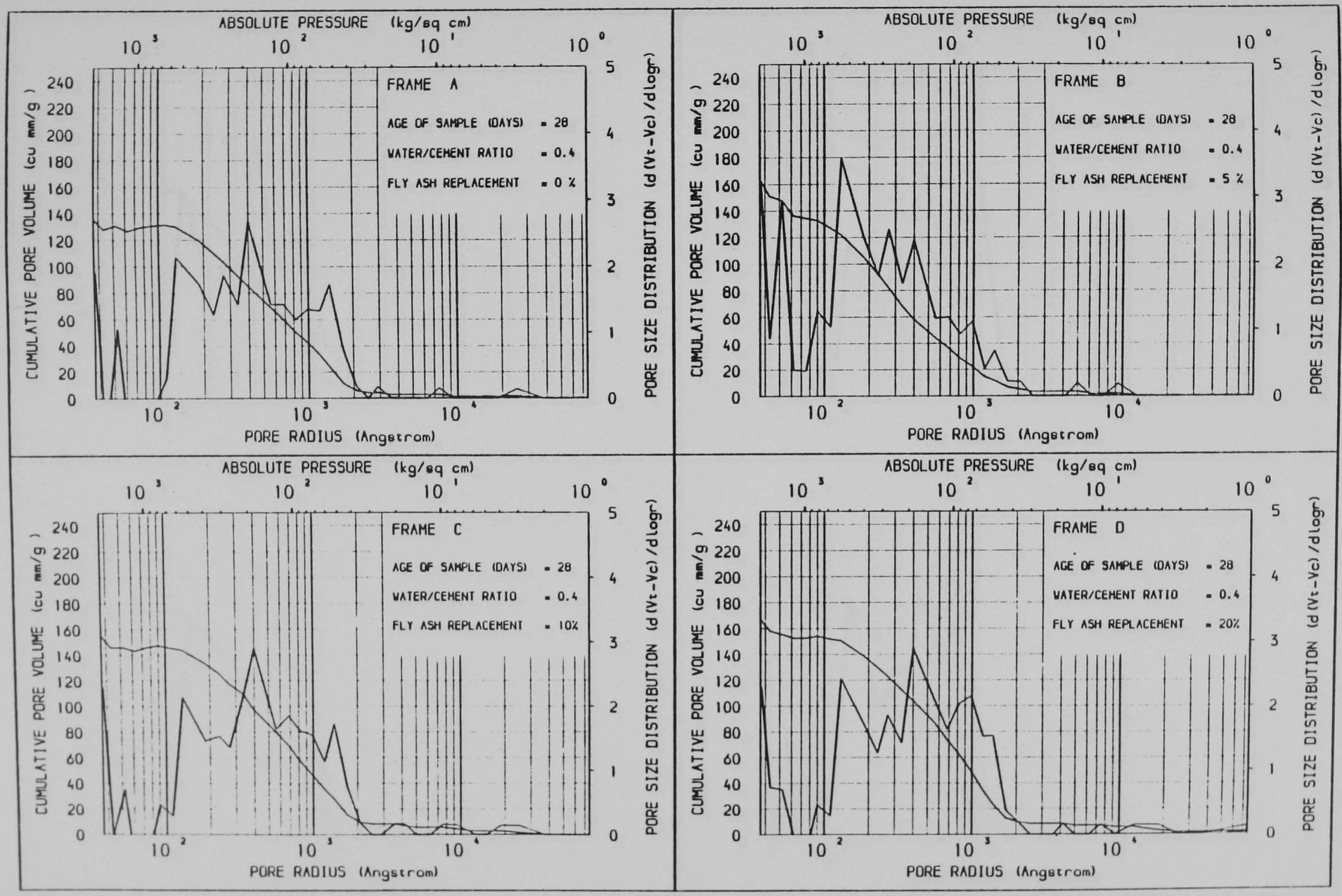

Figure A3.17 THE EFFECT OF FLY ASH REPLACEMENT OF CEMENT ON PORE SIZE DISTRIBUTION

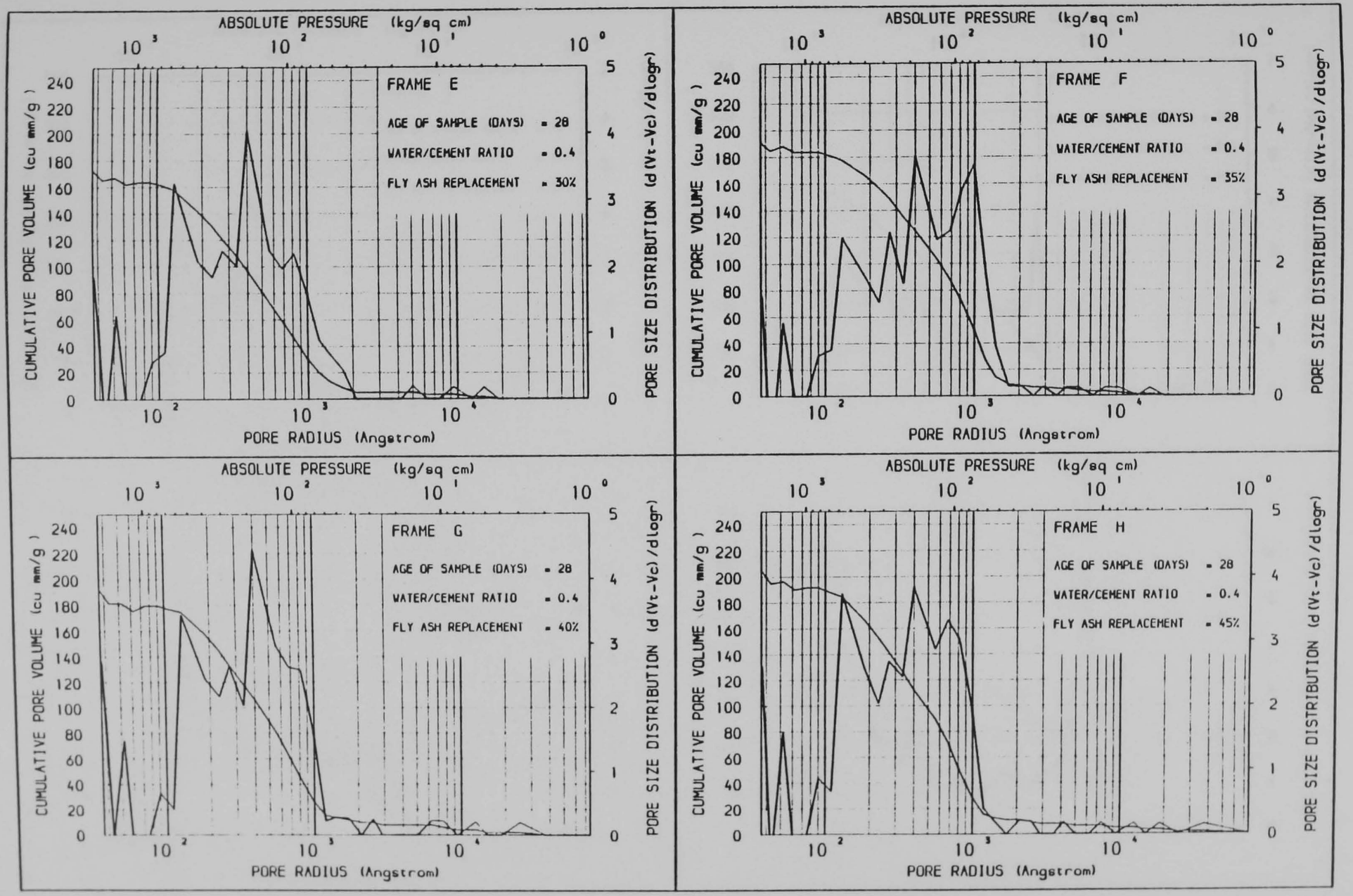

Figure A3.18 THE EFFECT OF FLY ASH REPLACEMENT OF CEMENT ON PORE SIZE DISTRIBUTION

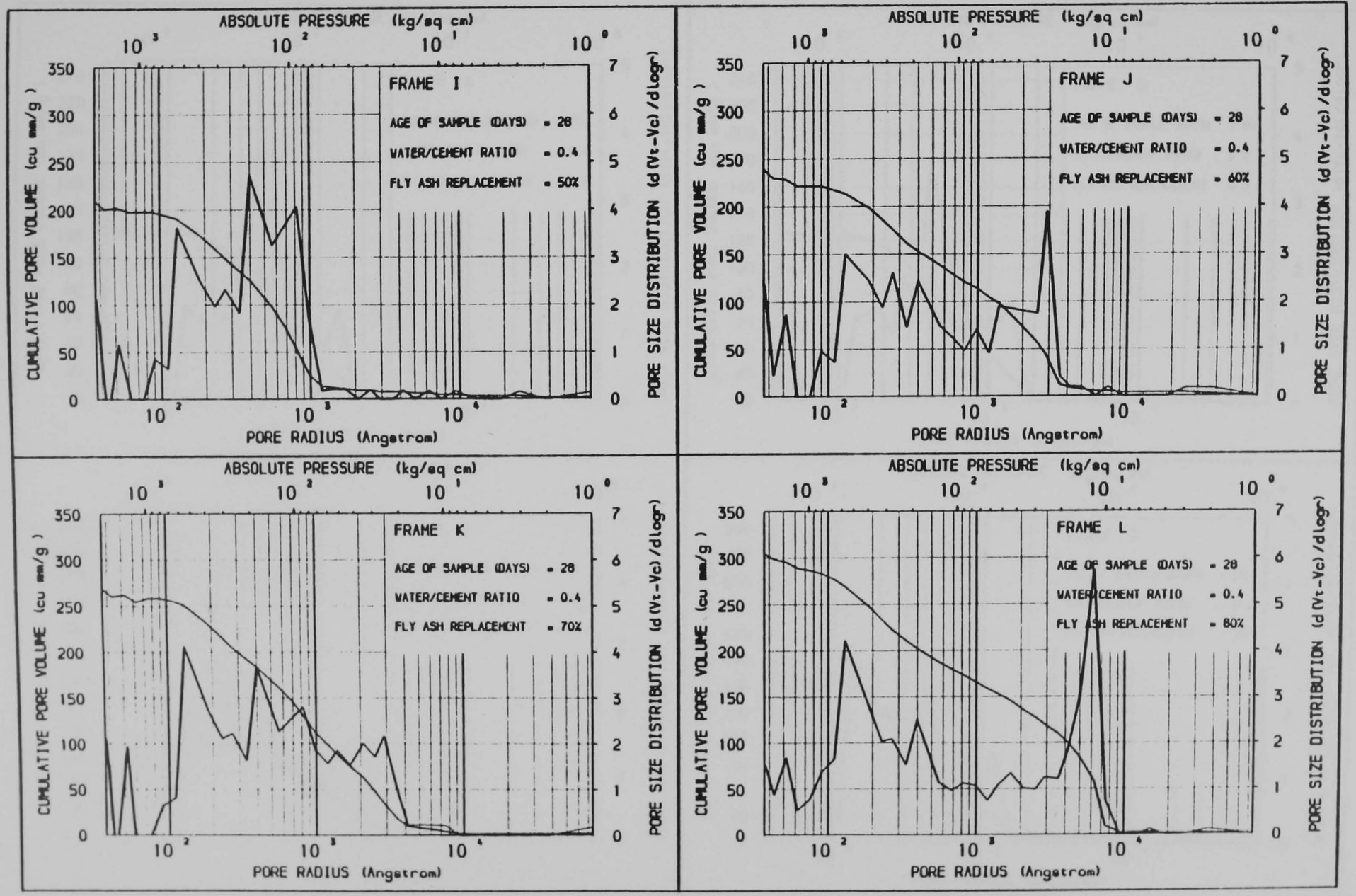

Figure A3.19 THE EFFECT OF FLY ASH REPLACEMENT OF CEMENT ON PORE SIZE DISTRIBUTION

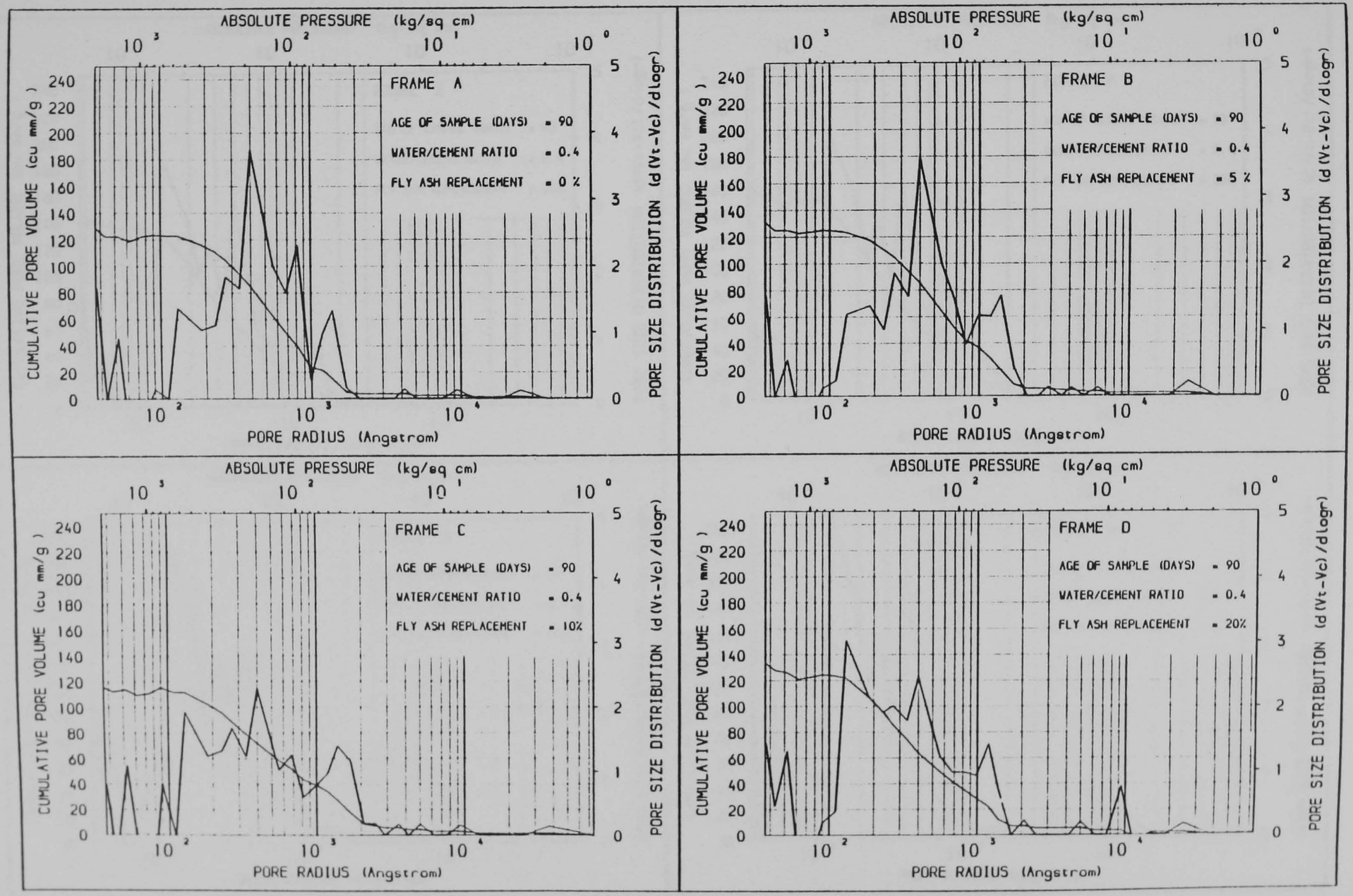

Figure A3.20 THE EFFECT OF FLY ASH REPLACEMENT OF CEMENT ON PORE SIZE DISTRIBUTION

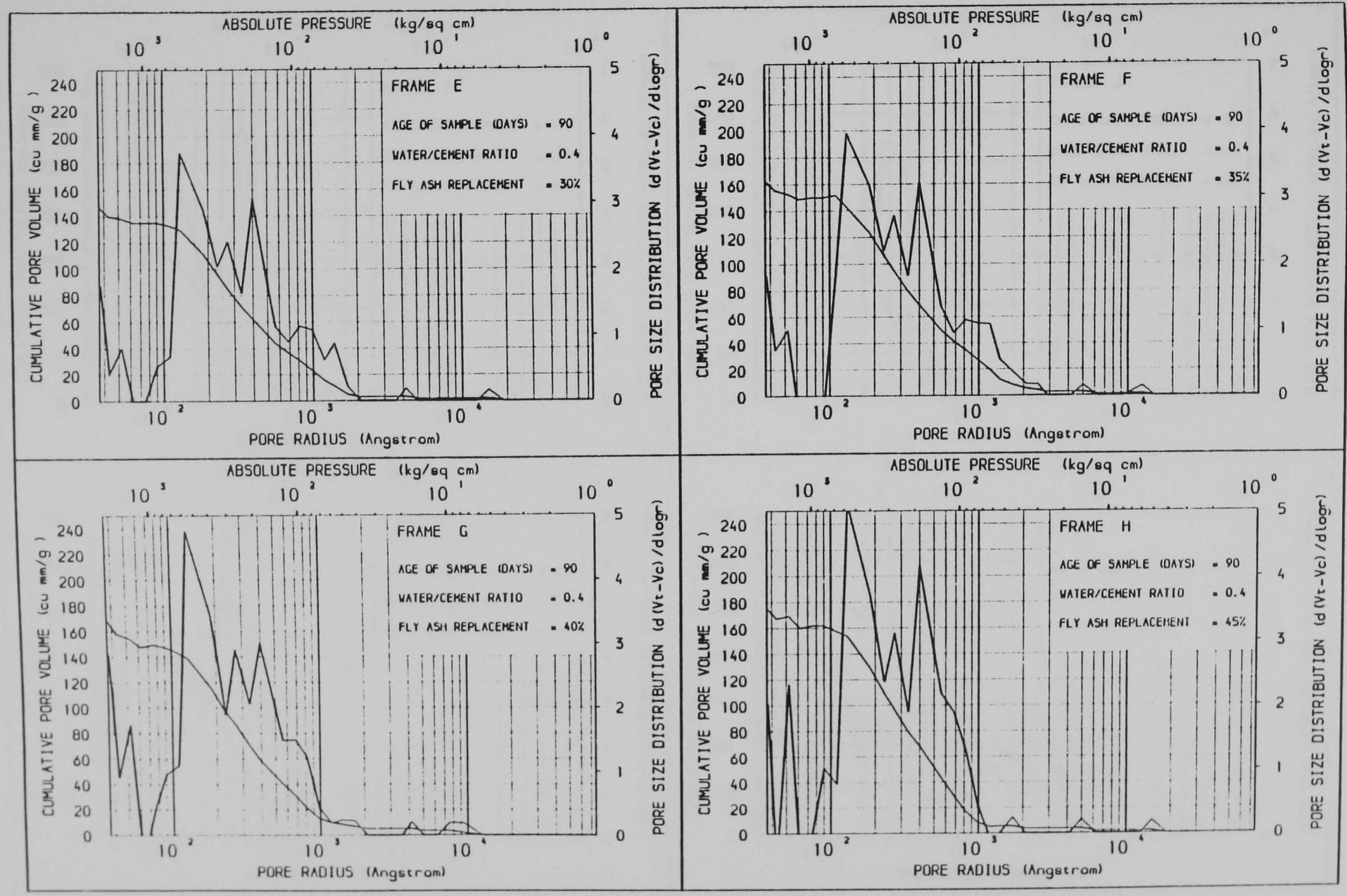

Figure A3.21 THE EFFECT OF FLY ASH REPLACEMENT OF CEMENT ON PORE SIZE DISTRIBUTION

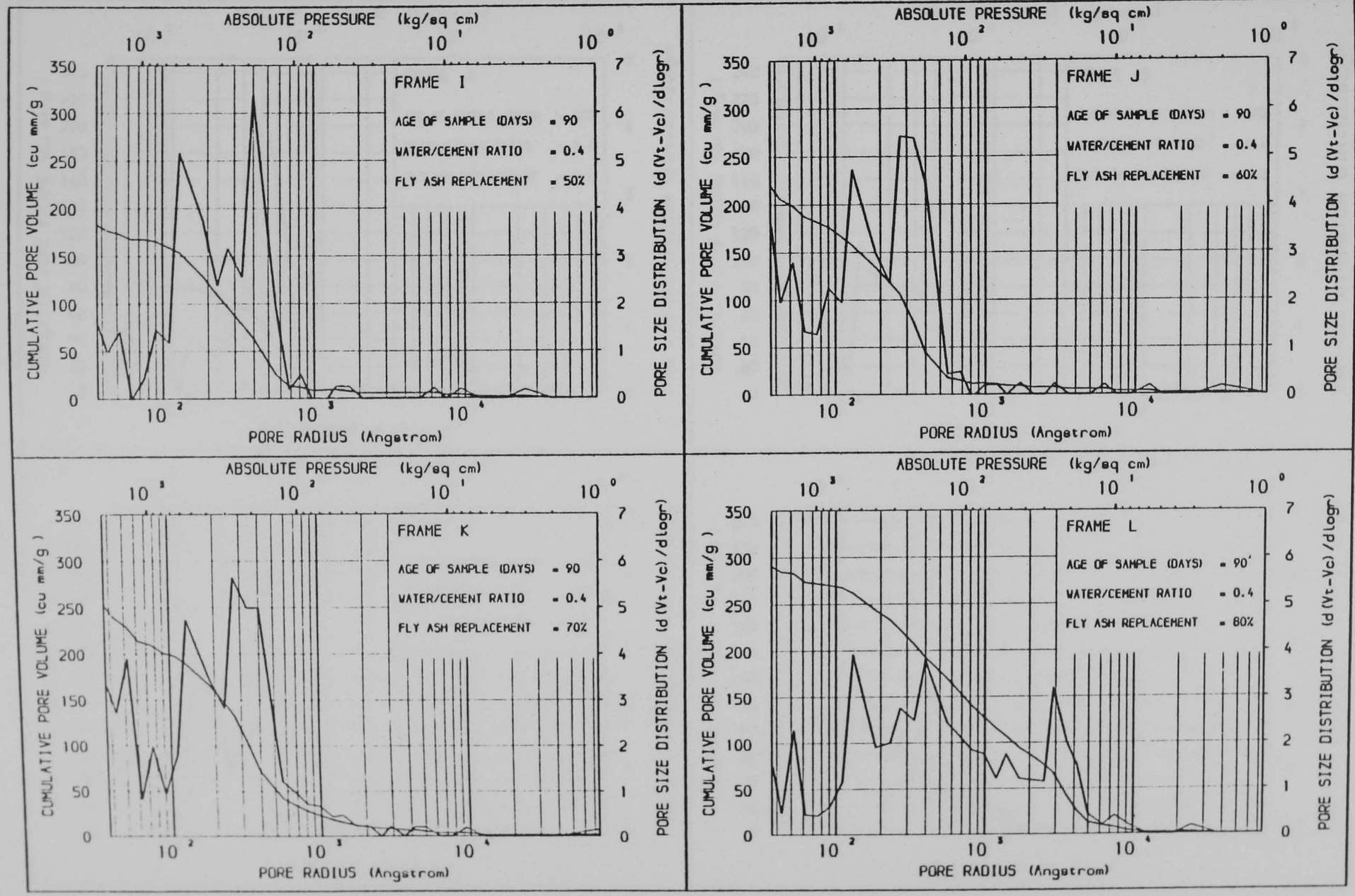

Figure A3.22 THE EFFECT OF FLY ASH REPLACEMENT OF CEMENT ON PORE SIZE DISTRIBUTION

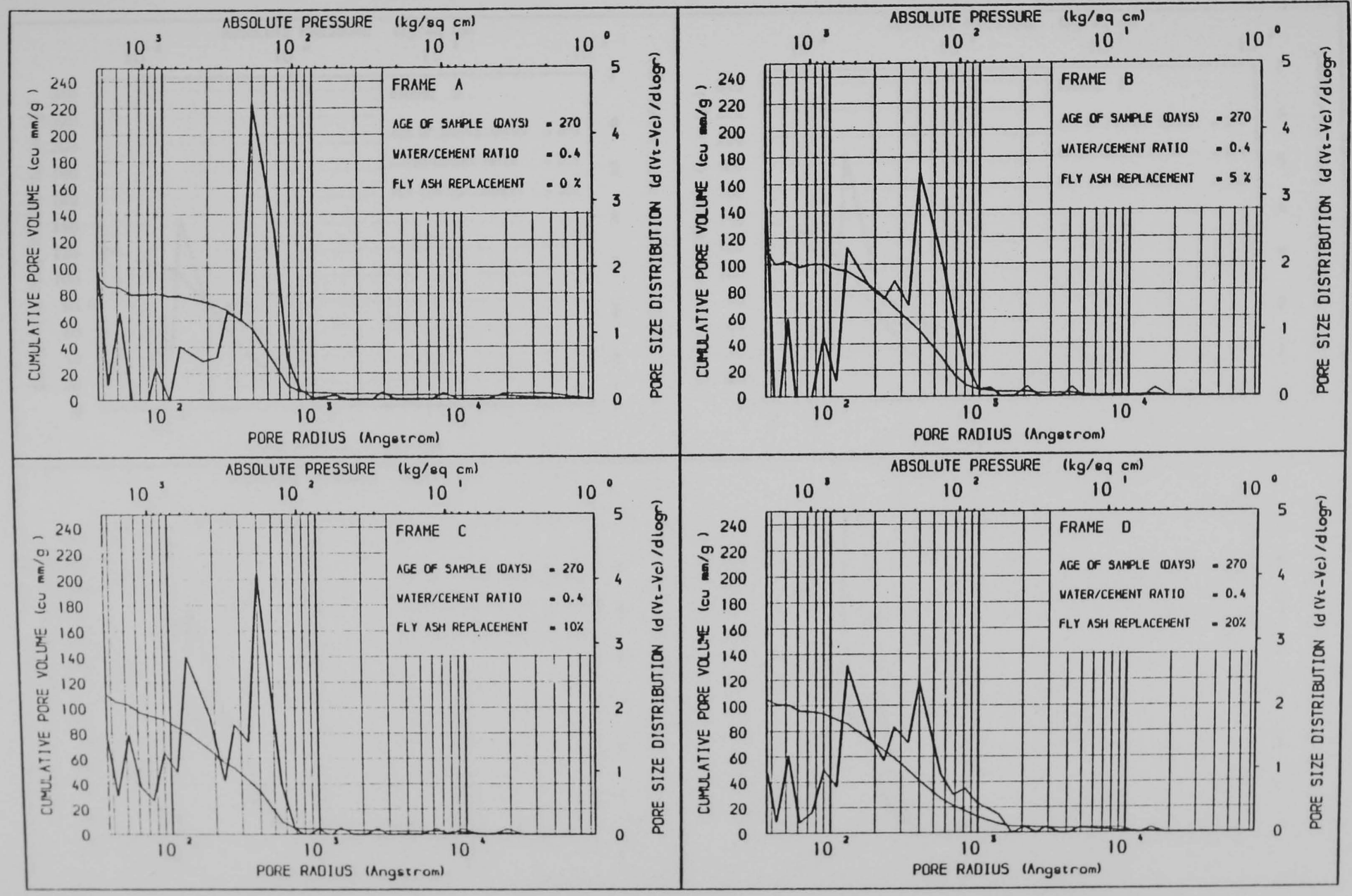

Figure A3.23 THE EFFECT OF FLY ASH REPLACEMENT OF CEMENT ON PORE SIZE DISTRIBUTION

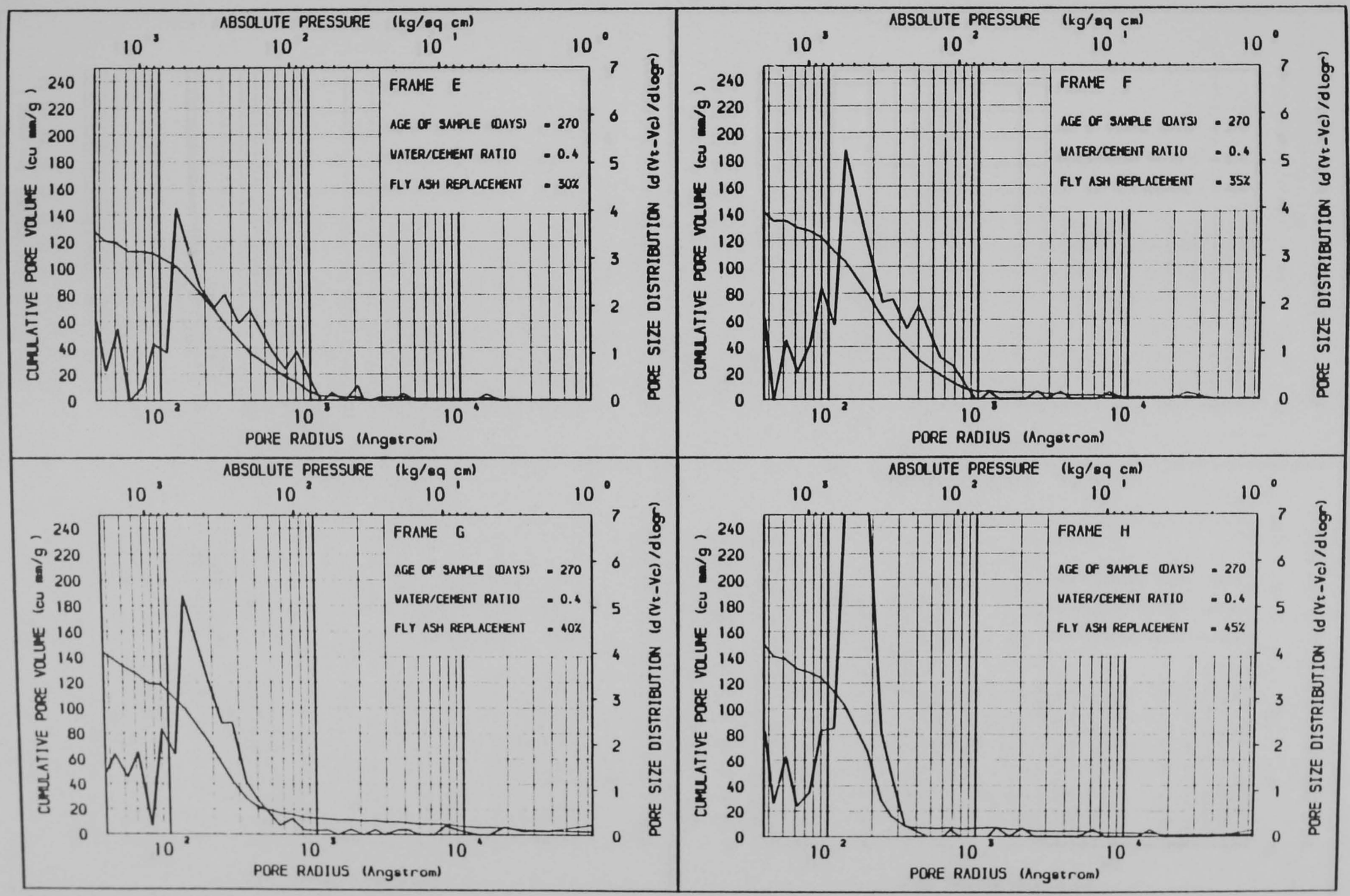

Figure A3.24 THE EFFECT OF FLY ASH REPLACEMENT OF CEMENT ON PORE SIZE DISTRIBUTION

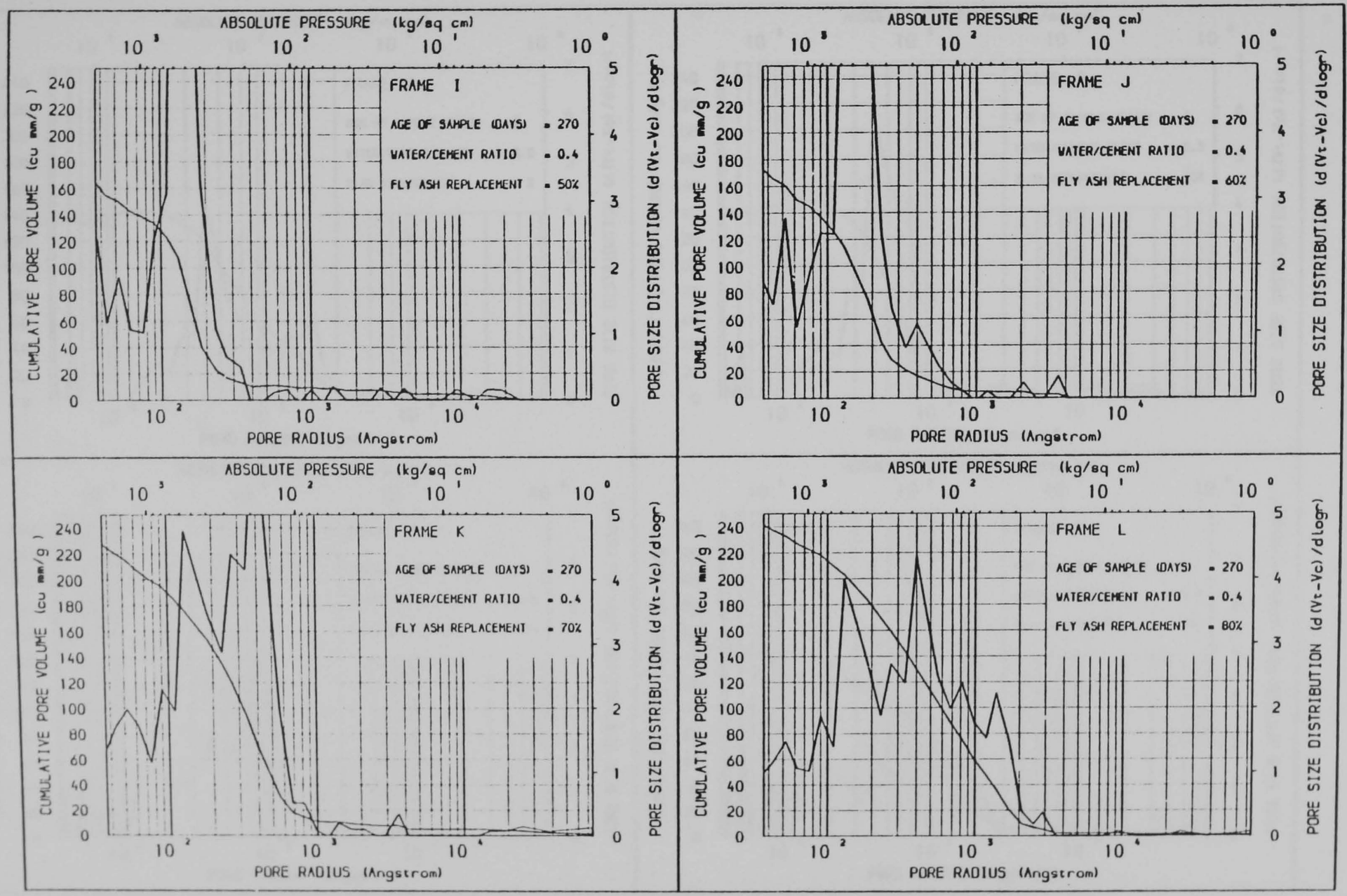

Figure A3.25 THE EFFECT OF FLY ASH REPLACEMENT OF CEMENT ON PORE SIZE DISTRIBUTION

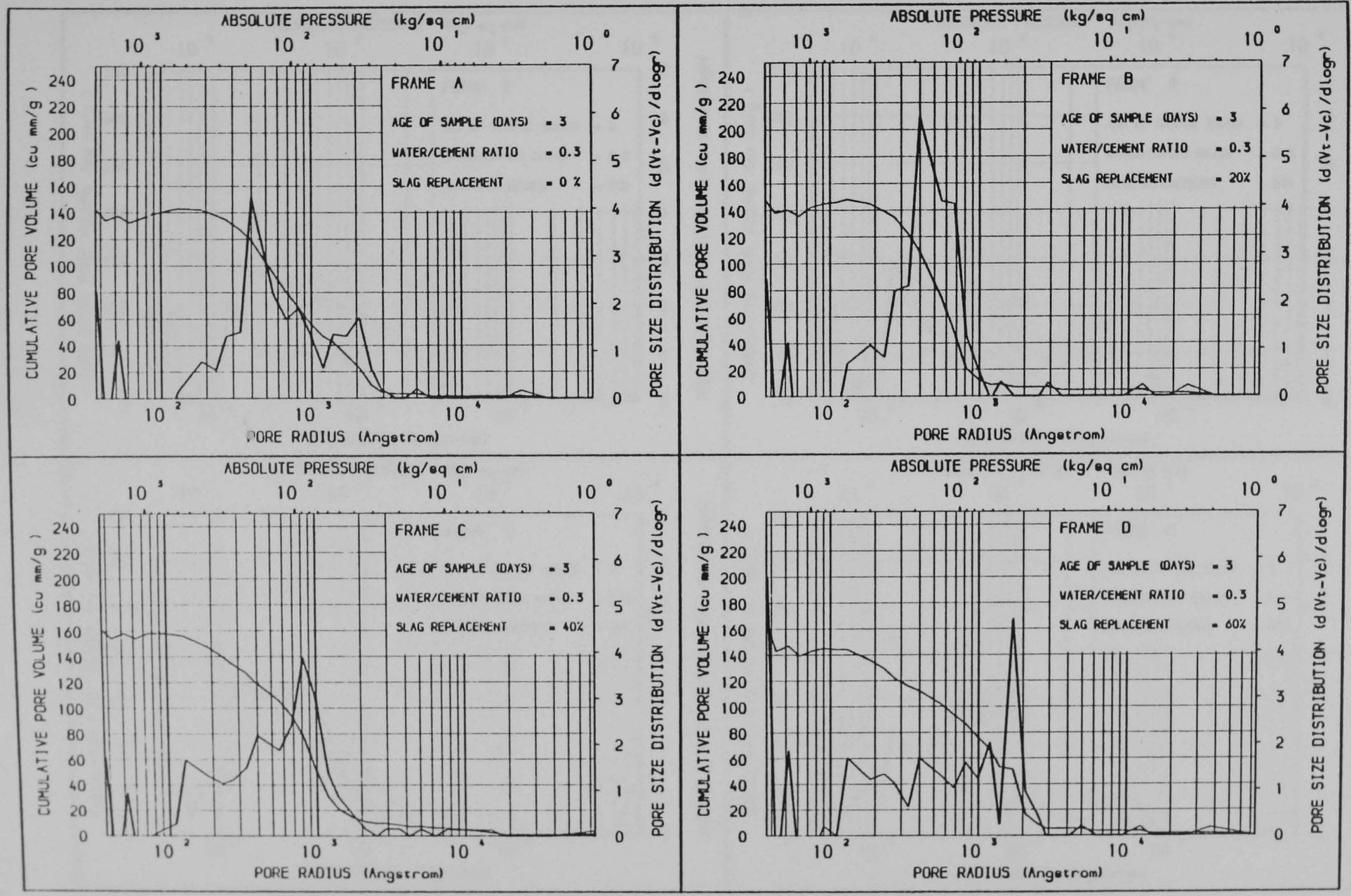

Figure A3.26 THE EFFECT OF BLASTFURNACE SLAG REPLACEMENT OF CEMENT ON PORE SIZE DISTRIBUTION

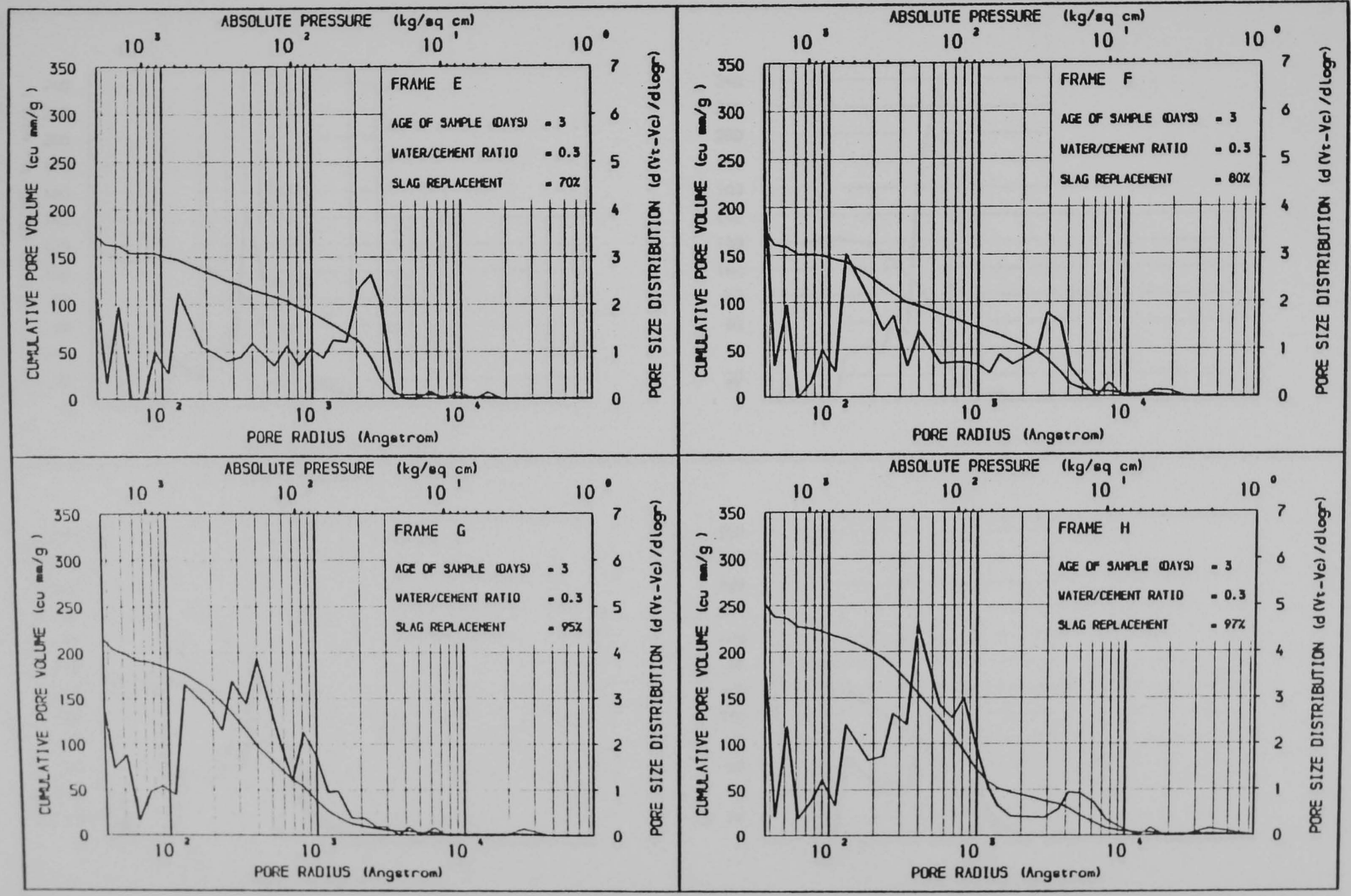

Figure A3.27 THE EFFECT OF BLASTFURNACE SLAG REPLACEMENT OF CEMENT ON PORE SIZE DISTRIBUTION

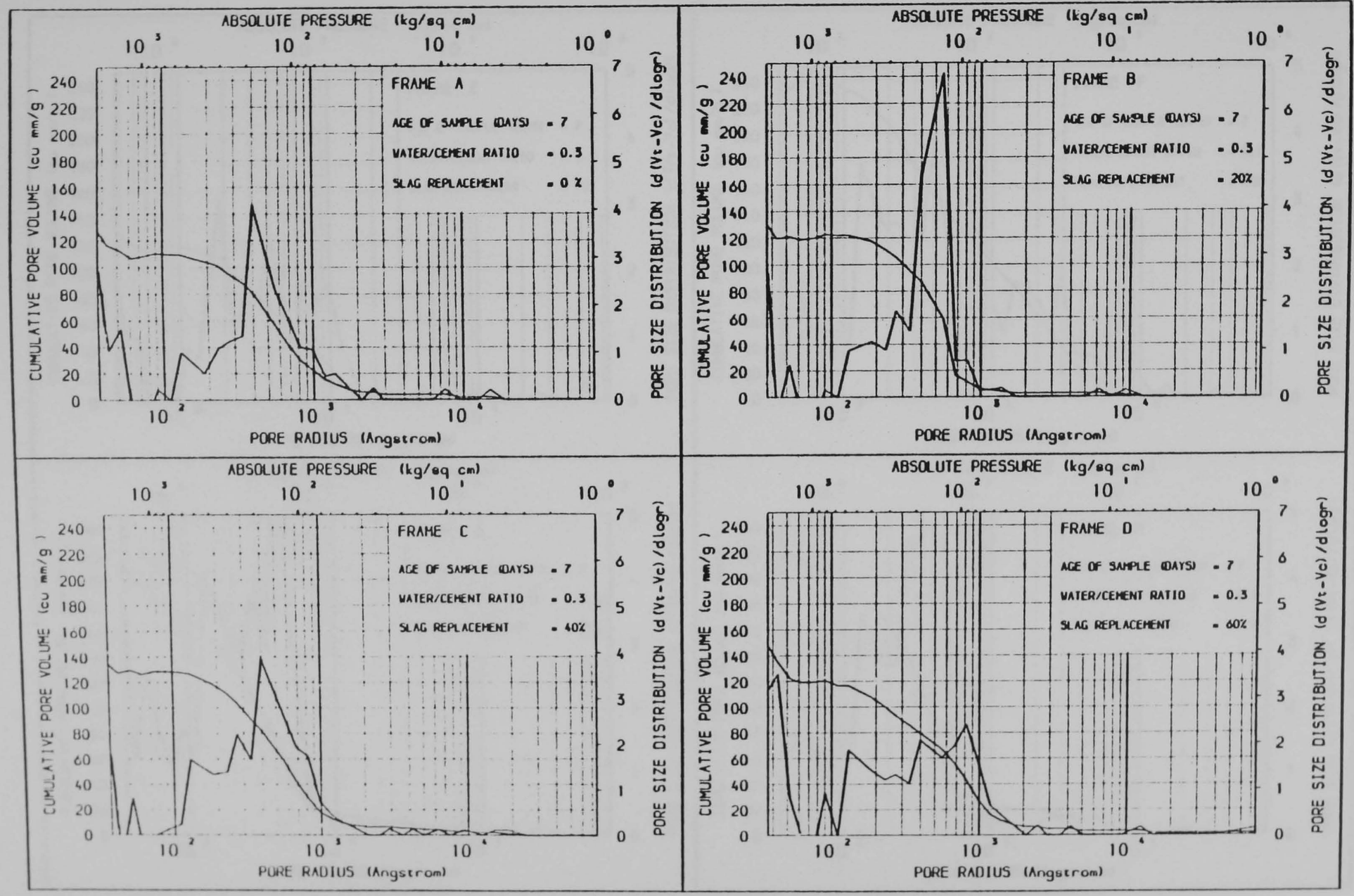

Figure A3.28 THE EFFECT OF BLASTFURNACE SLAG REPLACEMENT OF CEMENT ON PORE SIZE DISTRIBUTION

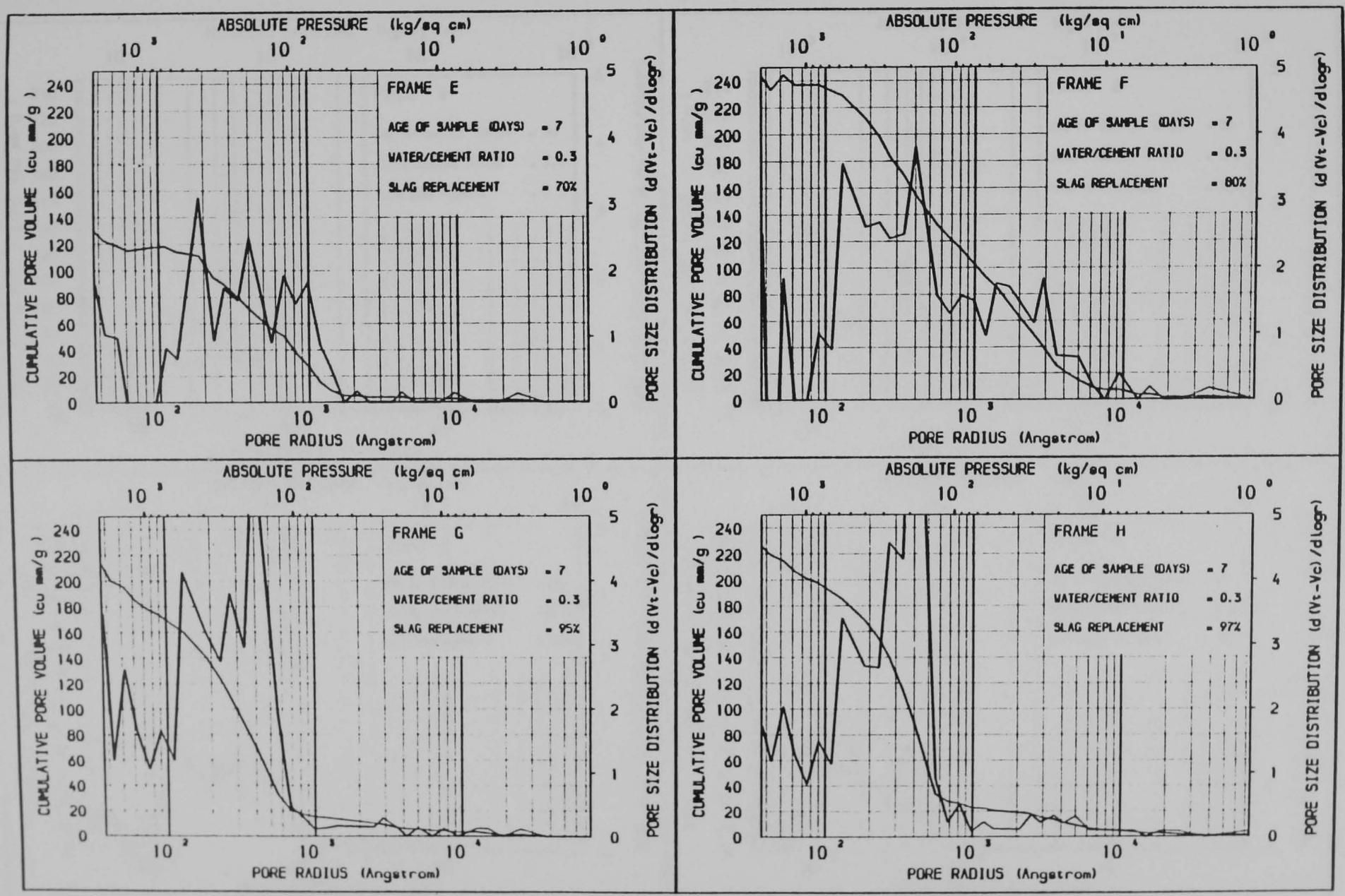

Figure A3.29 THE EFFECT OF BLASTFURNACE SLAG REPLACEMENT OF CEMENT ON PORE SIZE DISTRIBUTION

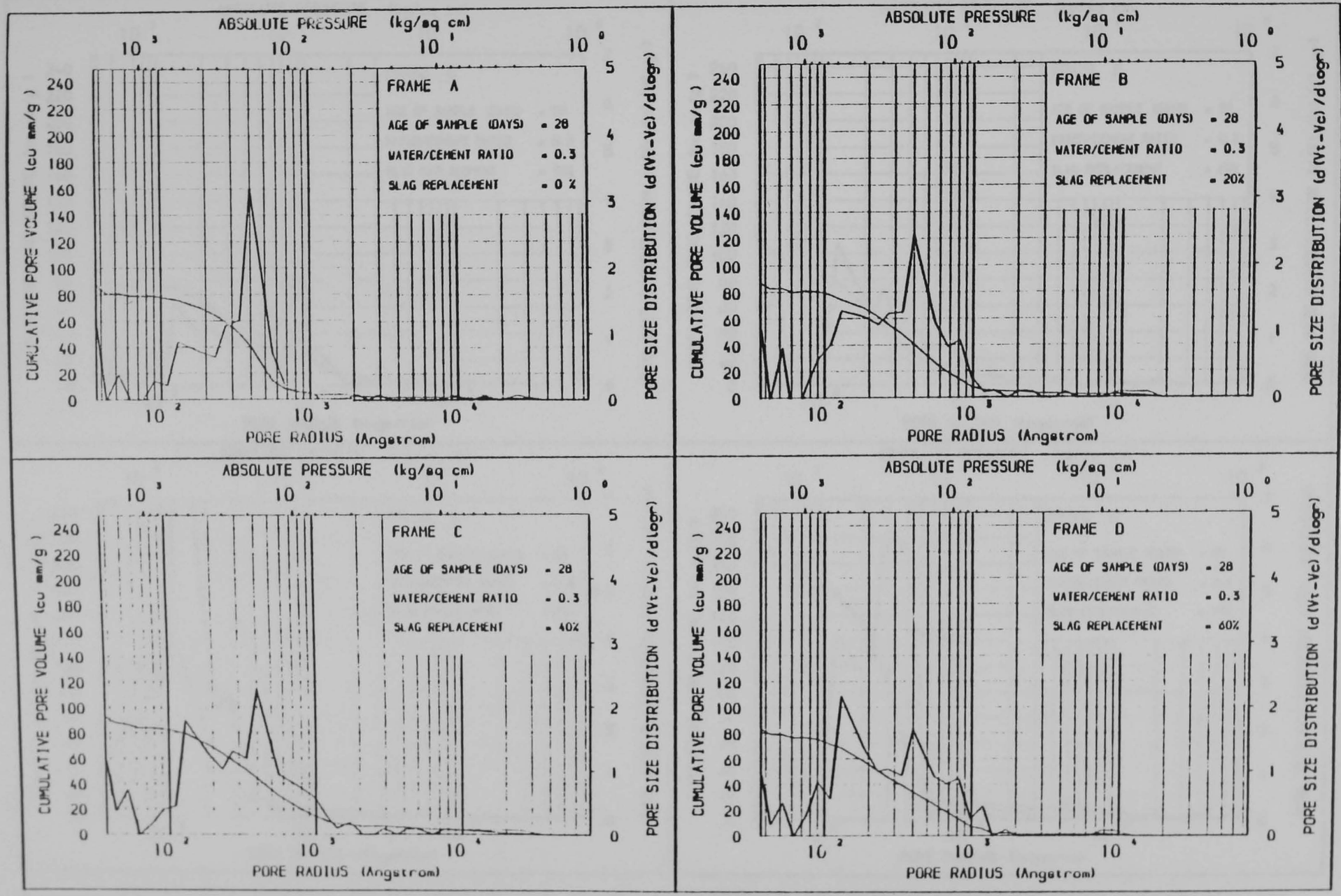

Figure A3.30 THE EFFECT OF BLASTFURNACE SLAG REPLACEMENT OF CEMENT ON PORE SIZE DISTRIBUTION

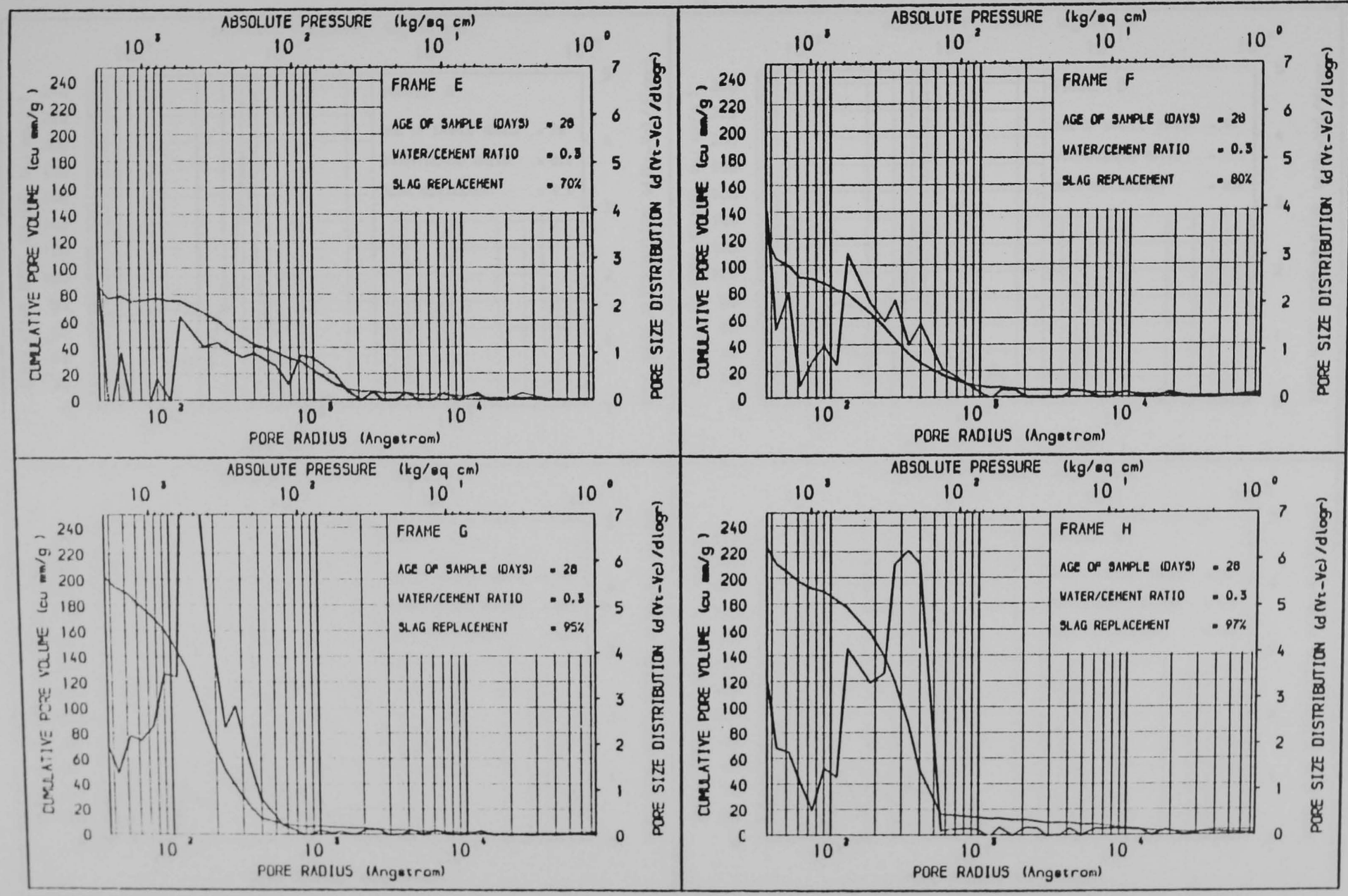

Figure A3.31 THE EFFECT OF BLASTFURNACE SLAG REPLACEMENT OF CEMENT ON PORE SIZE DISTRIBUTION

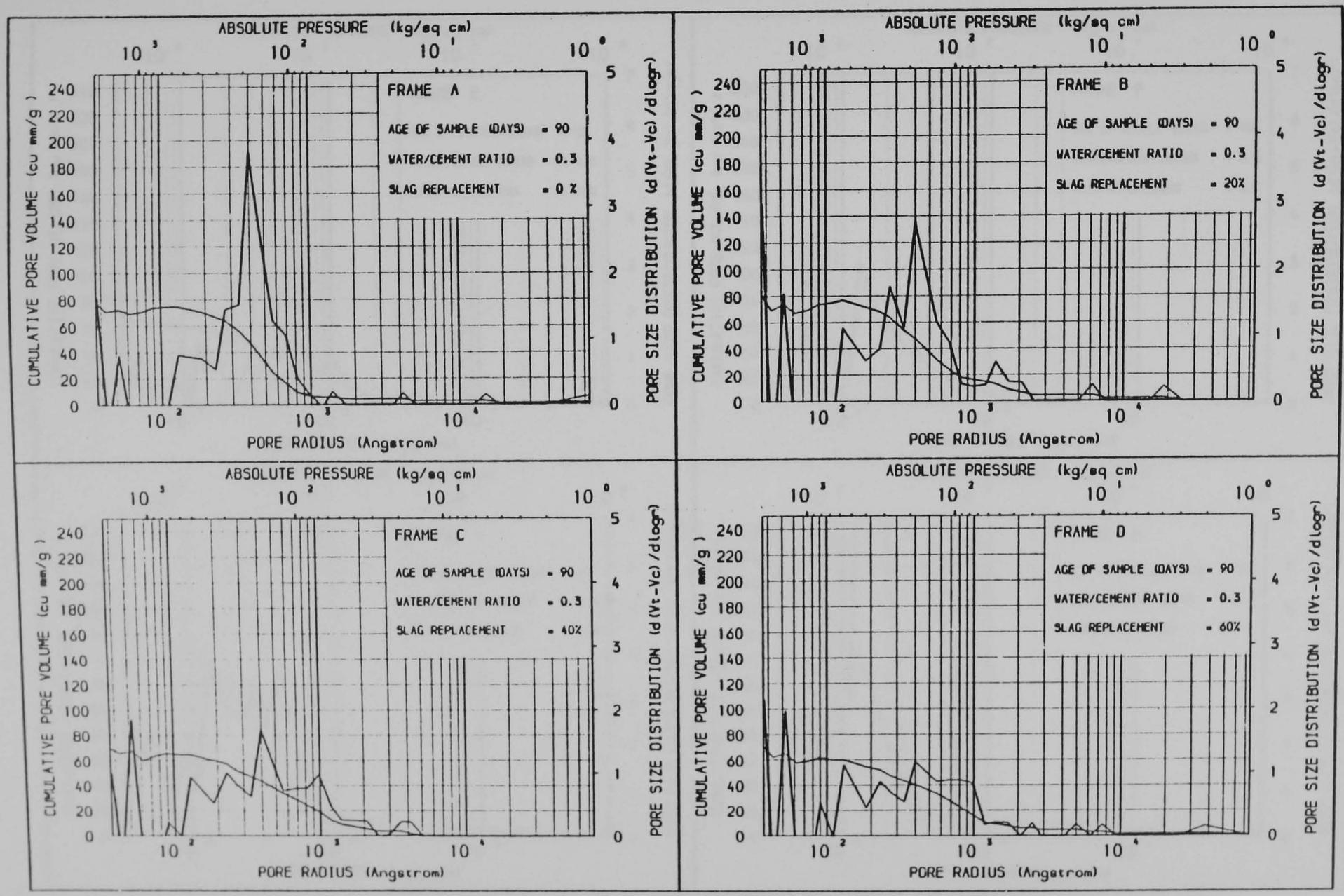

Figure A3.32 THE EFFECT OF BLASTFURNACE SLAG REPLACEMENT OF CEMENT ON PORE SIZE DISTRIBUTION

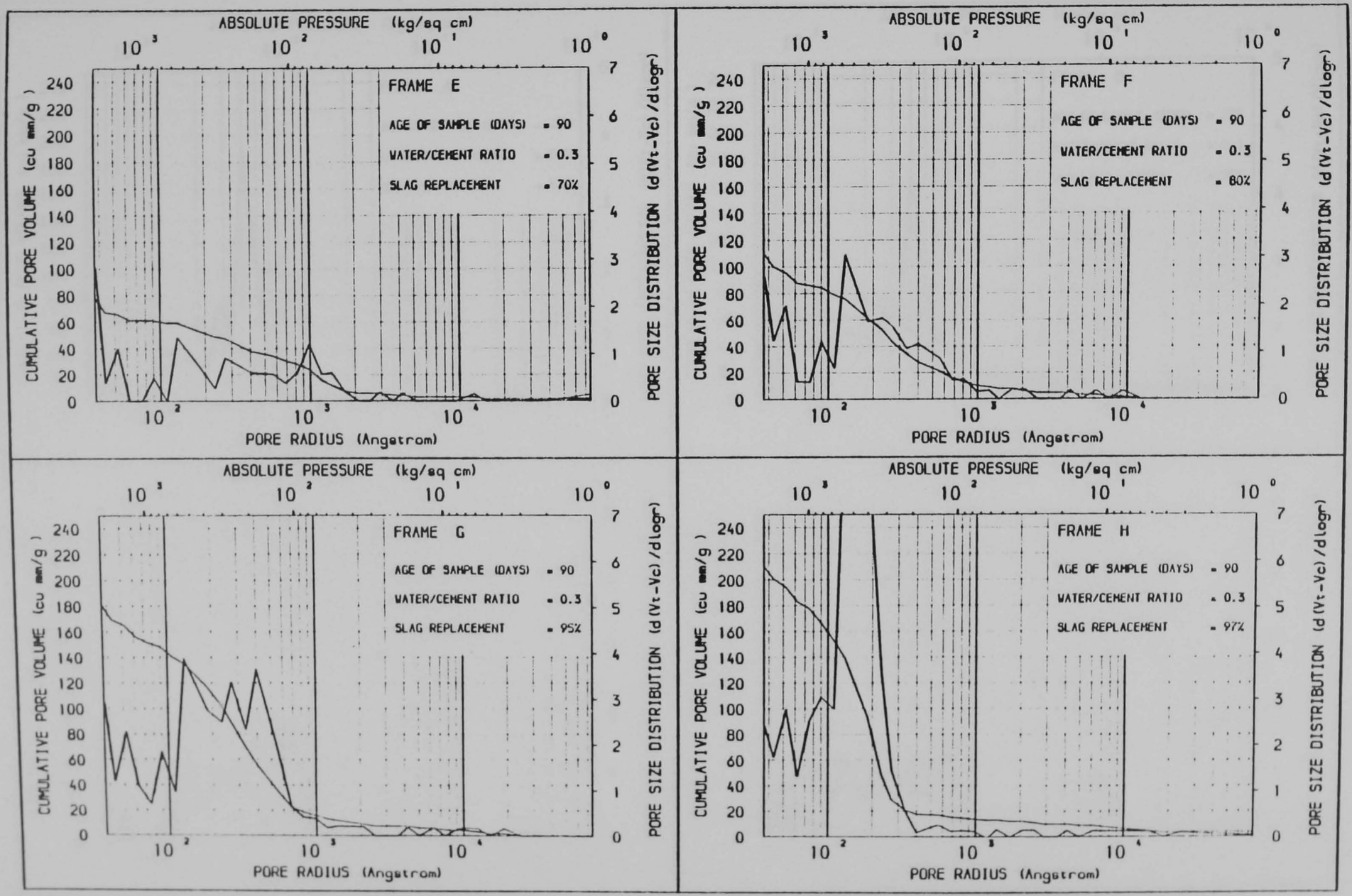

Figure A3.33 THE EFFECT OF BLASTFURNACE SLAG REPLACEMENT OF CEMENT ON PORE SIZE DISTRIBUTION

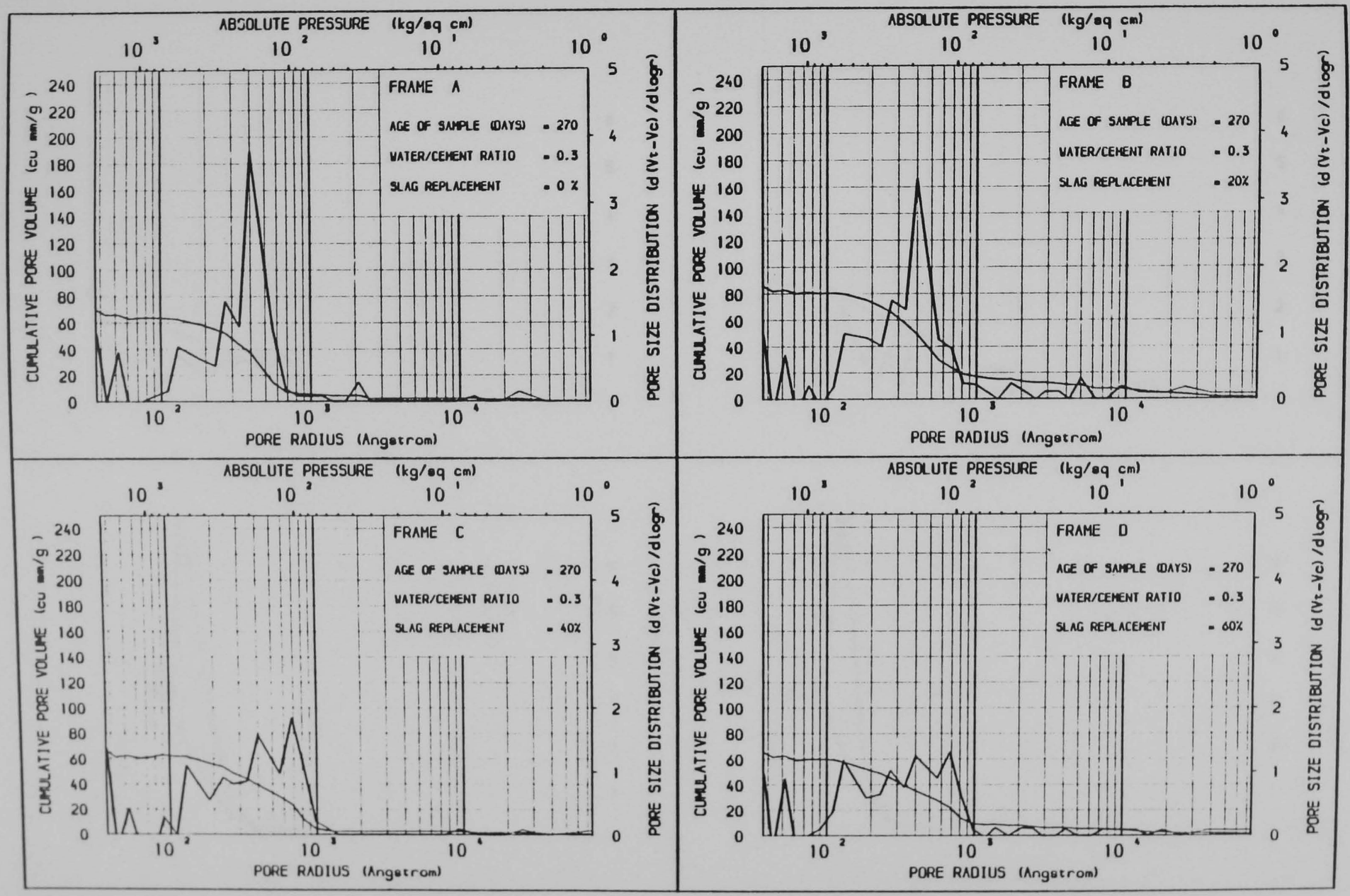

Figure A3.34 THE EFFECT OF BLASTFURNACE SLAG REPLACEMENT OF CEMENT ON PORE SIZE DISTRIBUTION

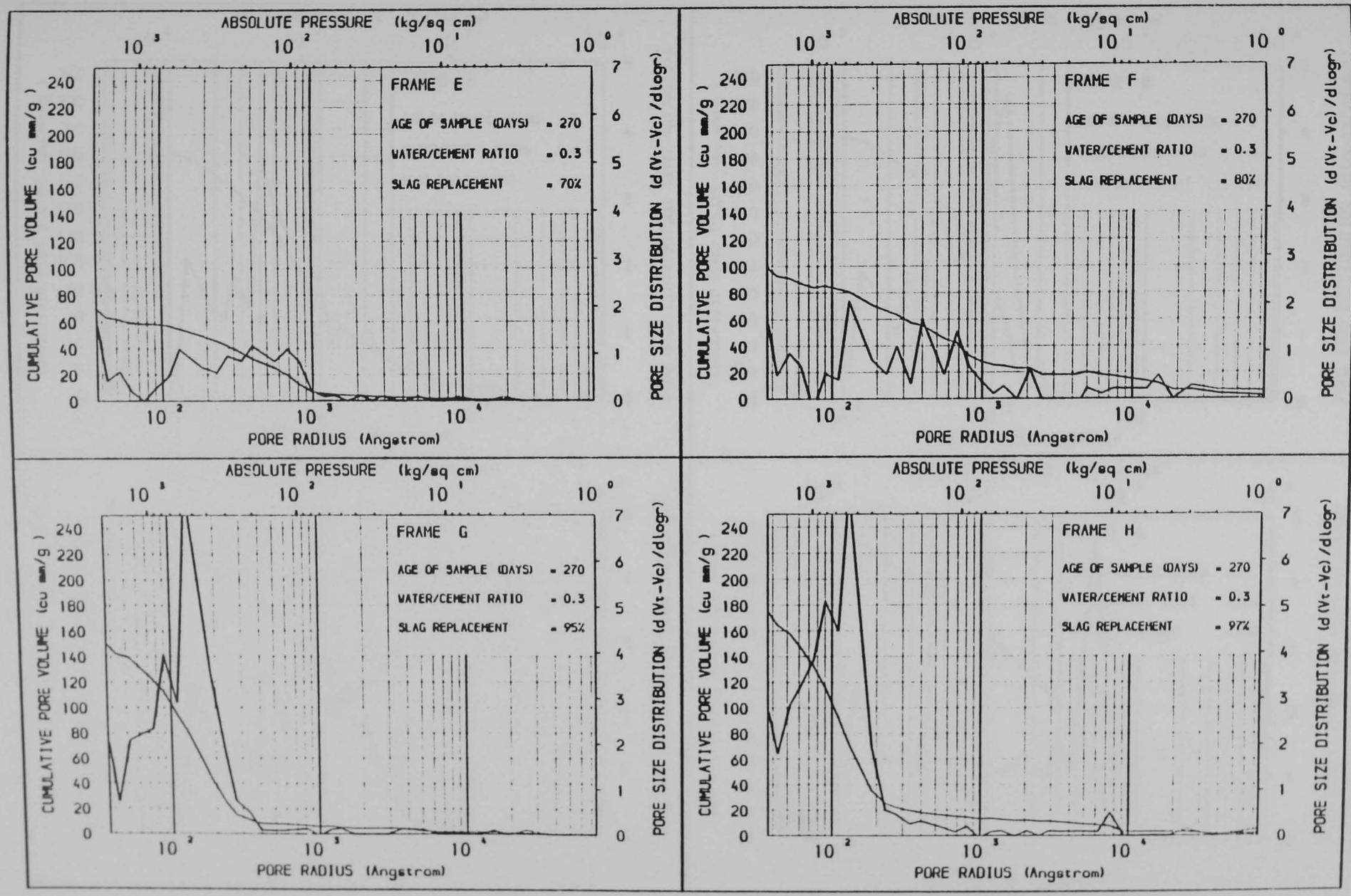

Figure A3.35 THE EFFECT OF BLASTFURNACE SLAG REPLACEMENT OF CEMENT ON PORE SIZE DISTRIBUTION

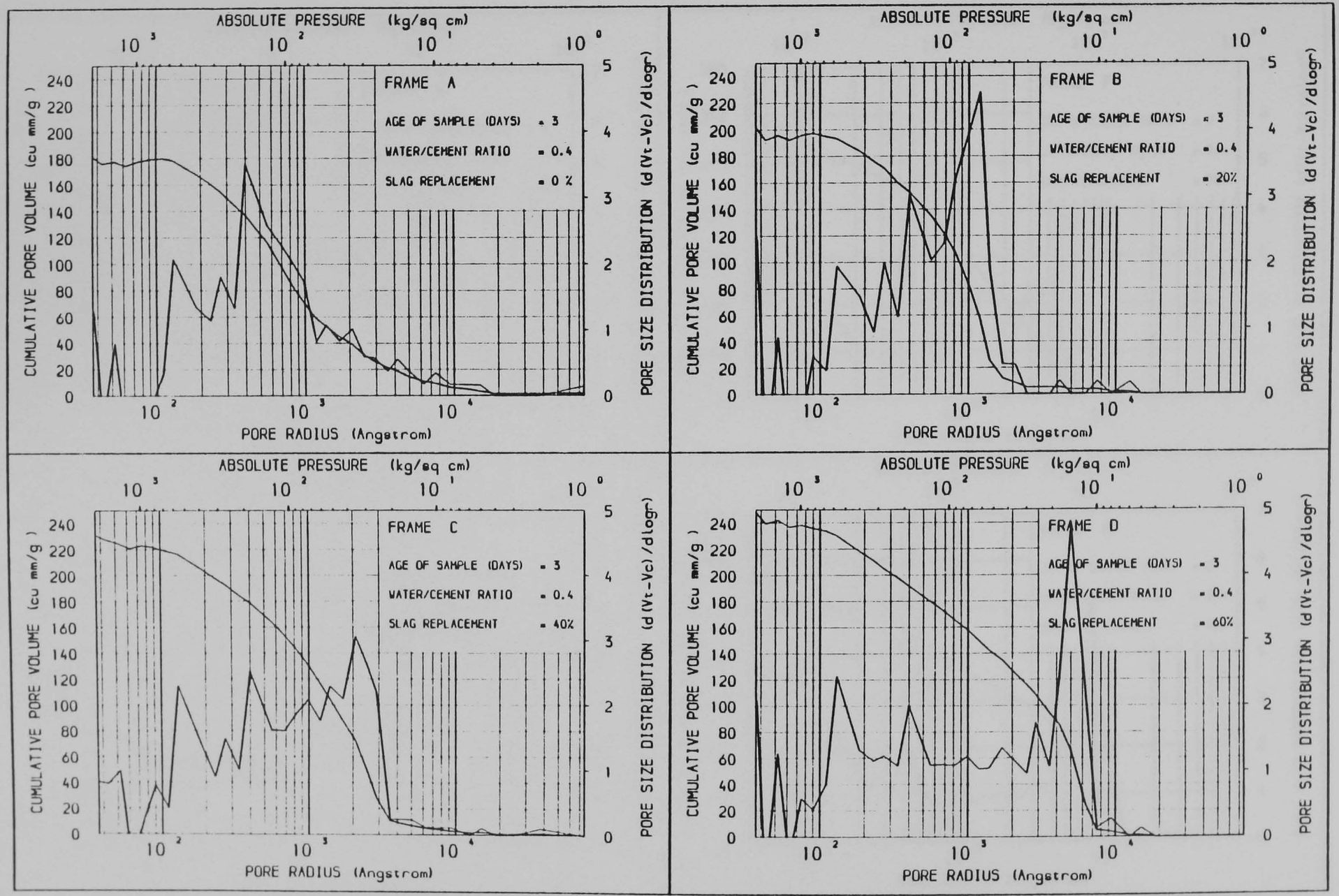

Figure A3.36 THE EFFECT OF BLASTFURNACE SLAG REPLACEMENT OF CEMENT ON PORE SIZE DISTRIBUTION

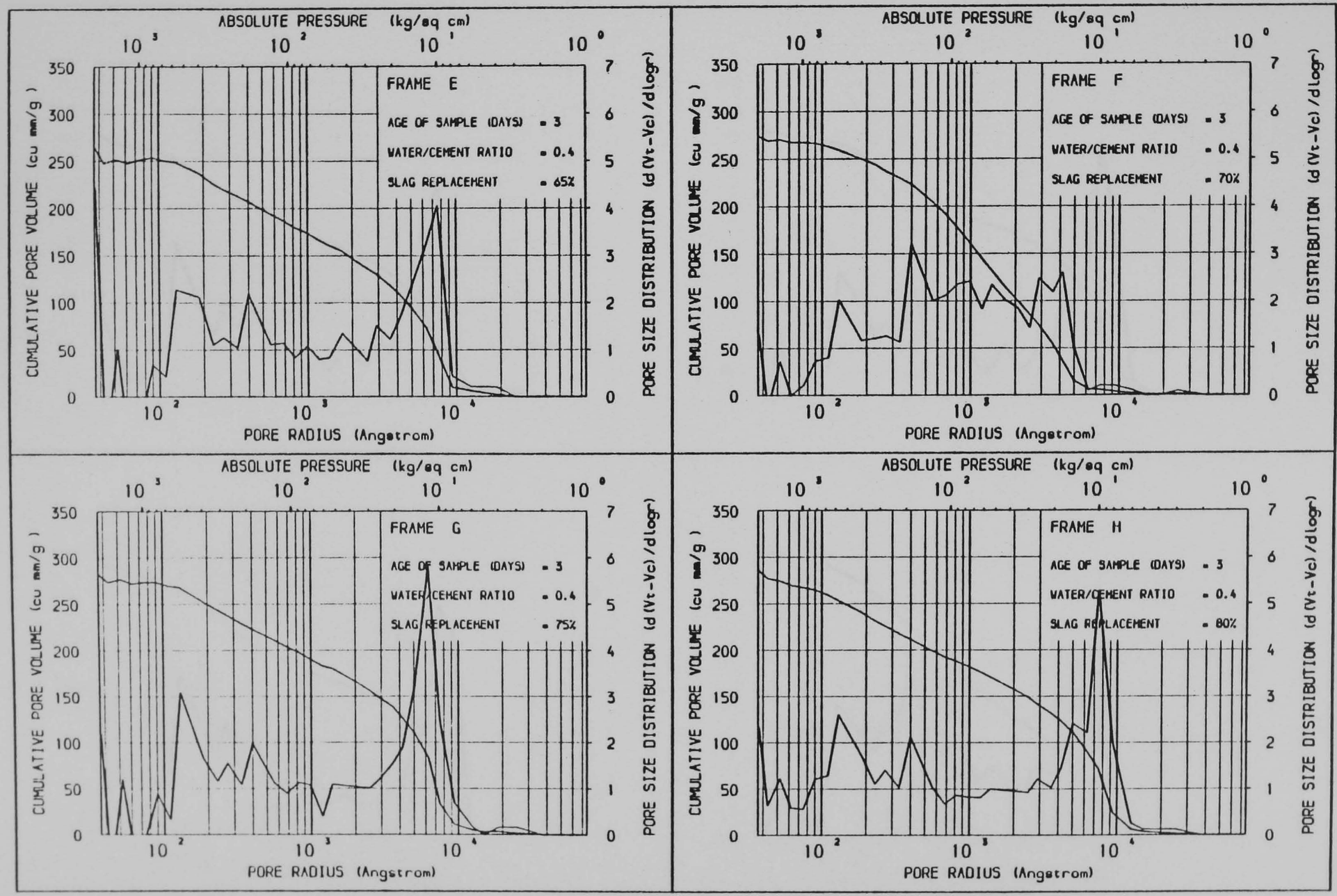

Figure A3.37 THE EFFECT OF BLASTFURNACE SLAG REPLACEMENT OF CEMENT ON PORE SIZE DISTRIBUTION

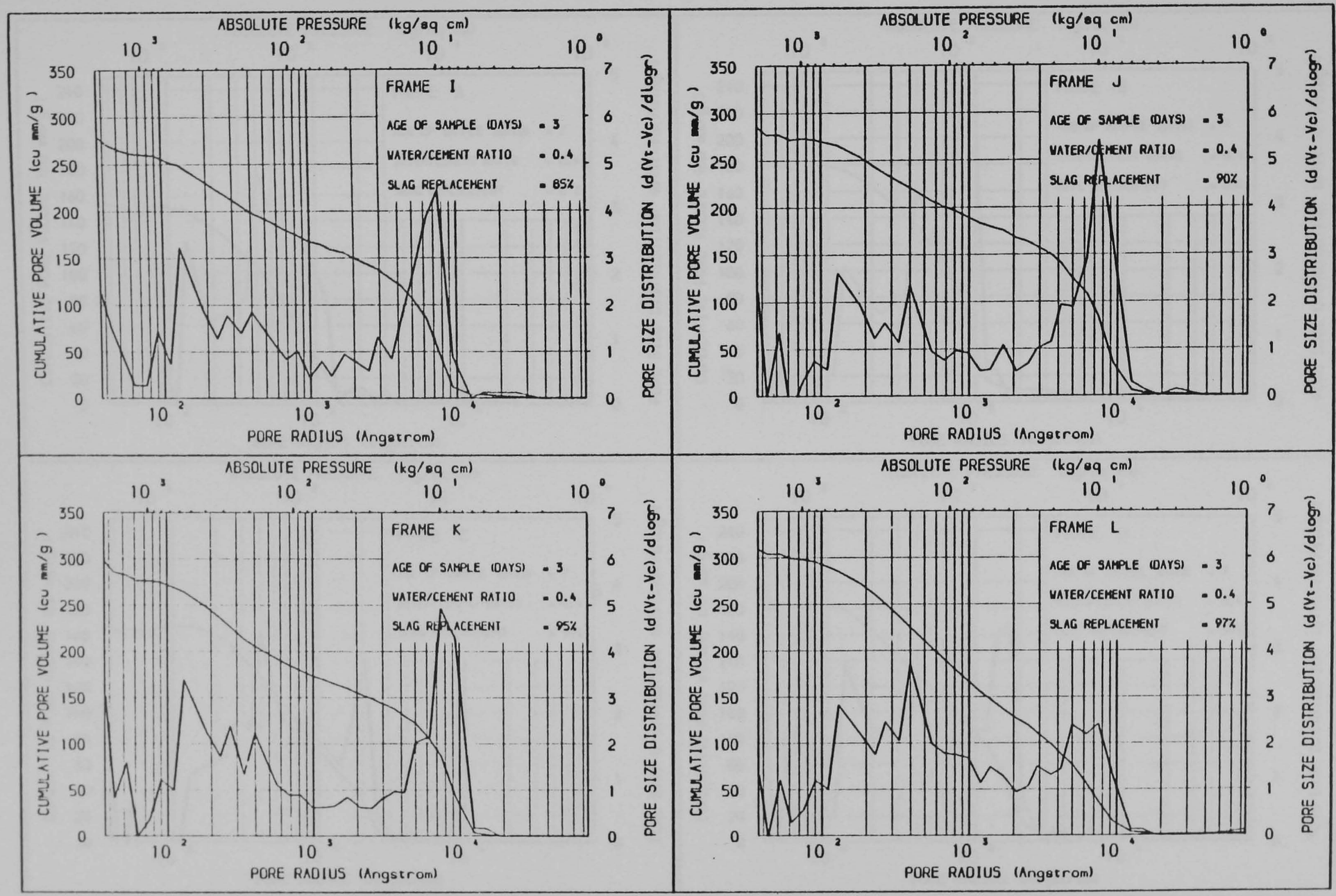

Figure A3.38 THE EFFECT OF BLASTFURNACE SLAG REPLACEMENT OF CEMENT ON PORE SIZE DISTRIBUTION

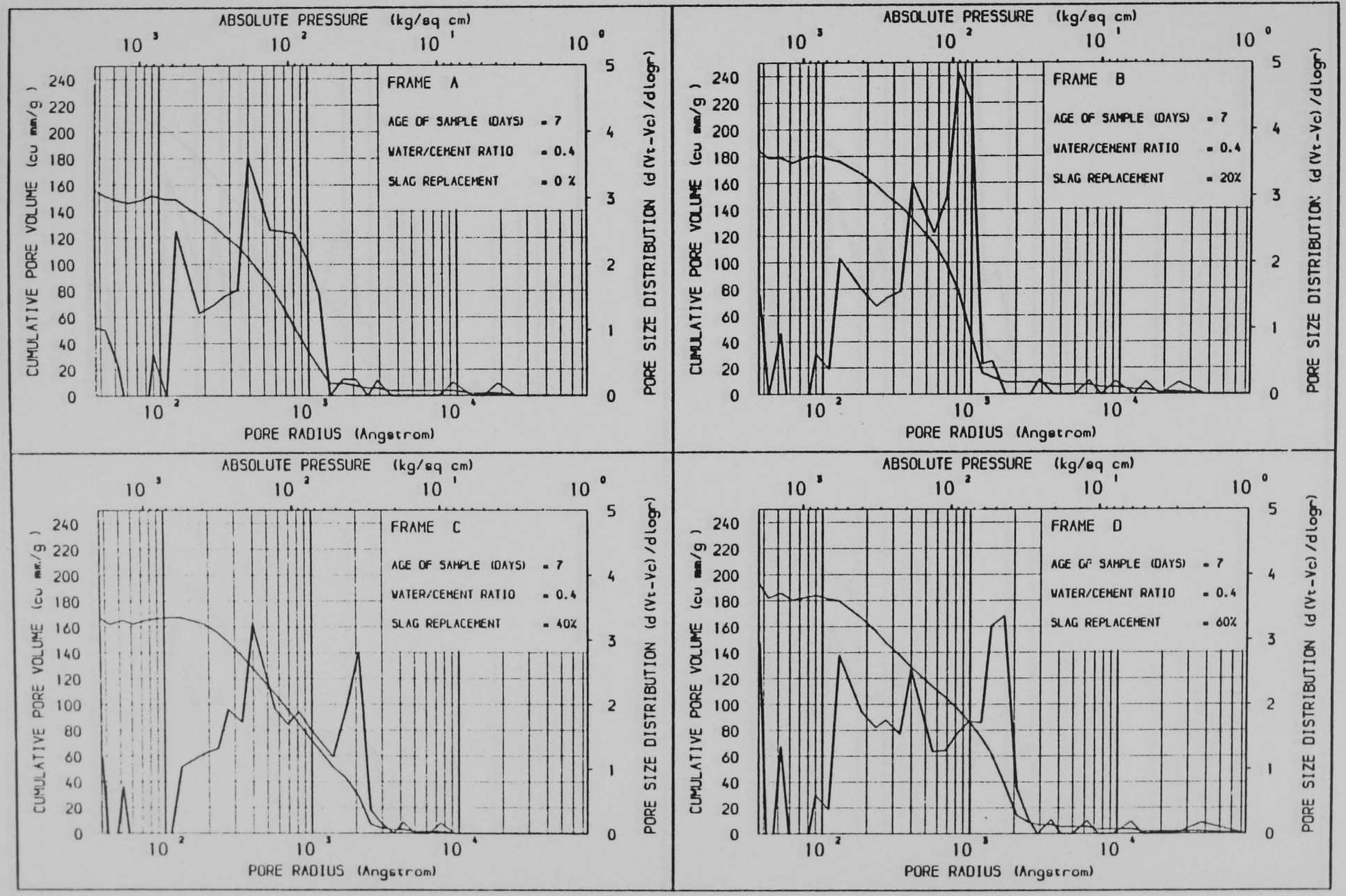

Figure A3.39 THE EFFECT OF BLASTFURNACE SLAG REPLACEMENT OF CEMENT ON PORE SIZE DISTRIBUTION

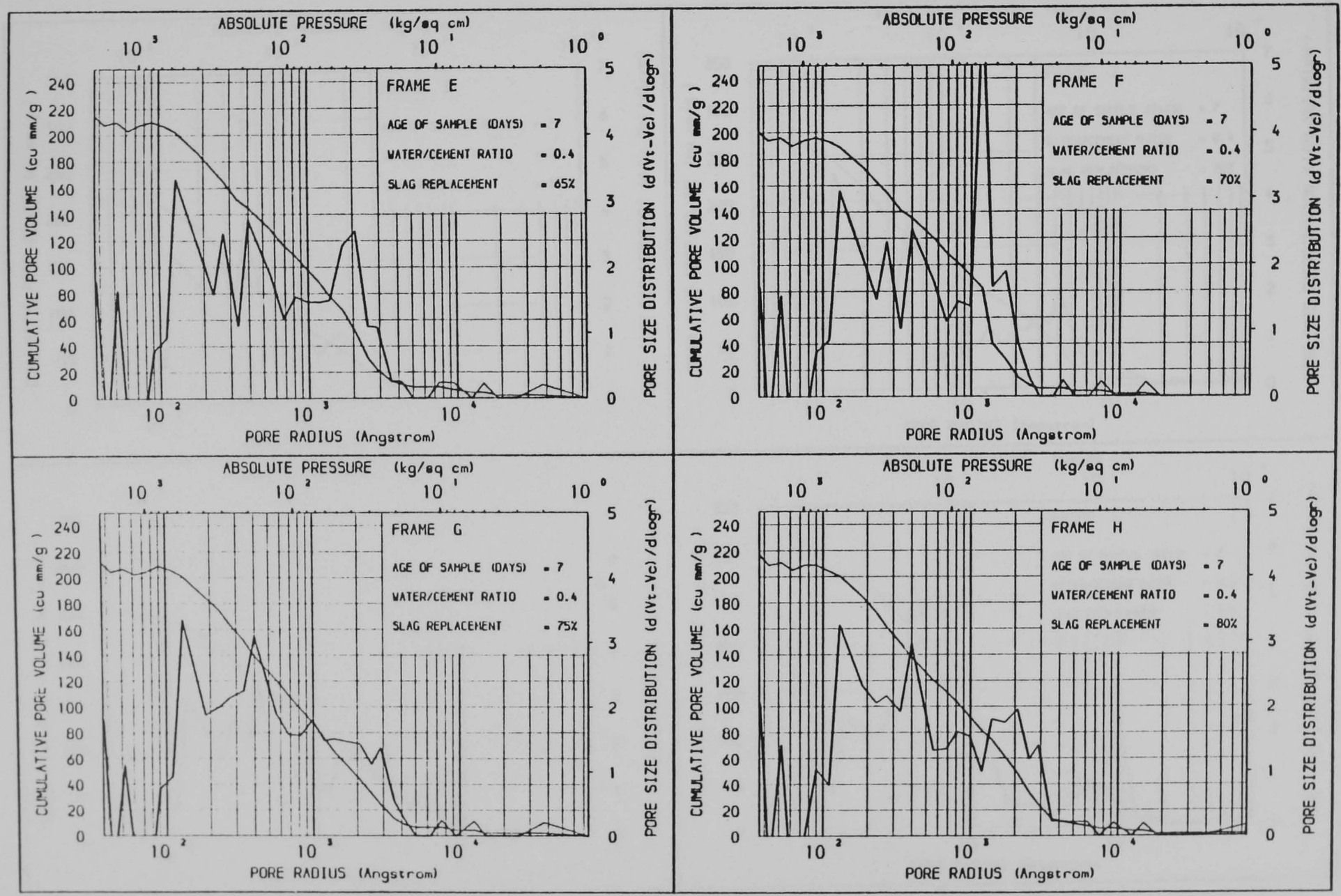

Figure A3.40 THE EFFECT OF BLASTFURNACE SLAG REPLACEMENT OF CEMENT ON PORE SIZE DISTRIBUTION

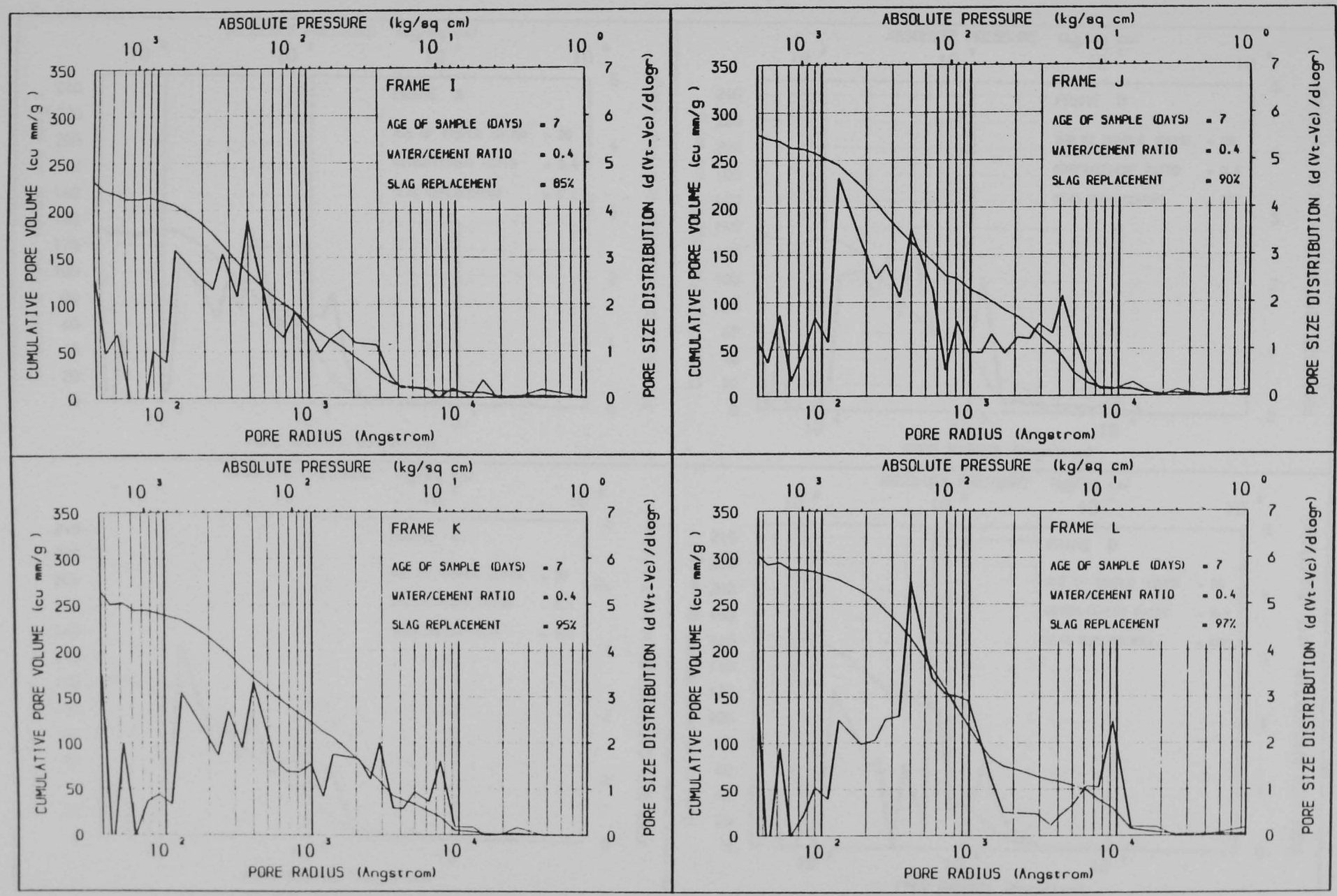

Figure A3.41 THE EFFECT OF BLASTFURNACE SLAG REPLACEMENT OF CEMENT ON PORE SIZE DISTRIBUTION

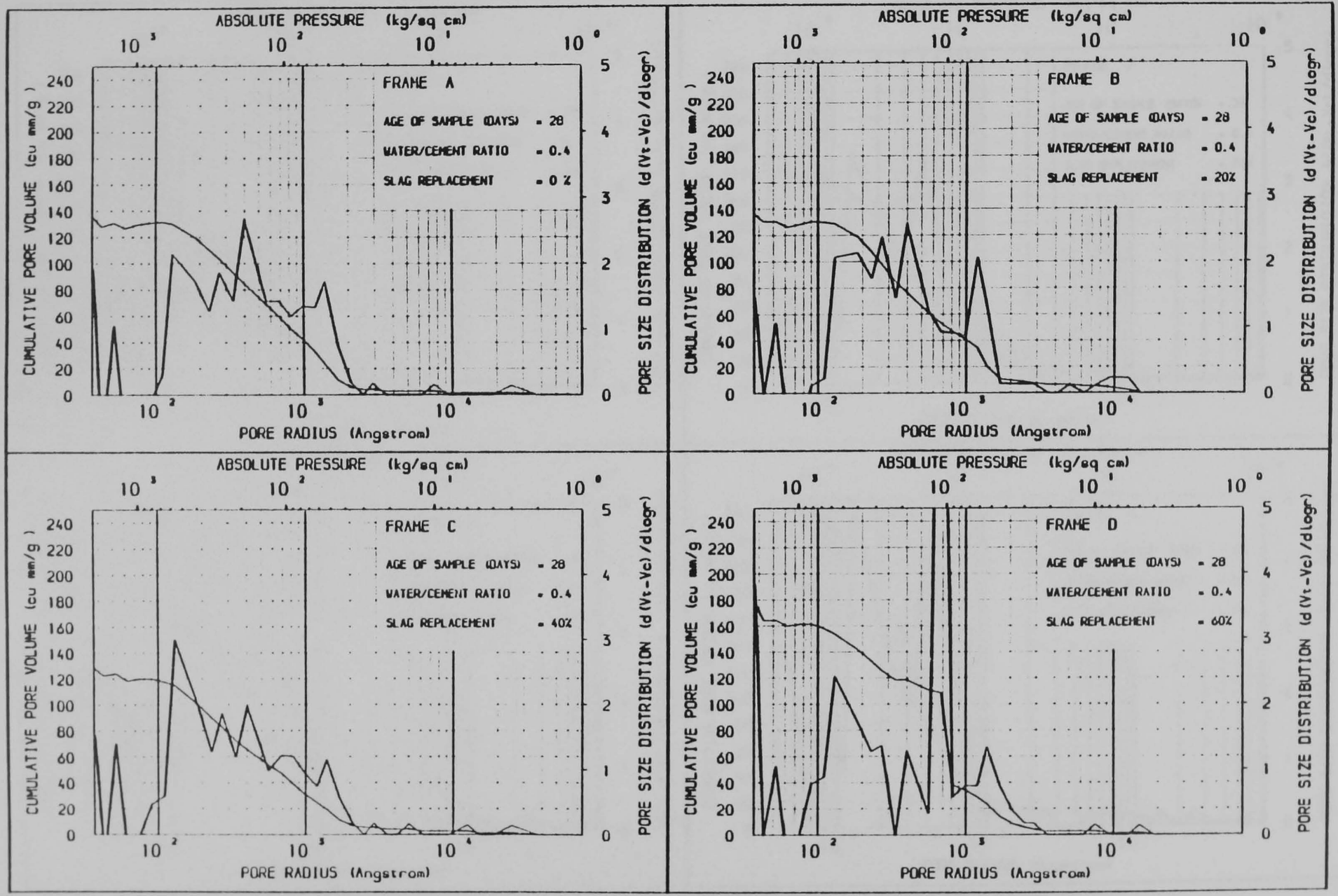

Figure A3.42 THE EFFECT OF BLASTFURNACE SLAG REPLACEMENT OF CEMENT ON PORE SIZE DISTRIBUTION

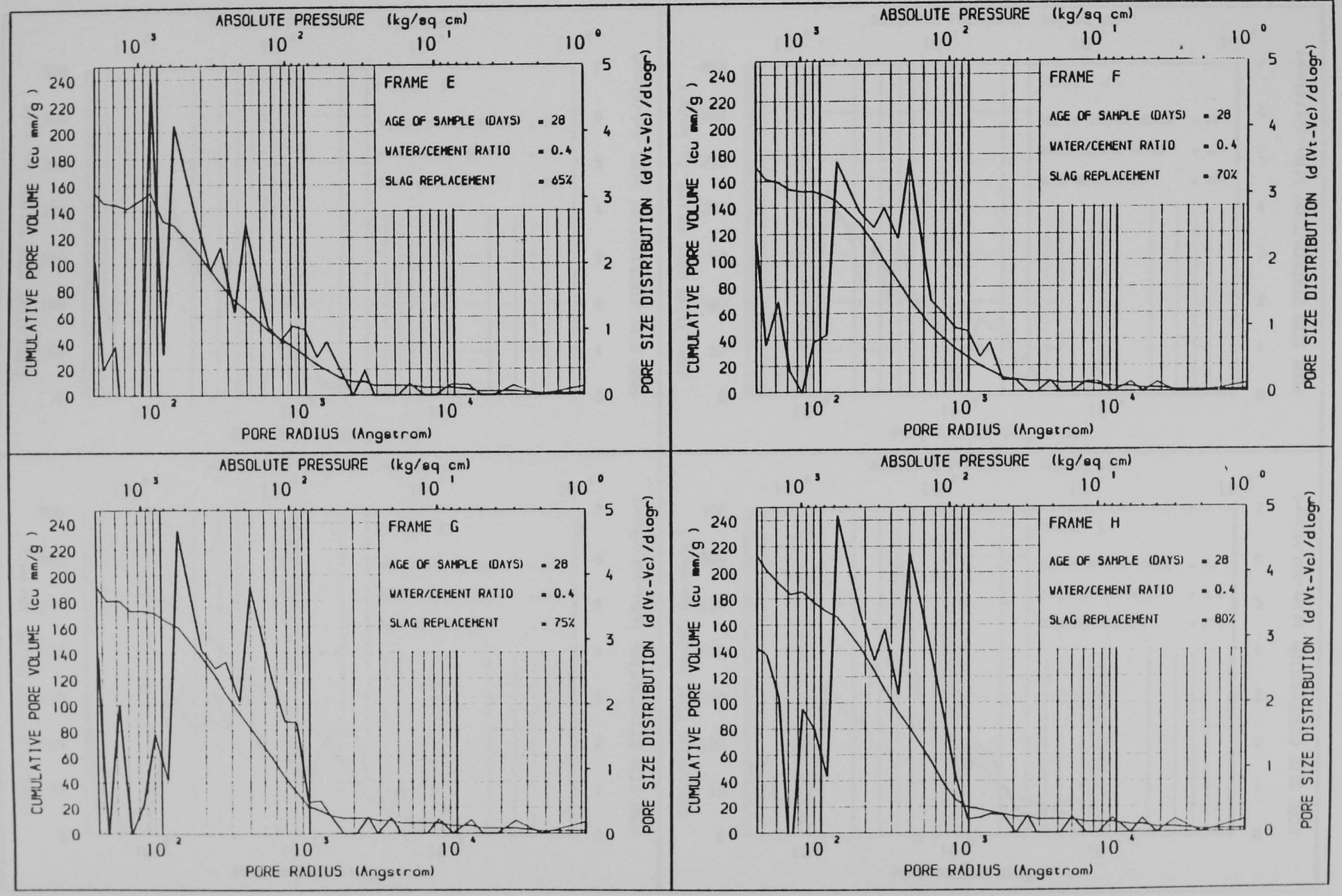

Figure A3.43 THE EFFECT OF BLASTFURNACE SLAG REPLACEMENT OF CEMENT ON PORE SIZE DISTRIBUTION

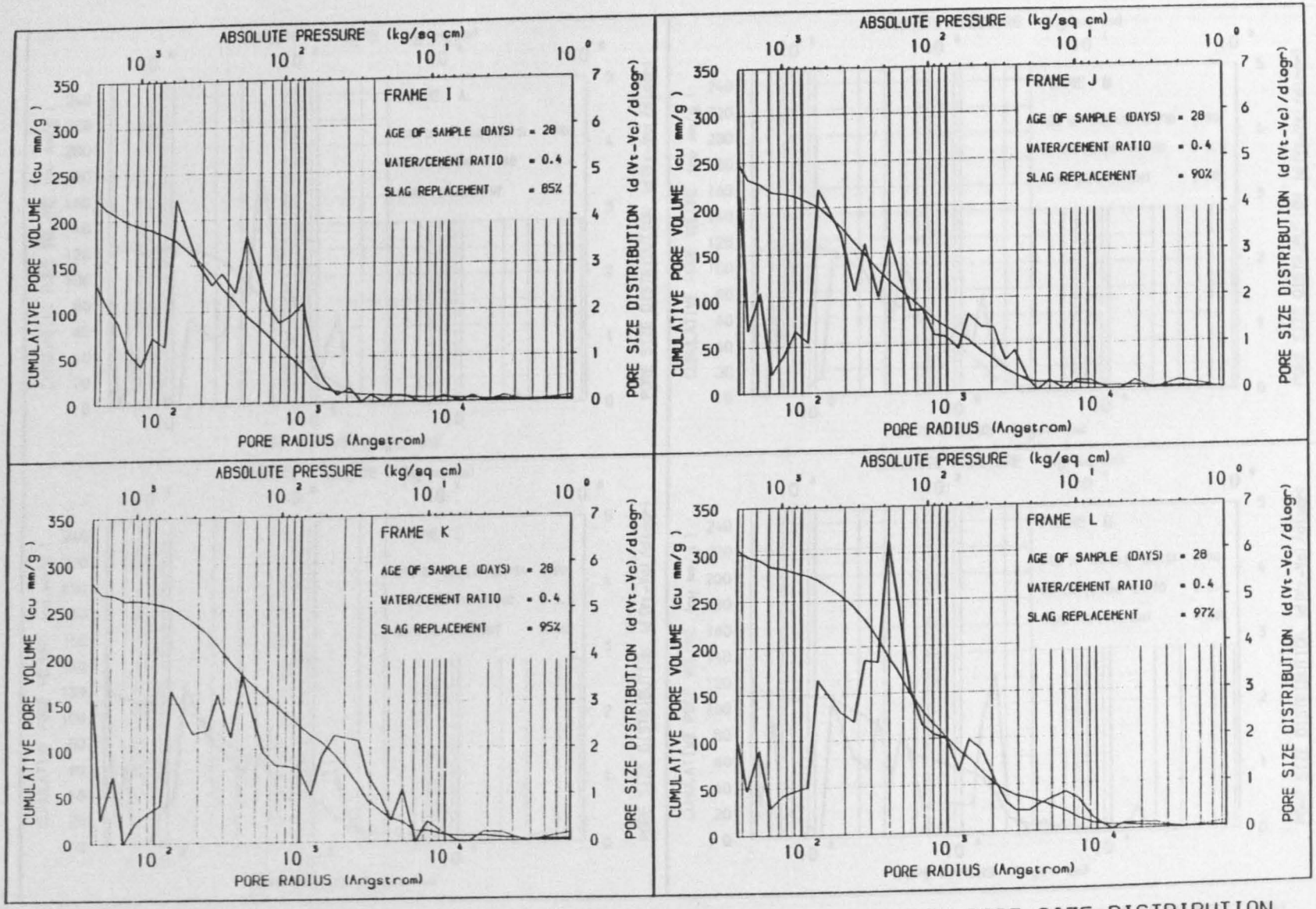

Figure A3.44 THE EFFECT OF BLASTFURNACE SLAG REPLACEMENT OF CEMENT ON PORE SIZE DISTRIBUTION

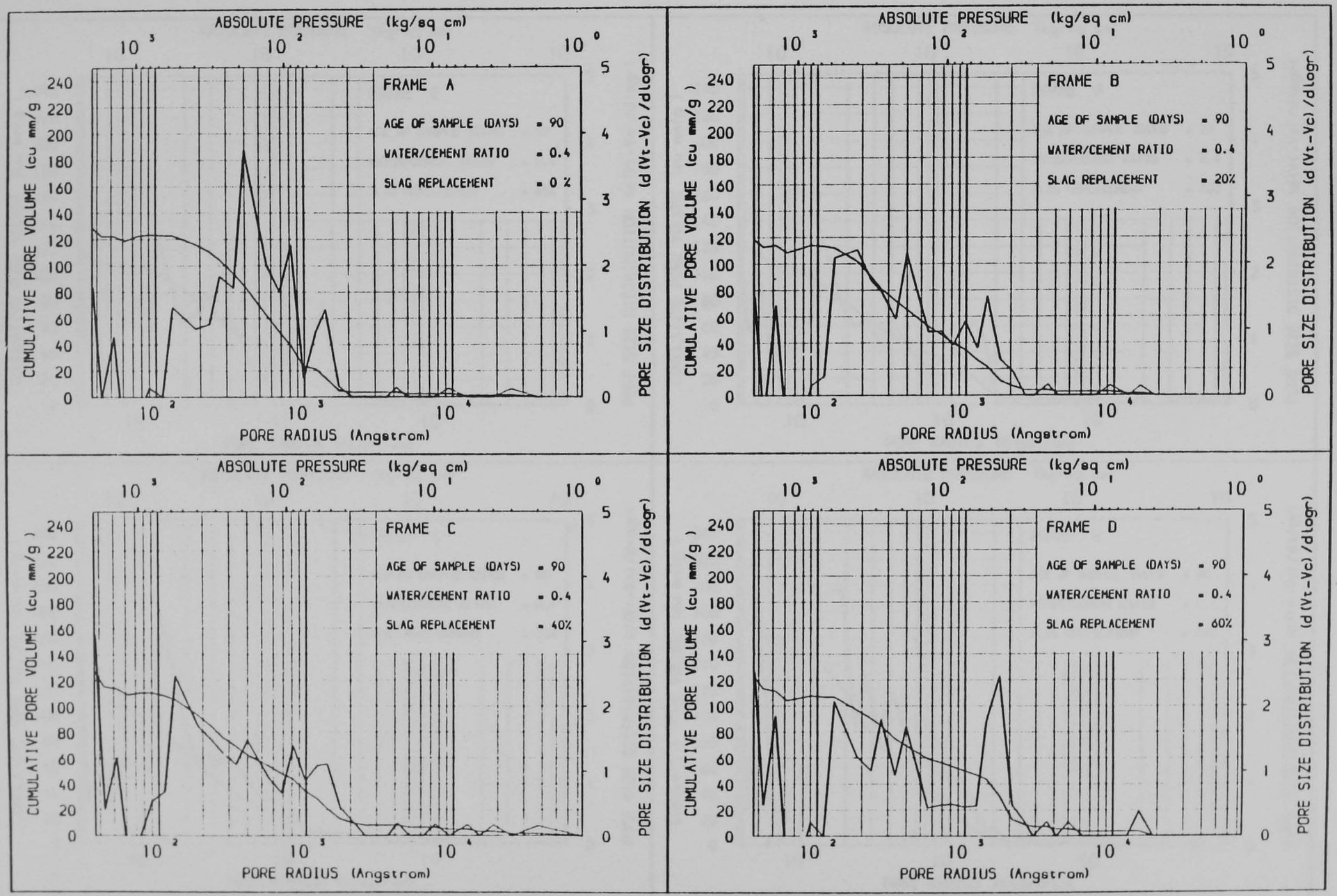

Figure A3.45 THE EFFECT OF BLASTFURNACE SLAG REPLACEMENT OF CEMENT ON PORE SIZE DISTRIBUTION

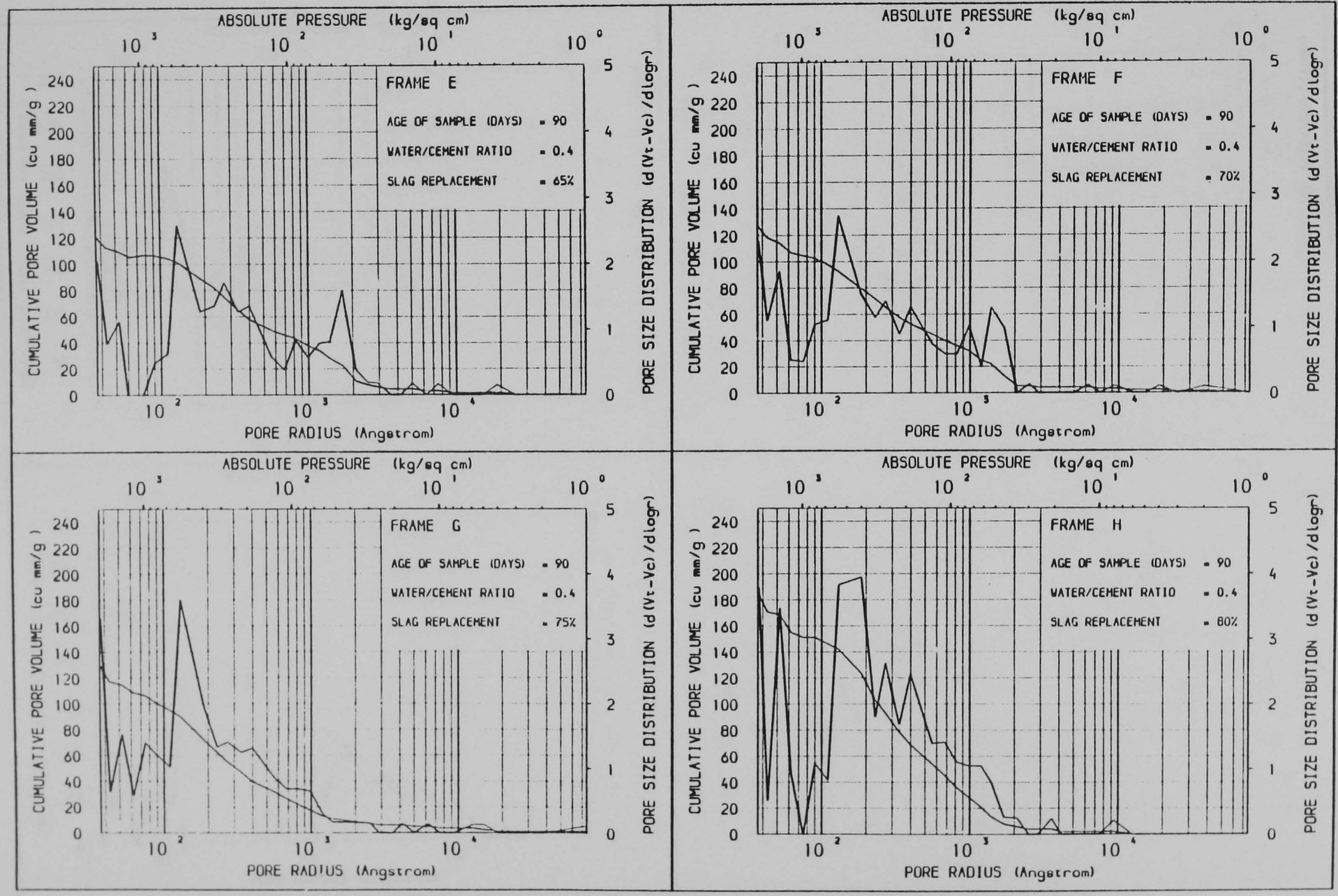

Figure A3.46 THE EFFECT OF BLASTFURNACE SLAG REPLACEMENT OF CEMENT ON PORE SIZE DISTRIBUTION

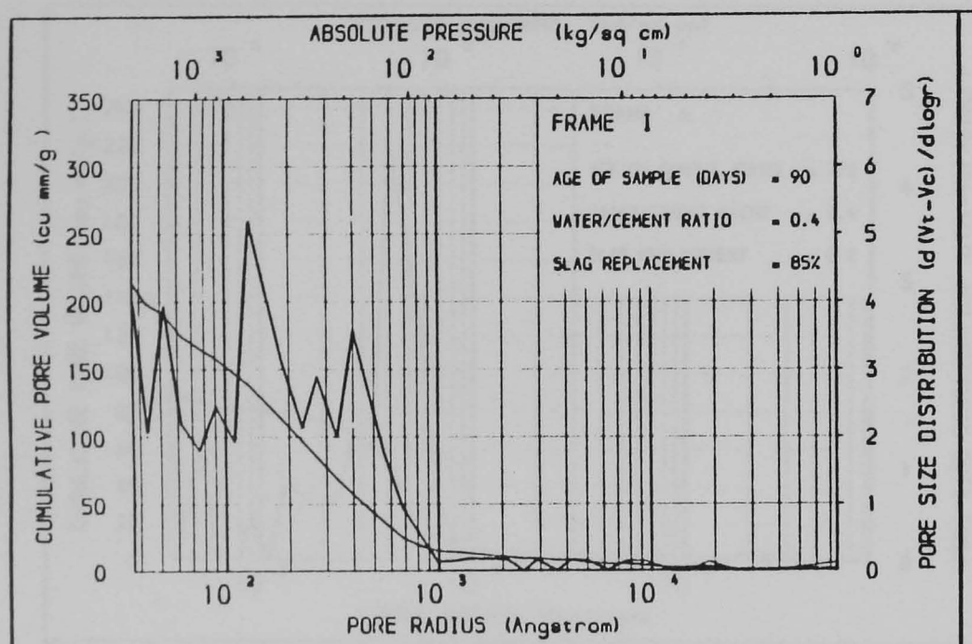

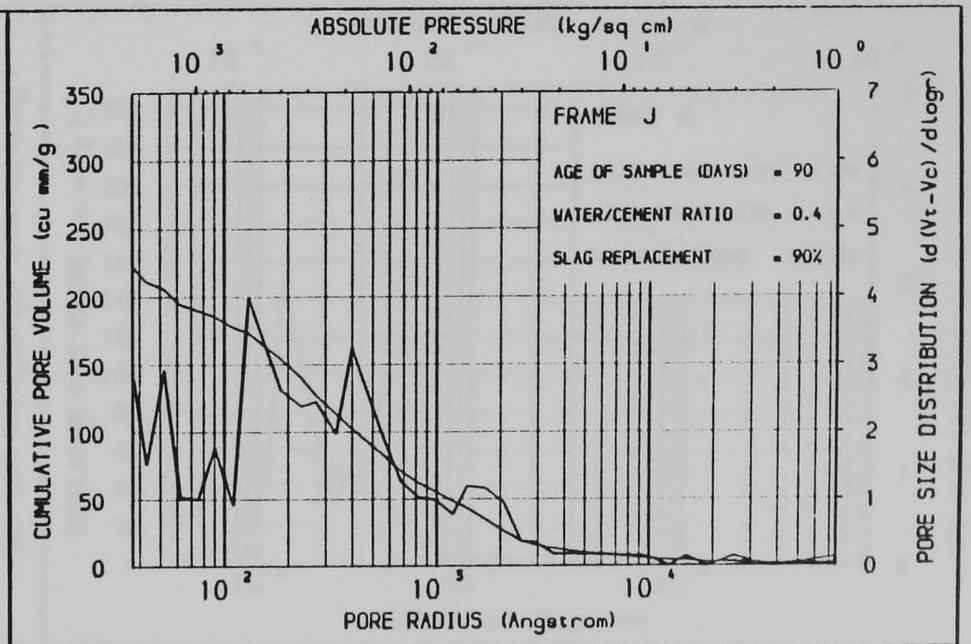

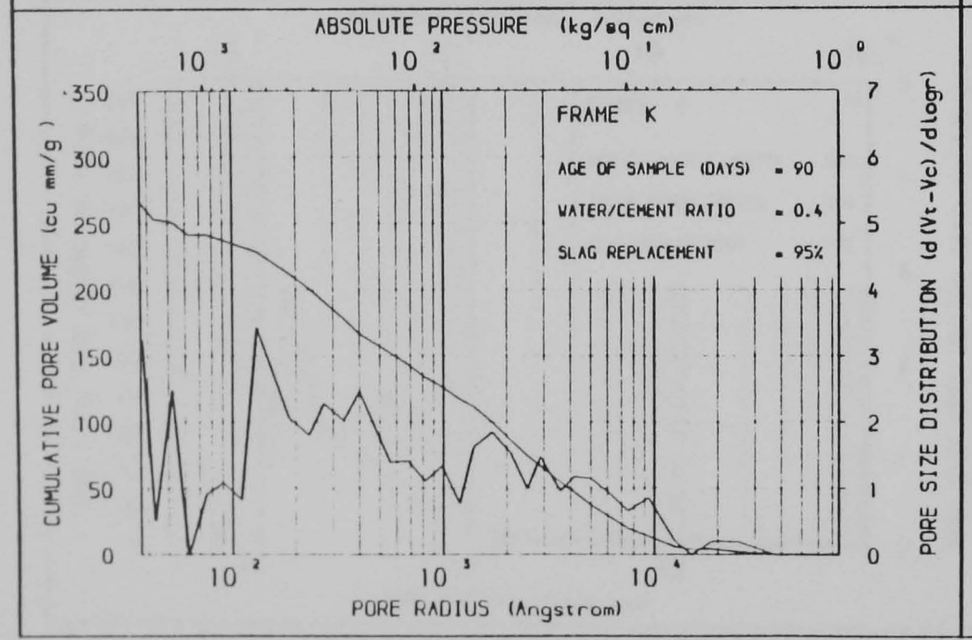

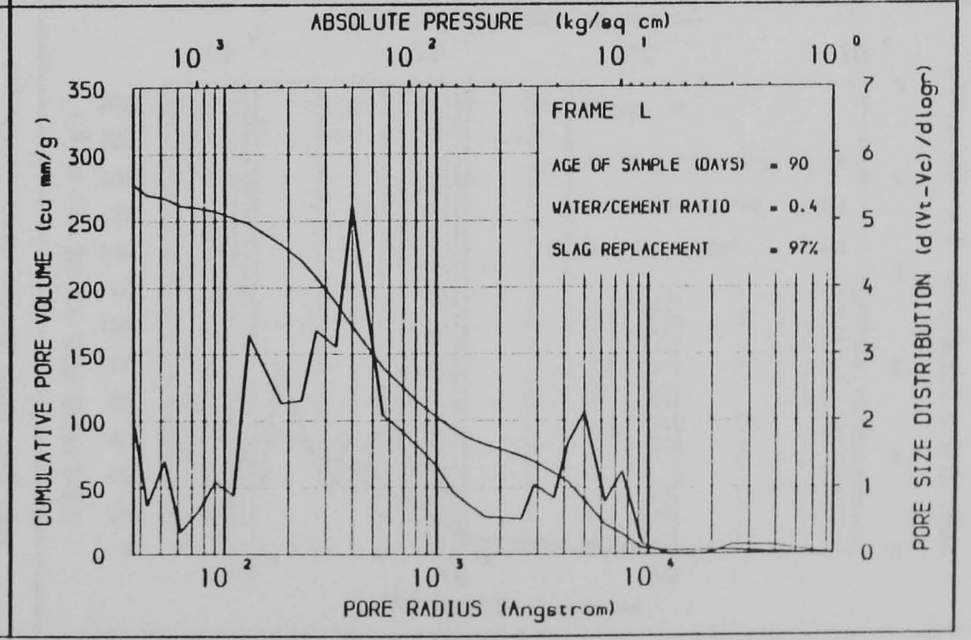

Figure A3.47 THE EFFECT OF BLASTFURNACE SLAG REPLACEMENT OF CEMENT ON PORE SIZE DISTRIBUTION

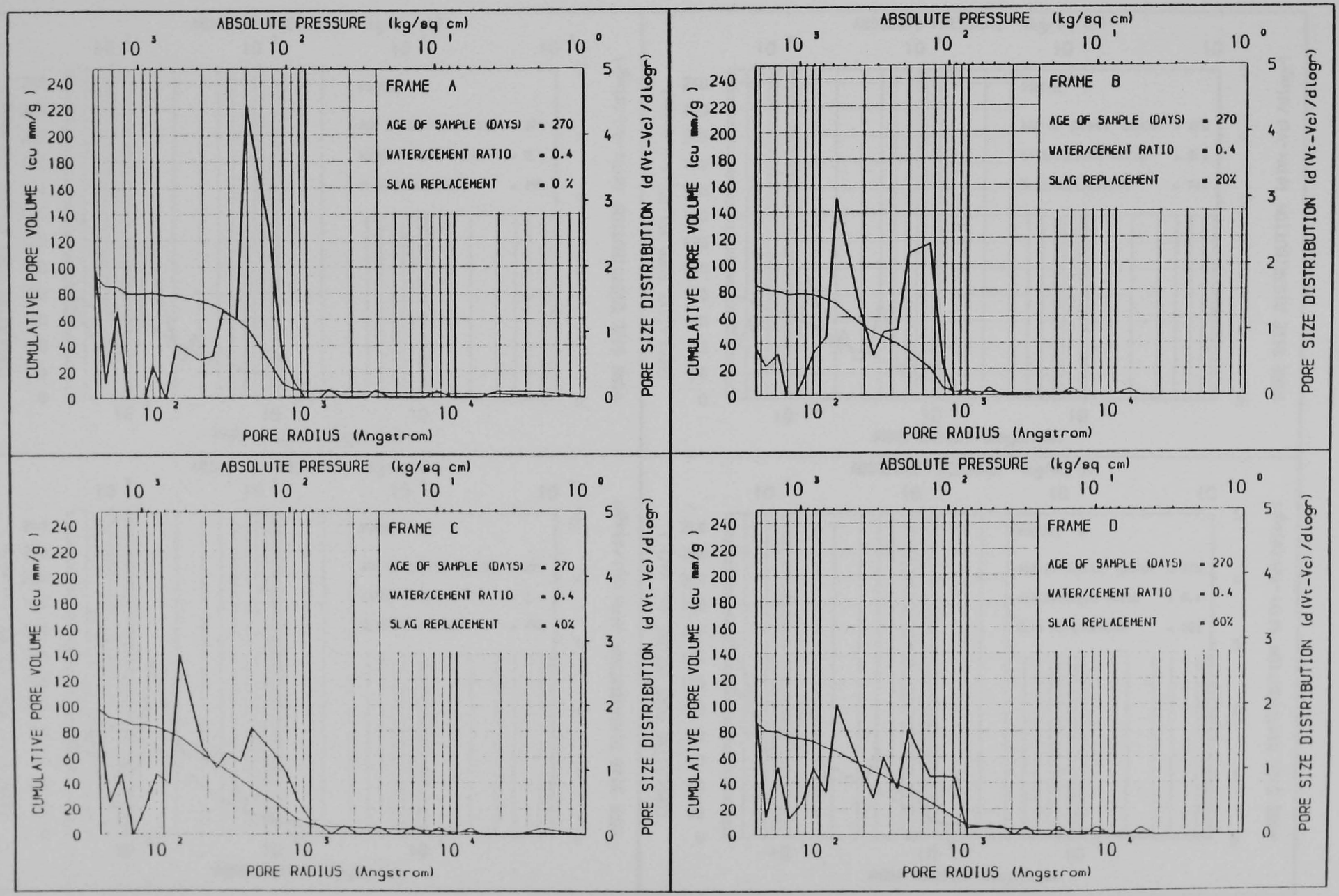

Figure A3.48 THE EFFECT OF BLASTFURNACE SLAG REPLACEMENT OF CEMENT ON PORE SIZE DISTRIBUTION

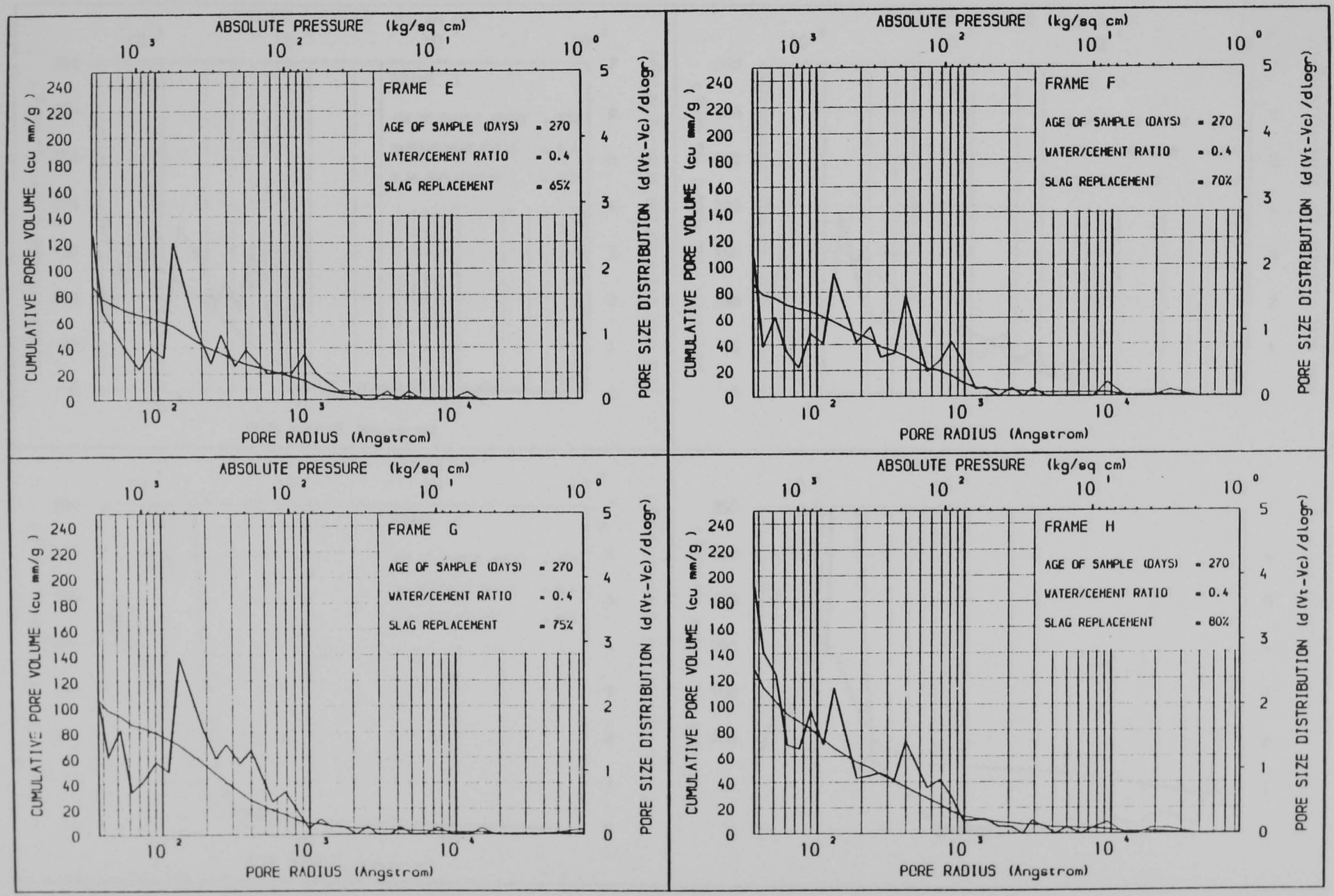

Figure A3.49 THE EFFECT OF BLASTFURNACE SLAG REPLACEMENT OF CEMENT ON PORE SIZE DISTRIBUTION

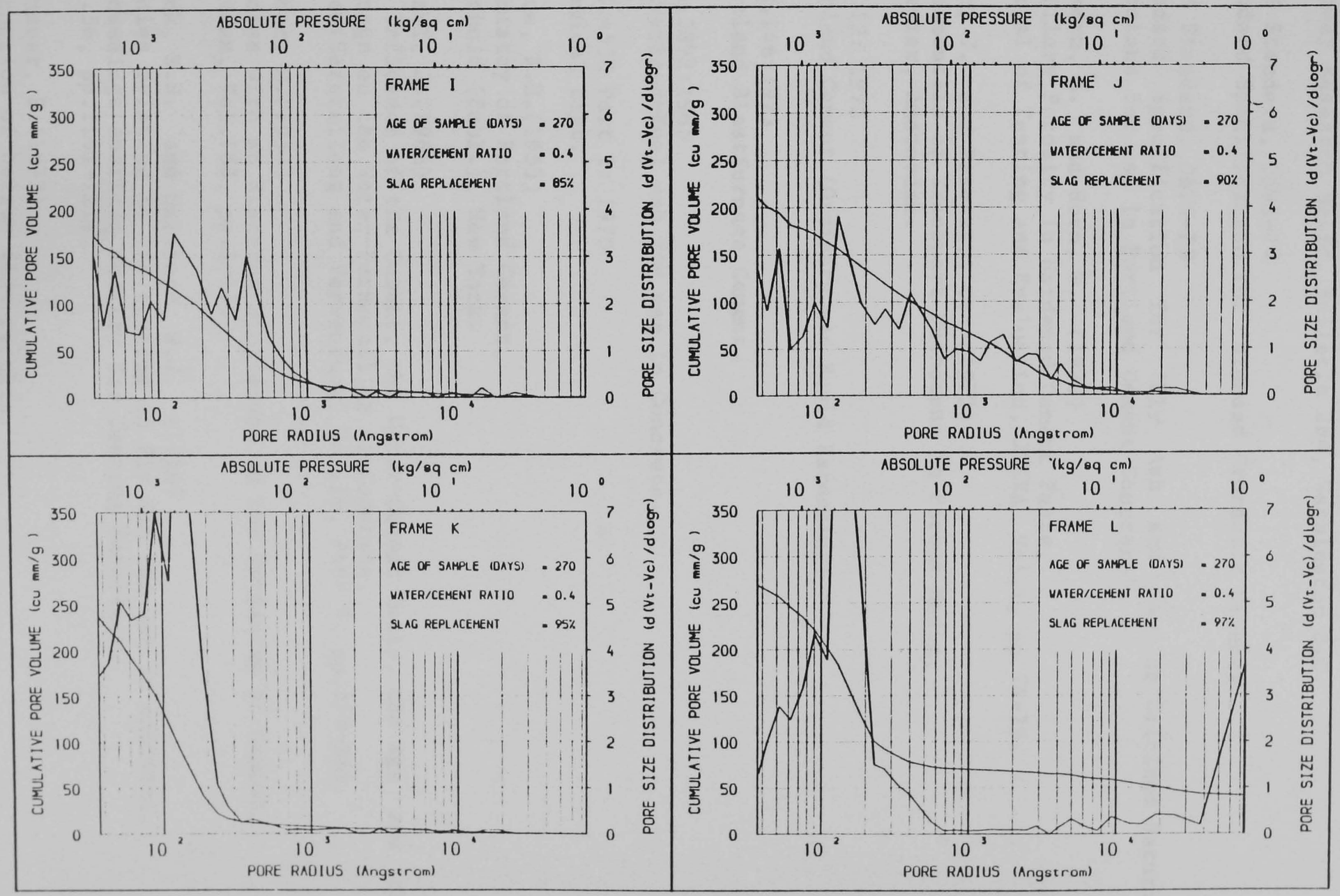

Figure A3.50 THE EFFECT OF BLASTFURNACE SLAG REPLACEMENT OF CEMENT ON PORE SIZE DISTRIBUTION

REFERENCES

Abdun-Nur, E.A.(1961)
Fly ash in concrete - an evaluation
Highway Research Board, Bulletin 284, Washington D.C.

ASTM Standard, C595-79
Standard Specification for `Blended Hydraulic Cements'.

ASTM Standard, C618-78
Standard Specification for `Fly Ash and Raw or Calcined Natural Pozzolans for use in Portland Cement Concrete'.

Auskern, A. and Horn, W. (1973)
Capillary Porosity in Hardened Cement Paste,
Journal of Testing and Evaluation, JTEVA, Vol.1, pp.74-79.

Bear, J. and Braester, C. (1972)
Fundamentals of Transport Phenomena in Porous Media,
Elsevier, Amsterdam.

B.S.12: 1978
Portland Cement (Ordinary and Rapid Hardening)

B.S.146:1973
Portland Blastfurnace Cement.

B.S.3892:1965
Pulverised-Fuel Ash for use in Concrete.

B.S.4550 Part 2: 1970
Chemical test.

Bogue, R.H.(1955)
Chemistry of Portland Cement,
Reinhold (Publ.), New York.

Bonzel, J.(1966)
The Influence of the Cement, the Water-Cement Ratio, the Age and the Storage on the Water-Permeability of Concrete,
Beton(Herstellung and Verwendung) Vol.16, Part 9, pp.379-383.

Boutet, D.(1950)
Studies with an Electron Microscope on the Hardening of Cement,
Travaux, Vol.183, pp.1-11.

Brink, R.H. and Halstead, W.J. (1956)
Studies relating to the testing of Fly ash for use in concrete,
Proceedings American Society for Testing Materials,
Vol.56, pp.1161-1214.

Brunauer, S.(1972)
Discussion of helium flow results,
Cement and Concrete Research, Vol.2, No.4, pp.489-492;
No.6, pp.749-753.

Brunauer, S. and Copeland, L.E. (1964),
Chemistry of hydration of Portland cement at ordinary temperature,
in: The chemistry of cement, Vol. 1,
edited by H.F.W. Taylor, Academic Press,
London, New York, pp.

Brunauer, S., Oder, I. and Yudenfreund, M.(1970)
The new model of hardened Portland cement paste,
Highway Res. Rec., No.328, p.89.

Brunauer, S., Mikhail, R.Sh. and Bodor, E.E. (1967)
Pore structure analysis without a pore shape model,
Journal of Colloid and Interface Science, Vol.24, pp.451-463.

Bruthans, Z. (1963),
Influence of hydration of cement on the properties of grouts for prestressed joints.
Proceedings of the Seventh Conference on the Silicate Industry,
(SILICONF, 1963), Budapest, pp. 234-246

Card, G.B. (1981),
The properties and performance of Bentonite-cement slurries for use as hydraulic cut-offs.
(Ph.D. thesis), King's College, London.

Carman, P.C.(1937)
Fluid flow through granular beds,
Transactions of the Industrial and Engineering Chemistry,
Vol.15, p.150.

Childs, E.C. and Collis-George, N.(1950)
The Permeability of porous materials,
Proceeding of the Royal Society, Vol.201A, pp.392-405.

Cook, H.K.(1951)
Permeability tests of lean mass concrete,
Proceedings American Society for Testing Materials,
Vol.51, pp.1156-1165.

Copeland, L.E. and Kantro, D.L. (1964)
Chemistry of hydration of Portland cement at ordinary temperatures,
in: The Chemistry of Cement, Vol.1,
edited by H.F.W. Taylor, Academic Press,
London, New York, pp.313-370.

Copeland, L.E., Kantro, D.L. and Verbeck, G. (1960)
Chemistry of hydration of Portland cement,
Proceedings of the Fourth International Symp. on the Chemistry of Cement, Washington D.C., pp.429-65.

Cranston, R.W., Inkley, F.A. (1957)
Advances in Catalysis
edited by A. Farkas, Vol. 9,
Academic press, New york, pp 143-154.

Davis, R.E., Carlson, R.W., Kelly, J.W. and Davis, H.E. (1937)
Properties of cements and concretes containing Fly ash,
Proceedings American Concrete Institute, Vol.33, pp.577-612.

Diamond, S.(1971)
A critical comparison of mercury porosimetry and capillary condensation pore size distribution of Portland cement paste,
Cement and Concrete Research, Vol.1, pp.531-545.

Diamond, S.(1973)
Pore structure of hardened cement paste as influenced by hydration temperature,
RILEM/IUPAG, Vol.1, pp.73-88.

Diamond, S. and Dolch, W.L. (1972)
Generalised log-normal distribution of pore sizes in hydrated cement paste,
Journal of Colloid and Interface Science, Vol.38, No.1, pp.234-244.

Drake, L.C. and Ritter, H.L. (1945)
Pressure porosimeter and determination of complete macropore size distributions,
Industrial and Engineering Chemistry, Vol.17, No.12, pp.787.

Dubinin, M.M.(1973)
On physical feasibility of Brunauer's microscope analysis method,
Journal of Colloid and Interface Science, Vol.46, No.3, pp.351-56.

Dunagan, W.M. and Ernst, G.G. (1934)
A study of the permeability of a few integrally water proofed concrete,
Proceedings American Society for Testing Materials, Vol.34, pp.384-92.

Dunstan, M.R.H. and Mitchell, P.B. (1976)
Results of a thermocouple stud in mass concrete in the Upper Tamer Dam,
Proceedings Institution Civil Engineers, pp.27-52.

Feldman, R.F.(1968)
Sorplion and length-change scanning isotherms of methanol and water on hydrated Portland cement pastes,
Proceedings of the Fifth International Symp. on the Chemistry of Cement, Tokyo, Part 3, Vol.3.

Feldman, R.F.(1971)
The flow of Helium into the interlayer spaces of hydrated Portland cement paste,
Cement and Concrete Research, Vol.1, pp.285-300.

Feldman, R.F.(1972)
Helium flow and density measurements of hydrated tricalcium silicate water system,
Cement and Concrete Research, Vol.2, No.1, pp.123-136.

Feldman, R.F.(1972)
Density and porosity studies of hydrated Portland cement paste,
Cement Technology, Vol.3, pp.5-14.

Feldman, R.F.(1972)
Reply to discussions by Brunauer,
Cement and Concrete Research, Vol.2, No.4, pp.493-98.

Feldman, R.F.(1973)
Helium flow characteristics of rewetted specimens of dried hydrated Portland cement paste,
Cement and Concrete Research, Vol.3, No.6, pp.777-90.

Feldman, R.F. and Sereda, P.J. (1970)
A new model for hydrated Portland cement and its practical implications,
Engineering Journal, Vol.53, No.8/9, pp.53-59.

Feldman, R.F. and Sereda, P.J. (1968)
A model for hydrated Portland cement paste as deduced from Sorption length-change and mechanical properties material and structures,
RILEM, Vol.1, No.6, pp.509-20.

Figg, J.W.(1973)
Methods of measuring the air and water permeability of concrete,
Magazine of Concrete Research, Vol.25, No.85, pp.213-19.

Gregg, S.J. and Sing, K.S.(1967)
Adsorption, Surface area and Porosity,
Academic Press Inc., London.

Guner, A.(1978)
The properties and behaviour of Bentonite/Cement Slurries,
(Ph.D. thesis), King's College, London.

Hagymassy, J., Brunauer, S. and Mikhail, R.Sh.(1969)
Pore structure analysis by water vapour adsorption 1: t-curves for water vapour,
Journal of Colloid and Interface Science, Vol.29, No.3, pp.485.

Hancox, N.L.(1968)
An electrical measurement of the effective cross-sectional area for conduction of flow processes in cement paste,
Magazine of Concrete Research, Vol.20, No.64, pp.171-76.

Hansbo, S.(1960)
Consolidation of clay, with special reference to influence of vertical sand drains,
Proceedings Swedish Geotechnical Institute, No.18, pp.1-160.

Higginson, E.C.(1966)
Mineral admixture,
A.S.T.M. sp. Tech. Publicn., No.169A, pp.453-55.

Hughes, B.P. and Ash, J.E. (1969)
Water gain and its effect on concrete,
Concrete, Vol. 3, December, pp. 494-496.

Jayner, L.G., Barrett, E.P. and Skold, R. (1951)
The Determination of pore volume and Area Distribution in porous substances. II. Comparison between Nitrogen Isotherm and Mercury Porosimeter Methods,
Journal of the American Chemical Society, Vol.73, pp.3155.

Jefferis, S.A. (1972)
The composition and uses of slurries in civil engineering practice. (Ph.D thesis), King's College, London.

Kozeny, I.(1927)
Concerning capillary conduction of water in the soil,
Proceedings of the Royal of the Academy Science, class.1.
Vol,136, pp.217-306, Vienna.

Lea, F.M.(1970)
The chemistry of cement and concrete,
Edward Arnold (Publ.) Ltd., Glasgow.

Lea, F.M.(1976)
The chemistry of cement and concrete,
3rd edition, Edward Arnold (Publ.) Ltd.

Lea, F.M. (1980)
The chemistry of cement and concrete,
3rd edition, Edward Arnold (Publ.) Ltd.

Lea, J.A. and Maskett, W.C. (1973)
Correction factors involved in mercury porosimetry,
Powder Technology, Vol.7, pp.259-262.

Lee, A.R.(1974)
Blastfurnace and steel slag production properties and uses,
Edward Arnold (Publ.) Ltd., London.

Manning, D.G. and Hope, B.B. (1971)
The effect of porosity on the compressive strength and elastic modulus of polymer impregnated concrete,
Cement and Concrete Research, Vol.1, pp.631-44.

Mayer, R.P. and Stowe, R.A. (1965)
Mercury Porosimetry - Breakthrough pressure for penetration between packed spheres,
Journal of Colloid Science, Vol.20, pp.893-911.

Midgley, H.G.(1979)
Private conversation

Minnick, L.J.(1959)
Fundamental characteristics of pulverized coal Fly ashes,
Proceedings American Society for Testing Materials,
Vol.59, pp.1155-1177.

Mikhail, R.Sh., Brunauer, S., and Bodor, E.E. (1967)
Investigations of a complete pore structure analysis,
Journal of Colloid and Interface Science, Vol.26, pp.45-53.

Mikhail, R.Sh. and Abo-El-Enein (1972)
Studies on water and Nitrogen Adsorption on hardened cement pastes,
Cement and Concrete Research, Vol.2, pp.401-14.

Mikhail, R.Sh., Turk, D.H. and Brunauer, S. (1975)
Dimensions of the average pore, the number of pores, and surface area of hardened Portland cement paste,
Cement and Concrete Research, Vol.5, pp.433-42.

Mikhail, R.Sh., Youssef, A.M. and Shater, M. (1977)
Air entrainment in Portland Blastfurnace slag cement paste: effects on strength and pore structure,
Cement and Concrete Research, Vol.7, pp.515-22.

Muskat, M.(1937)
The flow of homogeneous fluids through porous media,
McGraw-Hill Book Co.(Publ.), New York.

Muskat, M.(1946)
The flow of homogeneous fluids through porous media,
Edwards, Ann. Arbor, Ch.3.

McBain, J.W.(1932)
Sorption of gases and vapours by solids,
London, George Routledge and Sons, pp.79.

McMillan, F.R. and Lyse, I. (1929)
Some permeability studies of concrete,
Proceedings American Concrete Institute, Vol.26, pp.101-42.

Nyame, B.K.(1980)
Permeability and pore structure of hardened cement paste and mortar,
(Ph.D. thesis), King's College, London.

Nyame, B.K. and Illston, J.M.(1981)
Relationships between permeability and pore structure of hardened cement paste,
Magazine of Concrete Research, vol. 33, No. 116, pp 139-46.

Neville, A.M.(1977)
Properties of concrete,
Pitman Publishing, Bath.

Norton, P.T. and Pletta, D.H. (1931)
The permeability of Gravel Concrete,
Proceedings American Concrete Institute, Vol.27, pp.1093-132.

Nurse, R.W. and Midgley, H.A.(1951)
The mineralogy of Blastfurnace slag,
Silic.Ind., Vol.16, No.7, pp.211-17.

Odler, I., Hagymassy, J., Bodor, E., Yudenfreund, M. and Brunauer, S. (1972),
Hardened Portland cement paste of low porosity,
Cement and Concrete Research, Vol.2, pp.377-89.

Olsen, H.W.(1961)
Hydraulic flow through saturated clays,
(Ph.D. thesis), M.I.T.(Multilithed).

Orr, C.(1970)
Application of mercury penetration to materials analysis,
Powder Technology, Vol.3, pp.117-23.

Oulton, T.D.(1948)
The pore size - surface area distribution of a cracking catalyst,
Journal of Physical Colloid Chemistry, Vol.52, pp.1296.

Owens, P.L.(1978)
The essential quality control criteria for Fly ash for use as a separate pozzolanic ingredient for concrete,
The Conference on Ash Technology and Marketing, London.

Owens, P.L.(1979)
Fly ash and its usage in concrete,
The Journal of Concrete Society, Vol.13,

Palmer, H.K.(1975)
An alternative filling technique for use with micromeritics mercury intrusion porosimeter,
Powder Technology, Vol.11, pp.195-96.

Pihiajavaara, S.E. and Paroll, H. (1975)
On the correlation between permeability properties and strength of concrete,
Cement and Concrete Research, Vol.5, pp.321-28.

Powers, T.C.(1939)
The bleeding of Portland cement paste, mortar, and concrete,
Proceedings of the American Concrete Institute, Vol.35, pp.465-79.

Powers, T.C.(1939)
The bleeding of Portland cement paste, mortar, and concrete,
Bulletin No.2, Research Laboratory Portland Cement Association.

Powers, T.C.(1949)
The nonevaporable water content of hardened Portland cement paste,
ASTM Bulletin, ASTBA, No.158, pp.68.

Powers, T.C.(1958)
Structure and physical properties of hardened Portland cement paste,
Journal of American Ceramic Society, Vol.41, No.1, pp.1-6.

Powers, T.C.(1960)
Chemistry of cement,
Proceedings of the Fourth International Conference on the Chemistry of Cement, Washington, D.C., pp.577.

Powers, T.C.(1964)
The physical structure of Portland cement paste,
Chapter 10 of "The Chemistry of Cement", H.F.W.Taylor, Ed.,
Academic Press, New York.

Powers, T.C.(1968)
The properties of Fresh concrete,
John Wiley and Sons (Publ.) Ltd., London.

Powers, T.C. and Brownyard, T.L. (1947)
Studies of the physical properties of hardened Portland cement paste (Nine parts),
Journal of American Concrete Institute, Vol.43.

Powers, T.C. and Brownyard, T.L. (1948)
Studies of the physical properties of hardened Portland cement paste,
Portland Cement Association, Research and Development Laboratory Bulletin No.22, Skokie, Illinois, p.342.

Powers, T.C., Copeland, L.E., Hayes, J.C. and Mann, H.M. (1954)
Permeability of Portland cement paste,
Journal of American Concrete Institute, Vol.26, No.3, pp.285-300.

Powers, T.C., Copeland, L.E. and Mann, H.M. (1959)
Capillary continuity or discontinuity in cement paste,
Portland Cement Association, Research and Development Laboratory, Vol.1, No.1, pp.38-48.

Ritter, H.L. and Drake, L.C. (1945)
Pore size distribution in porous materials,
Industrial and Engineering Chemistry, Vol.17, No.12, pp.782-86.

Roberts, B.F.(1967)
A procedure for estimating pore volume and area distribution from sorption isotherms,
Journal of Colloid and Interface Science, Vol.23, pp.266-73.

Robson, R.A., (1965)
Mobility of water in porous media of high surface area,
Bulletin Rilem, No. 27 p. 65.

Rootare, H.M. (1967)
Surface area from mercury porosimeter neasurements,
The Journal of Physical Chemistry, Vol. 71, No. 8, pp. 2733-36.

Roy, D.M. and Gouda, G.R. (1975)
Optimization of structure in cement pastes,
Cement and Concrete Research, Vol.5, pp.153-62.

Ruettgera, A., Vidal, E.N. and Wing, S.P. (1935)
An investigation of the permeability of Mass concrete with particular reference to Boulder dam,
Journal of American Concrete Institute, Vol.31, pp.382-416.

Scheidegger, A.E.(1974)
The physics of flow through porous media,
3rd edition (University of Torouto Press).

Scholz, H.(1968)
German Black coal combusion residues, types and uses,
Conference on Ash Technology and Marketing, London.

Schull, C.G.(1948)
The determination of pore size distribution from gas adsorption data,
Journal of the American Chemical Society, Vol.70, pp.1405.

Sellvold, E.J.(1974)
Mercury porosimetry of hardened cement paste,
Cement and Concrete Research, Vol.4, pp.399-404.

Simons, H.S. and Jeffery, J.W. (1960)
An X-ray study of pulverised Fuel ash,
Journal of Applied Chemistry, Vol.10, pp.328-336.

Sing, K.S.(1980)
Private conversation

Skalny, J. and Odler, J. (1972)
Pore structure of Calicum Silicate hydrates,
Cement and Concrete Research, Vol.2, No.4, pp.387-400.

Slattery, J.C.(1972)
Momentum, energy and mass transfer in continua,
McGraw Hill.

Smith, M.A.(1975)
Review of standard specifications for Fly ash for use in concrete.
Department of the Environment, Building Research Establishment Current Paper CP8/75.

Steinour, H.H.(1944)
Rate of Sedimentation,
Portland Cement Association Research and Development Laboratory, Bulletin No.3.

Steinour, H.H.(1945)
Further studies of the Bleeding of Portland cement paste,
Portland Cement Association Research Bulletin, No.4.

Svata, M. and Zabransky, Z. (1970)
Comparison of mercury porosimetry, sedimentation and microscopy for determining the grain size distribution of powdered particles,
Powder Technology, Vol.3, pp.296-98.

Taylor, H.F.W. (1964),
The chemistry of cement,
Vol.1 Edited by H.F.W. Taylor, Academic Press,
London and New York, pp. 1-24.

Van Brakel, J. (1975)
Pore space models for capillary liquid transport,
Powder Technology, Vol.11, pp.205.

Van Der Meulen and Van Dijk, J. (1969)
A Permeability-Testing Apparatus for Concrete,
Magazine of Concrete Research, Vol.21, No.67, pp.121-123.

Valore, R.C., Bowling, J.E. and Blaine, R.L. (1949)
The direct and continuous measurement of bleeding in Portland Cement mixtures,
Proceedings American Society for Testing Materials, Vol.49, pp.891.

Verbeck, G.J.(1955)
Hardened concrete - pore structure,
ASTM Sp. Tech. Publicn., No.169, pp.136-42.

Verbeck, G.J.(1965)
Cement hydration reactions at early ages,
Portland Cement Association Research and Development Laboratories,
Vol.7, No.3, pp.57-63.

Verbeck, G.J.(1966)
Cement hydration reactions at early ages.
Portland Cement Association Research, Bulletin No.197, Skokie, Illinois.

Washburn, E.W.(1921)
Proceedings of the National Academy of Science, Vol.7, pp.115-16.

Watt, D. and Thorne, D.J.(1965)
Analyses for many British Fly ashes,
Journal of Applied Chemistry, Vol.15, pp.585-94.

Wiley, B. and Coulson, D. (1937)
A simple test for water permeability of concrete,
Proceedings American Concrete Institute, Vol.34, pp.65.